Analysis of the Subcellular Distribution and Trafficking of the Insulin-Responsive Glucose Transporter, GLUT4

A thesis submitted to the

FACULTY OF SCIENCE

for

the degree of

DOCTOR OF PHILOSOPHY

BY

CAROLINE ANN MILLAR

Division of Biochemistry & Molecular Biology

Institute of Biomedical & Life Sciences

University of Glasgow

October 1998

ProQuest LLC.
789 East Eisenhower Parkway
P.O. Box 1346
Ann Arbor, MI 48106 – 1346

Abstract

The translocation of a facilitative glucose transporter, GLUT4, from an intracellular site to the cell surface accounts for the large insulin-dependent increase in glucose transport observed in muscle and adipose tissue. Recent studies have indicated that a large proportion of intracellular GLUT4 is segregated from the recycling endosomal system in a post-endocytic storage compartment in 3T3-L1 adipocytes. However, the nature of this GLUT4 storage compartment, and the mechanism by which GLUT4 reaches the cell surface upon insulin stimulation are poorly understood.

Here, I have used Tf-HRP-mediated endosomal ablation analysis to examine the protein composition of the post-endocytic compartment with the aim of further defining the relationship of this compartment to other, well characterised, intracellular membrane structures. The results provide further evidence for the existence of a GLUT4 compartment segregated from the endosomal system, which is devoid of cell surface to endosome recycling markers including the TfR and SCAMPs. The observation that within this compartment, GLUT4 co-localises with TGN marker proteins, γ-adaptin and the CD-M6PR, suggests that GLUT4 traffics through the TGN as part of its recycling itinerary.

I further exploited this technique to examine the translocation of GLUT4 to the cell surface in response to insulin and GTPγS. The results indicate that insulin is still capable of stimulating GLUT4 translocation following endosomal ablation under conditions where GTPγS-stimulated GLUT4 translocation was effectively inhibited. In addition, both insulin- and GTPγS-stimulated GLUT1 translocation were blocked following ablation of the recycling endosomal system. On the basis of these and other data, I propose that insulin stimulates the exocytosis of two distinct compartments, one being the post-endocytic storage compartment and the other being the endosomal system, which may also be stimulated by GTPγS.

Recent studies have implicated ARF proteins to function as regulators of regulated exocytosis. To investigate the role of ARF proteins in insulin-stimulated GLUT4 translocation, we examined the effect of myristoylated ARF peptides on insulin-stimulated GLUT4 translocation and glucose transport in permeabilised 3T3-L1 adipocytes. A myristoylated peptide corresponding to the N-terminus of ARF6 markedly inhibited insulin-stimulated GLUT4 translocation and 2-deoxy-D-glucose transport, whereas ARF5 and ARF1 peptides were without effect. In addition, an effective inhibitor of PLD, butan-1-ol was observed to have no effect on insulin-stimulated GLUT4 translocation and glucose transport. These results suggest that ARF6 plays a crucial role in insulin-stimulated GLUT4 translocation. However, PLD does not appear to function as a downstream effector of ARF in this event.

Finally, I have shown that a chimeric protein comprising the signal sequence of the human growth hormone and HRP (ssHRP) may be targeted to the exocytic pathway and secreted from 3T3-L1 adipocytes. However, due to the time constraints of this study, I was unable to use this HRP probe to ablate the TGN, thus enabling me to investigate the role of this sorting compartment in GLUT4 trafficking.

Acknowledgements

Firstly, I am indebted to Professor Gwyn Gould for his supervision throughout my Ph.D. I wish to thank him for providing me with the opportunity to pursue a career in science and for showing great enthusiasm towards my work. I also wish to thank the British Diabetic Association for funding this project.

Special thanks must go to members of Lab C36 past and present, all of which have been a great help and a source of entertainment for the last three years. In particular, I wish to thank my Ph.D 'soulmate' Derek, a fair player and a great friend. Thanks must also go to Valerie for all her help in the latter stages and to Di for her proof reading skills.

I wish to thank my parents for providing me with every opportunity to further my education, for their constant love and support and for making sure I always did my homework!!

Last, but by no means least, I wish to thank Dave for his patience, support and encouragement, especially during the writing up of this thesis.

To mum and dad,

with all my love.

'Only fools live lives without alternatives.'

Mitchell Wilson

Contents

	Page
Abstract	i
Acknowledgements	iii
Dedication	iv
Quotation	v
Contents	vi
List of Figures	xvi
List of Tables	xx
Abbreviations	xxi

		Page
Chapter 1	**Introduction**	1
1.1	Glucose Transport	2
1.1.1	Insulin Resistance	2
1.1.2	GLUT4 - The Insulin-Responsive Transporter	3
1.2	Subcellular Trafficking - a General Background	4
1.3	The Endocytic System - Receptor-Mediated Endocytosis	5
1.3.1	Clathrin-Coated Pit Formation	6
1.3.2	Non-Clathrin-Mediated Endocytosis	8
1.3.3	Endosomal Compartments	9
1.3.4	Rab Proteins in Vesicle Transport	9
1.4	The Secretory System	11
1.4.1	The *trans*-Golgi Network (TGN)	12
1.4.2	Vesicle Budding at the TGN	12
1.4.3	Sorting at the TGN	14
1.5	Membrane Targeting and Fusion	21
1.6	The Role of Phosphoinositides in Membrane Trafficking	23
1.7	The Facilitative Glucose Transporter Family	24
1.7.1	The Tissue-Specific Distribution of the Facilitative Glucose Transporters	25
1.7.2	GLUT1	26
1.7.3	GLUT2	27

1.7.4	GLUT3	28
1.7.5	GLUT4	29
1.7.6	GLUT5	29
1.7.7	GLUT6	30
1.7.8	The Structure and Membrane Topography of the GLUTs	30
1.8	GLUT4-The Insulin-Responsive Glucose Transporter	32
1.9	GLUT4 Translocation	33
1.10	GLUT4 Subcellular Trafficking	35
1.11	The GLUT4 Intracellular Compartment	37
1.12	The Nature and Biogenesis of the GLUT4 Storage Compartment	40
1.13	GLUT4 Trafficking Signals	45
1.14	GLUT4 Trafficking: The Role of SNAREs and Rab Proteins	46
1.15	Signalling Mechanisms that Regulate GLUT4 Translocation	51
1.15.1	IRS Proteins and GLUT4 Translocation	53
1.15.2	PI3-Kinase and GLUT4 Translocation	54
1.15.3	Downstream Targets of PI3-Kinase	56
1.16	Aims of this Study	58

Chapter 2	**Materials and Methods**	83
2.1	Materials	84
2.1.1	General Reagents	84
2.2	General Buffers	87
2.2.1	Phosphate Buffered Saline (PBS)	87
2.2.2	Krebs Ringer Phosphate (KRP) Buffer	87
2.2.3	HES Buffer	87
2.3	Cell Culture	88
2.3.1	3T3-L1 Murine Fibroblasts	88
2.3.2	Trypsinisation and Passage of 3T3-L1 Fibroblasts	88
2.3.3	Differentiation of 3T3-L1 Fibroblasts	88
2.3.4	Freezing and Storage of Cells	89
2.3.5	Resurrection of Frozen Cell Stocks from Liquid Nitrogen	90
2.3.6	Collagen Coating of Cell Culture Plastic Ware	90
2.4	Antibody Preparations	90
2.4.1	Purification of Anti-GLUT4 Antibody	91
2.5	Protein Assay	91
2.6	SDS/Polyacrylamide Gel Electrophoresis	92
2.7	Western Blotting of Proteins	92
2.8	Immunodetection of Proteins	93
2.8.1	Using Autoradiography	93
2.8.2	Using the Enhanced Chemiluminescence (ECL) Detection System	94

2.9	Endosome Ablation	94
2.9.1	Preparation of Tf-HRP Conjugate	94
2.9.2	Use of Tf-HRP	96
2.10	Subcellular Fractionation of 3T3-L1 Adipocytes	96
2.11	Immunoadsorption of GLUT4 Vesicles	97
2.12	Indirect Immunofluorescence Microscopy	99
2.12.1	Plasma Memebrane Lawn Assay	99
2.12.2	Whole-Cell Indirect Immunofluorescence Microscopy	100
2.13	2-Deoxy-D-Glucose Transport Assay	101
2.14	Adipsin Release	102
2.15	Molecular Biology	103
2.15.1	Preparation of Competent Bacteria	103
2.15.2	Transformation of Competent Bacteria	103
2.15.3	Multiple Plasmid Minipreparations	104
2.15.4	Maxi Preparation of Plasmid DNA	105
2.15.5	Calculation to Determine the Plasmid DNA Concentration and Purity	106
2.15.6	Restriction Digestion of DNA	106
2.15.7	Dephosphorylation of Linearised DNA	107
2.15.8	Agarose Gel Electrophoresis	107
2.15.9	Gel Extraction of DNA	108

Chapter 3	**Compartment Ablation Analysis of the GLUT4 Intracellular Compartments**	109
3.1	Aims	110
3.2	Introduction	111
3.3	Materials and Methods	113
3.3.1	Ablation of the Intracellular (LDM) Membranes	113
3.3.2	Sucrose Density Gradient Analysis	114
3.3.3	Whole-Cell Immunoflurescence Microscopy	115
3.3.4	Antibodies	115
3.4	Results	116
3.4.1	Subcellular Distribution of Proteins In Basal and Insulin-Stimulated 3T3-L1 Adipocytes	116
3.4.2	Ablation of Proteins Localised to the Intracellular (LDM) Membranes	117
3.4.3	Co-Localisaton of γ-adaptin, the CD-M6PR and Syntaxin 4 with GLUT4-Containing Vesicles	120
3.4.4	Intracellular Distribution of GLUT4, γ-adaptin and the CD-M6PR in 3T3-L1 Adipocytes	121
3.5	Discussion	142
3.5.1	SCAMPs, Syntaxin 4 and CSPs: Markers for Exocytosis	143
3.5.2	Rab4	146
3.5.3	γ-adaptin and the CD-M6PR: Markers for the TGN	148
3.6	Summary	152

Chapter 4	**Compartment Ablation Analysis of Insulin- and GTPγS-Stimulated GLUT4 Transloaction from Multiple Intracellular Pools**	153
4.1	Aims	154
4.2	Introduction	155
4.3	Materials and Methods	157
4.3.1	Transferrin Receptor Externalisation Assay	157
4.3.2	Cell-Surface Transferrin Receptor Internalisation Assay	158
4.3.3	Cell-Surface Transferrin Receptor Externalisation Assay	159
4.3.4	Plasma Membrane Lawn Assay	159
4.3.5	Permeabilisation of 3T3-L Adipocytes	160
4.3.6	Adipsin Release:	
	Endosome Ablation	161
	Wortmannin Treatment	161
4.3.7	Antibodies	162
4.3.8	Statistical Analysis	162
4.4	Results	162
4.4.1	Effect of Endosomal Ablation on Transferrin Receptor Trafficking in 3T3-L1 Adipocytes	162
4.4.2	Effect of Endosomal Ablation on Insulin-Stimulated GLUT4 and GLUT1 Translocation	163
4.4.3	Effect of Endosomal Ablation on GTPγS-Stimulated GLUT4 and GLUT1 Translocation	164
4.4.4	Effect of Wortmannin on Insulin- and GTPγS-Stimulated GLUT4 Translocation	165

4.4.5	Effect of Endosomal Ablation on Cell-Surface Transferrin Receptors	166
4.4.6	Effect of Endosomal Ablation and Wortmannin on Constitutive Secretion in 3T3-L1 Adipocytes	167
4.5	Discussion	193
Chapter 5	**Analysis of the Role of ARF Proteins and Phospholipase D in Insulin-Stimulated GLUT4 Translocation**	199
5.1	Aims	200
5.2	Introduction	201
5.3	Materials and Methods	202
5.3.1	Permeabilisation of 3T3-L1 Adipocytes	202
5.3.2	2-Deoxy-D-Glucose Transport Assays:	
	Effect of Myristoylated Peptides	203
	Effect of Butan-1-ol	204
5.3.3	Double-Labelled Immunofluorescence Microscopy	204
5.3.4	Adipsin Release:	
	Effect of Butan-1-ol	204
5.3.5	Peptide Synthesis	205
5.3.6	Antibodies	205
5.3.7	Statistical Analysis	205
5.4	Results	206

5.4.1	Distribution of ARF Proteins and the Effect of Insulin and Wortmannin in 3T3-L1 Adipocytes	206
5.4.2	Co-Localisation of ARF5 and GLUT4 within 3T3-L1 Adipocytes	207
5.4.3	Role of ARFs in Insulin-Stimulated GLUT4 Translocation	209
5.4.4	Subcellular Distribution of PLDs and the Effect of Insulin in 3T3-L1 Adipocytes	210
5.4.5	Role of Phospholipase D In Insulin-Stimulated Trafficking in 3T3-L1 Adipocytes	210
5.5	Discussion	234
Chapter 6	**Constuction of an ssHRP Chimera for Compartment Ablation Analysis in 3T3-L1 Adipocytes**	241
6.1	Aims	242
6.2	Introduction	243
6.3	Materials and Methods	244
6.3.1	Construction of pOP13.ssHRP.aP2	
6.3.2	Calcium Phosphate Transfection of 3T3-L1 Fibroblasts and Selection of Stable Transfectants	245
6.3.3	HRP Assay	246
6.3.4	Ablation of the Intracellular (LDM) Membranes using ssHRP	246
6.3.5	Antibodies	247
6.4	Results	247

6.4.1	Restriction Digestion Analysis of pOP13.ssHRP.aP2	247
6.4.2	Secretion of HRP from 3T3-L1 Adipocytes and the Effect of Insulin	247
6.4.3	Ablation of Intracellular (LDM) Membranes using ssHRP	249
6.5	Discussion	262
6.6	Future Work	265
Chapter 7	**Overview**	266
References		270

List of Figures

		Page
Chapter 1	**Introduction**	
1.1	Model of the Potential Sites of Insulin Resistance in Adipose Tissue	63
1.2	Model for the Intracellular Organisation of the Endocytic Pathway in a Mammalian Cell	65
1.3	The Proposed Functional Cycle of Rab Proteins	67
1.4	Sorting Events at the TGN	69
1.5	Models of NSF/α-SNAP Action in SNARE-Mediated Docking and Fusion Reactions	71
1.6	Hypothetical Model for the Structure of the Facilitative Glucose transporters	73
1.7	Membrane Protein Recycling Models	75
1.8	Models for the Biogenesis of the GLUT4 Storage Compartment in Insulin-Sensitive Cells	77
1.9	The Potential Role of SNARE Proteins in GLUT4 Trafficking	79
1.10	Insulin Signalling Pathways	82
Chapter 3	**Compartment Ablation Analysis of the GLUT4 Intracellular Compartments**	
3.1	Subcellular Distribution of GLUT4, γ-adaptin, SCAMPs, the CD-M6PR, Syntaxin 4, CSP and Rab4 in 3T3-L1 Adipocytes and the Effect of Insulin	125

3.2	The Effect of Endosomal Ablation on the Intracellular Levels of GLUT4, TfR, γ-adaptin and CD-M6PR in 3T3-L1 Adipocytes	127
3.3	Sucrose Density Gradient Analysis of γ-adaptin Distribution in the Intracellular (LDM) Membranes of 3T3-L1 Adipocytes Before and After Ablation	129
3.4	Sucrose Density Gradient Analysis of Rab4 Distribution in the Intracellular (LDM) Membranes of Basal and Insulin-Stimulated 3T3-L1 Adipocytes Before and After Ablation	131
3.5	Sucrose Density Gradient Analysis of GLUT4 and SCAMPs Distribution in the Intracellular (LDM) Membranes of 3T3-L1 Adipocytes Before and After Ablation	133
3.6	Co-Localisation of the CD-M6PR and Syntaxin 4 with GLUT4-Containing Vesicles	135
3.7	Co-Localisation of γ-adaptin with GLUT4-Containing Vesicles	137
3.8	Double-Labelled Immunofluorescence Analysis of Basal 3T3-L1 Adipocytes	139
3.9	Immuno-EM of γ-adaptin and GLUT4 in Isolated Vesicles	141
Chapter 4	**Compartment Ablation Analysis of Insulin- and GTPγS-Stimulated GLUT4 Transloaction from Multiple Intracellular Pools**	
4.1	Effect of Endosomal Ablation on Transferrin Receptor Exocytosis	170

4.2A&B	Effect of Endosomal Ablation on Insulin-Stimulated GLUT4 Translocation	172-173
4.3	Effect of Endosomal Ablation on Insulin-Stimulated GLUT1 Translocation	175
4.4	Effect of Endosomal Ablation on GTPγS-Stimulated GLUT4 Translocation	177
4.5	Effect of Endosomal Ablation on GTPγS-Stimulated GLUT1 Translocation	179
4.6	Effect of Wortmannin on Insulin-Stimulated GLUT4 Translocation	181
4.7	Effect of Wortmannin on GTPγS-Stimulated GLUT4 Translocation	183
4.8	Effect of Endosomal Ablation on the Internalisation of Cell-Surface Transferrin Receptors	185
4.9	Effect of Endosomal Ablation on the Recycling of Cell-Surface Transferrin Receptors	187
4.10	Effect of Endosomal Ablation on Adipsin Secretion from 3T3-L1 Adipocytes	189-190
4.11	Effect of Wortmannin on Insulin-Stimulated Adipsin Secretion from 3T3-L1 Adipocytes	192
Chapter 5	**Analysis of the Role of ARF Proteins and Phospholipase D in Insulin-Stimulated GLUT4 Translocation**	
5.1	Subcellular Distribution of GLUT4, ARF1/3 and ARF6 in 3T3-L1 Adipocytes and the Effect of Insulin	214
5.2	Subcellular Distribution of GLUT4, ARF5 and ARF6 in 3T3-L1 Adipocytes and the Effect of Insulin and Wortmannin	216

5.3	Immunoadsorption of GLUT4-Containing Vesicles	218
5.4	Double-Labelled Immunofluorescence Analysis of GLUT4 and ARF5 in Basal and Insulin-Stimulated 3T3-L1 Adipocytes	220
5.5	Effect of Myristoylated ARF Peptides on Insulin-Stimulated GLUT4 Translocation in Permeabilised 3T3-L1 Adipocytes	222
5.6	Effect of Myrisoylated ARF Peptides on Insulin-Stimulated 2-Deoxy-D-Glucose Transport in Permeabilised 3T3-L1 Adipocytes	224
5.7	Subcellular Distribution of GLUT4, PLD1 and PLD2 in 3T3-L1 Adipocytes and the Effect of Insulin	226
5.8	Effect of Butan-1-ol on Insulin-Stimulated GLUT4 Translocation in 3T3-L1 Adipocytes	228
5.9	Effect of Butan-1-ol on Insulin-Stimulated 2-Deoxy-D-Glucose Transport in 3T3-L1 Adipocytes	230
5.10A&B	Effect of Butan-1-ol on Adipsin Secretion in 3T3-L1 Adipocytes	232-233

Chapter 6	**Construction of an ssHRP Chimera for Compartment Ablation Analysis in 3T3-L1 Adipocytes**	
6.1	Structure of ssHRP	250
6.2	Construction of pOP13.ssHRP.aP2	252
6.3	Restriction Digestion Analysis of the pOP13.ssHRP.aP2 Construct	254
6.4	Cell-Associated HRP Activity of SS-2 and SS-3 Adipocytes	256
6.5A&B	Secretion of HRP Activity from SS-2 and SS-3 Adipocytes	258-259
6.6	Ablation of Intracellular (LDM) Membranes using ssHRP	261

List of Tables

		Page
1.1	Localisation and Functional Properties of Rab Proteins in Mammalian Cells	60
1.2	Characterised Mammalian SNAREs Hypothesised to be Involved in Golgi to Plasma Membrane Transport	61
3.1	Analysis of Vesicle Labelling and Co-Localisation of GLUT4 with γ-adaptin and the CD-M6PR	123
5.1	Sequence Alignment of ARF Proteins at the Amino Terminus	212

Abbreviations

ANF	Atrial natriuretic factor
AP-1	Adaptor protein-1
AP-2	Adaptor protein-2
AP-3	Adaptor protein-3
ARF	ADP Ribosylation Factor
ARL	ARF-like
ARNO	ARF nucleotide binding-site opener
ATB-BMPA	(2-N-4-(1-azi-2,2,2-trifluoroethyl)- benzoyl 1,3-bis (D-mannos-4-yloxy)-2-propylamine
SNAP	Soluble NSF attachment protein
ATP	Adenosine 5'-triphosphate
bp	Base pairs
BSA	Bovine Serum Albumin
CD-M6PR	Cation-dependent mannose 6-phosphate receptor
cDNA	Complementary deoxyribonucleic acid
CGN	*cis*-Golgi network
CHO	Chinese Hamster Ovary
CI-M6PR	Cation-independent mannose 6-phosphate receptor
CIP	Calf intestinal phosphatase
COP1	Coatomer 1
cpm	Counts per minute
CSP	Cysteine string proteins
DAB	3,3' Diaminobenzidene
DeGlc	2-Deoxy-D-glucose
DFP	Diisopropyl fluorophosphate
DMEM	Dulbecco's modified Eagle's medium
DMSO	Dimethylsulphoxide

DNA	Deoxyribonucleic acid
DTT	Dithiothreitol
ECL	Enhanced chemiluminescence
EDTA	Diaminoethanetetra-acetic acid, disodium salt
EM	Electron microscopy
EGFR	Epidermal growth factor receptor
ER	Endoplasmic reticulum
E64	L-transepoxysuccinyl-leucylamido-4-guanidiniobutane
FCS	Foetal calf serum
FITC	Fluoroscein isothiocyanate
GDI	GDP dissociation inhibitor
GEF	Guanine nucleotide exchange factor
GLUT	Glucose transporter
GTP	Guanosine 5'-triphosphate
GTPγS	Guanosine 5'-[y-thio] triphosphate
HDM	High density microsome
HEPES	*N* -2-hydroxyethylpiperazne-*N* '-2-ethane sulphonic acid
h	Hours
HRP	Horseradish peroxidase
IBMX	Isobutylmethylxanthine
IC	Intermediate compartment
IgG	Immunoglobulin gamma
IGs	Immature secretory granules
IRS-1	Insulin receptor substrate-1
IRS-2	Insulin receptor substrate-2
KRP	Krebs ringer phosphate
lamp 1	Lysosome-associated membrane glycoprotein 1
LDL	Low density lipoprotein
LDLR	Low density lipoprotein receptor

LDM	Low density microsome
min	Minutes
mA	Milliamps
MGs	Mature secretory granules
NCS	New born calf serum
NIDDM	Non-insulin-dependent diabetes mellitus
NSF	*N*-ethylmaleimide sensitive factor
O.D.	Optical density
PA	Phosphatidic acid
PAGE	Polyacrylamide gel electrophoresis
PBS	Phosphate buffered saline
PDGF	Platelet-derived growth factor
PEG	Polyethylene glycol
PH	Plectstrin homology
PI 3-kinase	Phosphatidylinositide 3-kinase
PIP_2	Phosphatidylinositol 4,5-bisphosphate
PIP_3	Phosphatidylinositol 3,4,5-triphosphate
PLD	Phospholipase D
PM	Plasma membrane
RNase A	Ribonuclease A
s	Seconds
SCAMPs	Secretory carrier-associated membrane proteins
SDS	Sodium dodecyl sulphate
SDS-PAGE	Sodium dodecyl sulphate polyacrylamide gel electrophoresis
SNAP25	Synaptosome-associated 25kDa protein
SNARE	SNAP receptor
SP	Soluble protein
SSV	Synaptic Secretory Vesicle
Staph. a.	*Staphloccocus aureus*

TAE	Tris-acetate EDTA
TBST-1	Tris buffered saline Tween
TCA	Trichloroacetic acid
TEMED	*N, N, N', N'* -tetramethylenediamine
Tf-HRP	HRP-conjugated transferrin
TfR	Transferrin receptor
TGN	*Trans*-Golgi network
TRITC	Tetramethylrhodamineisothiocyanate
Tris	Tris(hydroxymethyl)aminoethane
VAMP	Vesicle-associated membrane protein
UV	Ultra violet
v/v	volume/volume ratio
WT	Wild type
w/v	weight/volume ratio
XTP	Xanthine 5'-triphosphate

Chapter 1

Introduction

1.1 Glucose Transport

1.1.1 Insulin Resistance

Muscle and adipose tissue play a central role in the maintenance of glucose homeostasis as they account for the majority of insulin-mediated glucose disposal in the post-prandial state. In response to insulin, glucose uptake into these peripheral tissues is mediated primarily by the glucose transporter, GLUT4. Exposure to insulin causes a rapid and pronounced increase in cell surface levels of GLUT4 following translocation of the transporter from an intracellular store(s), resulting in a paralleled increase in glucose uptake (reviewed in Rea *et al.*, 1997).

Insulin resistance is defined by a decrease in the ability of insulin to stimulate this peripheral glucose utilisation and is characterised by the development of a chronic hyperglycaemic state in the presence of a normal or elevated plasma insulin concentration. The insulin resistant state is exhibited by patients suffering from a range of conditions including non-insulin dependent diabetes mellitus (NIDDM) (Livingstone *et al.*, 1995), and has several serious complications including kidney failure, blindness, macrovascular disease and an increased risk of atherosclerosis, thus posing a major health problem for the Western world.

At the cellular level, insulin action involves a complex network of molecules. The insulin receptor is a cell surface receptor which contains intrinsic tyrosine kinase activity. Binding of insulin to its receptor elevates the tyrosine kinase activity, which leads to the phosphorylation of insulin receptor substrates such as IRS-1 and IRS-2, cytoplasmic proteins with multiple tyrosine phosphorylation sites. Upon stimulation, these serve as docking sites for SH2 domain-containing molecules such as phosphatidylinositol 3-kinase (PI 3-kinase) or adaptors which link insulin stimulation to other signalling pathways such as Grb2. Ultimately, this leads to the stimulation of glycogen, lipid and protein synthesis, as well as translocation of

GLUT4 to the surface of muscle and fat cells (Kahn, 1995). The abnormality(s) resulting in the decreased ability of insulin to stimulate glucose uptake into muscle and fat, thus leading to the insulin resistant state, may lie anywhere along this pathway.

As the overall levels of GLUT4 are normal in NIDDM patients (Kahn, 1992) a possible cause of the insulin resistant state in these subjects is impaired translocation of GLUT4 to the cell surface (Garvey *et al.*, 1998) (refer to Figure 1.1). Potential defects leading to the impairment of translocation include deficient signalling upstream of the translocation step, abnormalities within the trafficking machinery or indeed mistargeting of GLUT4 within the cell's intracellular compartments. Thus, understanding the expression, regulation and trafficking of GLUT4 will be critical to future progress in the treatment of this disease state. It is therefore this mode of glucose transport which is the focus of this thesis.

1.1.2. GLUT4 - The Insulin-Responsive Transporter

GLUT4 belongs to a family of homologous facilitative glucose transporters which transport glucose down a concentration gradient maintaining whole body glucose homeostasis (reviewed in Bell *et al.*, 1993; Gould *et al.*, 1993). Each transporter exhibits distinct kinetics and is expressed in a tissue specific fashion, with GLUT4 representing the acutely insulin-sensitive transporter of muscle and fat cells.

Although GLUT4 is the predominant transporter in insulin-sensitive tissues, muscle and adipose also express another glucose transporter isoform, namely GLUT1 (James *et al.*, 1993). Each transporter plays a different role in maintaining glucose homeostasis, clearly dictated by their subcellular distribution. Under basal conditions, the relatively even distribution of GLUT1 between the plasma membrane and intracellular compartments denotes this isoform as the 'housekeeping' transporter, maintaining basal glucose transport. In contrast, GLUT4 is almost

excluded from the plasma membrane in the absence of insulin with the majority residing in an intracellular compartment(s) (Slot *et al.*, 1991a; Slot *et al.*, 1991b). Insulin produces a 20- to 30-fold and a 7-fold increase in glucose transport in rat adipose (Holman *et al.*, 1990) and muscle cells (Ploug *et al.*, 1987) respectively, corresponding to a similar increase in GLUT4 levels at the plasma membrane. GLUT1 cell surface levels are also increased by insulin (~5-fold in fat cells) but to a significantly lesser extent than GLUT4 (Calderhead *et al.*, 1990), thus distinguishing the latter as the insulin-regulatable glucose transporter, mediating the vast majority of insulin-stimulated post-prandial glucose uptake.

A major part of understanding the mechanism by which insulin regulates hexose metabolism involves characterising both the GLUT4 intracellular compartment(s) and the pathways of subcellular trafficking of this glucose transport protein. In order to do this, a full understanding of the individual membrane compartments and the movement of proteins between these compartments is required. This introduction therefore includes a summary of subcellular trafficking, and reviews how some of these general mechanisms are thought to relate to GLUT4 intracellular sequestration and trafficking.

1.2 Subcellular Trafficking - a General Background

Compartmentalisation within eukaryotic cells has led to the requirement of vesicle mediated transport between morphologically distinct organelles. There are two main trafficking systems within cells, namely the endocytic and secretory pathways, both of which require special mechanisms to ensure the selective movement of proteins and lipids from the donor to the acceptor organelle (refer to Figure 1.2). The transport process, in principle, requires the packaging of cargo into a vesicle carrier and the transport, docking and fusion of the vesicle intermediate with the appropriate target membrane. Each of these processes in the endocytic and secretory systems, although distinct, show similarities in terms of the array of proteins, lipids and

enzyme complexes (coats, SNAREs [soluble NSF-attachment protein receptors], GTPases, ATPases, kinases and phosphoinositides etc.) involved, each of which will be discussed in this chapter.

1.3 The Endocytic System - Receptor-Mediated Endocytosis

Endocytosis of molecules into cells is involved in many processes including: nutrient capture, signal transduction, antigen presentation and neurotransmitter uptake (reviewed in Knutson *et al.*, 1996). As many of the molecules required for the aforementioned processes are too large to pass through plasma membrane pores and water-filled channels by diffusion, receptor mediated endocytosis has developed to enable their passage into the cell cytoplasm (Knutson *et al.*, 1996). The extracellular macromolecules bind to specific, high affinity receptors, thereby allowing concentration of the ligands at the plasma membrane before internalisation via clathrin-coated pits into membrane bound vesicles, endosomes. The ligands are then sorted in and transported through a series of distinct endosomal compartments before ultimate delivery to the lysosomes (Knutson *et al.*, 1996) (refer to Figure 1.2).

A well defined example of receptor-mediated endocytosis is the uptake of iron by the transferrin receptor (TfR) (Knutson *et al.*, 1996). Briefly, iron-loaded transferrin binds to the TfR on the plasma membrane. Following endocytosis, the endosome acidifies to a pH of ~ 5.1. Although this pH favours the release of iron, the apotransferrin remains associated with the receptor and is subsequently recycled back to the cell surface (Yamashiro *et al.*, 1984). The endocytic process of the TfR is very rapid, with a single cycle being complete in 3-4 min (Iacopetta *et al.*, 1983). Other examples of receptor-mediated endocytosis, although generally following the same process, exhibit distinct differences. For example, following the uptake of low density lipoprotein (LDL) by the low density lipoprotein receptor (LDLR), the receptor recycles back to the plasma membrane whereas the LDL is transported to the lysosomes to be degraded. The mannose-6-phosphate receptors (cation-

independent [CI-] and cation-dependent [CD-] M6PRs) 'scavenge' ligands with terminal mannose or fucose residues and degradation begins within the endosomal compartment (Knutson *et al.*, 1996).

Alternatively, the endocytic system may be used as a sorting mechanism. Following the biosynthesis of synaptic vesicle proteins in the endoplasmic reticulum (ER) they are transported via the Golgi to the plasma membrane, before being constitutively endocytosed and sorted into synaptic vesicles (Knutson *et al.*, 1996).

1.3.1 Clathrin-Coated Pit Formation

Following binding of cargo molecules to the extracellular domain of a transmembrane receptor at the plasma membrane, concentration of receptors occurs via interaction with a clathrin coat, required for vesiculation of the membrane. Clathrin provides a framework for other proteins which carry out receptor sorting and membrane budding. Clathrin-coated pits/vesicles are composed of clathrin, a trimeric scaffold protein which organises itself into cage-like lattices (reviewed in Kirchhausen *et al.*, 1997). Clathrin has the shape of a triskelion, each of the three legs having a heavy and light chain.

Clathrin-coat formation is driven by clathrin adaptors, heterotetramers that couple pit assembly to the entrapment of membrane receptors (reviewed in Lewin *et al.*, 1998). Endocytic coated pits contain the AP-2 complex, while coated buds and vesicles derived from the trans-Golgi network (TGN) contain the related AP-1 complex (Pearse *et al.*, 1990). AP-2 comprises two large chains (referred to as adaptins), one α chain and one $\beta1/\beta2$ chain, a medium chain ($\mu2$) and a small chain ($\sigma2$). AP-1 contains the adaptins γ and $\beta1$ together with $\mu2$ and a small $\sigma1$chain (reviewed in (Robinson, 1992; Robinson, 1994). A third adaptor-like complex, recently identified AP-3, contains δ and $\beta3$ chains together with the smaller $\mu3$ and $\sigma3$ chains (Simpson *et al.*, 1997; Dell'Angelica *et al.*, 1997). Although this complex is

also involved in sorting events at the TGN (refer to Section 1.4.3) it is not thought to interact with clathrin.

Initially, AP-2 is recruited from the cytosol to the plasma membrane allowing clathrin to bind and form the coated pit. Components of the pit then interact with the cytosolic tails of the transmembrane receptors, which have specific signals to direct rapid internalisation and other intracellular targeting steps (Kirchhausen *et al.*, 1997). The signal sequences usually have a critical tyrosine residue or a pair of dileucine or bulky hydrophobic residues (known as tyrosine/dileucine based signals) (reviewed in Marks *et al.*, 1997). Tyrosine based signals bind directly to the AP-2 complex, mediating the concentration of certain plasma membrane proteins within clathrin-coated pits. Examples include: the LDLR, the TfR and the epidermal growth factor receptor (EGFR), all of which have tyrosine internalisation motifs and are efficiently concentrated into clathrin-coated pits (Robinson *et al.*, 1996). However, proteins with these motifs are also found in other compartments suggesting that there may be a specific AP-2 receptor on the plasma membrane (and AP-1/AP-3 receptors on the TGN), yet to be identified (Kirchhausen *et al.*, 1997; Lewin *et al.*, 1998).

Another important component of the clathrin-coated vesicle machinery is dynamin. This large GTPase is thought to be involved in severing the neck of the coated pit to produce a coated vesicle (reviewed in Kelly, 1995). Concurrent studies by Hinshaw and Schmid, and Takei *et al* have shown that GTP binding regulates the spontaneous self assembly of dynamin into rings and stacks of interconnected rings (helical arrays) around the neck of the invaginated coated pit. Following GTP hydrolysis, the configuration of the helix changes, squeezing the neck further until molecular fission occurs in a sort of 'molecular garotting' (Hinshaw *et al.*, 1995; Takei *et al.*, 1995).

1.3.2 Non-Clathrin-Mediated Endocytosis

Although clathrin-mediated endocytosis is the most well characterised mechanism for gaining entry into the cell, non-clathrin-mediated pathways also exist. Three other morphologically distinct pathways which have been characterised include: macropinosomes (substantially contribute to constitutive bulk pinocytosis), non-coated vesicles and caveolae (small lipid-enriched microdomains of the plasma membrane) (reviewed in Lamaze *et al.*, 1995). Each of these pathways, including clathrin-mediated endocytosis, may be defined by vesicle size which is tightly regulated in each case. Caveolae are 50-80nm in diameter, clathrin-coated vesicles are 100-150nm in diameter, non-coated vesicles are in between, and macropinosomes are 0.5-2mm in diameter (Lamaze *et al.*, 1995; Robinson *et al.*, 1996). Although morphologically characterised, the purpose of these alternative pathways is still not clear. However, the inducible overexpression of a temperature sensitive dynamin mutant that displays a rapid and reversible block in clathrin-mediated endocytosis, has shown that after a shift to the non-permissive temperature, horseradish peroxidase (HRP) fluid-phase uptake was only partially inhibited, and recovered to wild-type levels within 30 min (Damke *et al.*, 1995). Based on this and similar studies, the prevailing view is that clathrin-mediated and non-clathrin-mediated endocytosis occur in parallel and the non-clathrin-mediated pathway may be up-regulated when the clathrin-mediated pathway is switched off (Robinson *et al.*, 1996). However, alternate fluid-phase and receptor-mediated endocytic pathways may be required to serve other purposes. As well as controlling the size of the plasma membrane, distinct endocytic vesicles provide an opportunity for targeting to distinct organelles and such pathways could also be differentially regulated (Lamaze *et al.*, 1995).

1.3.3 Endosomal Compartments

Following internalisation from the cell surface, membrane proteins (receptors) enter early sorting endosomes. This compartment consists of vacuoles, cisternae and tubules spread throughout the cytoplasm. From here, some receptors including the TfR, may pass through a highly tubulated recycling compartment, located in the peri-Golgi region, *en route* to the plasma membrane (Robinson *et al.*, 1996). From the early endosomes internalised molecules may proceed along the endocytic pathway to late endosomes and finally lysosomes (refer to Figure 1.2).

Although trafficking through the endocytic system is complex, many factors required to regulate transport along this pathway appear to be used at multiple stages and are also found in the secretory system. In particular, two classes of proteins namely SNAREs (soluble NSF-attachment protein [SNAP] receptors) (Hay *et al.*, 1997) and Rab proteins (Novick *et al.*, 1997) have emerged as specific and essential vesicle transport components in both endocytic and exocytic processes. SNAREs comprise integral membrane proteins, serving as receptors for soluble factors required for docking and fusion (refer to Section 1.5). Rab proteins are small GTPases which were initially implicated as regulators of SNARE pairing during vesicle docking (see below). However, these small GTPases may indeed play a more significant role as master regulators of membrane traffic as discussed below.

1.3.4 Rab Proteins in Vesicle Transport

Rab proteins constitute the largest family of small GTPases with almost 40 mammalian proteins being identified, correlating with the diversity of vesicle transport routes in mammalian cells (reviewed in Novick *et al.*, 1993; Novick *et al.*, 1997). To date many of the Rab proteins identified exhibit compartmentilisation, regulating specific transport events. For example, transport from the plasma membrane to the early endosomes is controlled by Rab5 whereas Rab4 has been

implicated in trafficking from the early endosomes to the plasma membrane (i.e. the recycling pathway) (Novick *et al.*, 1997). The prevailing view is that a different Rab protein may be required for each step of vesicular transport (refer to Table 1.1).

Briefly, the Rab protein is thought to associate with the transport vesicle budding from the donor membrane, moves to the acceptor membrane where docking and fusion take place and finally recycles back to the donor membrane via a cytosolic intermediate, Rab GDP-dissociation inhibitor (GDI). The GDI binds the Rab protein in the GDP-bound inactive conformation, thereby regulating membrane binding. In turn, GDI is displaced by a GDI-displacement factor, allowing Rab-GDP to bind the membrane. Following GDP/GTP exchange the Rab protein is resistant to removal by Rab GDI. As guanine nucleotide exchange factors (GEFs), effector molecules and GTPase activating proteins (GAPs) determine which nucleotide is bound to the Rab protein, these factors therefore regulate GDI accessiblity, thus keeping the proteins in a dynamic equilibrium between the cytosol and membranes (Novick *et al.*, 1997) (refer to Figure 1.3).

Although it is well established that Rab proteins are required for membrane docking and fusion events, the precise function of the proteins is still unclear. Studies using dynamin GTPase deficient mutants clearly indicate the requirement for GTP hydrolysis in the 'pinching' off of the invaginated vesicle (refer to Section 1.3.1). However, such studies are not as convincing with respect to the Rab proteins as Rab function may be inhibited or stimulated depending on the Rab protein studied. For example, in the case of Rab3a the GTPase deficient mutant inhibits exocytosis in neuroendocrine cells (Sudhof, 1995) whereas the Rab5 GTPase-deficient mutant stimulates endosome fusion (Stenmark *et al.*, 1994). This suggests that GTP-hydroysis, although possibly mediating membrane association, may not be directly coupled to membrane fusion. Initial studies using mutant Rab proteins with altered nucleotide specifity that bind xanthine 5'-triphosphate (XTP) support this view (Rybin *et al.*, 1996). With respect to Rab5, hydrolysis of [^{32}P] XTP occurred

constitutively suggesting that hydrolysis serves as a timer to switch off the protein and prevent prolonged activation (Rybin *et al.*, 1996). However, further studies are required to determine whether such a mechanism is applicable to other Rab proteins.

The recent discovery of Rab effector proteins, which function downstream of the Rab proteins, also suggests that like other GTPases of the Ras superfamily, Rab proteins may act as regulatable membrane anchors. Much in the same way that Ras serves as a membrane anchor for Raf kinase in signal transduction, and ARF recruits proteins in vesicle budding (refer to Sections 1.4.2 and 1.6), Rab5 recruits rabaptin 5, a cytosolic protein onto early endosomes in a GTP-dependent manner (Stenmark *et al.*, 1995). The over-expression of Rabaptin 5 alone, induces the expansion of early endosomes, indicating that this protein behaves as a direct Rab effector in the endocytic pathway (Robinson *et al.*, 1996). Although little is known about the biochemical activities of the effectors they may serve as down-stream intermediaries of a pathway leading to SNARE-complex formation. However, it is more plausible that Rab proteins, along with the appropriate effector, control several activities in parallel including motors needed for vesicle movement, vesicle-binding proteins needed for vesicle docking and, ultimately, the formation of SNARE complexes (Novick *et al.*, 1997).

1.4 The Secretory System

The secretory pathway of eukaryotes, like the endocytic system, comprises several morphologically distinct compartments [endoplasmic reticulum (ER), intermediate compartment (IC) and the Golgi complex] through which newly synthesised proteins and lipids move *en route* to the cell surface (reviewed in Lippincott-Schwartz, 1996). Briefly, the ER serves as port of entry while the Golgi complex serves as a site where membranes and proteins from the ER converge and are processed or sorted before transport to different destinations. Membranes of the secretory pathway are extremely dynamic exhibiting both anterograde and retrograde transport pathways

(Lippincott-Schwartz, 1996). However, anterograde vesicle mediated transport to the cell surface shall be the focus of this section, in particular trafficking from the *trans*-Golgi network (TGN) to the cell surface and/or the endosomes.

1.4.1 The *trans*-Golgi Network (TGN)

The Golgi complex plays a central role in processing and sorting proteins in the secretory pathway. It is a polarised structure of cisternal stacks with two distinct faces. The *cis*-Golgi network (CGN) is the site of entry from the ER, while the TGN forms the opposite face of the Golgi stack. As the last compartment of the Golgi complex, the TGN plays a pivitol role in directing proteins via the secretory pathway to the appropriate cellular destination (reviewed in Traub *et al.*, 1997). Several secretory pathways emerge from the TGN including a constitutive pathway which delivers proteins directly to the cell surface and a selective pathway which sorts protein traffic into the endosomal membrane system (Traub *et al.*, 1997) (refer to Figure 1.4). It is this selective endosomal route that allows communication between the secretory and endocytic pathways. In cells which undergo regulated exocytosis, the selective endosomal route may be modified allowing the formation and accumulation of mature secretory granules, ready for exocytic release (refer to Figure 1.4).

1.4.2 Vesicle Budding at the TGN

In terms of the molecular machinery required for vesicularisation and transport in the secretory system, most advances have come about through the study of yeast, with many of the homologous proteins also being isolated from mammalian cells, indicating a conservation across species. However, these studies have concentrated on ER to Golgi and intra-Golgi transport. Briefly, intra-Golgi transport requires coatomer (COPI), a large cytosolic protein complex, for vesicle formation and budding (reviewed in (Cosson *et al.*, 1997)). This vesicle coat is formed by the

polymerisation of COPI, (composed of seven subunits: α-, β-, β'-, g-, δ-, ε- and ζ-COP). As the coatomer coat can also specifically concentrate membrane proteins by interacting with their sorting motifs in their cytoplasmic domains, they appear to be functionally very similar to the previously described clathrin coat. Interestingly, one of the components of COPI, β-COP, is weakly homologous to β-adaptin, a component of the clathrin coat. COPII coat proteins, notably not homologous to COPI, mediate vesicle budding and transport in the ER (reviewed in Kuehn *et al.*, 1997).

The molecular events governing sorting, vesicle budding and transport from the TGN are rather ill defined compared to ER trafficking. However, studies with Brefeldin A (BFA), a fungal antibiotic, have cast some light on this issue. Treatment of cells with BFA reversibly arrests protein transport from the TGN (Miller *et al.*, 1992). As BFA is also known to inhibit a nucleotide exchange factor for ADP-ribosylation factor (ARF, a small GTPase) (Peyroche *et al.*, 1996), it is thought that ARF-GTP may regulate multiple TGN export sites. Consistent with this idea, the coatomer complexes previously described, cycle between a cytosol and membrane association, a process also shown to be mediated by ARF (Cosson *et al.*, 1997). The transport of proteins from the TGN to the endosomes may also be mediated by clathrin. As for clathrin-mediated endocytosis, budding requires the recruitment of cytosolic adaptors (AP-1) and clathrin onto the Golgi membrane (Pearse *et al.*, 1990). Again, ARF (in this case the ARF1 isoform) is implicated as the regulator of coat assembly, mediating the association of AP-1 with the membrane (Stamnes *et al.*, 1993), accounting for the sensitivity of this process to BFA. Regulation by this small GTPase may explain why clathrin-coated vesicles only assemble on particular intracellular membranes, even though other membranes contain suitable cargo. If the BFA-sensitive nucleotide exchange factor for ARF is localised to specific membranes, AP-1 recruitment and therefore coat assembly are limited (Traub *et al.*, 1993; Stamnes *et al.*, 1993; Seaman *et al.*, 1996b; Traub *et al.*, 1997).

1.4.3 Sorting at the TGN

The selective incorporation of cargo into budding vesicles at the TGN is an active process with cytosol-orientated sorting signals directing transmembrane proteins to the appropriate export site. These signals consist of short, linear stretches of amino acids within the cytosolic domain of a protein, and most fall into groups of consensus sequences or motifs. The most extensively studied motifs centre on either a critical tyrosine residue (Y) within the amino acid sequences NPXY or YXXØ (where X is any amino acid and Ø is an amino acid with a bulky hydrophobic group) (reviewed in Marks *et al.*, 1997) or a doublet of leucine residues (LL) referred to as a di-leucine motif (see Pond *et al.*, 1995 and references there in).

Tyrosine-based sorting signals conforming to the YXXØ motif have been implicated in directing protein localisation to various intracellular compartments including endosomes, lysosomes and to the basolateral surface of polarised epithelial cells (Marks *et al.*, 1996). Furthermore, most of the YXXØ-type signals are capable of mediating rapid internalisation from the plasma membrane into endosomes regardless of the ultimate compartment to which the proteins are eventually targeted (reviewed in Mellman., 1996). A subset of of YXXØ-type signals are also able to mediate other intracellular sorting events (reviewed in Gruenberg and Maxfield,. 1995) suggesting that such signals can be recognised differentially at more than one site in the cell. Thus, at the plasma membrane YXXØ-type signals may confer a rather broad specificity, whereas at some intracellular sites they may have a more restricted specificity.

The basis of such specificity, may in part depend on interactions between the tyrosine-based signals and a component of an organellar protein coat (Figure 1.4). In this regard, several laboratories have shown that the AP-1 and AP-2 heterotetrameric adaptor complexes that mediate association of clathrin with the TGN and plasma membrane, respectively (refer to Section 1.3.1), recognise tyrosine-based signals

conforming to the YXXØ motif (Ohno *et al.*, 1996; Nesterov *et al.*, 1995; Heilker *et al.*, 1996; Honing *et al.*, 1996). Interaction with AP-2 is likely to mediate rapid internalisation from the plasma membrane (Pearse., 1988), whereas interaction with AP-1 at the TGN is involved in endosomal and/or lysosomal targeting (Honing *et al.*, 1996). Specificity at both of these sites (plasma membrane and TGN), is thought to be maintained by the selectivity of the homologous μ chains of the adaptor complexes, on binding to the tyrosine signals. For example, in a yeast two-hybrid assay, the YXXØ motif from the endocytic TfR binds to μ2 (medium subunit of the AP-2 complex, see Section 1.3.1) but not detectably to μ1 (AP-1 complex), whereas the lysosomal membrane protein, LAMP 1 (lysosomal associated membrane protein 1), binds to both μ2 and μ1 (Ohno *et al.*, 1996; Ohno *et al.*, 1995). *In vitro* binding studies have also shown that some signals display higher avidity for AP-2 (Boll *et al.*, 1995), while others interact equally well with AP-1 and AP-2 (Heilker *et al.*, 1996; Honing *et al.*, 1996). Although care must be taken when extrapolating results from these types of assays to *in vivo* models, on the basis of these data it has been proposed that differential recognition of tyrosine-based signals by the AP-1 and AP-2 complexes may determine, at least in part, the targeting specificity of the signals (Marks *et al.*, 1997).

Signals conforming to a di-leucine motif can also mediate internalisation, and targeting to lysosomes, endosomal membranes and the basolateral surface of polarised epithelial cells (reviewed in Melman., 1996; Matter and Mellman., 1994). Although di-leucine- and tyrosine-based signals mediate localisation to similar end compartments, they do so through the interaction with different components of the sorting machinery (Marks *et al.*, 1996). In this regard, the μ2 and μ1 subunits of the AP-2 and AP-1 adaptor complexes respectively, do not appear to recognise di-leucine based signals (Ohno *et al.*, 1995). However, a very recent *in vitro* study has indicated that interaction of di-leucine motifs with AP-1 may be via the β1 subunit of the heterotetrameric adaptor complex (Rapoport *et al.*, 1998), suggesting that distinct regions of the adaptor complex may be responsible for recognition of tyrosine- and

di-leucine based signals. However, further studies are required to firmly establish a role for the β subunit of the adaptor complex in di-leucine-based signal recognition.

Additional features may also contribute to the recognition of a given sorting signal by specific sorting machinery. For example, binding of adaptor complexes to tyrosine-based signals may be influenced not only by the exact sequence of the signal but also by the nature of the amino acids in or surrounding the signal and the spacing of the signal from the membrane. Such an example has been provided by studies performed on LAMP 1 trafficking (Rohrer *et al.*, 1996). The insertion or the deletion of a single amino acid modifying the spacing of its GYXXI sorting motif almost completely blocks its lysosomal targeting but does not drastically affect its endocytosis. In the yeast two hybrid system, tyrosine-based sorting signals appear to be more efficiently recognised by the AP-1 and AP-2 μ chains when they are placed at the C-terminus of the polypeptide sequence and when it is appropriately distanced from the fusion partner domain (Ohno *et al.*, 1996). These results may predict enhanced adaptor binding *in vivo* to signals that are exposed to the C-terminus or appropriately distanced from the membrane, as is the case for several lysosomal membrane proteins such as LAMP 1 (Rohrer *et al.*, 1996).

Post-translational modifications of cytoplasmic domains may also regulate the accessibilty of sorting determinants. For example, the cation-dependent-mannose 6-phosphate receptor (CD-M6PR), a transmembrane protein required for lysosomal enzyme transport, has a casein-kinase II consensus phosphorylation site within an acidic cluster adjacent to the di-leucine motif at its C-terminus. The expression of CD-M6PRs mutated on this phophorylation site are unable to produce AP-1 coated vesicles when expressed in M6PR-negative fibroblasts (see below), suggesting that the phosphorylation of the caesin-kinase II consensus site may induce comformational changes and modulate the accessibilty of sorting determinants (Mauxion *et al.*, 1996). Palmitoylation is another example of post-translational modification. The CD-M6PR is transiently and reversibly palmitoylated on two

cysteine residues at positions 30 and 34 of its cytoplasmic domain (Schweizer *et al.*, 1996). The mutation of Cys-34 results in the accumulation of the mutant receptors in the lysosomes and a loss of its sorting function at the Golgi (Schweizer, *et al.*, 1996). These observations indicate that the anchoring of this region of the CD-M6PR tail in the lipid bilayer is essential for the normal trafficking of the receptor and further suggest that palmitoylation may confer a given conformation to the cytoplasmic tail necessary for the recognition of the tyrosine- and di-leucine-based sorting determinants. Finally, interactions with other proteins such as ARF1, the small GTP-binding protein thought to be involved in the association of AP-1 with the TGN (refer to Section 1.4.2) may also influence the interactions between sorting signals and the adaptor complexes (Traub *et al.*, 1993;Traub *et al.*, 1997), although this has not been formly demonstrated.

Several studies indicate that transmembrane proteins play some role in coat assembly. In the TGN, the two distinct but related M6PRs (cation-dependent and cation-independent M6PRs) involved in lysosomal enzyme targeting (reviewed in Ludwig *et al.*, 1995), appear to be key components required for AP-1 coat assembly (Figure 1.4). As for many transmembrane proteins, the M6PRs contain multiple sorting determinants in their cytoplasmic domains including tyrosine- and di-leucine-based motifs (reviewed in Sandoval and Bakke., 1994). Several studies have illustrated the importance of the carboxyl terminal di-leucine motif in efficient intracellular targeting of the M6PRs (Lobel *et al.*, 1989, Johnson and Kornfield., 1992). However, recent studies indicate that it is the acidic cluster motif containing the casein kinase II phosphorylation site which is critical for the interaction of AP-1 with its target membranes and the adjacent di-leucine motif appears to be more important for a post AP-1 step in the CD-M6PR cycling pathway (Mauxion *et al.*, 1996). Support for the role of the M6PRs in AP-1-coat assembly at the TGN comes from biochemical studies performed on mouse MPR-negative fibroblasts re-expressing physiological levels of either M6PR. Subcellular fractionation of these cells has revealed that M6PR-negative cells contain ~ 70% less AP-1 bound to the

TGN membranes than M6PR-positive cells or M6PR-negative cells re-expressing physiological levels of either M6PR (Le Borgne *et al.*, 1996). Furthermore, experiments carried out on the same cells has shown that the concentration of M6PRs determines the number of clathrin-coated vesicles formed in the TGN (Le Borgne *et al.*, 1997). Taken together, these observations strongly suggest that transmembrane protein sorting and AP-1 coat assembly are indeed coupled processes.

Some membrane proteins, although utilising the AP-1 sorting machinery at the TGN, contain sorting motifs that do not bind adaptors directly. For example, the endoprotease furin has an acidic cluster containing a pair of casein kinase II phosphorylation serines and a tyrosine motif in its cytosolic domain (Molloy *et al.*, 1994; Schafer *et al.*, 1995). Recent studies have shown that the phosphorylation of the furin acidic cluster is required for the the TGN localisation of the endoprotease and enhances its association with AP-1 (Ditte *et al.*, 1997), suggesting that TGN localisation of furin, like the M6PRs is mediated by an AP-1 sorting step. However, direct binding of AP-1 to the furin TGN localisation signal has not been demonstrated. Indeed, recent studies have shown that the acidic cluster sorting motif of furin requires a cytosolic connector protein, namely PACS-1 (phosphofurin acidic cluster sorting protein 1), to connect it to the clathrin sorting machinery (Wan *et al.*, 1998). PACS-1 is a partially membrane-associated cytosolic protein that binds phosphorylated furin, resulting in the localisation of the endoprotease to the TGN. *In vitro* binding assays and *in vivo* coprecipitation studies show that PACS-1 localises furin to TGN by connecting it to the AP-1 sorting machinery (Wan *et al.*, 1998). However, further studies involving furin mutants demonstrated that the cytosolic domain tyrosine motif but not the acidic cluster containing the phosphorylatable casein kinase II serine residues was required for budding at the TGN (Wan *et al.*, 1998). Together, these studies argue that PACS-1 localises furin to the TGN by a phosphorylation-dependent retrieval mechanism. This phosphorylated acidic cluster-dependent retrieval step is consistent with the AP-1-

associated removal of phosphorylated furin from clathrin-coated immature secretory granules (Ditte *et al.*, 1997).

Interestingly, in the same study Wan *et al* also showed a requirement for PACS- for the correct localisation of the CI-M6PR, suggesting that PACS-1 may direct the routing of a potentially large number of membrane proteins containing acidic cluster motifs within their cytosolic domains. This may also explain why Mauxion *et al* (see above; Mauxion *et al.*, 1996) found the casein kinase II consensus site to be important for AP-1 binding at the TGN and not the di-leucine-based motif, as the latter may be involved in budding whereas the casein kinase II consensus motif may be involved in retrieval and therefore localisation to the TGN.

Several other transmembrane proteins such as the lysosomal-associated membrane proteins (LAMP I, LAMP II), or the lysosomal integral membrane proteins (LIMP I, LIMP II) are also sorted in the TGN and follow an intracellular route to the endosomes/lysosomes (reviewed in Sandoval and Bakke., 1994; Mellman., 1996). Their lysosomal targeting depends on either a critical tyrosine-based (LAMP I, LAMP II, LIMP I) or di-leucine-based sorting determinants present in their 10-20-amino acid long cytoplasmic domains (Harter and Mellman., 1992; Guarnieri *et al.*, 1993; Honing *et al.*, 1996; Ogata and Fukuda., 1994). The presence of LAMP I in AP-1-coated structures suggests that their exit form the TGN, like that of the M6PRs may depend on such a pathway (Honing *et al.*, 1996). However, following the identification of the adaptor-like complex AP-3 (refer to Section 1.3.1), recent studies suggest that this heterotetrameric complex also functions in the intracellular targeting of transmembrane glycoproteins to lysosomes, consistent with the presence of this protein complex on buds/vesicles associated with the TGN (Simpson *et al.*, 1996).

A role for the AP-3 complex in recognition and sorting of lysosomal proteins is supported by recent *in vivo* studies which demonstrate that the overexpression of

LAMP I and LIMP II, promotes AP-3 recruitment onto perinuclear membranes (Le Borgne *et al.*, 1998). Furthermore, the expression of chimeric proteins mutated on the tyrosine residue of LAMP I and on the di-leucine based signal of LIMP II, failed to promote AP-3 recruitment onto membranes both *in vivo* and *in vitro,* suggesting that AP-3 may recognise the tyrosine- and di-leucine-based sorting signals of the transmembrane proteins (Le Borgne *et al.*, 1998). In the same study, inhibition of the synthesis of the μ3, the subunit intercating with tyrosine-based signals in the yeast two-hybrid system (Dell'Angelica *et al.*, 1997), by antisense oligonucleotides, resulted in the selective mis-routing of LAMP I and LIMP II to the plasma membrane (Le Borgne *et al.*, 1998). These data strongly indicate that AP-3 is essential for the proper intracellular targeting of LAMP I amd LIMP II to the lysosomes.

There is also accumulating evidence to suggest that AP-3 is involved in sorting cargo proteins to storage/secretory granules or lysosome-related organelles such as the melanosomes (reviewed in Odorizzi *et al.*, 1998). In this regard, a tailless mutant of tyrosinase, a membrane protein of melanosomes which contains a di-leucine motif, is delivered to the plasma membrane instead of melanosomes (Viyayasadhi *et al.*, 1995) Recent *in vitro* studies have also shown the cytoplasmic tail of tyrosinase to interact with AP-3 (Honing *et al.*, 1998). Synaptic vesicle recycling is also thought to involve protein sorting by AP-3 from the TGN to secretory granules in PC12 cells (Faundez *et al.*, 1998). Together, the above data suggest that the AP-3 complex is involved in sorting cargo proteins to both lysosome and lysosome-related storage/secretory granules, possibly through a common intermediate (Figure 1.4).

The existence of multiple coat complexes and their differential ability to bind to sorting determinants provide a framework for a hypothetical model in which the coat complexes act like filters for transmembrane proteins with one or more sorting signals on their cytoplasmic tails (see Marks *et al.*, 1997). In this model the TGN is the initial sorting sorting station for newly synthesised membrane proteins.

Transmembrane proteins with AP-1 or AP-3 directed di-leucine or tyrosine signals will be caputured by the appropriate coat complex (AP-1 or AP-3) and sorted to an endosomal/lysosomal or lysosomal-related storage compartment. Other transmembrane proteins will pass onto the plasma membrane. Those with AP-2 directed signals will be re-internalised. It should be noted that none of these steps are absolute with efficiencies depending on relative affinities for various signals.

1.5 Membrane Targeting and Fusion

Once transport intermediates have been formed in both the endocytic and secretory systems, they are targeted to the appropriate acceptor membrane where fusion occurs. The Rab family of proteins (refer to Section 1.3.4) are thought to play a major role in the regulation of this process, with additional components for the actual fusion process functioning further downstream.

Based on a linkage between ER and Golgi transport, and synaptic vesicle fusion in neurons, a model of vesicular fusion termed the SNARE (SNAP receptor) hypothesis was proposed (reviewed in (Rothman, 1994; Sudhof, 1995; Bennett, 1995; Hay *et al.*, 1997)). The model postulates that the specificity of vesicle targeting is generated by complexes which form between membrane proteins on the transport vesicle (v-SNAREs) and membrane proteins on the target membrane (t-SNAREs) (refer to Table 1.2). In the case of regulated exocytosis in neurons, the v- and t-SNAREs are VAMP2 (vesicle-associated membrane protein/synaptobrevin) and syntaxin 1A/SNAP-25 (synaptosome-associated protein, 25kDa), respectively (Rothman, 1994; Sudhof, 1995). Since the proposal of this model, studies have shown that the originally identified VAMP, SNAP-25 and syntaxin appear to represent protein families with homologues throughout the secretory pathway (Hay *et al.*, 1997). Originally, it was proposed that the assembly of the core complex in which the v- and t- SNAREs bound together exhibiting a 1:1:1 stoichometry, provided a receptor for α-SNAP (soluble NSF attachment protein, not related to SNAP-25). In turn this

created a receptor site for NSF (N-ethylmaleimide-sensitive factor), an ATPase which was thought to catalyse the fusion reaction by either disrupting the SNARE complex or conformationally destabilising it (Sudhof, 1995). However, recent studies have resulted in the migration of the proposed role of NSF from the last to an increasingly early step in the membrane fusion process. Convincing evidence for this altered role of NSF has been provided by a study of homotypic fusion in yeast carried out by Mayer *et al* (Mayer *et al.*, 1996). In this system, they have shown that both NSF and α-SNAP co-operate to activate v- and t-SNAREs independently into a docking competent state, implying that the major function of NSF occurs before vesicle docking (Mayer *et al.*, 1996) (refer to Figure 1.5).

The fundamental requirement for SNARE proteins in vesicular transport is illustrated by the treatment of neurons with botulinum and tetanus toxins resulting in the irreversible inhibition of synaptic vesicle exocytosis by specific proteolysis of VAMP2, syntaxin 1A and SNAP-25 (Sudhof, 1995). However, although these SNARE proteins have been characterised as the key components in vesicle fusion, additional molecules have been identified which act to either positively or negatively regulate the assembly of the SNARE complex. Under steady state conditions in the neuron, VAMP2 is bound to synaptophysin (a v-SNARE binding protein) (Johnston *et al.*, 1990) and at least some of syntaxin 1A is bound to Munc 18a (a syntaxin binding protein) over the entire plasma membrane (Hata *et al.*, 1993). Binding of Munc 18a to syntaxin 1A inhibits its interaction with SNAP-25, and VAMP2 is unable to bind to the SNAP-25/syntaxin complex when bound to synaptophysin (Sudhof, 1995). Thus, these proteins prevent the spontaneous assembly of the SNARE complex (Sudhof, 1995). The identification of many of these proteins in non-neuronal cells (refer to Section 1.13) has allowed the SNARE hypothesis to serve as a model for the docking, targeting and fusion of vesicles in many different trafficking pathways.

1.6 The Role of Phosphoinositides in Membrane Trafficking

As the generation, transport and fusion of vesicles clearly involves significant alterations in the membrane structure it is reasonable to assume that the transformation of lipid components either accompany or help to induce this processes. Indeed in mammalian cells, signal transduction pathways involving lipid second messengers not only stimulate regulated secretion but also affect the activity of constitutive transport pathways (reviewed in Roth *et al.*, 1997).

Studies in both yeast and mammalian cells suggest a role for phophatidylinositol 3-kinase (PI 3-kinase) in constitutive vesicle trafficking (reviewed in Shepherd *et al.*, 1996b). In *S. cerevisiae* the PI 3-kinase Vps34p is complexed to another protein Vps15p, and is required for the sorting of vacuolar proteins from the Golgi (Stack *et al.*, 1995). Recently, the mammalian homologues for both of these proteins have been identified, suggesting that yeast and mammalian cells share a common mechanism of regulation from the Golgi to endosomes (Volinia *et al.*, 1995). Furthermore, treatment of mammalian cells with wortmannin, an irreversible inhibitor of PI 3-kinase, has had adverse effects on TfR recycling, indicating that PI 3-kinase is involved in multiple sorting events in the receptor's membrane trafficking pathway (Spiro *et al.*, 1996; Martys *et al.*, 1996; Shpetner *et al.*, 1996).

Although clearly implicated in trafficking, the functional role of phosphoinositides remains to be determined. One possibility is the regulation of ARF proteins, monomeric GTP binding proteins required for secretory processes (reviewed in Boman *et al.*, 1995). Recently, the proteins required for guanine nucleotide exchange on ARFs have been identified in both yeast and mammalian cells (Peyroche *et al.*, 1996; Chardin *et al.*, 1996). Such proteins contain a sec7 homology domain (yeast sec7p is a protein required for transport to and from the Golgi complex). The mammalian guanine nucleotide exchange factor (GEF), ARNO (ARF nucleotide-binding-site opener) also contains a pleckstrin homology (PH) domain that mediates

stimulation of its exchange activity by phosphatidylinositol 4,5-bisphosphate (PIP_2) (Chardin *et al.*, 1996). Thus, a likely role for phosphatidlyinositols is activation of ARF through acceleration of its rate of GTP binding either through increased avidity of the exchange proteins for ARF or through localisation of the GEFs to membrane environments that are sites of ARF action (Roth *et al.*, 1997).

Further downstream, the stimulation of phospholipase D (PLD) activity by ARF proteins suggests a potential role for this enzyme in vesicularisation and transport. PLD hydrolyses phospholipids into phosphatidic acid (PA) and their respective polar head group, using PIP_2 as a co-factor (Roth *et al.*, 1997). Although several lines of evidence support this concept, Ktistakis *et al* employed a direct method by using ethanol to divert the action of PLD from PA production to the production of phophatidylethanol through a transphosphatidylation reaction (Ktistakis *et al.*, 1996). This treatment prevented the formation of coated vesicles from Golgi membranes in the presence of ARF. In the same study, treatment of Chinese Hamster Ovary (CHO) cell Golgi membranes with bacterial PLD to induce ARF-independent production of PA, also stimulated coatomer binding (Ktistakis *et al.*, 1996). Thus, these experiments suggest a role for PA or its metabolites in the binding of coat proteins to Golgi membranes and production of transport vesicles. Furthermore, a recent study using a permeabilised cell system and immunoaffinity purified PLD1 has shown that ARF regulation of PLD activity plays an important role in the release of nascent secretory vesicles from the TGN (Chen *et al.*, 1997b). Although the exact role of ARF is still unclear, together these studies suggest that the main role of the small GTP-binding protein in vesicle budding may be to stimulate PLD activity locally to 'prime' the membrane for coat binding.

1.7 The Facilitative Glucose Transporter Family

As glucose plays a fundamental role in cellular homeostasis and metabolism, the transport of this sugar across the plasma membrane of mammalian cells represents one of the most important cellular nutrient transport events. In most mammalian

cells, glucose transport is mediated by a family of proteins referred to as the facilitative glucose transporters, or GLUTs. These transporters allow uptake of glucose by the passive process of facilitated diffusion, which is driven solely by the concentration gradient existing across the plasma membrane. The transporters are specific for the D-enantiomer of glucose and are not coupled to any energy-requiring components, such as ATP hydroylsis or an H^+ gradient (reviewed in Baldwin., 1993; Gould and Holman., 1993).

The functional purification of the first member of this family of transporters was reported in 1977 by Kasahara and Hinkle (Kasahara and Hinkle., 1977). The transporter, isolated from erythrocyte membranes, was a heavy glycosylated, integral membrane protein that migrated as a broad band on SDS-PAGE with an average apparent molecular mass of 55kDa, which was reduced to a mass of 46kDa upon treatment with Endoglucosidase H. In 1985, this transporter (designated GLUT1) was sucessfully cloned and sequenced by Mueckler *et al* (Mueckler *et al*., 1985). In turn the availability of GLUT1 cDNA clones resulted in the rapid identification of the facilitative glucose transporter family through the low stringency screening of the appropriate cDNA libraries. To date six glucose transporters have been characterised and are referred to as GLUTs 1-6, in chronological order of the isolation of their cDNAs (Gould and Homan., 1993).

1.7.1 The Tissue-Specific Distribution of the Facilitative Glucose Transporters

The isolation and functional expression of a family of glucose transporter cDNAs subsequently lead to the realisation that the transporters were expressed in a tissue specific manner, exhibited distinct kinetics and were products of different genes (Gould and Holman., 1993). Indeed, the tissue specific expression of the GLUTs reinforced earlier findings which demonstrated that different tissue types exhibited distinct kinetics to D-glucose uptake (for review see Gould and Holman., 1993).

Such tissue specific expression may be explained in part on the basis of their functional properties as outlined below.

1.7.2 GLUT1

Following the isolation of a cDNA clone for GLUT1 (see above), the utilization of both cDNA and antibody probes demonstrated that both the GLUT1 protein and its mRNA are present in many different tissues and cell types (Gould and Bell,. 1990). Although expressed at high levels in brain and erythrocytes, it is also particularly abundant in endothelial and epithethial cells that form blood-tissue barriers such as the brain/nerve barrier, the placenta, the retina etc. (Froehner *et al*,. 1988). GLUT1 is also found at low levels in muscle and fat tissue. However, the bulk of glucose transport in these tissues is carried out by the insulin-regulatable transporter isoform, GLUT4 (see below). Low levels of GLUT1 are also present in the liver, which also has high levels of GLUT2 (see below). The fact that these tissues, which play a major role in maintaining whole body glucose homeostasis express high levels of other transporter isoforms, suggests that GLUT1 is probably of secondary importance. Indeed, GLUT1 is thought to fulfill a housekeeping function, maintaining a constant low level of glucose in muscle and fat required for resting cellular homeostasis. It has also been demonstrated that cultured cell lines possess elevated levels of GLUT1 protein and mRNA levels (reviewed in Gould and Holman,. 1993).

Kinetic studies on human erythrocytes have shown that GLUT1 has a very broad specificity, transporting a wide range of aldoses, including both pentoses and hexoses. Transport rate is determined by both the V_{max}, maximal velocity and the K_m ,which inversely reflects the affinity for substrate. The high affinity of GLUT1 for glucose (Km ~7mM) at physiological temperature, ensures that GLUT1 will function close to its V_{max} under normal physiological conditions (Lowe and Walmsley,. 1986).

Following the cloning and sequencing of GLUT1, low stringency screening of the appropriate cDNA libraries led to the rapid identification of homologous transporters from other tissues. The isoforms identified so far in this way are between 40 and 80% identical in amino acid sequence. Furthermore, hydropathy plots of their sequences are essentially super-imposable, suggesting that they must all be very similar in secondary structure to GLUT1.

1.7.3 GLUT2

The observation that GLUT1 was expressed at low levels in liver, coupled to the fact that the kinetics of glucose transport in hepatocytes were radically different from those in erythrocytes (Elliot and Craik., 1983) suggested the presence of a distinct transporter. Application of the aforementioned low stringency screening approach of human (Fukamoto *et al.*, 1988) and rat (Thorens *et al.*,1988) hepatocyte libraries led to the isolation of GLUT2 clones. The resulting human cDNA clone exhibited 55% sequence identity and 80% homology to GLUT1.

Subsequent immunocytochemical studies have shown that GLUT2 is expressed at highest levels in hepatocytes, in β cells of the Islets of Langerhans of the pancreas (Thorens *et al.*, 1988; Orci *et al.*, 1989) and in the absorptive epithelia of the small intestine and the kidney proximal tubule (Thorens *et al.*, 1988). Functional analysis of this transporter has shown that this protein has a supra-physiological K_m for glucose, a high transport capacity and exhibits the ability to transport D-fructose in addition to D-glucose.

The physiological role of glucose transport in the liver differs from that in most other tissues, as this organ may take up and release glucose in order to maintain blood glucose levels. The high K_m of GLUT2 may reflect a specific adaptation for this role, allowing glucose flux into or out of the hepatocyte to respond to changes in glucose concentration. The high transport capacity of GLUT2 compared to other

transporters may also provide a rationale for the localisation of this protein to the basolateral membranes of the absorptive epithelia of the small intestine and kidney (Thorens *et al*, 1988). Glucose transport in both the intestine and kidney is a two step process, with the active accumulation of glucose via a Na^+-dependent transporter on the apical membrane of the small intestine transporting glucose against its cocentration gradient (Heiger *et al.*, 1987). The accumulated glucose is subsequently released into capillaries via the high capacity GLUT2 which is present at the basolateral borders.

1.7.4 GLUT3

Further low stringency hybridisation studies resulted in the isolation of GLUT3 from human foetal muscle (Kayano *et al.*, 1988) and mouse (Nagamatsu *et al.*, 1992) cDNA libraries. The encoded proteins were found to share ~64% identity with the GLUT1 transporters from the same species. Northern blot analysis revealed that in humans, this transporter was barely detectable in adult skeletal muscle, but was rather expressed at high levels in the brain and neural tissues and at lower levels in fat, kidney, liver and placenta. However, subsequent immunological studies of human tissues only showed high levels of expression in the brain with much lower GLUT3 levels in the other tissues suggesting that post-transcriptional regulation of the transporter may occur in non-neuronal tissues (Shepherd *et al.*, 1992).

Thus, localisation of GLUT3 to tissues which exhibit a high glucose demand, such as the brain and CNS suggests that this transporter may be specialised to meet the high energy demands of such tissues. In this regard, GLUT3 exhibits the lowest K_m for hexoses of the facilitated glucose transporter family enabling glucose uptake by the brain under conditions of either high glucose demand or hypoglycemia where the extracellular glucose concentration may be very low (Gould *et al.*, 1991).

1.7.5 GLUT4

Following the successful identification of the GLUT2 and GLUT3 isoforms it was soon realised that insulin-regulatable transport exhibited in muscle and fat tissue may be due to a fourth isoform. By 1989, five independent groups (Fukumoto *et al.*, 1989; James *et al.*, 1989; Birnbaum,. 1989; Charron *et al.*, 1989; Kaestner *et al.*, 1989) reported the cloning and sequencing of GLUT4 which was predominantly expressed in insulin-responsive tissues including adipose, heart and skeletal muscle.

An important feature of GLUT4 is that in the absence of insulin this transporter is sequestered into a subcellular compartment, a property not shared with the other family members. In response to insulin there is a rapid and large mobilisation of the sequestered transporter to the plasma membrane, resulting in large increases in the number of GLUT4 transporters at the cell surface and glucose uptake. As this transporter is the focus of this study the properties of GLUT4 are examined in greater detail in the following sections of this thesis.

1.7.6 GLUT5

In 1990, another putative glucose transporter cDNA was isolated from human small intestine (Kayano *et al.*, 1990). Immunological analysis using specific anti-peptide antibodies showed that the transporter appears to be localised to the apical brush border on the luminal side of absorptive epithelial cells (Davidson *et al.*, 1992). As glucose transport from the lumen into epithelial cells was believed to be mediated predominantly by the unrelated Na^+-dependent glucose transporter, it was not immediately obvious as to what role this isoform may play as a hexose transporter. However, subsequent studies revealed that GLUT5 has a high affinity for fructose and a low affinity for glucose (Burant et al., 1992), suggesting that the primary role for GLUT5 in the small intestine is the uptake of dietary fructose. GLUT5 is expressed in a range of tissues including muscle, brain and adipose, where it is

thought to supply these tissues with fructose. However,it is not clear if other fructose transporters also exist.

1.7.7 GLUT6

The homology screening approach led to the identification of a further transporter-like transcript with a ubiquitous tissue distribution (Kayano *et al.*, 1990). This cDNA clone has a high level of base homology with GLUT3. However, as the cDNA was found to contain mutliple stop codons and frameshifts it is unlikely to encode a functional transporter (Kayano *et al.*, 1990). The extensive identity of the GLUT6 cDNA with the GLUT3 cDNA sequence suggests that the glucose transporter-like region of the the GLUT6 transcript may have arisen by the insertion of a reverse transcribed copy of GLUT3 into the non-coding region of a ubiquitously expressed gene (Kayano *et al.*, 1990).

1.7.8 The Structure and Membrane Topography of the GLUTs

Analysis of the predicted amino acid sequences of the GLUTs shows that they are a highly homologous family. Furthermore, they possess high levels of sequence identity with transporters found in many species including cyanobacteria, *E. coli*, yeast, algae and protozoa (reviewed in Walmsley *et al.*, 1998). This high level of sequence similarity is thought to relate to a common mechanism of transport catalysis and the transport of a common type of substrate.

Sequence alignment analysis of the GLUTs has revealed a common structure composed of 12 predicted amphipathic helices arranged so that both the N- and C-termini are at the cytoplasmic surface. There are large loops between helices 1and 2 and betwen helices 6 and 7 (Figure 1.6). The intracellular loop between helices 6 and 7 divides the transporter into two halves, denoted the N- and C-terminal domains.

The short loops between the remainder of the helices on the cytoplasmic surface are very short and are a conserved feature of the whole family. The length of these loops also places restrictions upon tertiary structure suggesting that the transporter may be composed of two groups of six helices in a bi-molecular structure as observed with low resolution electron microscopic images of *E. coli* lactose permease (Kaback,. 1996). The length and sequence identity of the loops at the extracellular surface are more varied and are generally longer in length than the cytoplasmic loops. This may potentially result in a less compact helical packing at the external surface allowing the protein some flexibility of movement during transport.

The two-dimensional topography with the N-and C-termini on the cytoplasmic surface as described above was confirmed using several different methods. Anti-peptide antibodies against peptides representing the C-terminal tail were found to bind to GLUT1 in inside-out vesicles (Davies *et al.*, 1987). Similarily, side-specific tryptic digestion of GLUT1 yields peptide fragments corresponding to the C-terminal tail and large central loop only when erythrocytes are permeabilised (Cairns *et al.*, 1987). However, perhaps the most convincing evidence in favour of the twelve membrane spanning domain model has been provided by glycosylation scanning mutagenisis. By introducing the GLUT4 glycosylation site into each of the short loops of a GLUT1 mutant lacking its native glycosylation sequence, followed by the analysis of their glycosylation status, Mueckler and colleagues could confirm the location of each loop (Hresko *et al.*, 1994). A change of mobility on SDS-PAGE after glycosidase digestion indicated that the inserted sequence was presented to the lumen of the ER and Golgi apparatus. Insertions into each predicted exofacial loop produced proteins which were glycosylated, the converse being true for insertions into predicted endofacial loops, thus, confirming the predicted twelve transmembrane helices model.

Protein secondary structure may be investigated using infra-red spectroscopy, a technique used to assess the relative proportions of α-helical, β-strand and random

coil confirmations. Fourier-transforming infra-red (FTIR) studies, which allow the the analysis of protein structure in dilute aqueous media, have shown that the GLUT1 protein in lipid bilayers contains predominantly α-helical structure, but also a proportion of β-sheet, β-turns and random coil conformation (Alvarez *et al.*, 1987). Polarised FTIR spectroscopy results suggest that the α-helices are preferentially oriented perpendicular to the plane of the lipid bilayer (Chin *et al.*, 1986). The above studies are consistent the twelve transmembrane α-helix structure and together with further experimental analysis (reviewed in Gould., 1997) suggest that D-glucose is transported across the lipid bilayer via a hydrophobic pore formed by bundle of helices which span the bilayer.

1.8 GLUT4 - The Insulin-Responsive Glucose Transporter

Although muscle is quantitatively the most important tissue for glucose disposal, many of the studies of the mechanism of GLUT4 translocation have been based on fat cells. This is due to a variety of reasons including the availability of adipocytes from rat epididymal fat pads and their experimental reliability with regard to hormone responsiveness, membrane fractionation and biochemical analysis (reviewed in Gould, 1997). In contrast, muscle myofibrils have posed problems in the fractionation techniques so readily used on adipocytes. In addition, the murine fat cell line, 3T3-L1, is insulin responsive and expresses quantitatively significant amounts of GLUT4. However, no comparable muscle cell line exists, a fact which has severely hampered studies of this tissue with regard to insulin-stimulated glucose transport. Thus, the following sections will refer to work based mainly on adipocytes, and studies of GLUT4 trafficking and translocation in muscle will not be discussed in any further detail.

1.9 GLUT4 Translocation

Insulin-sensitive tissues (muscle, heart and adipose) have the ability to rapidly augment their glucose transport rate in response to insulin by as much as 30-fold (James *et al.*, 1994). Initially, it was thought that insulin might alter the intrinsic catalytic activity of glucose transporters localised at the plasma membrane. However, in 1980, two independent groups reported that in basal adipose cells, most of the glucose transporters were located in an intracellular (microsomal) membrane compartment of the cells, and upon insulin stimulation the transporters translocated to the plasma membrane (Suzuki *et al.*, 1980; Cushman *et al.*, 1980). This transporter was subsequently shown to be GLUT4 (James *et al.*, 1988). Further studies involving immunoelectron microscopic analyses, photoaffinity labelling of GLUT4 by membrane impermeable reagents and subcellular fractionation, have formally demonstrated that insulin-stimulated increase in glucose uptake in fat, muscle and heart is a result of GLUT4 translocation to the cell surface in response to insulin (Gould *et al.*, 1993; James *et al.*, 1994).

Using immunoelectron microscopy Slot *et al* studied the cellular distribution of GLUT4 in brown adipose tissue in basal and insulin-stimulated states. Cryosections of fixed rat tissue were incubated with specific antibody for GLUT4, which was subsequently identified with Protein A /gold and examined by electron microscopy. In the basal state, the majority of GLUT4 was shown to be located in tubulo-vesicular elements clustered either in the *trans*-Golgi network (TGN) or in the cytoplasm often close to the cell surface. Upon insulin treatment there is a marked shift in GLUT4 from these sites to the plasma membrane, resulting in an increase of GLUT4 at the cell surface of rat brown adipose tissue by at least 40-fold (Slot *et al.*, 1991b). Further work by Slot *et al* in cardiac myocytes, showed that increased glucose transport in muscle may also be accounted for by the translocation of GLUT4 from intracellular tubulo-vesicular elements to the plasma membrane (Slot *et al.*, 1991a).

Studies using a bismannose photoaffinity labelling reagent, ATB-BMPA (2-N-4-(1-azi- 2,2,2-trifluroethyl) -benzoyl-1,3-bis (D-mannos-4-yloxy)-2-propylamine) have also played a major role in the elucidation of GLUT4 trafficking/translocation. Since the reagent is membrane impermeable it only labels the glucose transporters that are localised at the plasma membrane. Therefore, when photolabelling is carried out on intact cells, only those GLUT4 molecules at the cell surface become tagged (Holman *et al.*, 1994a). Experiments in which cell-surface glucose transporters in rat adipose cells in the basal and insulin-stimulated states have been labelled and immunoprecipitated show that cell-surface GLUT4 is increased 15- to 20-fold in response to insulin, whereas the level of cell-surface GLUT1 is only increased 3- to 5-fold, thus indicating that GLUT4 translocation accounts for the majority of insulin-stimulated glucose transport (Holman *et al.*, 1990; Calderhead *et al.*, 1990).

Further evidence for translocation has been provided by subcellular fractionation studies. Calderhead *et al* carried out studies involving immunoblotting of membrane fractions separated from plasma membranes on a sucrose gradient in conjunction with photoaffinity labelling. With respect to subcellular fractionation, insulin treatment caused GLUT4 to shift from the intracellular to the plasma membrane fraction (Calderhead *et al.*, 1990). However, the increase of GLUT4 in the plasma membrane containing fraction is considerably less than that found by the ATB-BMPA labelling method. This may be due to the contamination of these fractions with intracellular membranes containing the transporter. As previously mentioned the translocatable GLUT4 is thought to be located in the TGN and possibly also the endosomes. However, to date there is no known marker for the intracellular membranes containing the insulin-responsive transporters that may be used to assess the contamination of the plasma membrane fractions (Calderhead *et al.*, 1990).

Recent studies have also shown GLUT4 to be expressed in various cell types not considered to be insulin-responsive including neuronal tissue (hippocampus, medulla oblongata, ventricle and thalamus) (Kobasyashi *et al.*, 1996), endothelial cells of the blood brain barrier (McCall *et al.*, 1997) and specific parts of the kidney (distal

tubule, juxtaglomerular apparatus and afferent arterioles) (Rea *et al.*, 1997). However, GLUT4 is sequestered in intracellular tubulo-vesicular elements irrespective of the tissue type in which it is expressed, a unique property not shared with the other transporter isoforms which are localised at the cell surface (Rea *et al.*, 1997). Thus, it is possible that the translocation of GLUT4 may require different stimuli in brain and kidney tissue, yet to be determined.

1.10 GLUT4 Subcellular Trafficking

Immunocytochemical studies have shown the majority of GLUT4 molecules (~60%) to reside in tubulo-vesicular elements clustered in the cytoplasm often close to the cell surface (Slot *et al.*, 1991b). However, localisation of GLUT4 in clathrin-coated veisicles and endosomes (Slot *et al.*, 1991a; Slot *et al.*, 1991b) indicates that GLUT4 recycles via the endosomal system both in the absence and presence of insulin. Further evidence for the constitutive recycling of GLUT4 in basal and insulin-stimulated adipocytes, is provided by kinetic studies using impermeable photolabels. In these experiments, the photolabelling technique is used to study the transfer of tracer-tagged glucose transporters between the plasma membrane and the intracellular membranes. As only the cell-surface pool of transporters is labelled, the half-times for internalisation of tracer-tagged glucose transporters can be used to calculate both endocytosis and exocytosis rate constants, since the net loss of tagged transporters from the plasma membrane is dependent on both of these parameters (Yang *et al.*, 1993; Jhun *et al.*, 1992). Using the same approach, studies in rat adipose cells by Satoh *et al* (Satoh *et al.*, 1993) and 3T3-L1 adipocytes by Yang *et al* (Yang *et al.*, 1993), have shown that insulin primarily increases the exocytic rate constant while only slightly reducing the endocytic rate constant, providing further evidence for the translocation hypothesis.

However, the fact that there are multiple subcellular locations of GLUT4 (TGN, tubulo-vesicular elements and endosomes), each of which contribute to the

redistribution of GLUT4 to the cell surface in response to insulin, as revealed by immunocytochemical studies (Slot *et al.*, 1991b), suggests that the recycling of GLUT4 between the plasma membrane and a single intracellular compartment is an oversimplified model. Also, kinetic studies by Satoh *et al* have shown that the half-time for recycling in the continuous presence of insulin is significantly slower than the half-time for insulin-stimulated trafficking from the basal state (Satoh *et al.*, 1993). With only one intracellular pool, these processes should have the same half-times as both are are dependent on the same insulin-stimulated rate constants for trafficking between the two pools. Thus, these studies are not consistent with a single intracellular compartment.

Using mathematical analysis coupled with computer simulations, Holman *et al* have shown how trafficking through multiple pools can account for these experimental observations (refer to Figure 1.7) (Holman *et al.*, 1994b). The trafficking models employed included: a 3-pool model (with a plasma membrane pool and two intracellular compartments representing the tubulo-vesicular and early endosomal compartments), and 4 and 5-pool models (accounting for the presence of occluded pools in the plasma membrane). The 3-pool model is consistent with the possibility that most of the GLUT4 in the basal state is associated with the tubulo-vesicular compartment, thought to represent a storage pool, from which insulin stimulates a rapid GLUT4 exocytosis. At steady state, recycling from this compartment to the plasma membrane, followed by trafficking via the endosomes and sequestration into the storage compartment, can be slower than the initial rate of exocytosis, thus accounting for the slow steady-state recycling of cell surface GLUT4 in the presence of insulin and the fast initial insulin stimulation of the appearance of GLUT4 at the plasma membrane observed by Satoh *et al* (Satoh *et al.*, 1993). The 4-pool model takes into account the presence of occluded plasma membrane glucose transporters before or after the pool in which proteins are participating in glucose transport. The model in which there is a pool of vesicles which have docked with the plasma membrane but have yet to fuse is likely to account for the lag observed between the

appearance of GLUT4 at the plasma membrane and its participation in glucose transport as observed by Satoh et al (Satoh *et al.*, 1993). In the 5-pool model, two occluded plasma membrane pools are included occurring both before and after the fully functional plasma membrane form of the protein (Holman *et al.*, 1994b).

Taken together, these studies demonstrate that GLUT4 subcellular trafficking in isolated rat adipose cells and 3T3-L1 adipocytes exibits many of the properties observed in regulated secretory processess and neurosecretion. The rapid translocation of GLUT4 to the plasma membrane in response to insulin, and subsequent recycling resulting in sequestration into a storage pool, is analagous to the exocytosis of synaptic vesicles and their retrieval from the plasma membrane via clathrin-coated vesicles into endosomes, and sorting into a specialised secretory pool which is then available for further stimulated exocytosis (refer to Section 1.3).

1.11 The GLUT4 Intracellular Compartment

Although mathematical analysis of GLUT4 trafficking kinetics suggest that the tubulo-vesicular elements observed by immunocytochemical studies represent a distinct GLUT4 compartment, it must be noted that a mechanism by which GLUT4 is specifically sequestered within the endosomal system and then escorted to the cell surface in response to insulin would also be consistent with the data obtained. Insulin also causes a 2- to 4-fold increase in cell surface levels of many recycling proteins in adipocytes including the TfR, the CI-M6PR and the α2-macroglobulin receptor (Tanner *et al.*, 1987; Oka *et al.*, 1985). Thus, the insulin-dependent movement of GLUT4 in adipocytes may simply represent an efficient adaptation of this pathway. However, although it has been difficult to distinguish the GLUT4 compartment from other elements of the constitutive recycling pathway, there is increasing evidence to suggest that there is a separate GLUT4 storage compartment. A technique which has played a major role in several of the following studies is vesicle immunoisolation, a method initially described by Biber and Lienhard (Biber *et*

al., 1986) in which vesicles are immunoadsorbed onto a solid support such as *Staphloccocus aureus* cells coated with an appropriate antibody such as a monoclonal antibody against the carboxy terminal of GLUT4.

Direct evidence for the existence of a GLUT4 storage compartment, which is separate from the recycling endosomal system has recently been demonstrated by means of a technique referred to as compartment ablation analysis (Livingstone *et al.*, 1996). This method employs loading of the recycling pathway of the TfR (refer to Section 1.3) with transferrin conjugated to horseradish peroxidase (Tf-HRP). In the presence of peroxide (H_2O_2) and 3,3'-diaminobenzidine (DAB), the HRP converts DAB into a dense polymer. Integral membrane proteins present in the Tf-HRP containing endosomes become cross-linked by the DAB polymerisation reaction and are subsequently ablated. Using endosomal ablation in conjunction with vesicle immunoisolation in 3T3-L1 adipoctyes, Livingstone *et al* have shown that some 40% of the GLUT4 is localised to the early endosomal/ recycling system, but a larger proportion of GLUT4 (~60%) resides in a distinct 'non-ablatable' pool which is devoid of transferrin receptors and other endosomal recycling proteins (Livingstone *et al.*, 1996). Glycerol gradient analysis has also been used to identify a population of GLUT4 vesicles in adipocytes that are segregated from endosomal markers (Herman *et al.*, 1994; Laurie *et al.*, 1993).

GLUT1 also recycles between an intracellular pool and the plasma membrane. Co-localisation of this isoform with both the TfR and the CI-M6PR suggests that this occurs via the endosomal system (Tanner *et al.*, 1989), consistent with the quantitative ablation of GLUT1 following endosomal ablation (Livingstone *et al.*, 1996). As GLUT4 also constitutively recycles via the endosomal system (refer to Section 1.9), it is therefore not surprising that GLUT1 and GLUT4 were found to co-localise upon the isolation of GLUT1 and GLUT4 vesicles from bulk membranes of 3T3-L1 adipoctyes (Calderhead *et al.*, 1990). However, double-labelled immuno-fluorescence microscopy in 3T3-L1 adipoctyes has revealed differential intracellular

targeting of GLUT1 and GLUT4 (Piper *et al.*, 1991). Also, the immunoisolation of GLUT4 vesicles from intracellular membranes in rat cardiac myoctyes has recently identified two GLUT4 pools, only one of which is enriched in GLUT1 (Fischer *et al.*, 1997). Kinetic studies in which both GLUT4 and GLUT1 in 3T3-L1 adipocytes have been tracer-tagged by photolabelling, suggest that the rates of endocytosis of both transporters are very similar, but in the basal state the rate constant for exocytosis of GLUT4 is much slower than that of GLUT1. The slow exocytosis of GLUT4 in the basal state results in increased intracellular retention of GLUT4 relative to GLUT1, suggesting that the former isoform possesses additional intracellular retention signals, providing a possible explanation for the differential targeting of the two transporters (Yang *et al.*, 1993).

Recently, Malide *et al* have studied the subcellular distribution of GLUT4 and its co-localisation with compartment markers in rat adipose cells *in situ* using confocal microscopy and 3-D image reconstruction (Malide *et al.*, 1997a). Three-dimensional analysis of GLUT4 immunostaining in basal cells revealed an intracellular punctate distribution both in the perinuclear region and throughout the cytoplasm. VAMP2 was found to be co-localised with GLUT4 in many of these punctate structures with a small fraction of the transporter also overlapping with TGN38, γ-adaptin and the M6PR in the perinuclear region, corresponding to the late endosome and TGN structures. However, co-localisation was not observed with either the TfR or lgp120 (a lysosomal membrane protein), suggesting that in the basal state GLUT4 resides in a post-endosomal VAMP2-positive compartment, distinct from the recycling endosomes (Malide *et al.*, 1997a), a result in striking agreement with the data from Tf-HRP ablation analysis (Livingstone *et al.*, 1996). The co-localisation of GLUT4 with the v-SNARE, VAMP2, has been shown in several other studies (Cain *et al.*, 1992; Martin *et al.*, 1996), the relevance of which shall be discussed later in this chapter.

Several other observations also support the idea that the GLUT4 storage compartment is a separate entity from the endosomal recycling system. The aminopeptidase vp165, completely co-localises with GLUT4 in muscle and fat cells (Kandror *et al.*, 1994; Martin *et al.*, 1998; Ross *et al.*, 1996) and exhibits similar insulin-stimulated trafficking kinetics to GLUT4 in 3T3-L1 adipocytes (Ross *et al.*, 1997), suggesting that the GLUT4 storage compartment contains other proteins aside from GLUT4. Although insulin causes a 2- to 4-fold increase in cell surface levels of many recycling proteins, the translocation of GLUT4 and vp165 is considerably greater (10- to 40-fold) (James *et al.*, 1994). This dichotomous behaviour suggests that the major function of the GLUT4 storage compartment is to sequester GLUT4 and other resident proteins in the basal state and to facilitate their rapid access to the cell surface in response to insulin. Finally, GLUT4 is enriched in regulated secretory granules when expressed in endocrine cells, indicating that the transporter must contain sorting signals which enable it to be distinguished from other recycling proteins (Hudson, 1993).

1.12 The Nature and Biogenesis of the GLUT4 Storage Compartment

Taken together, these studies provide compelling evidence for the existence of a GLUT4 storage compartment. However, the nature of this compartment is still poorly understood and it is not known whether the storage compartment resides in an extension of a previously identified organelle such as the TGN or a specialised entity, yet to be identified. The aforementioned studies clearly show poor co-localisation between GLUT4 and the TfR, a marker of the endosomal system, probably excluding this compartment as being a possibility for the sequestration of GLUT4. Although GLUT4 shows partial co-localisation with the CI-M6PR (also known as the insulin-like growth factor II receptor [IGFIIR]) this is thought to be within the recycling endosomal system, and the majority of the CI-M6PR (Kandror *et al.*, 1996) and lgp120 (lysosomal membrane protein) (Malide *et al.*, 1997a) show no co-localisation with GLUT4, ruling out the late endosomes and the lysosomes,

respectively. As previously reported, early studies by Slot *et al* showed a small fraction of GLUT4 (~13%) to be associated with the TGN (Slot *et al.*, 1991a; Slot *et al.*, 1991b), consistent with the recent confocal studies observing partial overlap between the transporter and the putative TGN markers, TGN38 and γ-adaptin (a component of the AP-1 complex) (Malide *et al.*, 1997a). However, it has recently been shown by vesicle isolation that only ~10% of the intracellular complement of GLUT4 is present within TGN38 vesicles isolated from 3T3-L1 adipocytes (Martin *et al.*, 1994), suggesting that the GLUT4 storage compartment does not reside in the TGN. However, the TGN is a heterogenous compartment organised into discrete subdomains and therefore GLUT4 may be localised to certain regions devoid of TGN38 and *vice versa.* Thus, it is not possible to exclude a subdomain of the TGN as being a major site for intracellular GLUT4 storage until further studies regarding the nature of such a compartment are carried out.

An experimental approach exploited by several laboratories has been to elucidate the composition of GLUT4-rich vesicles in order to identify a 'reporter' protein that may be instructive in understanding their regulation by insulin. The rationale for this approach is based on the assumption that the insulin-induced biochemical changes which result in GLUT4 translocation are not directed to GLUT4 *per se*, but rather, take place in one or more regulatory proteins that are part of the GLUT4 vesicles. To date, several proteins have been identified in GLUT4 vesicles from adipocytes including: vp165 (Keller *et al.*, 1995), sortilin (Morris *et al.*, 1998), SCAMPs (secretory carrier-associated membrane proteins) (Laurie *et al.*, 1993), VAMPs (Cain *et al.*, 1992), phosphatidylinositol-4-kinase (Del Vecchio *et al.*, 1991) and Rab4 (Cormont *et al.*, 1991). As the aminopeptidase vp165 has been found to completely co-localise with GLUT4 and exhibit similar kinetics to the transporter both in the basal state and in response to insulin (Kandror *et al.*, 1994; Ross *et al.*, 1996; Ross *et al.*, 1997), this protein may prove to be a key component in the regulation of GLUT4 vesicles. However, the requirement for aminopeptidase activity in insulin-responsive cells is unknown. Interestingly, the vasopressin-sensitive, water channel-

containing vesicles from kidney are also rich in aminopeptidase activity (Sabolic *et al.*, 1992; Harrison *et al.*, 1994). In a similar way to GLUT4, these water channels translocate from a vesicular storage pool in a hormone-dependent manner, thus suggesting that aminopeptidases may be involved in hormone-sensitive vesicular traffic (Stephens *et al.*, 1995). As sortilin has only recently been identified, little is known about this novel membrane protein (Morris *et al.*, 1998). However, the relatively small increase in cell surface levels of this protein (~2-fold) in response to insulin, suggests that sortilin may associate with GLUT4 in the recycling endosomal system, in a manner similar to the TfR (Morris *et al.*, 1998). As the other proteins are ubiquitous in their expression, their identification has not provided any further clues towards the insulin-dependent regulation of GLUT4. However, the identification of SCAMPs (Laurie *et al.*, 1993), VAMPs (Cain *et al.*, 1992) and Rab4 (Cormont *et al.*, 1991) as constituents of GLUT4 vesicles supports the concept that GLUT4 translocation exhibits many similarities to secretory phenomena such as neurotransmitter release at synapses and hormone release from endocrine cells.

Using confocal microscopy, Malide *et al* have recently proposed that GLUT4 resides in a post-endocytic compartment (Malide *et al.*, 1997a). However, the nature of this compartment is ill-defined and it is still not clear whether or not it represents a specialised secretory compartment. Although GLUT4 has been localised to secretory granules in neuroendocrine cells, such cell lines do not express this transporter endogenously and therefore care must be taken when interpreting the results (Hudson, 1993). However, a recent study in rat atrial cardiomyocytes, a regulated secretory cell type in which GLUT4 is endogenously expressed, has shown a large proportion of GLUT4 (50-60%) to be localised in the atrial natriuretic factor (ANF)-containing secretory granules (Slot *et al.*, 1997). It must be noted that the effect of insulin on GLUT4 distribution was too small to measure shifts of GLUT4 labelling from the ANF granules and therefore it is still unknown whether this compartment contributes to the translocation of GLUT4. Further studies in other

insulin-responsive cell lines may provide insight into the physiological basis for the targeting of GLUT4 to a secretory organelle.

Relatively little progress has also been made in determining the biogenesis of the intracellular storage compartment. However, based on our current knowledge of GLUT4 and/or general trafficking systems, three possible models for the entry of GLUT4 into the intracellular storage compartment after leaving the plasma membrane have been proposed (refer to Figure 1.8) (reviewed in Rea *et al.*, 1997). The first model postulates that the GLUT4 storage compartment may bud directly from the endosomes. This is supported by the partial overlap between endosomal proteins and GLUT4 (Martin *et al.*, 1996) and electron microscopy studies which have clearly shown GLUT4 to be clustered in tubulo-vesicular elements adjacent to sorting endosomes (Slot *et al.*, 1991a;Slot *et al.*, 1991b), consistent with a specific sorting step at this location. Furthermore, the PI 3-kinase inhibitor wortmannin disrupts both GLUT4 and endosomal trafficking (Shepherd *et al.*, 1996b), suggesting a common mode of action. The co-localisation of Rab4 with GLUT4 vesicles, suggesting a potential role for this endosomal GTP-binding protein in GLUT4 trafficking (Cormont *et al.*, 1996; Shibata *et al.*, 1996) (see below), and the recent discovery of unique coat proteins involved in vesicle budding from the endosomes (Stoorvogel *et al.*, 1996), also support the idea that the storage compartment may be of endosomal origin.

The second model proposes that GLUT4 may traffic back to the TGN, with the subsequent budding of the storage compartment from this organelle. The partial overlap of GLUT4 with the M6PR-, TGN38- and γ-adaptin-positive structures observed using confocal microscopy, suggests the possibility that in the recycling pathway GLUT4 may indeed return as 'far back' as the TGN before reaching the storage compartment (Malide *et al.*, 1997a), consistent with electron microscopy studies showing GLUT4 to be localised to the TGN in insulin-sensitive cells (Slot *et al.*, 1991a; Slot *et al.*, 1991b). Also, the aforementioned ANF-secretory granules in

atrail cardiomyocytes were found to become GLUT4-positive in the TGN (Slot *et al.*, 1997). Cyclohexamide treatment had no effect on the TGN localisation of GLUT4 in these cells, suggesting that a large proportion of GLUT4 recycles via the TGN (Slot *et al.*, 1997). However, it is not known whether GLUT4 returns back to the endosomal system from the TGN or whether the storage compartment buds directly from this organelle. Clathrin-coated vesicles (containing the AP-1-complex) budding from the TGN are thought to fuse with endosomes (refer to Section 1.4.2). However, AP-1-containing coated vesicles have also been observed on immature secretory granules following budding from the TGN (refer to Section 1.4.3) (Traub *et al.*, 1993; Seaman *et al.*, 1996b). Further studies on GLUT4 trafficking are required to differentiate between these two possible processes. It is also possible that the GLUT4 storage compartment may emanate from both the endosomes and the TGN. This is supported by recent studies which have shown that sorting signals regulating the internalisation of membrane proteins from the cell surface may also facilitate sorting in the Golgi (Marks *et al.*, 1997). Similarly, the GLUT4 signal which mediates its entry into the storage compartment may operate both at the TGN and endosomes (Rea *et al.*, 1997). Also, the gross architecture of the cell may dictate the pathway followed by the recycling vesicles. For example, the specialised structure of the neurite dictates the need for a Golgi-independent vesicle recycling system. Both adipocytes and muscle cells are highly compartmentalised and therefore in some regions of the cell, the GLUT4 storage compartment may occur independently of the Golgi, analagous to the reformation of synaptic vesicles in neurons (Rea *et al.*, 1997).

Finally, the third model proposes that GLUT4 may be internalised via a separate endosome, compared with other recycling proteins. This model has recently been proposed for the re-formation of synaptic vesicle-like membranes in PC12 cells (Schmidt *et al.*, 1997). A characteristic feature of the specialised endosome in these cells is that traffic out of the compartment is blocked at low temperature. Interestingly, insulin-stimulated GLUT4 translocation is inhibited in adipocytes following a prolonged incubation at 18°C, consistent with this model (Robinson *et*

al., 1992a). However, the specific sorting of GLUT4 out of the recycling endosome may also be blocked at a low temperature. In addition, a 20°C incubation is known to reversibly block the transport of proteins from the TGN (Matlin *et al.*, 1983) and therefore this phenomenon may be explained by all three models. The co-localisation between GLUT4 and recycling proteins also casts doubt upon the viability of this last model.

1.13 GLUT4 Trafficking Signals

When considering the subcellular trafficking of GLUT4 there are at least three separate stages which may require a signalling motif including; internalisation of GLUT4 via clathrin-coated pits, sorting at the TGN and sorting and /or retention into the storage compartment. To date, two such motifs have been identified through studies involving the use of chimeric, truncated or mutated transporters.

The first motif is an aromatic-based signal (F^5QQI) located in the N-terminus while the second signal comprises a dileucine motif ($LL^{489-490}$) located in the C-terminus. Interestingly, both motifs resemble well described targeting signals identified in numerous other recycling proteins (refer to Section 1.4.3) (Marks *et al.*, 1997). In the N-terminus, mutation of the phenylalanine to alanine results in the accumulation of GLUT4 at the cell surface, thought to be due to impaired entry into clathrin-coated pits (Piper *et al.*, 1993). Furthermore, the construction of chimeric transporters between GLUT4 and the transferrin receptor has shown that the F^5QQI internalisation motif promotes effective internalisation of the chimera in CHO cells (Garippa *et al.*, 1994). Mutation of the leucine residues to alanines in the C-terminus also leads to the accumulation of GLUT4 at the cell surface under steady state conditions. However, although it is apparent that mutation of this motif impairs GLUT4 internalisation, in contrast to to the F^5QQI mutant, a high level of expression of the transporter is required (Verhey *et al.*, 1995; Marsh *et al.*, 1995). Based on the above data and other studies it is unlikely that either the F^5QQI or di-

leucine motifs regulate entry of GLUT4 into the storage compartment. Thus, there must be a separate motif which faciliates this function.

Recently, Lee *et al* have demonstrated the importance of the C-terminal cytoplasmic domain of GLUT4 in its intracellular sequestration (Lee *et al.*, 1997). By introducing a synthetic peptide corresponding to the C-terminal cytoplasmic domain of GLUT4, redistribution of GLUT4 from the intracellular pool to the plasma membrane was observed in basal adipocytes. Not only does this study underscore the importance of the C-terminal domain in GLUT4 targeting, it also suggests the existence of a regulatory protein that interacts with this domain, thus participating in GLUT4 sequestration (Lee *et al.*, 1997). As vp165 is also targeted to the GLUT4 storage compartment, a similar targeting motif might be expected to exist in this protein. Interestingly, the cytoplasmic tail (N-terminus) of vp165 contains two di-leucine motifs and several acidic regions similar to those which occur in the extreme GLUT4 C-terminus (Ross *et al.*, 1996). Furthermore, the introduction of a glutathione S-fusion protein containing the cytosolic portion of vp165 results in GLUT4 translocation to the plasma membrane in basal 3T3-L1 adipocytes, suggesting that the N-terminus of vp165 interacts with a retention/sorting protein that also regulates the distribution of GLUT4 (Waters *et al.*, 1997). Collectively, these studies suggest that the sorting of GLUT4 and vp165 within the cell is carried out by a common mechanism. The similarity between the C-terminus of GLUT4 and the N-terminus of vp165 indicates that this mechanism may act via a signalling motif within these domains. Further studies are required to define the nature of such a motif and also to identify cellular proteins that interact with this region.

1.14 GLUT4 Trafficking: The Role of SNAREs and Rab Proteins

The segregation of GLUT4 in a separate storage compartment and its translocation to the cell surface in response to insulin, shares many morphological and biochemical features with synaptic secretory vesicle (SSV) exocytosis in neurons. As several

molecules involved in targeting, docking and fusion of SSV with the presynaptic membrane have been characterised (refer to Section 1.5) this catalysed the search for SNAREs and other SSV proteins in insulin-sensitive tissues. Recently, homologues of these molecules have been identified in adipocytes and myocytes implying that the trafficking of the GLUT4 storage compartment is highly analagous to SSV exocytosis. Thus, the SNARE hypothesis also provides a working model for studies of vesicle targeting and fusion in adipocytes (refer to Figure 1.9).

The expression of neuronal VAMP analogues in adipocytes was first reported by Lienhard and colleagues (Cain *et al.*, 1992). Subsequent studies, have shown adipocytes to express both VAMP2 and an additional v-SNARE cellubrevin, both of which were surprisingly found to co-localise with GLUT4 in adipoctyes (Volchuk *et al.*, 1995; Martin *et al.*, 1996). However, using endosomal ablation analysis to further define their intracellular distribution in 3T3-L1 adipocytes, Martin *et al* have shown that the majority of cellubrevin resides in the endosomes whereas a large fraction of VAMP2 (~90%) was targeted to the 'non-ablatable' GLUT4 storage compartment, suggesting a specific role for VAMP2 in GLUT4 trafficking (Martin *et al.*, 1996). In the same study, immuno-electron microscopy of intracellular vesicles revealed co-localisation between VAMP2 and GLUT4, again, in striking agreement with GLUT4 localisation in a VAMP2-positive post-endocytic compartment recently observed by confocal microscopy (Malide *et al.*, 1997a).

Although providing conflicting data, the specific proteolytic cleavage of VAMP2 and cellubrevin by neurotoxins has been used to determine the role of these molecules in GLUT4 trafficking. Studies in 3T3-L1 adipocytes using Botulinum neurotoxins (BoNT) B and D specific for VAMP and cellubrevin, resulted in a 64% inhibition of insulin-evoked glucose uptake and a 61% inhibition of GLUT4 translocation to the plasma membrane, respectively (Chen *et al.*, 1997a; Macaulay *et al.*, 1997). In contrast, the introduction of tetanus toxin into rat adipocytes by electroporation, resulting in complete loss of cellubrevin and VAMP2 expression, had no effect on the

ability of insulin to stimulate glucose transport (Hajduch *et al.*, 1997). However, recently it has been shown that the introduction of synthetic peptides that comprise VAMP2 domains into 3T3-L1 adipocytes inhibit insulin-stimulated translocation by ~50% (Macaulay *et al.*, 1997), thus providing more conclusive evidence of the involvement of VAMP2 in GLUT4 trafficking . Taken together with the differential distribution of VAMP2 and cellubrevin in 3T3-L1 adipocytes, it is plausible that VAMP2 regulates insulin-dependent GLUT4 trafficking whereas cellubrevin may mediate the endosomal trafficking of the transporter.

As it became evident that insulin-sensitive cells employed the same v-SNARE as neurons, further investigations were carried out to determine whether they also utilised the same t-SNAREs, namely syntaxin-1A and SNAP-25 and other regulatory proteins. Among the syntaxins thought to regulate recycling through the endosomal system, only syntaxins 1A and 4 have been shown to bind to VAMP2. Syntaxin 1A is predominantly expressed in neurons and is absent from insulin-sensitive cells. Syntaxin 4, however, is expressed at high levels in fat and muscle cells and is predominantly targeted to the plasma membrane (Olson *et al.*, 1997; Tellam *et al.*, 1997). By the introduction of either the cytoplasmic domain of syntaxin 4, a GST-syntaxin 4 fusion protein or antibodies directed against syntaxin 4, insulin-stimulated GLUT4 translocation was found to be inhibited in 3T3-L1 adipocytes, thus establishing a role for the t-SNARE in GLUT4 trafficking (Olson *et al.*, 1997;Tellam *et al.*, 1997). Furthermore, the introduction of a mutant cytoplasmic domain of syntaxin 4 in which the putative VAMP binding domain was deleted had no significant effect on insulin-stimulated GLUT4 translocation, suggesting that the inhibition observed was specific for the interaction of syntaxin 4 with VAMP2 (Olson *et al.*, 1997).

The inability to detect significant expression of the t-SNARE SNAP-25 in adipocytes, has led to the recent identification of a SNAP-25 homologue, designated SNAP-23 (Araki *et al.*, 1997). SNAP-23 is located primarily at the plasma

membrane in 3T3-L1 adipocytes, exhibiting a similar distribution to that of syntaxin 4. *In vitro,* SNAP-23 has also been shown to associate strongly with syntaxin 4, analagous to the association of syntaxin 1A to SNAP-25 in neural cells (refer to Section 1.5). Furthermore, by expressing SNAP-23, syntaxin 4 and Munc 18c (a syntaxin binding protein, see below) in COS cells, syntaxin 4 was shown to bind to both SNAP-23 and Munc 18c, and as expression of Munc 18c increased the amount of SNAP-23 associated with syntaxin 4 decreased, suggesting that Munc 18c may regulate the formation of the SNAP-23-syntaxin 4 SNARE complex (Araki *et al.*, 1997). However, the role of SNAP-23 in the trafficking of GLUT4 in insulin-sensitive cells has yet to be established.

Upon establishing a role for syntaxin 4 as the functional t-SNARE in GLUT4 trafficking, subsequent studies have led to the identification of the syntaxin binding protein involved in the regulation of v-SNARE and t-SNARE interactions in GLUT4 exocytosis. Of the three Munc 18 isoforms participating in the endosomal recycling system of adipocytes (Munc 18a-c), Munc 18c is primarily targeted to the cell surface, again with a distribution indistinguishable from that of syntaxin 4 (Tellam *et al.*, 1997). In addition, *in vitro* studies by Tellam *et al* have recently shown that Munc 18c reduces the interaction between syntaxin 4 and VAMP2 (Tellam *et al.*, 1997), similar to the effect observed for Munc 18a on the interaction between syntaxin 1A and VAMP2 (Sudhof, 1995).

Collectively, these data provide further support for the similarity between the regulation of GLUT4 exocytosis in fat cells and synaptic vesicles in neurons. Modulation of the syntaxin binding proteins by insulin, thereby regulating the availability of the t-SNARE syntaxin 4 for the v-SNARE VAMP2, provides an attractive model for insulin-stimulated GLUT4 exocytosis, as shown in Figure 1.8.

The Rab family of small GTP-binding proteins are also known to play an important role in vesicle trafficking (refer to Section 1.3.4). Initial studies showing the

association of Rab4 with GLUT4 vesicles in adipocytes (Cormont *et al.*, 1993), in addition to the tight correlation observed between the subcellular redistribution of GLUT4 and Rab4 in response to insulin (Ricort *et al.*, 1994), suggested that this member of the Rab family may be important in GLUT4 trafficking. Recent studies have provided further evidence for a specific role for Rab4 in the insulin-stimulated translocation of GLUT4.

Le Marchand-Brustel and colleagues have shown that the transient co-expression of Rab4 with an epitope tagged GLUT4 in rat adipocytes leads to the enhanced intracellular retention of GLUT4 in the basal state (Cormont *et al.*, 1996). The overexpression of Rab4 at high endogenous levels, in addition to decreasing the levels of GLUT4 at the plasma membrane also blocked the insulin-induced recruitment of GLUT4 to the cell surface, suggesting that Rab4 is involved in both the biogenesis of the GLUT4 compartment and also translocation to the cell surface in response to insulin. Moreover, as the overexpressed protein was found to be mainly cytosolic, the inhibitory effect may be due to the sequestration of some protein/factor required for insulin action. The moderate expression of a Rab4 mutant lacking the geranylgeranylation sites required for membrane anchorage had the same effect as the wild type Rab4 when overexpressed at high levels, consistent with this idea (Cormont *et al.*, 1996). Two independent studies support the work carried out by Le Marchand-Brustel and colleagues. First, Shibata *et al* have inhibited insulin-induced GLUT4 translocation by ~50% by introducing a peptide corresponding to the hypervariable carboxy terminal of Rab4 into rat adipocytes (Shibata *et al.*, 1996). Second, by co-expressing Rab4 and GLUT4 in *Xenopus* oocytes, Mora *et al* have also observed an increase in the intracellular retention of GLUT4, similar to that observed in rat adipocytes (Mora *et al.*, 1997). Thus, both of these studies support the notion that Rab4 is involved in both insulin-induced GLUT4 translocation and the biogenesis of the storage compartment.

Recently, Shibata *et al* have shown that Rab4 may indeed be one of the possible intracellular targets of insulin action on intracellular vesicle traffic in rat adipocytes (Shibata *et al.*, 1997). By showing that insulin stimulates guanine nucleotide exchange on Rab4, Shibata *et al* have proposed that insulin may activate as yet unidentified guanine nucleotide exchange factor(s) (GEFs) for Rab4 (Shibata *et al.*, 1997). Furthermore, inhibition of this insulin-stimulated nucleotide binding by wortmannin, a specific inhibitor of phophatidylinositol 3-kinase (PI 3-kinase), suggests that insulin targets Rab4 via a PI 3-kinase-dependent signalling pathway (Shibata *et al.*, 1997). However, the exact mechanisms involved in the activation of Rab4 by PI 3-kinase remain to be explored.

1.15 Signalling Mechanisms that Regulate GLUT4 Translocation

The signalling cascade that results from the binding of insulin to its receptor is one of the most extensively studied signal transduction pathways (reviewed in Shepherd *et al.*, 1996a; Holman and Kasuga,. 1997). Insulin has a dual role as it is both a weak mitogen and a regulator of glucose metabolism. There is growing evidence to suggest that two divergent signalling pathways result from the activation of the insulin receptor and that these pathways separately regulate the mitogenic response and metabolic effects, the latter of which includes the GLUT4 trafficking pathway (Haruta *et al.*, 1995; Van Den Berghe *et al.*, 1994). The divergence of mitotic stimulation and metabolic stimulation is clearly necessary in insulin-responsive tissues such as fat and muscle where there is a requirement for an acutely regulatable metabolic flux without a concomitant stimulation of cell growth and division.

The cascades leading to stimulated glucose transport and activation of cell growth and mitosis begin at the insulin receptor, an $\alpha 2/\beta 2$ tetramer (reviewed in Hausdorff *et al.*, 1997). The α-subunit is located entirely at the extracellular surface of the plasma membrane and contains the insulin binding site. The β-subunit is a transmembrane peptide that possesses tyrosine-specific protein kinase activity in the intracellular

domain. Insulin binding to the α-subunit leads to the phosphorylation of the β-subunit of the receptor on tyrosine residues. This auto-phosphorylation process is associated with increased tyrosine kinase activity toward intracellular substrates. The major substrates of the kinase include the adaptor protein Src-homology-collagen-like protein (Shc) (Skolnik *et al.*, 1993) and four related insulin receptor substrate (IRS) proteins (White., 1998) (Figure 1.10). Tyrosine-phosphorylated Shc recruits the small adaptor protein growth factor receptor-binding protein 2 (Grb2) which in turn recruits and activates the ras-GDP exchange factor mammalian son-of-sevenless protein (m-sos). Recruitment of m-sos into a receptor tyrosine kinase-induced complex at the plasma membrane results in the activation of the small GTP-binding protein ras. This in turn results in the activation of the mitogen-activated protein (MAP)-kinase cascade which is associated with the induction of many important events in mitogenesis. Thus, in this cascade a key switch in signalling occurs between tyrosine kinase activation and serine/threonine kinase activation through the G-protein Ras. However, such a switch has not been demonstrated for the reactions leading to the stimulation of glucose transport and it appears that the MAP-kinase cascade is not involved in the activation of this process (for review see Denton and Tavare., 1995).

Multisite tyrosine phosphorylation of IRS proteins appears to be the major mechanisn by which insulin transmits signals to regulate metabolic events including glucose transport (White., 1998). Phosphorylation of specific tyrosine residues on the IRS proteins allows the protein to recruit a number of signalling molecules through their src-homology-2 (SH2) domains. These include Grb2, the small adaptor protein Nck, the tyrosine phosphatase SH-PTP2 and the p-85-p110 PI 3-kinase (reviewed in Holman and Kasuga, 1997; Hausdorff *et al.*, 1997) (Figure 1.10). Since the identification of IRS signalling complexes, considerable effort has been made to determine which, if any, of these molecules mediate the acute insulin-stimulated increase in glucose uptake.

1.15.1 IRS Proteins and GLUT4 Translocation

As insulin causes very little recruitment of PI 3-kinase activity directly to the insulin receptor, the IRS proteins appear to provide a means of coupling the insulin receptor tyrosine kinase activity with the activation of intracellular PI 3-kinase activity. Four members of the IRS family have now been identified, namely IRS-1 (Sun *et al.*, 1991), IRS-2 (Sun *et al.*, 1995), IRS-3 (Lavan *et al.*, 1997a) and IRS-4 (Lavan *et al.*, 1997b). All the IRS proteins have the same overall architecture, sharing highly homologous N-terminal pleckstrin homology (PH) and phosphotyrosine-binding domain (PTB) domains. The PTB domain binds directly to the juxtamembrane region of the insulin receptor at an NPXY motif (Ile *et al.*, 1995; Wolf *et al.*, 1995), whereas the PH domain is thought to allow the interaction of IRS-1 with membrane phosphoinositides (Rameh *et al.*, 1997). The IRS proteins also contain multiple potential tyrosine phophorylation sites, of which the majority are in YMXM or YXXM motifs. As YMXM motifs have been shown to be the preferred substrate of the insulin receptor tyrosine kinase, the IRS proteins are ideally structured for the insulin-dependent recruitment and activation of PI 3-kinase (Shoelson *et al.*, 1992; Songyang *et al.*, 1995).

However, whether IRS proteins are required for PI 3-kinase signalling to act on GLUT4 translocation is unclear at present. Quite conflicting data have resulted from two differing experimental methods utilised thus far. Microinjection or expression of the PTB domain of IRS-1 in insulin-sensitive cultured adipocytes is able to block the mitogenic and membrane ruffling effects of insulin but not the stimulation of glucose transport (Sharma *et al.*, 1997). This dominant inhibitory construct is expected to block binding of all IRS protein isoforms to the insulin receptor through binding to the insulin receptor juxtamembrane sequence surrounding Tyr 960, the docking site for IRS and Shc protein PTB domains. Indeed, nearly complete inhibition of IRS-1 tyrosine phophorylation by insulin was observed in these studies (Sharma *et al.*, 1997).

In contrast, studies in animals in which the IRS-1 or the IRS-2 gene has been ablated provide support for a role of these proteins in glucose transport regulation. Mice lacking IRS-1 exhibit some insulin resistance although no diabetes (Araki *et al.*, 1994; Tamemoto *et al.*, 1994), and heterozygotes for loss of both IRS-1 and insulin receptor genes are both insulin resistant and develope diabetes (Bruning *et al.*, 1997). IRS-2 ablation in mice causes both impaired insulin signalling to glucose uptake and diabetes (Withers *et al.*, 1998) despite the presence of a functional insulin receptor and normal IRS-1 expression. It has been suggested that the insulin action observed on glucose uptake in adipocytes from animals lacking IRS-1 may involve the IRS-3 isoform, which is tyrosine phosphorylated in response to insulin (Kaburagi *et al.*, 1997). Such redundancy may account in part for some of these conflicting results. Thus, studies involving IRS knockout mice provide compelling evidence for a role for these proteins in insulin-stimulated glucose transport, with the caveat that unrelated changes changes in response to IRS loss during development may contribute to the phenotypes observed. Taken together, the above data do not provide conclusive proof for the role of IRS proteins in insulin-stimulated GLUT4 translocation, but instead suggest that the PI 3-kinase-IRS complexes are necessary but not sufficient for GLUT4 translocation in response to insulin.

Another IRS-1 binding protein is the protein tyrosine phosphatatse, SH-PTP2. SH-PTP2 associates with IRS-1 following stimulation by insulin (Kuhne *et al.*, 1993). However, microinjection of SH-PTP2 SH2 domains or antibodies to SH-PTP2 into 3T3-L1 adipocytes blocks insulin-induced but not insulin-stimulated GLUT4 translocation. Over longer incubations, increased expression of GLUT1 is observed and this leads to an increase in glucose transport activity (Hausdorff *et al.*, 1995).

1.15.2 PI 3-Kinase and GLUT4 Translocation

A family of PI 3-kinases phosphorylate the inositol ring at the D-3 position to give PI 3-phosphate from PI, PI 4,5-bisphosphate from PI 4-phosphate and PI 3,4,5-

trisphosphate from PI 4,5-bisphosphate. The only PI 3-kinases currently known to be stimulated by insulin are the class I heterodimeric p85/p110 PI 3-kinases. In this class, the p85 subunit acts as an adaptor, linking the p110 catalytic subunit to tyrosine phophorylated motifs on IRS proteins, resulting in the activation of the holoenzyme (reviewed in Shepherd *et al.*, 1998).

There is growing evidence to suggest that the p85-p110 PI 3-kinase plays a pivotal role in insulin-stimulated GLUT4 translocation, consistent with the concept that PI 3-kinase activity is a rate limiting step in various membrane trafficking events (reviewed in Shepherd *et al.*, 1996b). Initial studies using two structurally distinct PI 3-kinase inhibitors, namely wortmannin and LY294002, showed that these inhibitors blocked both the insulin-stimulated translocation of GLUT4 and consequently, the increase in glucose uptake in adipocytes (Cheatham *et al.*, 1994; Clarke *et al.*, 1994; Yang *et al.*, 1996). Kinetic studies by Yang *et al* have shown that treatment with wortmannin dramatically reduces the GLUT4 exocytic rate constant with no marked perturbation of the endocytic rate constant (Yang *et al.*, 1996) . The same study also showed a slow reduction of basal glucose transport activity in wortamnnin-treated cells, consistent with a wortmannin effect on constitutive recycling as well as insulin-regulated exocytosis (refer to Section 1.6) (Yang *et al.*, 1996) .

However, following concerns regarding the specificity of wortmannin and LY294002, recent studies have provided more conclusive evidence of the involvement of p85-p110 PI 3-kinase in GLUT4 trafficking. Expression of a mutant of the p85 subunit of PI 3-kinase which is unable to bind the p110 catalytic subunit results in a parallel blockade of insulin-stimulated glucose transpoter translocation and insulin-stimulated PI 3-kinase activity in 3T3-L1 adipocytes (Kotani *et al.*, 1995). Furthermore, microinjection of the SH2 domains of p85 expressed as fusion proteins, into 3T3-L1 adipocytes, blocks insulin stimulation of glucose transport (Haruta *et al.*, 1995), coupled with the induction of glucose transporter translocation following the overexpression of a constitutively active form of PI 3-kinase (Tanti *et al.*, 1996),

provide strong evidence that insulin stimulation of PI 3-kinase is linked to the stimulation of GLUT4 translocation.

However, there is evidence to suggest that p85-p110 PI 3-kinase is also involved in the mitogenic pathway (Cheatham *et al.*, 1994) and is not exclusively part of the GLUT4 translocation machinery. Indeed, platelet-derived growth factor (PDGF) also stimulates cellular PI 3-kinase activity in 3T3-L1 adipocytes, but only insulin significantly stimulates glucose transport (Navé *et al.*, 1996). A possible explanation for this discrepancy is the differential subcellular targeting of PI 3-kinase activity as insulin stimulates PI 3-kinase in the microsomal fraction from which the glucose transporters translocate, while PDGF stimulates PI 3-kinase activity almost exclusively in the plasma membrane fraction of 3T3-L1 adipocytes (Ricort *et al.*, 1996). The inability to recruit PI 3-kinase activity to the correct intracellular location may also explain why the introduction of phosphopeptides containing the two tyrosine phophorylation motifs corresponding to the p85 association sites on IRS-1 in 3T3-L1 adipocytes, results in the activation of cellular PI 3-kinase but only produces a small stimulation in glucose transport (Herbst *et al.*, 1995).

1.15.3 Downstream Targets of PI 3-Kinase

The elements downstream of PI 3-kinase in the insulin-stimulated signalling pathways regulating GLUT4 translocation are poorly understood. A potential mechanism by which PI 3-kinase may affect membrane trafficking is the activation of members of the Ras superfamily of small GTP-binding proteins via GEFs (refer to Section 1.6). Interestingly, the stimulatory effect of guanosine 5'-[γ-thio]triphosphate (GTPγS) on glucose transport activity can overcome the wortmannin induced inhibition of insulin-stimulated glucose transport in 3T3-L1 adipocytes, suggesting that a GTP-binding protein lies downstream of PI 3-kinase activity (Clarke *et al.*, 1994). An obvious candidate for such a role is Rab4 as Shibata *et al* have recently shown Rab4 to lie downstream of PI 3-kinase activity (refer to

Section 1.13) (Shibata *et al.*, 1997). It is also possible that PI 3-kinase activation may enhance the budding of GLUT4 vesicles in response to insulin by promoting nucleotide exchange on an ARF-like small GTPase required for 'coat' formation (refer to Sections 1.4.2 and 1.6) (Seaman *et al.*, 1996a). Recently, GRP1, a molecule which specifically binds the product of PI 3-kinase, phosphoinositide-3,4,5-trisphosphate (PIP_3), and contains pleckstrin and sec7 homolgy domains which may be involved in nucleotide exchange (refer to Section 1.6) has been identified in adipocytes (Klarlund *et al.*, 1997). Furthermore, GRP1 has been shown to catalyse guanine nucleotide exchange of ARFs 1 and 5 *in vitro* (Klarlund *et al.*, 1998), consistent with the possibility that GLUT4 trafficking may indeed be regulated by ARF proteins. However, further *in vivo* studies are required to determine a role for both GRP1 and ARFs in GLUT4 trafficking.

Recent research has also focused on serine/threonine kinases downstream of PI 3-kinase that may regulate GLUT4. A prime candidate is Akt/protein kinase B (PKB), which has been found to be inhibitable by wortmannin (Burgering *et al.*, 1995) and activatable by insulin (Kohn *et al.*, 1995). Recent studies also suggest that insulin causes the recruitment of the β isoform of PKB to GLUT4-containing microsomal vesicles (Calera *et al.*, 1998). Furthermore, constitutively active PKB stimulates GLUT4 translocation in a range of cell types (Kohn *et al.*, 1996; Cong *et al.*, 1997; Hajduch, 1998), and it is claimed that a dominant inhibitory construct blocks this process (Cong *et al.*, 1997). However, in well controlled experiments using a mutant PKB with alanines substituted at phosphorylation sites threonine 308 and serine 473 as a dominant inhibitory construct in both CHO cells and 3T3-L1 adipocytes, protein synthesis but not insulin-stimulated transport was inhibited (Kitamaru *et al.*, 1998).

Other possible downstream targets include the protein kinase C ζ and λ, however studies are on going to determine whether these kinases contribute to glucose transport regulation. Taken together, there is not a clear consensus of data that any

of the known protein kinases downstream of PI 3-kinase directly mediates insulin action on glucose transport.

The characterisation of PI 3-kinase as a mediator of insulin-regulatable glucose transport has been a major advance as it acts as a point of convergence of signalling and membrane trafficking processes. However, the link between PI 3-kinase and the effector molecules that have been suggested as facilitating the complex process of insulin-stimulated GLUT4 translocation is incomplete at present but is subject to intense investigation.

1.16 Aims of this Study

The basis of this study was to further define the nature of the non-ablatable GLUT4 storage compartment and to characterise the mechanism of translocation of GLUT4 from this compartment to the plasma membrane in response to insulin.

To address these issues, I employed a technique referred to as compartment ablation analysis (refer to Section 1.10) to examine the protein composition of the non-ablatable storage compartment with the aim of further defining the relationship of this compartment, to other well characterised, intracellular membrane structures. I also used this technique to examine insulin-stimulated translocation of GLUT4 from the endosomal and non-ablatable post-endocytic compartments to the cell surface in response to insulin. The purpose of this was to determine whether insulin stimulates the translocation of GLUT4 to the cell surface independently of the recycling endosomal pathway.

It should be noted that some aspects of the above studies were carried out in collaboration with D. E. James and colleagues (University of Queensland, Australia). However, data provided by this group is included for comparative purposes only and is clearly indicated.

In addition, I analysed the role of ARF proteins and phospholipase D in insulin-stimulated GLUT4 translocation. As these proteins are known to be involved in regulated exocytosis, I wished to examine whether they may be components of the insulin-regulatable GLUT4 trafficking machinery.

Finally, as an extension of the compartment ablation studies, I set out to construct a chimeric cDNA comprising the signal sequence of the human growth hormone and horseradish peroxidase with the intention of targeting the resultant protein to the exocytic pathway in 3T3-L1 adipocytes. This would enable me to carry out ablation studies on the secretory pathway in these cells.

Table 1.1

Localisation and Functional Properties of Rab Proteins in Mammalian Cells

A summary of the involvement of Rab proteins in membrane traffic in mammalian cells is shown below (Novick *et al.*, 1997) (refer to Section 1.3.5).

Proteins	Localisation	Function
Rab 1A, 1B	ER-Golgi intermediate compartment	ER to Golgi transport, intra-Golgi transport
Rab 2	ER-Golgi intermediate compartment	ER to Golgi transport
Rab 3A	Synaptic vesicle, chromaffin granules	Regulated exocytosis in pancreatic acinar cells, adrenal chromaffin cells and mast cells
Rab 3B	Tight junction region in polarised epithelial cells	n.d
Rab 3C	Synaptic vesicles	n.d
Rab 3D	Zymogen granules in pancreatic acinar cells	n.d
Rab 4A, 4B	Early endosomes	Recycling pathway from endosomes to plasma membrane
Rab 5A, 5B, 5C	Plasma membrane; clathrin-coated vesicles; early endosomes	Plasma membrane to early endosome transport and homotypic fusion between endosomes
Rab 6	Middle Golgi-TGN	Intra-Golgi retrograde transport?
Rab 7	Late endosomes	Transport from early to late endosomes and lysosomes
Rab 8	Post-Golgi exocytic vesicles; tight junction in epithethial cells	Golgi to plasma membrane transport
Rab 9	Late endosomes and TGN	Transport from late endosomes to TGN
Rab 10	Golgi complex	n.d
Rab 11	TGN; constitutive secretory vesicles; secretory granules; recycling endosomes	Transport through recycling endosomes

n.d not determined

Table 1.2

Characterised Mammalian SNAREs Hypothesised to be Involved in Golgi to Plasma Membrane Transport

A summary of the SNARE proteins and the steps in membrane traffic between the Golgi and the plasma membrane in which they are thought to be involved, are shown below (Hay *et al.*, 1997) (refer to Section 1.5).

Name	Function or localisation	v- or t- SNARE?
Syntaxin 1A, B	Neurotransmission	t
VAMP1, 2	Neurotransmission & GLUT4 trafficking	v
SNAP25	Neurotransmission	t
Syntaxin 4	GLUT4 trafficking	t
Syntaxin 2, 3	Plasma membrane	t
SNAP23	Plasma membrane?	t
Cellubrevin	Constitutive endocytosis/exocytosis & GLUT4 trafficking	v

Figure 1.1

Model of the Potential Sites of Insulin Resistance in Adipose Tissue

Under basal conditions, approximately 95% of GLUT4 is sequestered within an intracellular compartment(s), the nature of which is poorly understood. GLUT4 undergoes a slow rate of constitutive recycling between the plasma membrane and the intracellular site, a process which is thought to occur through clathrin-coated pits and entry into the endosomal system. Upon insulin-stimulation, 40-50% of the intracellular pool translocates rapidly, giving rise to 20- to 30-fold increases in cell surface GLUT4 levels, and so accounting for the large increase in glucose transport under such conditions. As circulating glucose and insulin levels fall, GLUT4 is sequestered in the intracellular compartment. Potential sites of insulin resistance shown are as follows: (1) Reduced binding of insulin to the plasma membrane insulin receptor (IR) or impaired activation of the receptor associated tyrosine kinase. (2) Impaired intracellular insulin signalling pathway. Both defects would render cells insulin-resistant for glucose transport independently of any defects in transporter expression or function. (3) Defective translocation of GLUT4 to the cell surface. In this case, normal levels of GLUT4 are present in the intracellular compartment, but a defect in the mechanism responsible for moving this pool to the cell surface results in a reduced insulin-stimulated transport. (4) Reduction in the level of GLUT4 in the intracellular compartment. In this scenario, translocation of GLUT4 occurs as normal, but there is a reduced level of insulin-stimulated glucose transport due to a profound reduction in the GLUT4 available for translocation. (5) Mistargeting of GLUT4 to a non-translocatable compartment. This mislocalisation of GLUT4 to a site from which it cannot be targeted would have the effect of reducing insulin-stimulated glucose transport.

Figure 1.1

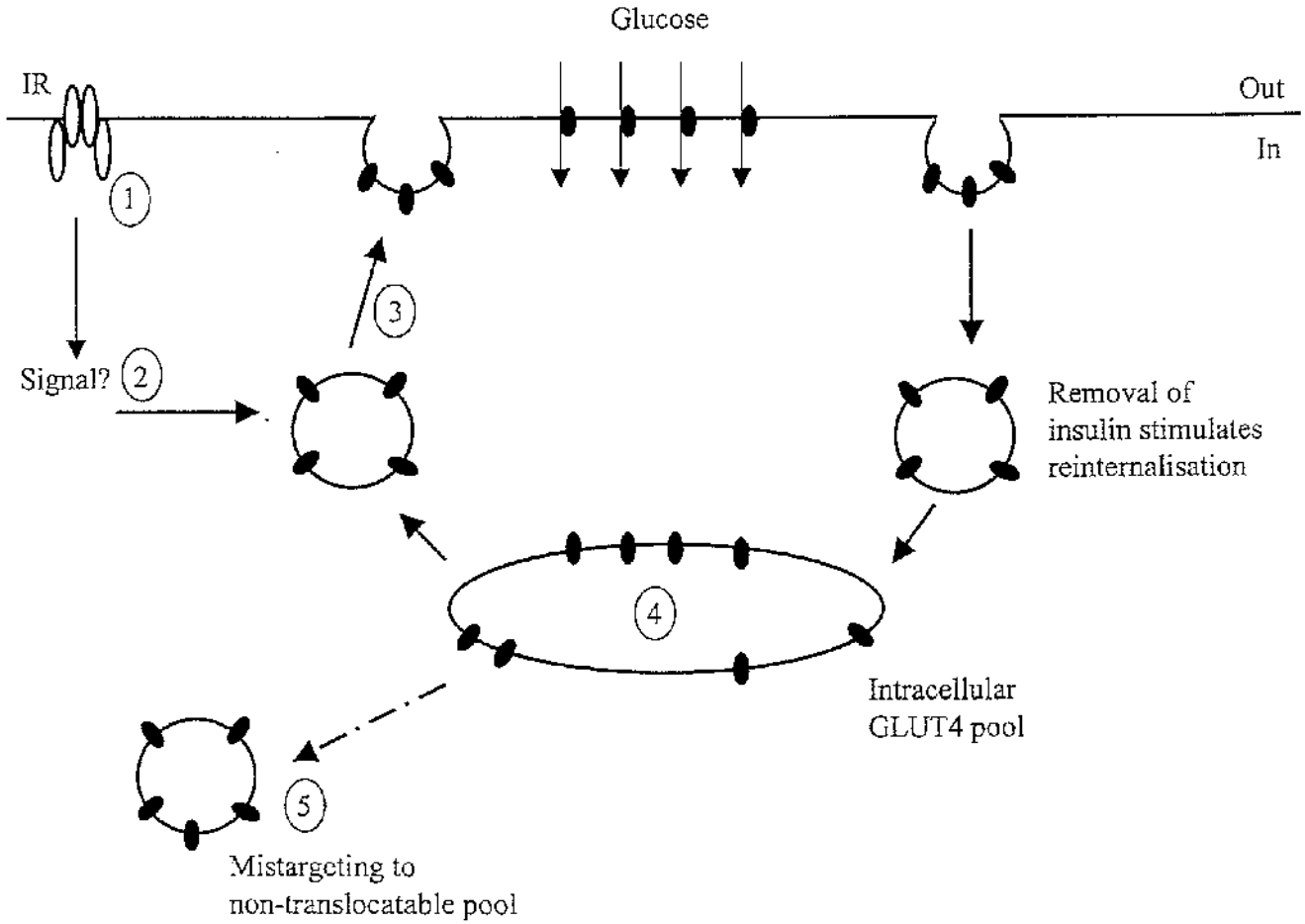
Glucose
IR
Out
In
1
Signal?
2
3
Removal of
insulin stimulates
reinternalisation
4
Intracellular
GLUT4 pool
5
Mistargeting to
non-translocatable pool

Figure 1.2

Model for the Intracellular Organisation of the Endocytic Pathway in a Mammalian Cell

Entry into the cell is mediated by caveolae, non-clathrin-coated vesicles (N-CCV), clathrin-coated pits and vesicles (CCP and CCV) and macropinosomes. The clathrin-coated vesicles that bud from the plasma membrane are coated with AP-2 adaptors as well as clathrin, and their formation is regulated by the GTPase dynamin. These vesicles deliver their cargo to early endosomes (EE), a process controlled by the small GTPase Rab5. Receptors that recycle back to the plasma membrane transit through a recycling endosome (RE) that is enriched in TfRs and in the SNARE protein cellubrevin. Whether this is a subcompartment of the early endosome or a distinct compartment, as drawn here, is not clear. Rab4 is proposed to control access into the recycling endosome. M6PRs (MPR), together with the small GTPase ARF1, promote the recruitment of AP-1 adaptors onto the TGN to drive assembly of CCVs from this compartment. Transport from the early endosome to the late endosome (LE) is mediated by endosomal carrier vesicles (ECVs).

Figure 1.2

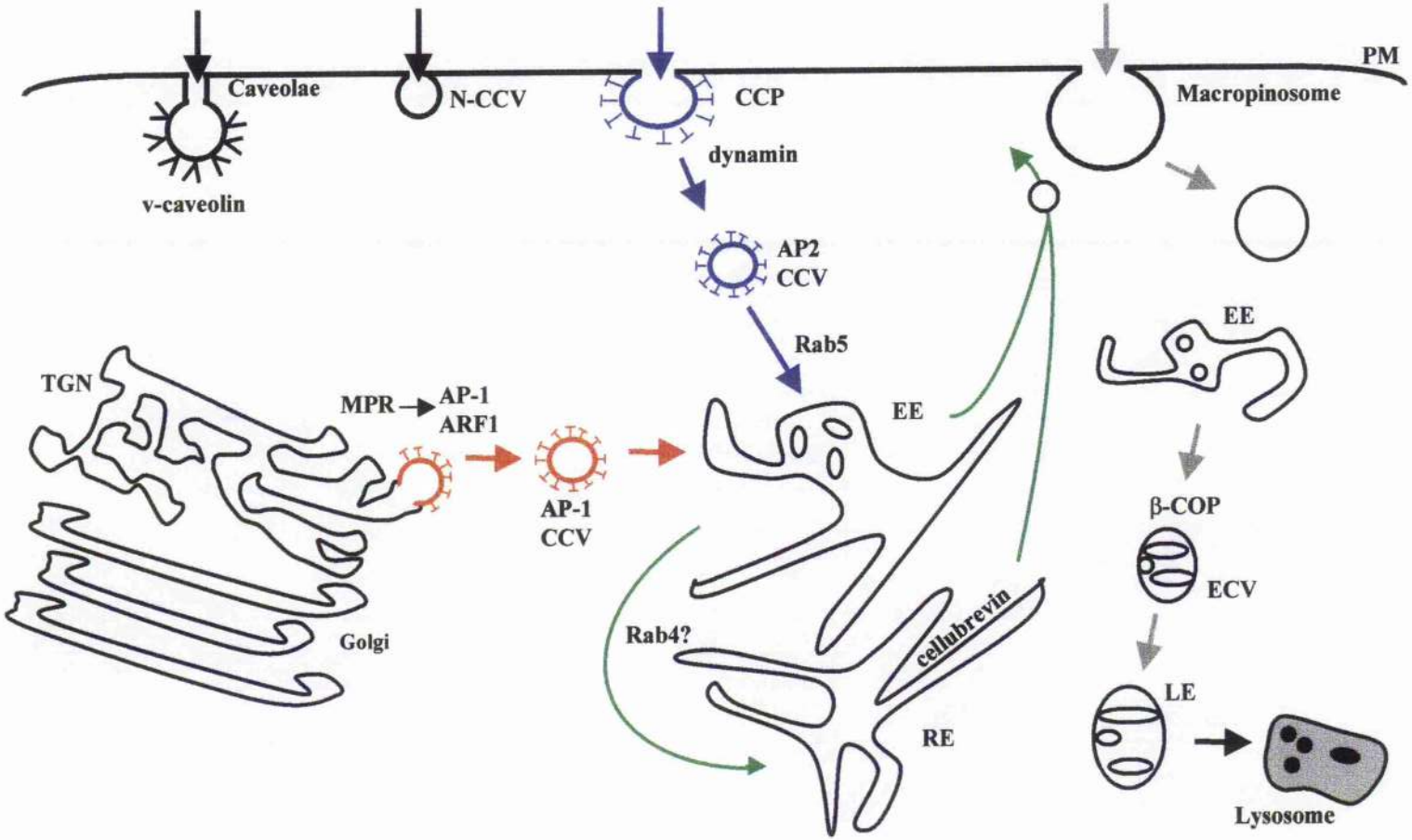
PM
Caveolae
N-CCV
CCP
Macropinosome
dynamin
v-caveolin
AP2
CCV
Rab5
EE
TGN
MPR
AP-1
ARF1
EE
β-COP
AP-1
CCV
ECV
Rab4?
cellubrevin
LE
RE
Golgi
Lysosome

Figure 1.3

The Proposed Functional Cycle of Rab Proteins

Rab-GDP is shown as a black circle labelled GDP with zigzagged lines indicating the attached isoprenyl lipid moieties; Rab-GTP is shown as a black oval labelled GTP with zigzagged lines attached; and Rab proteins that are in a state of nucleotide exchange/hydrolysis are shown as unlabelled black circles with zigzagged lines attached. (a) In the cytosol, Rab proteins are maintained in the GDP-bound inactive confirmation by Rab GDI. Rab GDI prevents indiscriminate membrane binding by Rab. (b) As Rab-GDP binds to the membrane of the donor organelle compartment or vesicle, GDI is displaced by a GDI displacement factor (GDF). (c) Exchange of GDP for GTP on Rab is catalysed by a GEF. Nucleotide exchange serves to activate the Rab protein and render it resistant to removal from the membrane by Rab GDI. (d) The transport vesicle buds from the donor compartment. (e) Binding of transport vesicles to acceptor compartments is mediated by Rab-GTP on the transport vesicle and probably an effector on the acceptor compartment. GTP hydrolysis is mediated by GAP. The release of vesicle contents (represented by dots) into the acceptor compartment is shown. (f) GDI can release Rab-GDP from the acceptor compartment and the cycle can begin again.

Figure 1.3

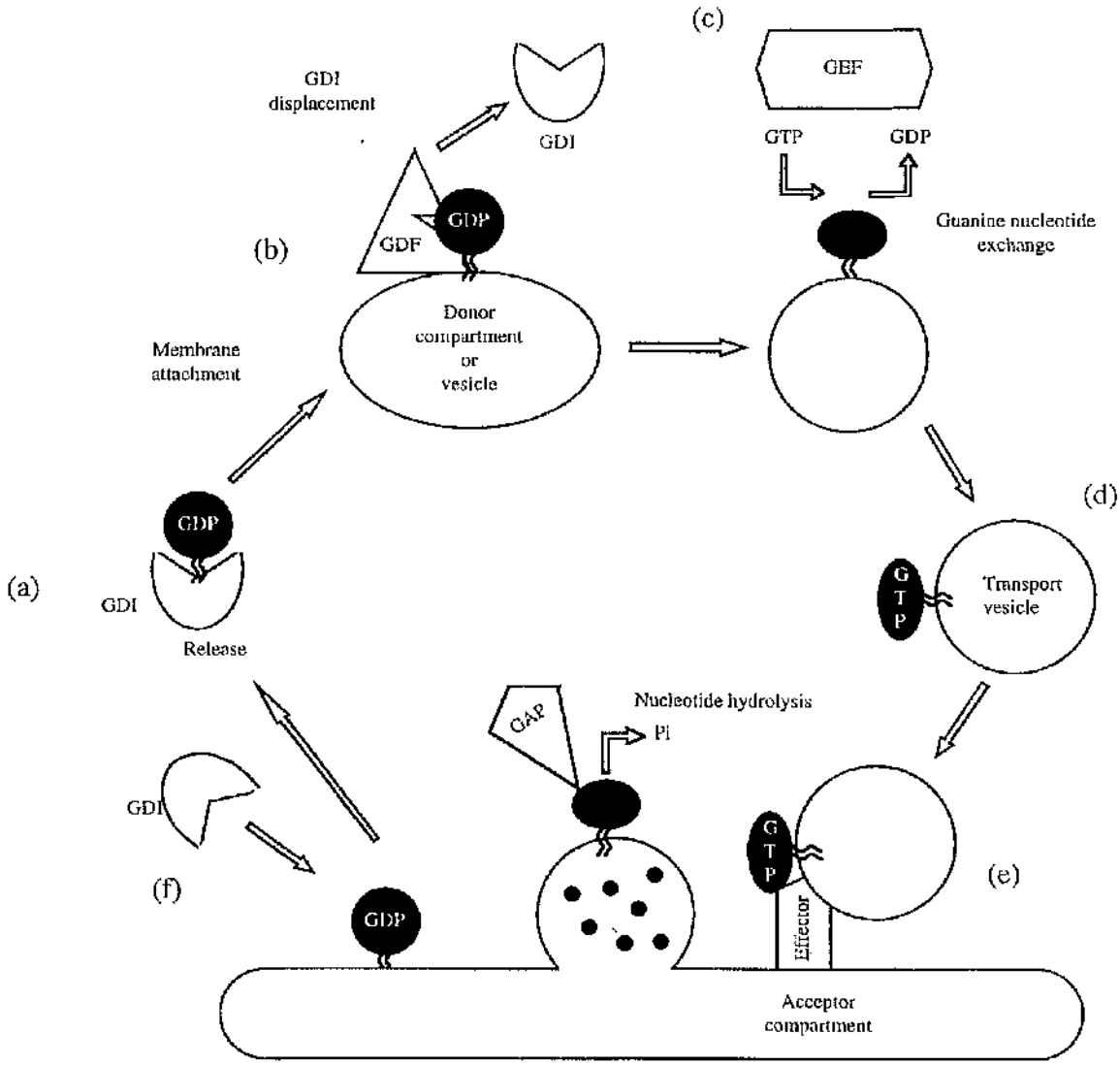
(c)
GEF
GTP
GDP
GDI
displacement
GDI
GDP
GDF
(b)
Guanine nucleotide
exchange
Donor
compartment
or
vesicle
Membrane
attachment
(d)
GDP
(a)
GDI
G
T
P
Transport
vesicle
Release
Nucleotide hydrolysis
GAP
Pi
GDI
(f)
G
T
P
(e)
GDP
Effector
Acceptor
compartment

Figure 1.4

Sorting Events at the TGN

Biochemicaly distinct coats are likely to specify protein sorting at the TGN. To attempt to distinguish the different sorting routes from each other, these coats are indicated by coloured symbols. The AP-1 complex (red) associates with clathrin at the TGN and sorts M6PRs to the endosome, whereas the AP-2 complex (green) associates with clathrin at the plasma membrane to mediate endocytosis. The AP-3 complex (red) is depicted as having a role in vesicle formation and anterograde transport from the TGN to sort cargo proteins such as LIMP II to lysosomes. In some specialised cells, AP-3 also appears to be involved in transport to lysosome-related storage granules such as melanosomes (Odorizzi *et al.*, 1998).

Figure 1.4

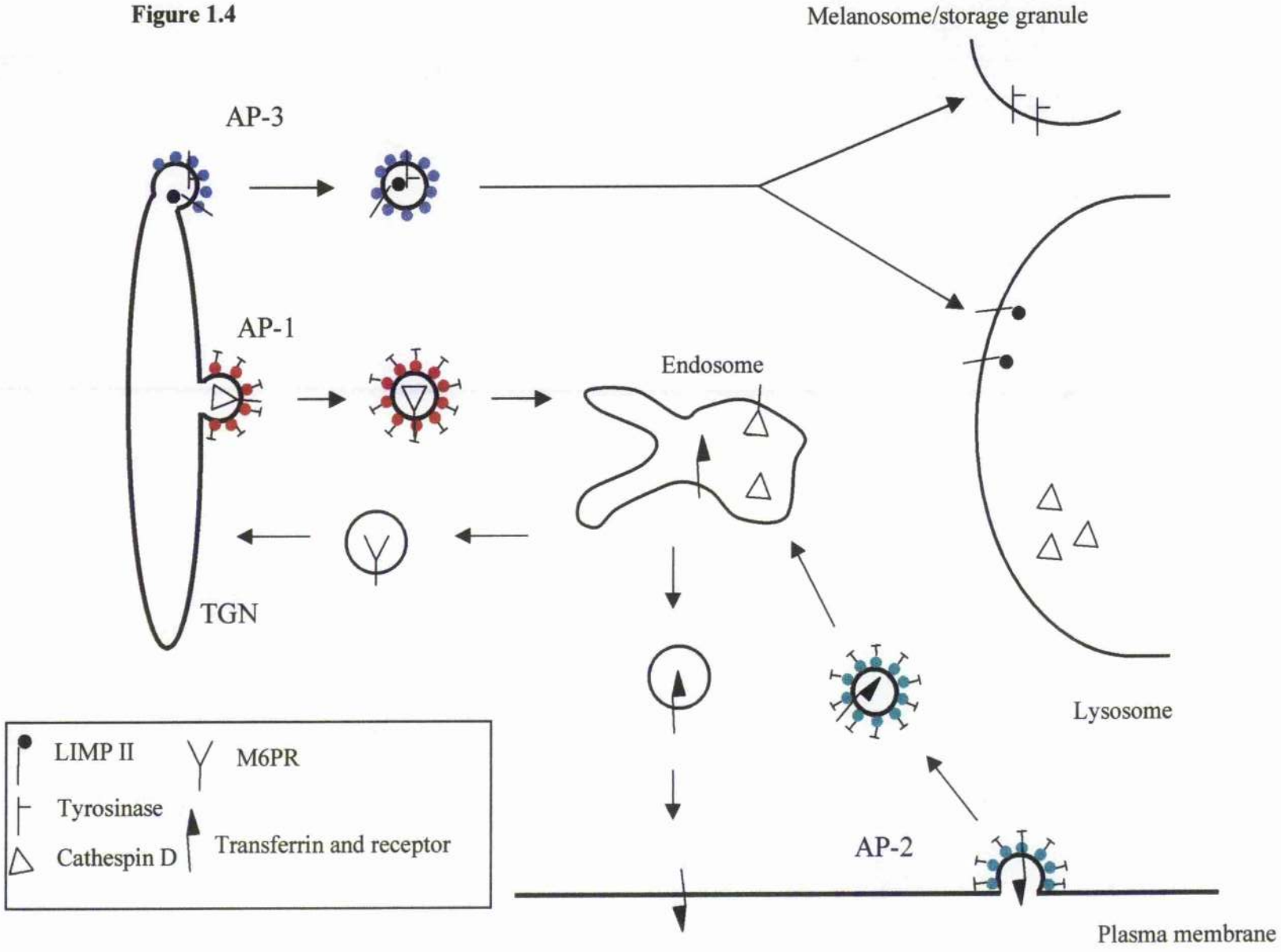
Melanosome/storage granule
AP-3
AP-1
Endosome
TGN
Lysosome
LIMP II
M6PR
Tyrosinase
Cathespin D
Transferrin and receptor
AP-2
Plasma membrane

Figure 1.5

Models of NSF/α-SNAP Action in SNARE-Mediated Docking and Fusion Reactions

(a) Original proposal, in which NSF/α-SNAP assembles onto the docked complex and rearranges protein-protein interactions to allow membrane fusion. This proposal suggested that the motion created by NSF/α-SNAP-dependent events directly triggered membrane fusion. (b) New model, which is consistent with vacuolar assembly, in which NSF/α-SNAP is required prior to SNARE docking. NSF/α-SNAP may be required to activate SNAREs for docking interactions. Although their role is not well understood, it is believed that Rab proteins may function to promote SNARE-complex assembly.

Figure 1.5

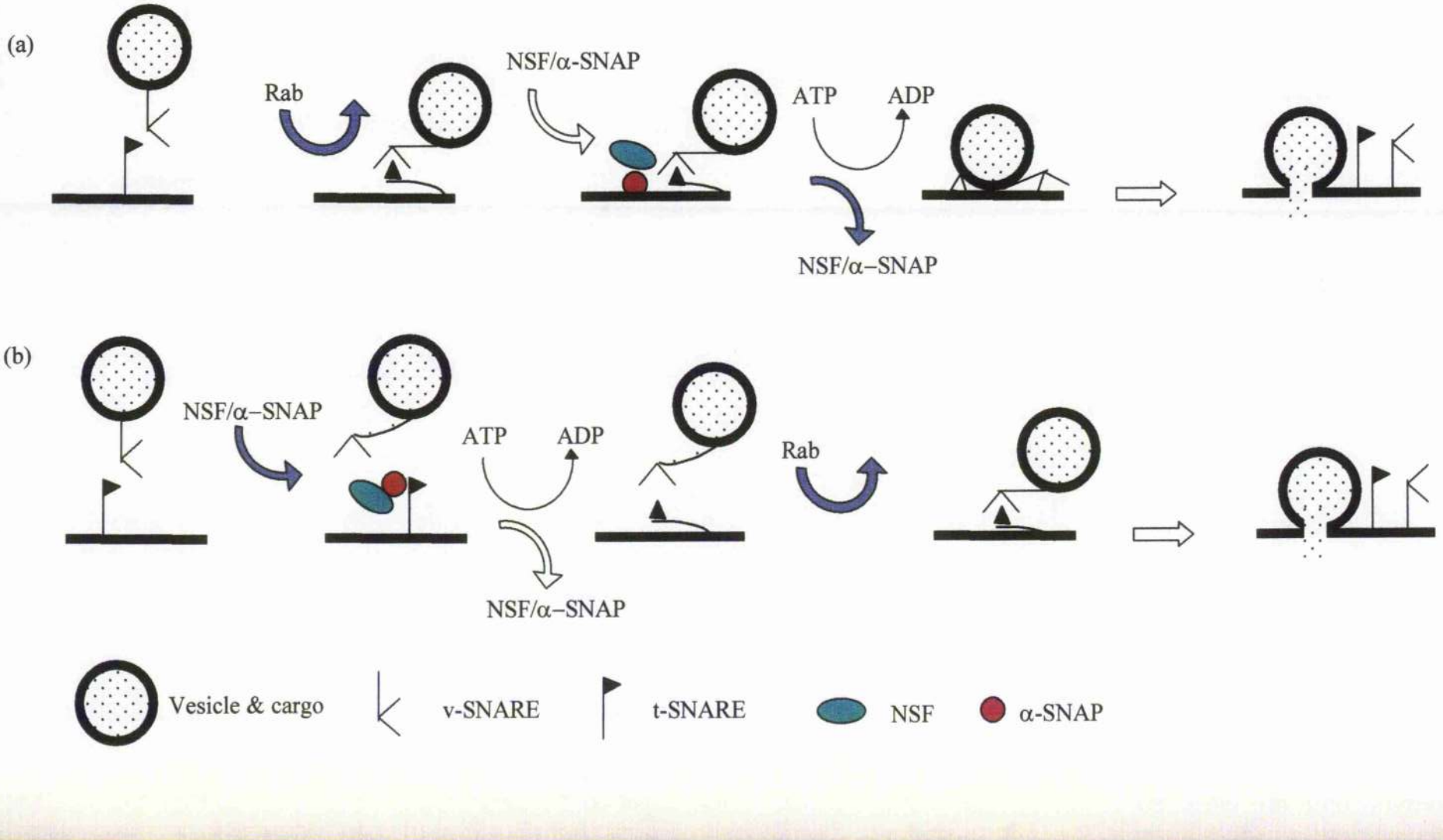
(a)
Rab
NSF/α-SNAP
ATP
ADP
NSF/α–SNAP
(b)
NSF/α–SNAP
ATP
ADP
Rab
NSF/α–SNAP
Vesicle & cargo
v-SNARE
t-SNARE
NSF
α-SNAP

Figure 1.6

Hypothetical Model for the Structure of the Facilitative Glucose Transporters

The protein is predicted to contain 12 transmembrane helices (1-12), with both the N- and C-termini intracellularly disposed. N-linked glycosylation can occur in the intracellular loop between helices 1 and 2. Conserved amino acids are indicated by the appropriate single letter code.

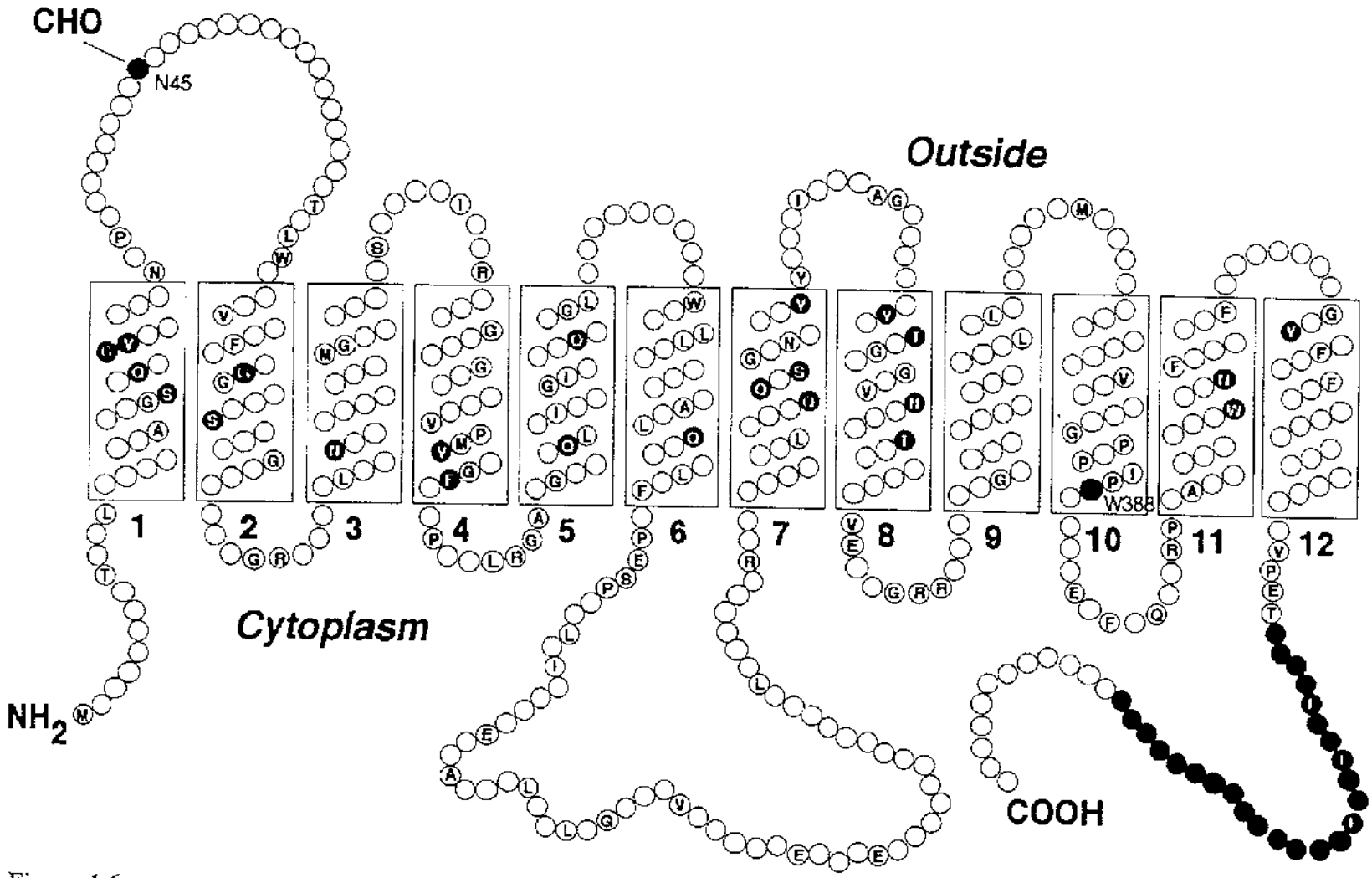

Figure 1.6

Figure 1.7

Membrane Protein Recycling Models

In the 2-pool model, the fully functional plasma membrane protein (T_p) is in equilibrium with only one intracellular pool (T_{ec}). In the 3-pool model, two distinct intracellular pools are designated, the early endosome pool (T_{ee}) and the tubulovesicular compartment (T_{tv}). In the 4-pool models, occluded forms are added to the plasma membrane occurring either before (T_{po}, the 4a-pool model) or after (T_{pc}, the 4b-model) the fully functional plama membrane pool. In the 5-pool model, two occluded plasma membrane pools are included occurring both before (T_{po}) and after (T_{pc}) the fully functional plasma membrane form of the protein (T_p). Two intracellular pools are also included, one associated with the early endosomes (T_{ec}) and the other associated with a tubulovesicular system (T_{tv}).

Figure 1.7

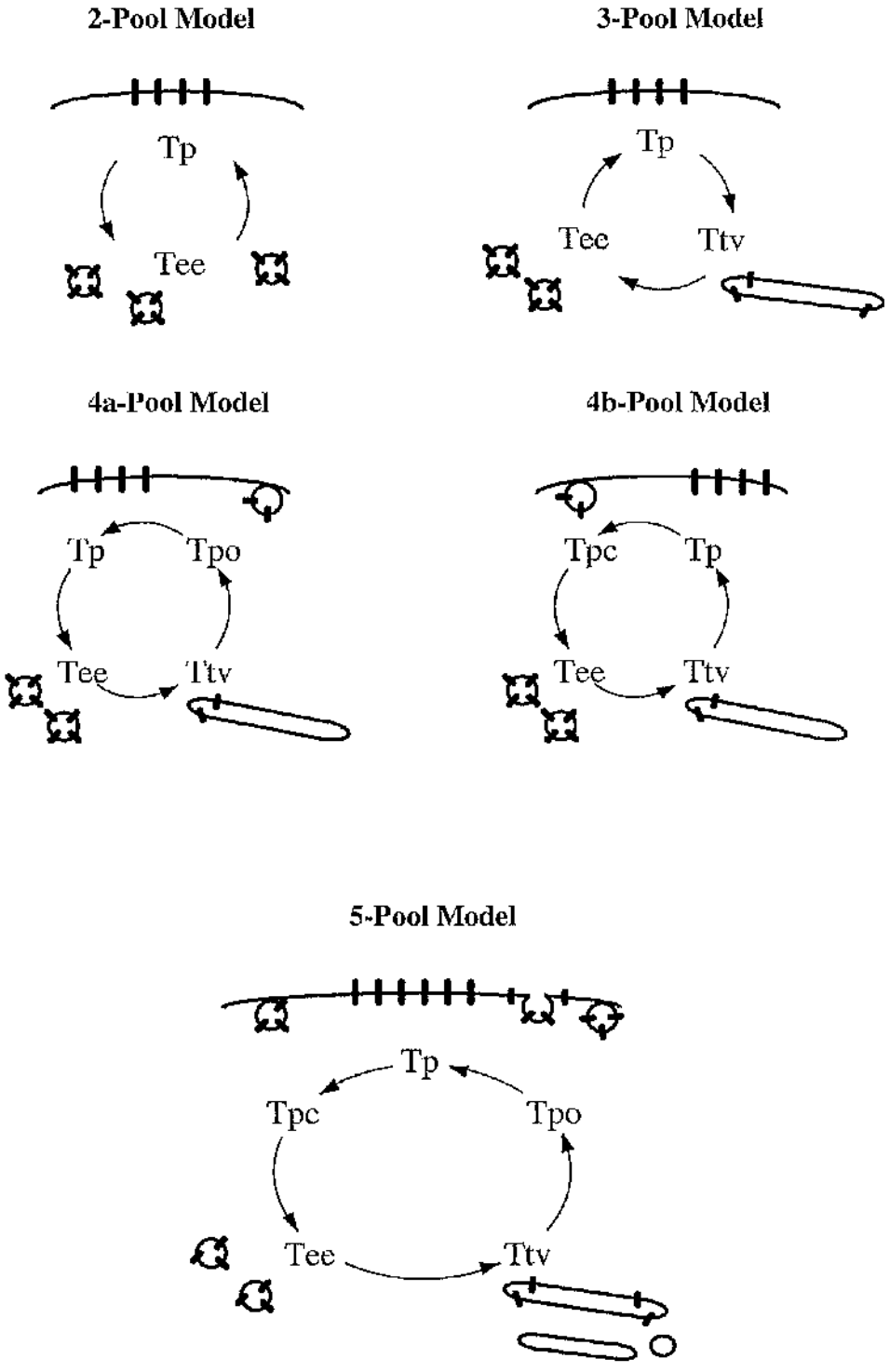
2-Pool Model
Tp
Tee
3-Pool Model
Tp
Tee
Ttv
4a-Pool Model
Tp
Tpo
Tee
Ttv
4b-Pool Model
Tpc
Tp
Tee
Ttv
5-Pool Model
Tp
Tpc
Tpo
Tee
Ttv

Figure 1.8

Models for the Biogenesis of the GLUT4 Storage Compartment in Insulin-Sensitive Cells

Each model (a-c) compares the trafficking of GLUT4 to a constitutively recycling protein such as the transferrin receptor (TfR) throughout the endosomal (E) and/or Golgi (G) systems. While models (a) and (b) suggest that GLUT4 and the TfR traffic through the same endosome, model (c) suggests that each molecule may traffic via distinct endosomes.

Figure 1.8

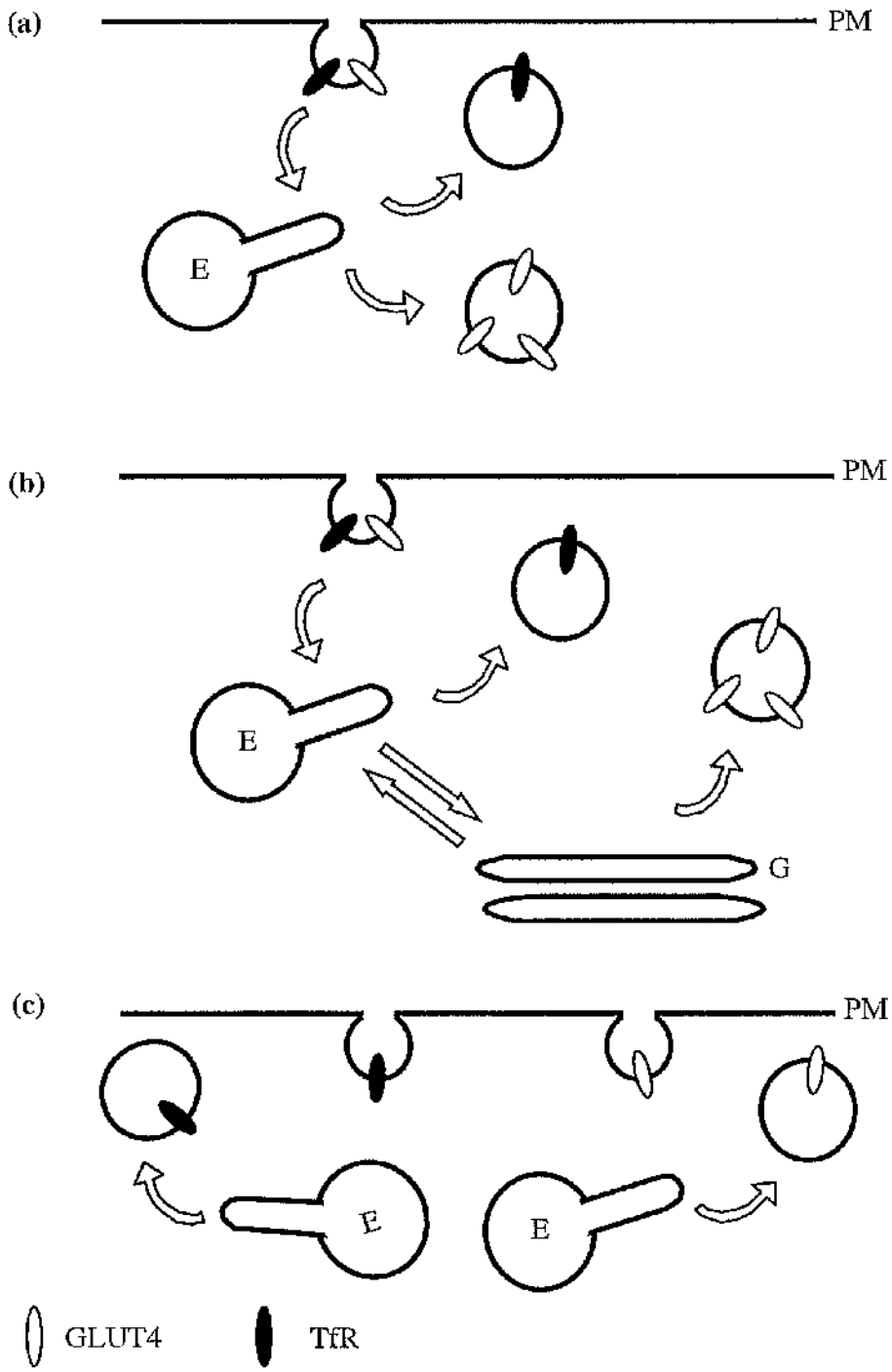

Figure 1.9

The Potential Role of SNARE Proteins in GLUT4 Trafficking

Based on the neuronal system, the following scheme of events is proposed for the insulin-dependent translocation of GLUT4 to the cell surface. A: in the non-insulin stimulated state, the core SNARE proteins VAMP2, syntaxin 4 and SNAP23 are prevented from interacting. Additional molecules predicted to be important for directing the interaction of SNAREs are also in an inactive state. Numbers include potential sites of insulin action and include: 1) activation of a GLUT4 vesicle specific Rab GTP exchange factor (GEF); 2) release of a putative VAMP2 blocking protein; 3) modulation of the affinity of Munc 18c for syntaxin 4; 4) release of a putative SNAP23 blocking protein. B: following the action of insulin, NSF and α–SNAP prime v- and t-SNAREs into a docking competent state in an ATP-dependent manner. GEF loads the GLUT4 vesicle Rab with GTP and the latter protein adopts an activated confirmation and/or recruits additional molecules to the vesicle surface (not shown). C: GLUT4 vesicles are actively transported to the cell surface where a SNARE complex is assembled. GTP-Rab displaces Munc 18c from syntaxin 4. This may be the rate limiting step in the formation of the SNARE complex. D: following SNARE docking, several additional steps may be necessary for lipid mixing and bilayer fusion. Lipid kinases and other GTPases are probably involved. Ultimately, insulin leads to an increase in the number of GLUT4 molecules at the cell surface and to the net rate of glucose transport into the cell. Question marks (?) refer to unidentified and/or hypothetical steps and proteins.

Figure 1.9

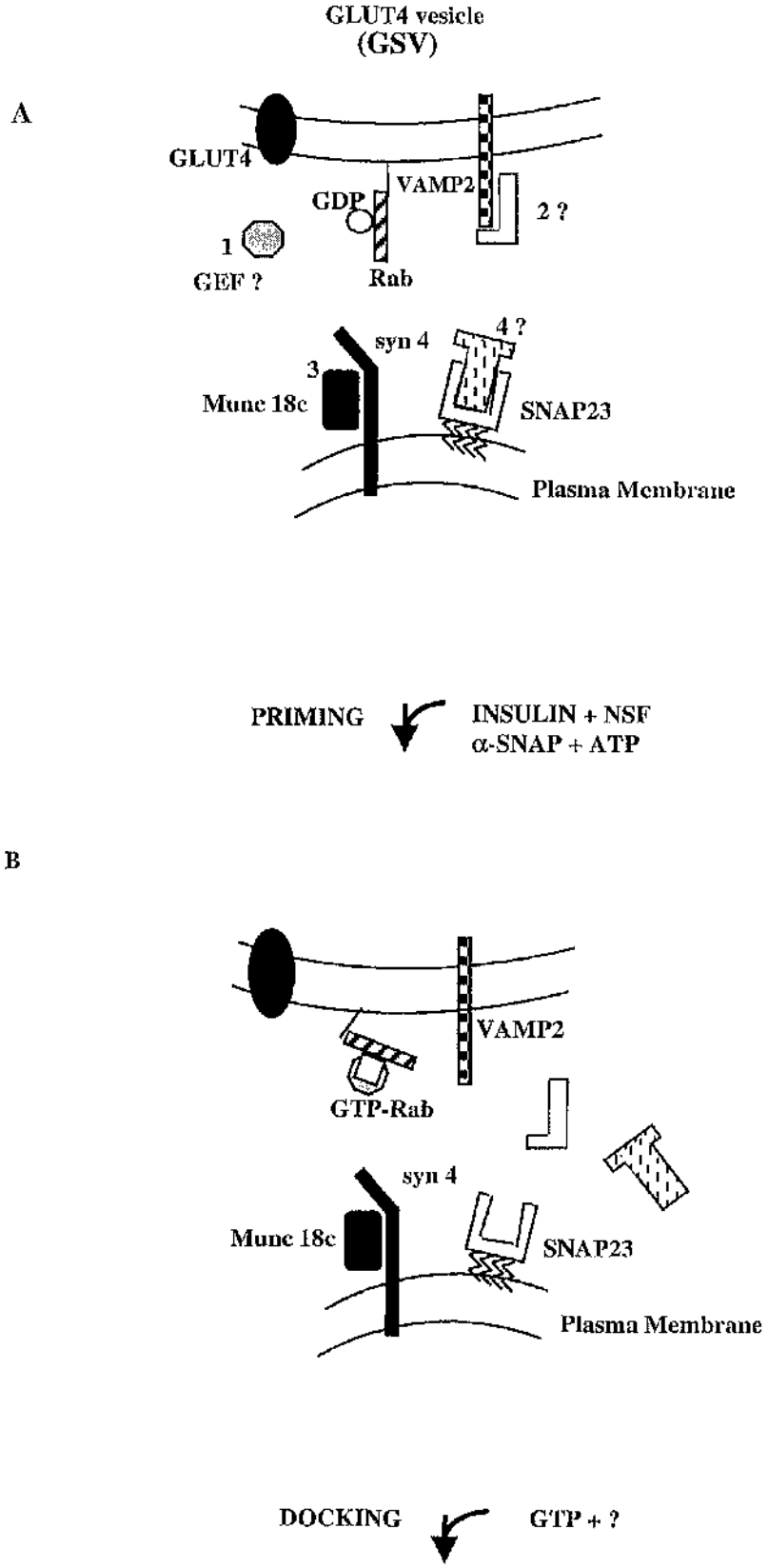
GLUT4 vesicle
(GSV)
A
GLUT4
GDP
VAMP2
2 ?
1
GEF ?
Rab
syn 4
4 ?
3
Munc 18c
SNAP23
Plasma Membrane
PRIMING
INSULIN + NSF
α-SNAP + ATP
B
VAMP2
GTP-Rab
syn 4
Munc 18c
SNAP23
Plasma Membrane
DOCKING
GTP + ?

Figure 1.9 cont:

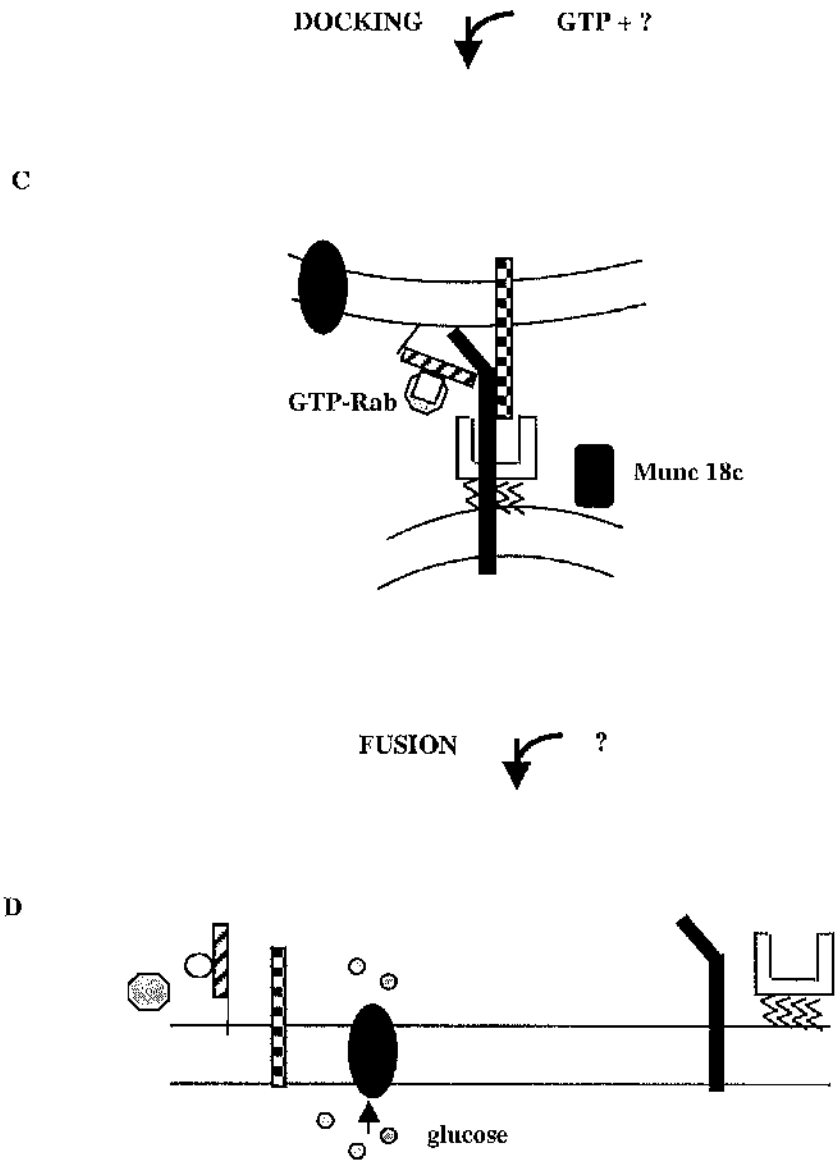

Figure 1.10

Insulin Signalling Pathways

Schematic diagram showing the role of receptor substrates such as IRS-1 as a multisite docking protein for SH-2 containing proteins and the progression of both mitogenic and metabolic signals (Yenush and White., 1997).

Figure 1.10

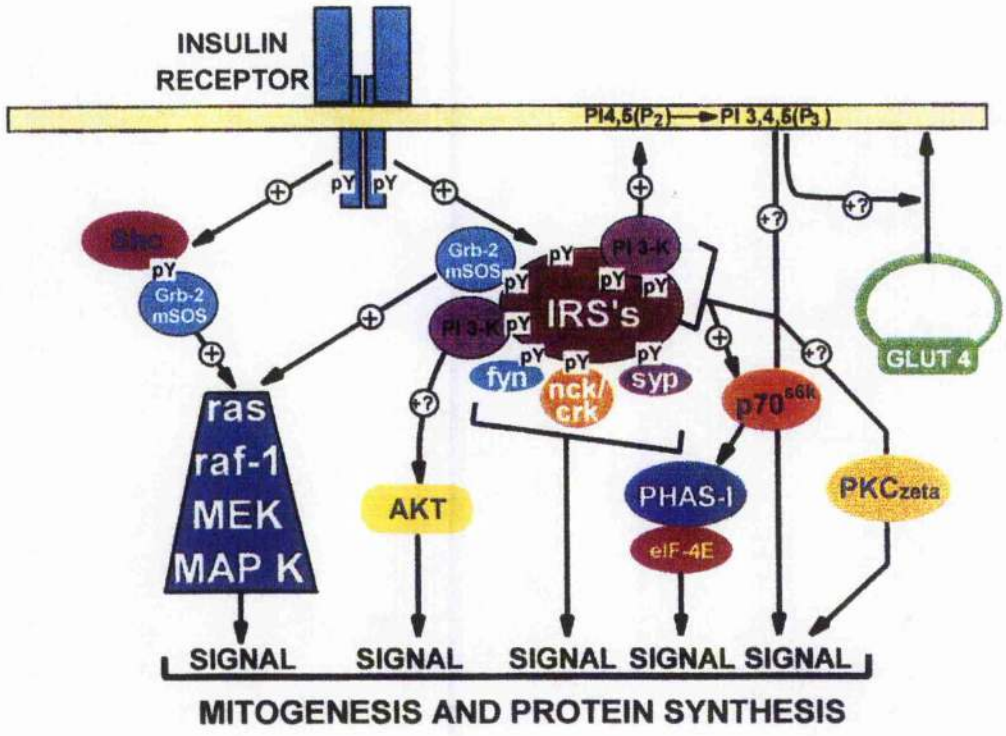
INSULIN
RECEPTOR
PI4,5(P2) → PI 3,4,5(P3)
pY
pY
Shc
pY
Grb-2
mSOS
Grb-2
mSOS
PI 3-K
pY
pY
pY
IRS's
PI 3-K
pY
pY
pY
pY
fyn
nck/
crk
syp
p70 s6k
GLUT 4
ras
raf-1
MEK
MAP K
AKT
PHAS-I
eIF-4E
PKCzeta
SIGNAL
SIGNAL
SIGNAL
SIGNAL
SIGNAL
MITOGENESIS AND PROTEIN SYNTHESIS

Chapter 2

Materials and Methods

2.1 Materials

All reagents used in the course of the project were of a high quality and were obtained from the following suppliers:

2.1.1 General Reagents

Bio-Rad Laboratories Ltd, Hemel Hempstead, Hertfordshire, UK

Cellophane membrane backing

N, N, N', N'-tetramethylethylenediamine (TEMED)

Bio-Rad protein assay dye reagent concentrate

New England Biolabs (UK), Ltd, Hitchin, Hertfordshire, UK

Prestained protein marker, broad range (6-175kDa)

Fisons, Loughborough, Leicestershire, UK

Ammonium persulphate

Glucose

Glycerol

Glycine

N-2-hydroxyethylpiperazine-N'-2-ethanesulphonic acid (HEPES)

Hydrochloric acid (HCL)

Methanol

Potassium chloride (KCl)

Sodium dodecyl sulphate (SDS)

Sodium chloride (NaCl)

Sodium dihydrogen orthophosphate dihydrate ($NaH_2PO_4.2H_2O$)

Sodium diaminoethanetetra-acetic acid (EDTA)

Sodium hydrogen carbonate ($NaHCO_3$)

Trichloroacetic acid

Gibco BRL, Paisley, Lanarkshire, UK

Tris base

30% acrylamide/bisacrylamide

Kodak Ltd, Hemel Hempstead, Hertfordshire, UK

X-Omat S film

Merck Ltd (BDH), Lutterworth, Leicestershire, UK

Calcium chloride hexahydrate

Dimethyl sulphoxide

Magnesium chloride hexahydrate

Packard Instrument B.V. -Chemical Operations, Groningen, The Netherlands

Ultima-Flo scintillation fluid

Premier Brands UK, Knighton Adbaston, Staffordshire, UK

Marvel powdered milk

Schleicher & Schuell, Dassel, Germany

Nitrocellulose membrane (pore size:0.45μM)

Whatman International Ltd, Maidstone, UK

Whatman No.1 filter paper

Whatman No.3 filter paper

Amersham International Plc, Aylesbury, Buckinghamshire, UK

Horseradish peroxidase (HRP)-conjugated donkey anti-rabbit IgG antibody

Horseradish peroxidase (HRP)-conjugated sheep anti-mouse IgG antibody

ECL Western blotting detection reagents

East Acres Biologicals, Southbridge, Massachusetts, USA

Rabbit anti-human GLUT-1 antibody

NEN Dupont (UK) Ltd, Stevenage, Hertfordshire, UK

[^{3}H] 2-deoxy-D-glucose

[^{14}C] sucrose

[^{125}I] conjugated goat anti-rabbit IgG antibody

[^{125}I] transferrin

Calbiochem-Novabiochem (UK) Ltd, Nottingham, UK

α-toxin, *Staphlococcus aureus*

2.1.2 Cell Culture Materials

American Type Culture Collection, Rockville, USA

3T3-L1 fibroblasts

Gibco BRL, Paisley, Lanarkshire, UK

Foetal calf serum (FCS)

Sigma Chemical Company Ltd, Poole, Dorset, UK

Dulbecco's modified Eagle's medium (without sodium pyruvate, with 4500mg/L glucose) (DMEM)

10000U/ml penicillin, 10000U/ml streptomycin

New born calf serum (NCS)

Trypsin/EDTA solution

Collagen

AS Nunc, DK Roskilde, Denmark

50 ml centrifuge tubes

Costar

6 cm cell culture plates

75cm^2 cell culture flasks

Falcon

10 cm cell culture plates

6-well cell culture plates

Bibby Sterilin Ltd, Stone, Staffordshire, UK

Sterile pipettes

13.5 ml centrifuge tubes

Bayer plc, Newbury, Berkshire, UK

Ciproxin

2.2. General Buffers

2.2.1 Phosphate Buffered Saline (PBS)

150mM NaCl, 10mM $NaH_2PO_4.2H_2O$, pH 7.4.

2.2.2 Krebs Ringer Phosphate (KRP) Buffer

64mM NaCl, 2.5mM KCl, 2.5mM $NaH_2PO_4.2H_2O$, 0.6mM $MgSO_4.7\ H_2O$, 0.6mM $CaCl_2$, pH 7.4.

2.2.3 HES Buffer

255mM sucrose, 20mM N-2-hydroxyethylpiperazine-N'-2-ethanesulphonic acid (HEPES) and 1mM EDTA, pH 7.4.

Unless otherwise indicated, all remaining chemicals were supplied by Sigma Chemical Company Ltd, Poole, Dorset, UK.

2.3 Cell Culture

2.3.1 3T3-L1 Murine Fibroblasts

3T3-L1 fibroblasts were cultured in 75cm^2 flasks containing DMEM/10% (v/v) newborn calf serum and 1% (v/v) penicillin and streptomycin. 1% (v/v) ciproxin was added to the media when required to prevent bacterial infection. Cells were cultured at 37°C in a humidified atmosphere of 10% CO_2 and the media was replaced every 48 h. When subconfluent (showing 80% confluency) the cells were passaged into 6-well or 10cm culture plates and a 75cm^2 carry over flask. Cells were cultured to 4 days post confluency and then differentiated into adipocytes.

2.3.2 Trypsinisation and Passage of 3T3-L1 Fibroblasts

Following aspiration of media from a 75cm^2 flask, 1ml of trypsin/EDTA solution was added to wash the remaining media from the monolayer of cells. In turn, this was aspirated and 3ml of trypsin/EDTA solution was added and the flask was incubated at 37°C in a humidified atmosphere of 10% CO_2 for 5 min. Careful agitation of the flask resulted in the cells being lifted from the surface of the flask. This cell suspension was then added to a maximum volume of 230ml DMEM/10% (v/v) newborn calf serum and 1% (v/v) penicillin and streptomycin. With continuous agitation the cells were split between 10cm culture plates and /or 6-well culture plates and 2 x 75cm^2 flasks.

2.3.3 Differentiation of 3T3-L1 Fibroblasts

Differentiation media of DMEM/10% (v/v) foetal calf serum, 1% (v/v) penicillin and streptomycin, 0.25μM dexamethasone, 0.5mM methyl isobutylxanthine and 1μg/ml insulin was prepared as outlined below.

A stock of 2.5mM dexamethasone (in ethanol) was diluted 1:20 with DMEM/ 10% (v/v) foetal calf serum, 1% (v/v) penicillin and streptomycin immediately prior to use yielding a 500X stock solution. A 500X sterile solution of methyl isobutylxanthine (IBMX) was prepared by dissolving 55.6mg IBMX in 1ml of 2M KOH and passing the solution through a 0.22 micron filter. Insulin (1mg/ml) was prepared in 0.01M HCL and filter sterilised using a 0.22 micron filter as before. Differentiation media was prepared by adding both the dexamethasone and IBMX solutions to a 1X concentration in DMEM/10% (v/v) foetal calf serum, 1% (v/v) penicillin and streptomycin and then adding insulin to a final concentration of 1μg/ml.

3T3-L1 fibroblasts were cultured on 6-well or 10cm culture plates until 4 days post confluency. The growth media was aspirated and replaced with differentiation media. After 48 h, this media was replaced with DMEM/10% (v/v) foetal calf serum, 1% (v/v) penicillin and streptomycin and 1μg/ml insulin. The cells were incubated in this media for a further 48 h. Following differentiation, the media was replaced with DMEM/10% (v/v) foetal calf serum, 1% (v/v) penicillin and streptomycin. The media was changed every 48 h and the cells were used 8-14 days post differentiation.

2.3.4 Freezing and Storage of Cells

Cells were cultured to 80% confluency, the media was aspirated and 1ml of trypsin/EDTA solution was added to wash the remaining media from the monolayer of cells. In turn, this was aspirated and 3ml of trypsin/EDTA solution was added and the flask was incubated at 37°C in a humidified atmosphere of 10% CO_2 for 5 min. Careful agitation resulted in the cells being lifted from the surface of the flask. 3ml of DMEM/10% (v/v) newborn calf serum, 1% (v/v) penicillin and streptomycin was added to the cell suspension and gently triturated over the surface of the flask. The cell suspension was then transferred to a sterile falcon tube and centrifuged at 2000 x g for 4 min. Following aspiration of the supernatant the pellet was 'flicked'

gently and then resuspended in 1ml of DMEM/10% (v/v) newborn calf serum, 1% (v/v) penicillin and streptomycin and 10% (v/v) DMSO. The suspension was then transferred to a 1.8ml polypropylene cryo-vial and placed at -80°C overnight to freeze slowly before being stored in a liquid nitrogen vat.

2.3.5 Resurrection of Frozen Cell Stocks from Liquid Nitrogen

A vial of cells was removed from from liquid nitrogen, transferred immediately to a 37°C water bath and thawed. The cell suspension was then pipetted into a 75cm culture flask containing DMEM/10% (v/v) newborn calf serum, 1% (v/v) penicillin and streptomycin and ciproxin which had previously been equilibrated at 37°C in a humidified atmosphere of 10% CO_2. The media was replaced after 48 h and the cells were cultured as described above.

2.3.6 Collagen Coating of Cell Culture Plastic Ware

Collagen-coated plates were often used for permeabilisation experiments, PM lawn assays and stable transfectants to enhance adhesion of the cells to the plate surface upon differentiation. A solution of collagen in acetic acid was used to wash the plates leaving a thin film coating. Plates were then dried in a sterile flow hood and irradiated with U.V light overnight. Prior to use, plates were washed with serum-free DMEM to remove any traces of acetic acid.

2.4 Antibody Preparations

The anti-GLUT4 antibodies used were either a mouse monoclonal antibody (1F8) (James *et al.*, 1988) provided by Professor David James (University of Queensland, Australia), or rabbit polyclonal antibodies against a peptide comprising the C-terminal 14 amino acid residues of the human isoform of GLUT4 .

2.4.1 Purification of Anti-GLUT4 Antibody

This procedure required the use of an affinity column consisting of Sepharose beads to which an antigenic peptide (C-terminal 14 amino acid residues) of the human GLUT4 isoform was covalently attached (Brant *et al.*, 1993).

Following equilibration of the column with approximately 20ml of PBS (see Section 2.2.1) 300µl of 10X PBS was added to 2.7ml antisera (raised against the GLUT4 C-terminal peptide) and applied to the column. The column was incubated for 15 min at room temperature and then washed with PBS until all the brown coloured eluant had been collected. The eluant was reapplied and again incubated in the column for 15 min at room temperature. This procedure was repeated a further four times allowing the antibodies which recognised the Sepharose-conjugated peptide to bind. Following the final incubation, the column was washed with PBS, until the eluant gave an O.D. reading at 280nm of zero. The GLUT4 antibody was eluted with 2M glycine, pH 2, collected in 1ml fractions and the O.D. reading at 280nm determined for each fraction. The fractions with the highest O.D. readings were pooled and 1M Tris (pH 6.8) was added to pH 7.0. This was dialysed overnight against PBS, at 4°C and finally, aliquoted, snap frozen and stored at -80°C.

2.5 Protein Assay

Protein concentration was measured using the Bradford assay. Protein samples were made up to a final volume of 25µl with distilled H_2O in plastic cuvettes. A standard curve was produced by preparing a series of BSA samples 0, 1, 2, 5, 10, 12, 15 and 20µg (i.e 0, 1, 2, 5, 10, 12, 15 and 20µl of BSA 1mg/ml in 25µl). Bio-Rad protein assay reagent concentrate was diluted 1:4 with distilled H_2O and 1ml was added to each sample. The cuvettes were covered with parafilm and inverted to ensure mixing before the absorbance was read at 495nm. A standard curve was plotted and the concentrations of the unknown protein samples determined.

2.6 SDS/Polyacrylamide Gel Electrophoresis

SDS/polyacrylamide gel electrophoresis was carried out using Bio-Rad mini-PROTEAN II or Hoefer large gel apparatus. The percentage of acrylamide in each gel ranged between 7.5% - 15%, according to the molecular weight of the protein to be detected. All reagents were of electrophoresis grade.

On assembly of either Bio-Rad mini-PROTEAN II or Hoefer large gel units, the separating gel was prepared using 30% acrylamide/bisacrylamide, 100mM Tris-HCL (pH 8.8), 10% (w/v) SDS, polymerised with 0.1% (w/v) ammonium persulphate and 0.019% (v/v) N,N,N',N'-tetramethylethylenediamine (TEMED). The stacking gels of 2 and 5cm respectively, were prepared using 30% acrylamide/bisacrylamide, 150mM Tris-HCL (pH 6.8), 10% (w/v) SDS polymerised with 0.1% (w/v) ammonium persulphate and 0.019% TEMED.

Protein samples were resuspended in 1X SDS PAGE sample buffer (93mM Tris-Cl pH6.8, 20mM dithiothreitol [added immediately before use], 1mM sodium EDTA, 10% (w/v) glycerol, 2% (w/v) SDS, 0.002% (w/v) bromophenol blue) and loaded onto the wells in the stacking gel. Broad-range pre-stained molecular weight markers [Mr 6-175 kDa (Biolabs)] were used routinely. Gels were electrophoresed in electrode buffer (120mM Tris, 40mM glycine and 0.1% (w/v) SDS, pH 8.3) at a constant voltage to ensure good separation of the molecular weight markers.

2.7 Western Blotting of Proteins

Proteins were separated by SDS/polyacrylamide gel electrophoresis as previously described. A sponge pad, two sheets of Whatman 3mm filter paper and a sheet of nitrocellulose membrane (pore size 0.45mM), cut to size and previously soaked with transfer buffer (25mM $NaH_2PO_4.2H_2O$, pH 6.5) were placed on the black plate of the gel cassette holder. The gel was then placed on top of the nitrocellulose

membrane and any air bubbles were gently removed. The 'sandwich' was completed with two more sheets of filter paper and a sponge pad as before. Transfer was carried out using a Bio-Rad mini or Bio-Rad trans-blot electrophoretic cell containing transfer buffer at a constant current of 250mA for 3 h. The efficiency of transfer was determined by staining the nitrocellulose with Ponceau S solution prior to blocking.

2.8 Immunodetection of Proteins

Following transfer, non-specific binding sites on the nitrocellulose membrane were blocked by shaking for 1 h in 5% (w/v) dried skimmed milk (see section 2.1.1) in TBST-1 buffer (20mM Tris, 150mM NaCl, 0.2% Tween-20, pH 7.4).

The nitrocellulose membrane was then transferred to a plastic pocket containing primary antibody in 1% (w/v) dried skimmed milk in TBST-1 buffer at the appropriate dilution and shaken overnight at room temperature. Following five washes with TBST-1 buffer over a period of 1 h, the membrane was incubated in 1% (w/v) dried skimmed milk in TBST-1 buffer with secondary antibody, either ^{125}I-labelled goat anti-rabbit IgG (1μCi/20ml) or the appropriate HRP-linked IgG (1:1000 dilution) for 1 h at room temperature. The membrane was then washed a further five times as before.

2.8.1 Using Autoradiography

Following incubation with ^{125}I-labelled goat anti-rabbit and subsequent washing, the membrane was dried overnight between two sheets of Bio-Rad cellophane membrane backing at room temperature. The dried membrane was then mounted in an autorad holder and exposed to Kodak X-Omat S film for 12-24 h at -80°C. The film was developed using an X-OMAT processor.

2.8.2 Using the Enhanced chemiluminescence (ECL) Detection System

Following incubation with the appropriate HRP-linked IgG and subsequent washing, the membrane was washed in distilled H_2O. Equal volumes of Amersham 'detection reagent 1' and 'detection reagent 2' were mixed and the membrane was immersed and shaken in this mixture for 90 s. The membrane was then 'blotted' dry with blue roll, wrapped in cling film and exposed to Kodak film. The film was developed using an X-OMAT processor.

2.9 Endosome Ablation

2.9.1 Preparation of Tf-HRP Conjugate

Preparation of Tf-HRP protein conjugate was carried out as described by Kishida *et al* (Kishida *et al.*, 1975)

Buffer 1 (0.1M NaCl/10mM $NaPO_4$, pH7.2) was prepared by adding acid ($NaCl/NaH_2PO_4$) to alkali ($NaCl/Na_2HPO_4$) to pH7.2. 150mg of horseradish peroxidase (HRP) was dissolved in 7.5ml of buffer 1, transferred to dialysis tubing (previously boiled in 2% $NaHCO_3$, 10mM EDTA and stored in 50% ethanol:50% H_2O) and dialysed at 4°C overnight against 2-4 litres of the same buffer. Following dialysis, 3g of succinate (disodium salt) was added to the protein solution at room temperature. At 0°C, 1.05g of crushed succinic anhydride was added and the mixture was stirred for 30 min at 0°C and then for a further 30 min at room temperature.

Meanwhile, 4 X 20ml G-50 sephadex columns were prepared. Buffer 2 (0.1M NaCl/1mM $NaPO_4$) was prepared by adding acid ($NaCl/NaH_2PO_4$) to alkali ($NaCl/Na_2HPO_4$) to pH7.2. 9g of G-50 sephadex was slowly added to 100ml of buffer 2 and 4 X 20ml syringes, plugged with glass wool, were packed with this sephadex and equilibrated with the same buffer.

The mixture was then resolved using 3 of the columns (the remaining column being stored at 4°C to be used later) and eluted with buffer 2. The elutant was then concentrated using Centriprep 3 columns (Amicon Ltd, UK) by centrifugation at 2000 x g, at 4°C to a final volume of 1.5-3ml. At 0°C, 375mg of N-hydroxy succinimide and 600mg of N-ethyl-N-(3-dimethylaminopropyl) carbodi-imide hydrochloride (EDAC) were added and the mixture was stirred at 0°C for 3 h. The resultant solution was then resolved using the remaining G-50 sephadex column as before.

At this stage the 'active' HRP was ready to be coupled to transferrin. This was carried out immediately to prevent hydrolysis of the active NHS esters. 6ml of 25mg/ml apo-transferrin (in buffer 2) and 10^6-10^7 cpm ^{125}I-transferrin were added to the elutant and stirred at 2°C for 48 h. The solution was then quenched with glycine and either stored at 2°C with the addition of azide or snap frozen and stored at -80°C.

Meanwhile, a sephacryl S-300 column (1m in length) was equilibrated overnight with buffer 2 at 10ml/h. The conjugate was concentrated to 2-3ml as before and applied to the column. When the brown band of conjugate reached approximately half way down the column, 0.5ml fractions were collected. The fractions were then counted using a γ-counter and a graph of cpm versus fraction number was plotted. The fractions representing the first two peaks were pooled (the first two being the smallest of three peaks, with the third peak corresponding to unconjugated ^{125}I-transferrin) and concentrated to 3-4ml as before. The conjugate was reapplied to the column and fractions were collected and counted as before. On plotting a graph, the fractions representing the largest peak were pooled and concentrated to 3-4ml as before. The protein concentration was determined by a Bradford assay (see Section 2.5) before the conjugate was iron loaded by adding 375µl $FeSO_4$ and 112.5µl $KHCO_3$. The conjugate was then filtered through Whatman No.1 paper, aliquoted, snap frozen and stored at -80°C.

2.9.2 Use of Tf-HRP

Ablation of the recycling endosomal system was carried out as described by Livingstone *et al* (Livingstone *et al.*, 1996).

During a 2 h incubation in serum-free DMEM, 3T3-L1 adipocytes were incubated with Tf-HRP conjugate (20μg/ml final concentration) for 60 min at 37°C. The cells were then placed on ice, washed gently three times over a period of 10 min with ice-cold isotonic citrate buffer (150mM NaCl, 20mM Tri-sodium citrate, pH 5.0) and once with ice-cold PBS (see Section 2.2.1). Chilling the cells prevented any further vesicle trafficking during the DAB cytochemistry while acid washing with citrate buffer removed any cell-surface-attached Tf-HRP. 3,3'-diaminobenzidine (DAB) (2mg/ml stock prepared freshly in PBS, vortexed thoroughly and filtered through a 0.22 μm-pore-size-filter) was added at 100 μg/ml to all cells and H_2O_2 (final concentration 0.02% v/v) was added to experimental plates only. After a 60 min incubation at 4°C in the dark the reaction was stopped by washing the cells with ice-cold PBS.

2.10 Subcellular Fractionation of 3T3-L1 Adipocytes

Subcellular fractions (PM, HDM, LDM and SP) were obtained as described for the fractionation of rat adipocytes by Piper *et al* (Piper *et al.*, 1991), modified by Martin *et al* (Martin *et al.*, 1994).

Cells cultured on 10cm plates were incubated at 37°C in serum-free DMEM for 2 h. For the last 15 min of the incubation insulin (1μM) was added to experimental plates only. Following the transfer of plates onto ice the cells were washed 3 times with ice-cold HES buffer (see Section 2.2.3). On addition of 5ml HES buffer containing proteinase inhibitors (1μg/ml pepstatin A, 0.2mM di-isopropylflurophosphate [DFP] and 20μM L-transepoxysuccinyl-leucylamido-4-guanidiniobutane [E64]) the

cells were scraped and then homogenised with 20 hand strokes in a Dounce homogeniser. Homogenates were transferred to pre-chilled Oakridge centrifuge tubes and centrifuged at 19,000 x g for 20 min at 4°C.

The resulting pellet was resuspended in 1ml ice-cold HES buffer and layered onto 1ml of 1.12mM sucrose in HE buffer in an Ultra-clear Beckman tube and centrifuged at 100,000 x g for 60 min at 4°C in a swing out rotor. The upper layer was aspirated off to leave a brown band at the interface (plasma membrane) and a brown pellet (mitochondria/nuclei fraction). The plasma membrane fraction was transferred to an Oakridge centrifuge tube, resuspended in 15ml HES buffer and pelleted at 41,000 x g for 20 min at 4°C.

Meanwhile, the supernatant from the initial spin was centrifuged at 41,000 x g for 20 min at 4°C, yielding a pellet designated as the high density microsomal fraction (HDM). The resulting supernatant was centrifuged at 100,000 x g for 60 min at 4°C yielding a pellet designated the low density microsomal fraction (LDM). The soluble protein fraction was precipitated from the resulting supernatant with 1.5ml TCA and centrifuged at 41,000 x g for 20 min at 4°C. All fractions were resuspended in HES buffer, snap frozen in liquid nitrogen and stored at -80°C prior to analysis.

2.11 Immunoadsorption of GLUT4 Vesicles

3T3-L1 adipocytes were fractionated as above with minor modifications. For preparation of intracellular (LDM) membranes for immunoadsorption, cells cultured on 10cm plates were incubated at 37°C in serum-free DMEM for 2 h at 37°C. The plates were transferred onto ice and washed 3 times with ice-cold HES buffer (see Section 2.2.3). On addition of 1ml of the same buffer containing proteinase inhibitors (1μg/ml pepstatin A, 0.2mM DFP and 20μM E64), the cells were scraped and then homogenised in a Dounce homogeniser as before. Homogenates were transferred to pre-chilled Oakridge centrifuge tubes and centrifuged at 41,000 x g for 20 min at 4°C

to remove plasma membranes, mitochondria, nuclei and high-density microsomes. The resulting supernatant was centrifuged at 100,000 x g for 60 min at 4°C to yield a pellet containing the low density microsomal (LDM) membranes, which was resuspended in HES buffer (200µl HES per plate of cells) containing NaCl (100mM final).

Meanwhile, formaldehyde-fixed *Staph. a* cells (~50µl cells per two plates) were washed twice in HES buffer containing 1% bovine serum albumin (BSA), and loaded with either a monoclonal GLUT4 antibody 1F8 (see Section 2.4.1), affinity purified polyclonal anti-GLUT4 (see Section 2.4.1) or non-specific IgG as a control by incubation for 1 h at room temperature with occasional agitation. *Staph. a.* cells were then washed three times with HES/1%BSA by centrifugation at 10,000 x g for 30 s in a microfuge to remove unbound antibody .

For immunoadsorption, 400µl of resuspended LDM (two 10cm plates of cells) was placed in an Eppendorf tube and incubated with the immunoadsorbent for 2-4 h at 4°C with slow end-over-end rotation. Samples were then centrifuged in 13.5ml centrifuge tubes for 5 min at 2000 x g to pellet the immunadsorbent. The immunoadsorbent was resuspended in 1ml HES/NaCl, transferred to an Eppendorf and centrifuged at 10,000 x g for 30 s in a microfuge. Following a further two washes, the pellet was resuspended in 90µl of 1% Triton X-100 in PBS, vortexed briefly and the vesicle proteins were solubilised by incubation with occasional agitation for 20 min at room temperature. The *Staph. a.* cells were pelleted by centrifugation at 10,000 x g for 30 s using a microfuge. The supernatant was collected to a fresh tube and again centrifuged for 30 s before carefully removing the supernatant. Samples for electrophoresis were prepared by the addition of 30µl of 4X SDS-PAGE sample buffer (see Section 2.6) directly to this supernatant.

The supernatant recovered from the initial centrifugation of the *Staph. a.* cells following the 2 h rotation at 4°C was centrifuged at 2000 x g for 10 min to remove

any remaining cells. The resulting supernatant was added to 5ml Beckman Ultra-clear tubes and centrifuged at 100,000 x g for 60 min at 4°C. The resulting pellet was resuspended in 120µl 1X SDS-PAGE sample buffer (see Section 2.6). All fractions were snap frozen in liquid nitrogen and stored at -80°C prior to analysis.

2.12 Indirect Immunoflourescence Microscopy

2.12.1 Plasma Membrane Lawn Assay

The plasma membrane lawn assay was carried out as described by Robinson *et al* (Robinson *et al.*, 1992c; Robinson *et al.*, 1992b) to generate highly purified plasma membrane (PM) fragments in order to determine the relative levels of different proteins at the cell surface.

3T3-L1 adipocytes cultured on collagen-coated coverslips on 6-well plates were treated as described by the individual experiments. At the conclusion of the experiment, cells were rapidly washed once with ice-cold buffer A (50mM HEPES (pH7.2) and 10mM NaCl) and then twice with ice-cold buffer B (20mM HEPES (pH7.2), 100mM KCl, 2mM $CaCl_2$, 1mM $MgCl_2$, pepstatin A (1µg/ml), Trypsin inhibitor (2µg/ml) and 0.5mM Benzamide). While immersed in buffer B, the cells were sonicated using a 0.8mm tapered Dawa Ultrasonics probe at 50 watts for 3 s to generate a lawn of PM fragments attached to the coverslip.

Lawns were washed three times with PBS (see Section 2.2.1) and then fixed to the coverslips for 15 min by using freshly prepared 2% paraformaldehyde in PBS (see Section 2.2.1). Cells were then washed three times with PBS and the reaction was quenched with 50mM NH_4Cl/PBS over a period of 10 min. Cells were washed a further three times in each case with PBS, PBS/0.2% gelatin (PBS, 0.2% fish-skin gelatin and 0.1% goat serum, to block non-specific binding sites) and again with PBS over a 5 min period each time.

An aliquot of primary antibody was centifuged in a microfuge, diluted to required concentration in PBS/0.2% gelatin and stored on ice prior to use. Following the addition of 100µl of antibody solution on parafilm, the coverslips were placed cells down on the solution and incubated at room temperature for 1-2 h. PM lawns were washed three times sequentially with PBS/0.2% gelatin and PBS over a 5 min period.

Due to fluorescent dyes on secondary antibodies the preparation of PM lawns is continued in the dark from this point. Secondary antibody, fluoroscein isothiocyanate (FITC)-conjugated goat anti-rabbit IgG was prepared as for primary antibody and staining was carried out as described above. Coverslips were covered with aluminium foil during the 1-2 h incubation to avoid bleaching of dyes. As before, the PM lawns were washed three times sequentially with PBS/0.2% gelatin and PBS over a 5 min period. Coverslips were then mounted onto slides by placing them lawn down onto a 15µl drop of moviol. Again, to prevent bleaching the slides were covered with aluminium foil and allowed to dry overnight. The slides were stored in the dark prior to analysis.

Coverslips were viewed using x 40 and x 63/1.4 Zeiss oil immersion objectives on a Zeiss Axiovert fluorescence microscope (Carl Zeiss, Germany) equipped with a Zeiss LSM4 laser confocal imaging system.

2.12.2 Whole-Cell Indirect Immunofluorescence Microscopy

3T3-L1 adipocytes cultured on coverslips on 6-well plates were incubated in serum-free DMEM for 2 h at 37°C, washed three times in PBS (see Section 2.2.1) and then fixed in 2% paraformaldehyde in PBS for 15 min at room temperature. Subsequently the cells were washed three times with PBS, quenched with 50mM NH_4Cl/PBS over a period of 10 min, and then washed a further three times with PBS. The cells were then permeabilised with 0.1% Triton X-100 in PBS for 4 min at room temperature. After this time, the cells were washed three times with PBS and a

further five times with PBS/0.2% gelatin. The cells were incubated with primary and secondary antibodies and mounted on glass slides as described above.

In double-labelling experiments, pairs of anti-GLUT4 antibody and the corresponding secondary antibody were used in conjunction with pairs of primary and secondary antibodies required for detection of the other protein. The primary and secondary antibodies were applied in two steps as described above, with the two primary antibodies being mixed together in PBS/0.2% gelatin and applied simultaneously, followed by the wash steps as described above and then the application of the secondary antibodies.

2.13 2-Deoxy-D-Glucose Transport Assay

Glucose transport was measured by the uptake of 2-deoxy-D-glucose according to the method of Gibbs *et al* (Gibbs *et al.*, 1988) and Frost and Lane (Frost *et al.*, 1985).

3T3-L1 adipocytes cultured on 6-well plates were treated as described by the individual experiments. Following 2 washes with 2ml of KRP buffer (see Section 2.2.2) warmed to 37°C, the cells in three of the wells per plate were incubated in 950µl of KRP while the remaining cells were incubated in KRP and 10µM cytochalasin B (to determine non-specific association of 2-deoxy-D-glucose with the cell monolayer) on a hot plate at 37°C. Cells were then stimulated with or without 1µM insulin for 15 min at 37°C. Glucose transport was initiated by the addition of 50µl of [^{3}H] 2-deoxy-D-glucose (final concentration of 50µM and 0.5µCi/ml).

After 3 min, the transport was terminated by 'flipping' the plates rapidly to remove the incubation buffer and then 'dipping' them sequentially into 3 volumes of ice-cold PBS (see Section 2.2.1). The plates were left to air dry and 1ml of 1% Triton X-100 in H_2O was added to each well. Following incubation for 1 h at room temperature,

the detergent solubilised [^{3}H] 2-deoxy-D-glucose was determined by liquid scintillation counting.

It has been calculated by members of this lab and others that one well of a 6-well contains 2.1 million cells and as a result the rate of 2-deoxy-D-glucose transport is expressed as pmol/min/million cells which is the standard unit used within the field of glucose transport.

2.14 Adipsin Release

The release of adipsin from 3T3-L1 adipocytes was measured as described exactly by Kitagawa *et al* (Kitagawa *et al.*, 1989).

3T3-L1 adipocytes cultured on 10cm plates were treated as described by in the individual results chapters and corresponding figure legends. Thereafter, the cells were washed twice with KRP buffer (see Section 2.2.2) at 37°C and then incubated in 10ml of KRP/BSA (10μg/ml) ± 1μM insulin at 37°C. 1ml aliquots of media were removed at defined times (0, 2, 5, 10 and 30 min) and the protein was precipitated by adding 110μl of 70% trichloroacetic acid and 20μl of deoxycholate as a carrier. The samples were incubated on ice for 10 min and centrifuged at 10,000 x g for 10 min in a microfuge. The protein pellets were resuspended in 40μl 1X SDS-PAGE sample buffer (see Section 2.6) and 10μl 2M Tris, snap frozen and stored at -80°C prior to analysis. Adipsin release into the media was quantitated by immunoblotting and subsequent detection with ^{125}I goat anti-rabbit IgG and is therefore expressed in arbitrary units.

2.15 Molecular Biology

2.15.1 Preparation of Competent Bacteria

To revive the cells a splinter of ice was scraped off with a wire loop from a glycerol stock of XLI-Blue *E. coli* bacteria stored at -80°C. The bacteria were then streaked out on a minimal plate (L-broth and agar containing the appropriate antibiotic - in the case of the XLI-Blue strain tetracycline) and incubated at 37°C overnight. A single colony was picked and used to innoculate a universal tube containing 5ml L-broth (1% peptone, 1% NaCl and 0.5% yeast extract). This was cultured overnight at 37°C. The 5ml culture was then added to 100ml L-broth and incubated at 37°C for ~1.5-1.75 h until the optical density at 550nm was 0.48 The cells were then chilled on ice for 5min before being transferred to 50ml sterile Nunc centrifuge tubes and spun at 2000 x g for 10min at 4°C. On discarding the supernatant each pellet was resuspended in 20ml buffer 1 (1M KAc, 1M $RbCl_2$, 1M $CaCl_2$, 1M $MnCl_2$ and 80% glycerol) by gently pipetting up and down. The cells were then chilled on ice for 5min and spun as before. Each pellet was then resuspended in 2ml buffer 2 (100mM MOPS, pH 6.5, 1M Ca Cl_2, 1M $RbCl_2$ and 80% glycerol) by pipetting. The cells were placed on ice for 15min, divided into 220µl aliquots, snap frozen using liquid nitorgen and stored at -80°C.

2.15.2 Transformation of Competent Bacteria

On thawing an aliquot of competent bacterial cells, 50µl per transformation was added to a sterile 13.5ml conical based tube and placed on ice. 1-5µl of DNA (~1-10ng) was added and the cells were placed on ice for 15 min. The tubes were then placed in a water bath at 42°C for 90 s in order to induce heat shock. The cells were returned to ice for 2 min before 450µl of L-broth (see Section 2.14.1) was added and the tubes were placed in an orbital shaker at 37°C for 45 min. 100µl of cells was plated out on the appropriate antibiotic plate and incubated at 37°C overnight.

2.15.3 Multiple Plasmid Minipreparations

To perform multiple plasmid minipreparations the QIAprep® 8 Turbo Miniprep kit was used as described below. It should be noted that details of the individual buffers used below were not available (refer to manufacturer's handbook).

Following transformation of competent XL1-Blue *E.Coli*, single colonies of interest were picked from an agar plate and dispensed into 3ml of L-Broth (see Section 2.14.1) in a Universal tube containing 50µg/ml ampicillin. The cultures were shaken overnight at 37°C and then 1.5ml was transferred to Eppendorf tubes which were centrifuged at 10,000 x g for 5 min in a microfuge. The supernatant was discarded and the pellet of bacterial cells was resuspended in 250µl of Buffer P moving all visible cell clumps. 250µl of Buffer P2 was then added and the tubes were gently inverted 4-6 times to ensure mixing before incubation at room temperature for 5 min. As the solutions became viscous and slightly clear 350µl of Buffer N3 was added to each sample and again the tubes were inverted immediately but gently 4-6 times. The cloudy lysates (850µl) were then pipetted into the wells of the TurboFilter strips and the vacum was applied until all the samples had passed through the TurboFilter into the QIAprep® strips below. On turning the vacum off, the TurboFilter strips were discarded and replaced with the now filled QIAprep® strips with the waste tray being positioned below. Again the vacum was applied allowing the flow throughs to be collected as waste. With the aid of the vacum the QIAprep® strips were washed two times by the addition of 1ml of Buffer PE to each well (the vacum being switched off before Buffer PE was added for a second time). At the end of the second wash the vacum was left on for an additional 5 min to dry the membrane. The QIAprep® strips were then rapped on a stack of absorbent paper until no drops were observed and the nozzles were blotted dry.

To elute DNA, 100µl of sterile H_2O was added to the centre of each well of the QIAprep® strips and left to stand for 1 min. The waste tray was replaced with

collection microtubes and then the vacum was applied for 5 min allowing elution of bound DNA. The DNA was stored at -20°C.

2.15.4 Maxi Preparation of Plasmid DNA

500ml of sterile L-broth (containing the appropriate antibiotic) was innoculated with 500µl of culture previously prepared by the innoculation of a small volume of L-broth (see Section 2.14.1) with a single colony of XL1-blue *E. Coli*. The culture was shaken overnight at 37°C. The cells were then pelleted by centrifugation in Beckman 250ml polypropene bottles at 4000 x g for 10 min at 4°C. On discarding the supernatant, the pellets were pooled and resuspended in 25ml total volume of ice-cold glucose buffer (50mM glucose, 10mM EDTA, 25mM Tris, pH6.8). Keeping the cells on ice, 25ml of alkaline lysis buffer (1% SDS, 0.2M NaOH) was added slowly with continual swirling and then 25ml of 5M potassium acetate buffer, pH5.5 was added. The bottle was then shaken vigorously before centrifugation at 4000 x g for 10 min at 4°C. The supernatant was filtered through 2 layers of muslin into a fresh 250ml Beckman polypropene bottle, mixed with 100ml propan-2-ol and incubated at -20°C for 10min. After centifugation at 4000 x g for 10 min at 4°C, the supernatant was discarded and the pellet was resuspended in 7.5ml TE buffer (10mM Tris, 1mM EDTA, pH8.8) and transferred to a 50ml Beckman polypropene tube. Following the addition of 10ml of 5M LiCl, the solution was incubated on ice for 2-5 min and then centrifuged at 3000 x g for 10 min at 4°C. The supernatant was then transferred to a fresh 50ml Beckman polypropene tube, mixed with an equal volume of 100% ethanol and incubated for 30 min at -20°C. After centrifugation at 3000 x g for 20 min at 4°C, the supernatant was discarded and the pellet was washed with 95% ethanol and allowed to dry. The pellet was then resuspended in 0.6ml TE buffer and transferred to an Eppendorf tube. Following the addition of RNAse (20µg/ml), the solution was incubated at 37°C for 15 min. After the addition of 0.5 volumes of polyethylene glycol (PEG), the solution was incubated on ice for 15 min and spun in a microfuge at 10, 000 x g for 10 min. On discarding the supernatant the

pellet was resuspended in 0.6ml TE buffer. The DNA was subsequently cleaned by phenol:chloroform extraction. An equal volume of phenol: chloroform (1:1) was added to the sample and vortexed vigorously. The aqueous (top) layer was carefully removed with the aid of a pipette and transferred to a clean Eppendorf. This was repeated and then followed by two chloroform extractions, again with the aqueous layer being removed each time. 2.5 volumes of absolute ethanol and 0.1 volumes of 3M NaOAc were added and the DNA was precipitated overnight at -20°C. The sample was then spun at 10,000 x g for 20 min in a microfuge, the supernatant decanted off and the pellet was washed with 70% ethanol and allowed to air dry before resuspension in 100-200µl H_2O. The DNA concentration and purity was determined by reading the absorbance at 260 and 280nm.

2.15.5 Calculation to Determine the Plasmid DNA Concentration and Purity

absorbance value of 1.0 at 260nm = 50µg of double stranded DNA

absorbance value of "y" at 260nm = "y" X 50µg of double stranded DNA

$$\frac{\text{absorbance at 260nm}}{\text{absorbance at 280nm}} = \text{"Z"}$$

DNA has a lower protein concentration and has a higher purity when Z is nearer to 2.0.

2.15.6 Restriction Digestion of DNA

Approximately 10µg of DNA was used for a large scale digest in a reaction volume of 100µl. 10µg of DNA, 10µl of 10X buffer (optimising salt and pH for individual enzymes) and 10 units of enzyme were added with sterile water to 100µl to a 1.5ml Eppendorf tube and incubated at 37°C for 2 h. For digestions with more than one

enzyme, the reaction was carried out as before with the first enzyme (the one which utilises a lower salt concentration), and then salt added to the reaction to optimise conditions for the second digest which is subsequently carried out. Alternatively, if both enzymes utilised similar optimum reaction conditions, both digests could be carried out simultaneously. Following the addition of 5X DNA loading buffer (0.25% bromophenol blue, 30% (v/v) glycerol/H_2O), the sample was electrophoresed on a 1% agarose gel.

2.15.7 Dephosphorylation of Linearised DNA

For plasmids linearised with a single restriction endonuclease or cut to receive an insert, de-phosphorylation was carried out to reduce the efficiency of re-ligation of sticky ends. 10µg of DNA, 5µl of 10X buffer and 5 units of enzyme were added with sterile water to 50µl to a 1.5ml Eppendorf tube and incubated at 37°C for 1 h as before. 10µl of 10X de-phosphorylation buffer, 1 unit of alkaline phosphatase with sterile water to 100µl were added and incubated at 37°C for a further 2 h. A fraction of the sample was electrophoresed as before to verify linearisation and the remaining DNA was cleaned by phenol:chloroform extraction (refer to Section 2.15.4). 2.5 volumes of absolute ethanol and 0.1 volumes of 3M NaOAc were added and the DNA was precipitated overnight at -20°C. The sample was then spun at 10,000 x g for 20 min in a microfuge, the supernatant decanted off and the pellet was washed with 70% ethanol and allowed to air dry before resuspension in 20µl H_2O.

2.15.8 Agarose Gel Electrophoresis

For standard 1% gels, agarose was dissolved by boiling in distilled water. On cooling to a hand hot temperature, 50X TAE buffer (2mM Tris, 50mM EDTA, 5.7% (v/v) glacial acetic acid) was added to produce a final concentration of 1X TAE. Ethidium bromide (10mg/ml) was added, mixed thoroughly and the gel solution was then poured into a horizontal electrophoresis gel cartridge (with a comb inserted) and

allowed to set at room temperature. The gel cartridge was transferred to an electrophoresis tank containing 1X TAE buffer and the comb was carefully removed. The DNA samples were then loaded adjacent to a sample of either *Bst E* II-digested l DNA or 1Kb DNA ladder, required to determine the size of the digested DNA fragments. Electrophoresis was carried out at 50-100mA until the dye front had migrated two thirds of the way along the gel towards the anode. DNA was visualised under U.V using an Ultraviolet Products Inc. transilluminator and photographs were taken using a Mitsubushi video copy processor.

2.15.9 Gel Extraction of DNA

This was carried out using materials from a Wizard™ *Plus* Minipreps DNA Purification system.

Following agarose gel electrophoresis, the appropriate DNA fragments were excised as gel slices and transferred to a 1.5ml microcentrifuge tube. 1ml of Wizard™ Minipreps DNA Purification Resin (thoroughly mixed) was added and the gel slice was incubated at 55°C for 5-10 min to allow the gel to melt. The 1.5ml microcentrifuge tube was agitated several times during the incubation to ensure mixing of the DNA and resin. A Wizard™ Minicolumn was prepared by removing the plunger from a 3ml syringe and attaching the syringe barrel to a Luer-Lok® extension of the Minicolumn. The 1ml of 'slurry' was then pipetted into the barrel and pushed into the Minicolumn with the aid of the syringe plunger. The syringe was detached from the column before removing the plunger. The syringe barrel was reattached and 2X 2ml of isopropanol was used to wash Minicolumn. On removal of the syringe, the Minicolumn was transferred to a 1.5ml microcentrifuge tube and centrifuged at 10,000 xg in a microfuge for 2 min to dry the column. The Minicolumn was transferred to a fresh 1.5ml microcentrifuge, 50µl of H_2O was added. After 1 min, the Minicolumn was centrifuged at 10, 000 xg for 20 s to elute the DNA. The DNA was stored in the microcentrifuge tube at -20°C prior to further analysis.

Chapter 3

Compartment Ablation Analysis of the GLUT4 Intracellular Compartments

3.1 Aims

1. To examine the subcellular distribution of SCAMPs (secretory carrier associated membrane proteins), syntaxin 4, CSPs (cysteine string proteins), syntaxin 4, Rab4, γ-adaptin and the cation-dependent mannose-6-phosphate receptor (CD-M6PR) in basal and insulin-stimulated 3T3-L1 adipocytes.

2. To examine the effect of endosome ablation on the proteins localised to the intracellular (LDM) membranes enriched in GLUT4.

3. To determine the extent of co-localisation of the proteins localised to the non-ablatable compartment with GLUT4.

3.2 Introduction

The acute stimulation of glucose transport in adipose and muscle tissue in response to insulin is associated with the rapid translocation of GLUT4 transporters to the cell surface from an intracellular compartment(s) (reviewed in James *et al.*, 1994). Although the intracellular sequestration of this transporter is fundamental to the insulin response, the nature of the intracellular compartment(s) and the exact mechanism of translocation remain poorly defined. In the basal state, morphological studies have localised > 95% of GLUT4 to tubulovesicular elements adjacent to early and late endosomes, at the *trans*-Golgi network (TGN) or in the cytoplasm often close to the plasma membrane (Slot *et al.*, 1991b; Slot *et al.*, 1991a). In response to insulin, GLUT4 levels are decreased by 40-50% at each of these locations suggesting that each of these compartments participate in insulin-stimulated GLUT4 trafficking (Slot *et al.*, 1991b; Slot *et al.*, 1991a).

GLUT4 continuously recycles between the plasma membrane and the intracellular compartment(s) in the absence and presence of insulin (Yang *et al.*, 1993; Jhun *et al.*, 1992). Internalisation of GLUT4 via clathrin-coated pits (Slot *et al.*, 1991b) and partial co-localisation with endosomal proteins including the TfR and the CI-M6PR (Tanner *et al.*, 1989), suggests that this recycling is by way of the endosomal system. However, the kinetics of GLUT4 trafficking in the absence and presence of insulin suggests that more than one intracellular compartment is responsible for GLUT4 sequestration (refer to Section 1.9) (Holman *et al.*, 1994b). On the basis of these data, and mathematical analysis, a three compartment model has been proposd for the subcellular trafficking of GLUT4 (Holman *et al.*, 1994b). In the model GLUT4 is associated with two intracellular compartments; one is the recycling endosomal system, and the second is a more specialised compartment where GLUT4 is sequestrated in the basal state. It is this latter compartment which is thought to represent the insulin-responsive storage compartment from which GLUT4 is recruited to the plasma membrane upon insulin stimulation. Following recruitment to

the plasma membrane GLUT4 is internalised *via* the recycling endosomal system, and subsequently sorted back into the specialised storage compartment (refer to Figure 1.9) (Holman *et al.*, 1994b).

Biochemical evidence for the sequestration of GLUT4 in an intracellular compartment segregated from the recycling endosomal system has recently been provided by means of a technique referred to as compartment ablation analysis (Livingstone *et al.*, 1996). Ablation may be achieved by the introduction of horseradish peroxidase (HRP) or HRP-conjugates into the appropriate compartment(s) (West *et al.*, 1994). On incubation with 3,3' -diaminobenzidine (DAB) and H_2O_2, proteins within the compartment carrying the HRP probe are cross-linked and rendered 'insoluble' (i.e. ablated) (West *et al.*, 1994). To determine the relationship between the intracellular sequestration of GLUT4 and the recycling endosomal system, this technique was exploited by using a transferrin-HRP (Tf-HRP) conjugate (Livingstone *et al.*, 1996). By saturating the recycling pathway of the TfR with Tf-HRP in 3T3-L1 adipocytes, proteins present in the recycling endosomal system including the TfR, GLUT1 and the CI-M6PR were quantitatively ablated in the presence of DAB and H_2O_2 (Livingstone *et al.*, 1996). In contrast, only 40% of intracellular GLUT4 was ablated under the same conditons, suggesting that a larger proportion (~60%) of intracellular GLUT4 resides in a 'non-ablatable' storage compartment withdrawn from the endosomal system (Livingstone *et al.*, 1996). Further ablation studies have shown GLUT4 to co-localise with the v-SNARE VAMP2 in this non-ablatable compartment (Martin *et al.*, 1996). In striking agreement with the ablation data, a recent immunocytochemical study on rat adipocytes has localised GLUT4 with VAMP2 in a post-endocytic compartment, distinct from the TfR in the constitutively recycling endosomes (Malide *et al.*, 1997a).

In the present study, I wished to further characterise the non-ablatable GLUT4 compartment and investigate the relationship of this compartment with the

endosomal and secretory pathways. In order to do this, I studied the co-localisation of GLUT4 with marker proteins that define distinct intracellular compartments (γ-adaptin, the CD-M6PR and Rab4) and proteins known to be involved in exocytosis (SCAMPs [secretory carrier-associated membrane proteins], syntaxin 4 and cysteine string proteins [CSPs]) in 3T3-L1 adipocytes before and after endosomal ablation. The results obtained provide further evidence for the existence of two distinct intracellular GLUT4 pools in 3T3-L1 adipocytes. I have shown that after endosomal ablation a smaller pool (~38%) of GLUT4 is localised to the endosomal system along with markers for cell surface to endosome recycling such as the TfR and SCAMPs, consistent with the constitutive recycling of GLUT4 between the plasma membrane and the early endosomes via the recycling endosomal system. The co-localisation of syntaxin 4 with GLUT4 within the larger non-ablatable intracellular pool suggests that this t-SNARE may be involved in GLUT4 intracellular trafficking. Moreover, the presence of TGN markers within this pool implies that GLUT4, along with the CD-M6PR, recycles through the TGN in AP-1 positive vesicles *en route* to the endosomal system.

3.3 Materials and Methods

3.3.1 Ablation of the Intracellular (LDM) Membranes

Ablation of the recycling endosomal system was carried out as described by Livingstone *et al* (Livingstone *et al.*, 1996).

3T3-L1 adipocytes were cultured on 10cm plates and incubated in serum-free DMEM at 37°C for 3 h prior to use. For the last hour of the incubation, Tf-HRP conjugate (20μg/ml final concentration) was added to all plates. On transferring the plates onto ice, the cells were washed gently three times over a 10 min period with ice-cold isotonic citrate buffer (150mM NaCl, 20mM Tri-sodium citrate, pH 5.0) and once with ice-cold PBS (see Section 2.2.1). 9.5ml of PBS and 0.5ml of 3,3'-

diaminobenzidine (DAB) (2mg/ml stock prepared freshly in PBS, vortexed thoroughly and filtered through a 0.22 μm-pore-size-filter) were added to each plate. H_2O_2 (0.02%) was then added to experimental plates only. The plates were wrapped in aluminium foil and incubated in the dark at 4°C for 1 h. On discarding the buffer, the plates were washed with ice-cold PBS. The cells were then scraped upon adding 1ml of ice-cold HES buffer (see Section 2.2.3) and added to a Dounce homogeniser. Proteinase inhibitors (1μg/ml pepstatin A, 0.2mM DFP and 20μM E64) were added and the cells were homogenised with 20 handstrokes. Homogenates were transferred to pre-chilled Oakridge centrifuge tubes and centrifuged at 19,000 x g for 20 min at 4°C. The resulting supernatant was added to 5ml Ultra-Clear tubes and centrifuged at 100,000 x g for 60 min at 4°C. The resulting pellet, designated as the low density microsomes (LDM) was resuspended in HES buffer, snap frozen in liquid nitrogen and stored at -80°C prior to analysis.

3.3.2 Sucrose Density Gradient Analysis

The intracellular (LDM) membranes (± ablation) prepared as described above were resuspended in 200μl HE buffer (20mM N-2-hydroxyethylpiperazine-N'-2-ethanesulphonic acid (HEPES), pH 7.4 and 1mM EDTA) containing proteinase inhibitors (1μg/ml pepstatin A, 0.2mM DFP and 20μM E64). A discontinuous sucrose gradient was prepared by adding 200μl aliquots of sucrose solutions in HE buffer of decreasing sucrose concentration (50%, 45%, 42.5%, 40%, 37.5%, 35%, 32.5%, 30% and 25%w / v sucrose) to a pre-chilled Beckman tube. The resuspended LDM sample was then loaded onto the gradient and centrifuged at 100,000 x g at 4°C for 24 h. A series of 125μl fractions was collected by tube puncture into Eppendorf tubes. 30μl of 0.15% w / v deoxycholate and 200μl of 72% Trichloroacetic acid were added to each tube which were then vortexed briefly and incubated on ice for 10 min. Following centrifugation of each fraction at 10,000 x g in a microfuge for 10 min, the supernatant was aspirated off and the precipitated protein was resuspended in 40μl

1X SDS-PAGE sample buffer (see Section 2.6) and 10µl 1M Tris before each fraction was snap frozen in liquid nitrogen and stored at -80°C.

3.3.3 Whole-Cell Immunofluorescence Microscopy

Whole-cell immunofluorescence microscopy was carried out as described in Section 2.12.2. For GLUT4 staining alone whole cells were labelled with an affinity purified rabbit polyclonal anti-GLUT4 primary antibody (refer to Section 2.4) and the corresponding secondary antibody (FITC-conjugated goat anti-rabbit IgG). In the case of double-labelling experiments, Triton-permeabilised 3T3-L1 adipocytes were incubated with a mouse monoclonal anti-GLUT4 antibody (refer to Section 2.4) and the corresponding secondary antibody (tetramethylrhodamineisothiocyanate [TRITC]-conjugated goat anti-mouse IgG) in conjunction with either a rabbit anti-γ-adaptin antibody (see Section 3.3.5) or a rabbit anti-CD-M6PR antibody (see Section 3.3.5) and the corresponding secondary antibody (FITC-conjugated goat anti-rabbit IgG).

3.3.4 Antibodies

The anti-GLUT4 antibody used for immunoblotting was a rabbit polyclonal against a peptide comprising the C-terminal 14 amino acid residues of the human isoform of GLUT4 (see Section 2.4). For vesicle immunoadsorption and double-labelled immunofluorescence a monoclonal GLUT4 antibody (1F8) was used (see Section 2.4). An anti-transferrin receptor monoclonal antibody was purchased from UBI (Lake Placid, New York, USA). Anti-γ-adaptin antibody was the generous gift of Dr M.S. Robinson (Addenbrooks Hospital, University of Cambridge, UK), and the anti-CD-M6PR antibody was from Dr A. Hille-Rhefeld (Utrecht, Netherlands). Anti-Rab4 antibodies were provided by Dr Y. LeMarchand-Brustel (INSERM, Nice, France) and Dr P. van der Sluijs (Utrecht, Netherlands). Anti-SCAMP antibodies

were from Dr D. Castle (University of Virginia, USA) and antiserum against CSPs was generously provided by Dr R. Burgoyne (University of Liverpool, UK).

3.4 Results

3.4.1 Subcellular Distribution of Proteins in Basal and Insulin-Stimulated 3T3-L1 Adipocytes

Initially I examined the subcellular distribution of several proteins including: γ-adaptin, SCAMPs, the CD-M6PR, CSPs, syntaxin 4 and Rab4 in basal and insulin-stimulated 3T3-L1 adipocytes. Subcellular fractionation was carried out using both basal and insulin-stimulated adipocytes as described in Section 2.10. Figure 3.1 shows Western blots of plasma membrane (PM), low-density microsome (LDM) and high-density microsome (HDM) fractions analysed for the distribution of GLUT4 and these proteins.

The cellular distribution of the CD-M6PR was similar to that of GLUT4 with an increase at the PM in response to insulin and a concomitant decrease in the LDM fraction. The majority of γ-adaptin, a marker for the AP-1 complex which is a component of clathrin-coated vesicles associated with the TGN (Robinson, 1990) was found in the LDM fraction, consistent with this fraction being enriched in the Golgi complex. There was no redistribution of this protein upon insulin treatment. As integral membrane proteins of secretory and transport vesicles (Sudhof, 1995), SCAMPs are important components involved in trafficking to and from the cell surface. As expected, SCAMPs were localised predominantly in the LDM fraction enriched in GLUT4, with no significant change in distribution in response to insulin, consistent with a previous study in adipocytes (Laurie *et al.*, 1993). In agreement with a previous study, syntaxin 4 was highly enriched in the PM fraction with a smaller intracellular pool in the LDM fraction in 3T3-L1 adipocytes (Tellam *et al.*, 1997). It must be noted that in order to examine this intracellular pool twice as much

protein sample had to be loaded to the lanes representing the LDM fractions of syntaxin 4. In response to insulin there was a decrease in syntaxin 4 levels in the LDM fraction, consistent with the aformentioned study. However an increase at the PM is not apparent as the amount of this protein lost from the LDM fraction is very small compared to the high levels already present at the PM.

I also studied the distribution of the small GTP-binding protein, Rab4. Several studies have previously suggested a role for Rab4 in GLUT4 trafficking with the LDM fraction containing the majority of both Rab4 and GLUT4 in the basal state with movement to the cytosol and plasma membrane respectively, upon insulin stimulation (Ricort *et al.*, 1994; Cormont *et al.*, 1993; Shibata *et al.*, 1996; Cormont *et al.*, 1991). Consistent with these studies I found Rab4 to be localised to the LDM fraction in basal adipocytes. However, in response to insulin the immunoblot shows little if any change in cellular distribution (see below). CSPs were also found to be expressed in 3T3-L1 adipocytes. Intriguingly these proteins, previously identified as membrane proteins localised to secretory vesicles in neuroendocrine and endocrine cells (Chamberlain *et al.*, 1996a; Chamberlain *et al.*, 1996b), were confined to the plasma membrane both in basal and insulin-stimulated adipocytes.

3.4.2 Ablation of Proteins Localised to the Intracellular (LDM) Membranes

Ablation of the recycling endosomal system has led to the identification of a distinct GLUT4 compartment segregated from the TfR in which the majority (~60%) of intracellular GLUT4 resides in the basal state, and which is thought to represent a unique intracellular GLUT4 compartment (referred to as the non-ablatable compartment) (Livingstone *et al.*, 1996). This approach exploits the recycling of the TfR through the endosomal system by loading the receptor with a protein conjugate of transferrin and horseradish peroxidase (Tf-HRP). Previous studies have shown that this procedure selectively ablates markers for the recycling endosomal system (TfR, Rab5, cellubrevin, GLUT1 and the CI-M6PR), with little or no effect on

markers for the TGN or lysosomes (Livingstone *et al.*, 1996). Here, I have employed this procedure to determine the co-localisation of the proteins previously localised to the LDM fraction (CD-M6PR, γ-adaptin, syntaxin 4, and SCAMPs) to this non-ablatable compartment.

Duplicate plates of 3T3-L1 adipocytes were incubated with Tf-HRP for either 1h at 4°C or 1h at 37°C, the latter set of conditions being sufficient to allow full equilibration of the TfR pool with Tf-HRP in 3T3-L1 adipocytes (Livingstone *et al.*, 1996). At 4°C, trafficking will effectively be stopped and therefore the Tf-HRP conjugate will not be recycled through the endosomal system, thus rendering the ablation procedure ineffective. This is clearly shown by the immunoblots (Figure 3.2) as there is no change in the amount of protein in the two lanes labelled ± H_2O_2 at 4°C. Following ablation (DAB ± peroxide), LDM fractions were prepared as described in *Materials and Methods* and the extent of ablation was determined by quantitative immunoblot analysis. Figure 3.2 shows immunoblots for the TfR, GLUT4, the CD-M6PR, γ-adaptin and syntaxin 4. Following the loading of Tf-HRP at 37°C, the TfR exhibits a significant degree of ablation (79 ± 8%, mean ± s.e.m, n = 3, $p<0.01$), but in contrast, only a relatively modest degree of GLUT4 ablation is observed (38 ± 6%, mean ± s.e.m, n = 3). No significant ablation was observed in the case of γ-adaptin or the intracellular pool of syntaxin 4, suggesting that both of these proteins reside in an intracellular compartment distinct from the recycling endosomal system. The CD-M6PR also shows partial ablation (~35%), exhibiting a pattern similar to that for GLUT4. These data indicate that smaller intracellular pools of both of these proteins reside in the recycling endosomal system.

As the DAB-dependent protein complex forms in the lumen of endosomal vesicles containing the TfR, in order for a protein to become ablated, it must have a lumenal domain. As γ-adaptin is a coat protein it does not contain a lumenal domain and therefore will not be susceptible to ablation. Hence, the lack of ablation when immunoblotting the intracellular (LDM) membranes should not be taken as evidence

for this protein not residing in TfR positive membranes (Figure 3.2). However, membrane compartments which contain the DAB-dependent protein complex exhibit increased density following ablation. The association of proteins with vesicles which have undergone ablation is reflected by a change in the distribution of such proteins on density gradients, an approach which has previously been employed for analysis of Rab5 in adipocytes (Livingstone *et al.*, 1996). I therefore further examined the effect of ablation on γ–adaptin and also Rab4 using sucrose density gradient centrifugation.

Intracellular (LDM) membranes were prepared and further subfractionated on discontinuous sucrose density gradients as described (see Section 3.3.2). Fractions were collected from the gradients and analysed for the distribution of γ-adaptin, Rab4 and GLUT4. There was little if any change in the distribution of γ-adaptin on sucrose gradients upon ablation, suggesting that there was little formation of the DAB-dependent protein complex in the lumen of γ-adaptin vesicles, consistent with a low rate of TfR recycling through the TGN (Figure 3.3). In contrast, the distribution of Rab4 is markedly changed upon ablation. In control cells, Rab4 is detected in fractions also shown to contain GLUT4 (Figures 3.4 and 3.5). However, following ablation, there is a complete loss of signal for Rab4. This result may be reflective of a weak association of Rab4 with the endosomes which is disrupted by ablation. However, the lack of Rab4 association with dense membranes as was observed for Rab5 (Livingstone *et al.*, 1996) preludes a definitive conclusion in this regard. As previous studies have reported the dissociation of Rab4 from the intracellular (LDM) membranes into the cytosolic fraction in response to insulin (Cormont *et al.*, 1993) I immunoblotted a sucrose density gradient prepared from the LDM fraction of insulin-stimulated adipocytes for Rab4. As shown in Figure 3.4, insulin stimulation results in a significant loss of Rab4 immunoreactivity, consistent with the dissociation of the Rab protein from the membrane fraction. This loss of immunoreactivity due to the dissociation of Rab4 from the intracellular membranes in response to insulin is notably similar to that observed following ablation, suggesting

that the ablation procedure may have resulted in the dissociation of Rab4 from the intracellular membranes. However, it must be noted that the same procedure was without effect on the association of Rab5 with the intracellular membranes (Livingstone *et al.*, 1996).

As SCAMPs have previously been shown to co-localise with GLUT4 in rat adipocytes (Laurie *et al.*, 1993) I wished to compare the effect of ablation on the distribution of these two proteins determined by sucrose density gradient analysis (Figure 3.5). In control cells, GLUT4 and SCAMPs exhibit a similar distribution. After ablation, there is a loss of GLUT4 signal, consistent with a smaller pool of GLUT4 recycling through the endosomal system. In contrast, the distribution of SCAMPs is markedly changed in the presence of peroxide. As shown in Figure 3.5, essentially all of the SCAMPs undergo a density shift and are found in fraction 1 corresponding to the pellet at the bottom of the tube. This suggests that in adipoctyes, SCAMPs are associated with vesicles of the recycling endosomal system which become more dense as a result of ablation. These results suggest that the co-localisation previously observed between GLUT4 and SCAMPs is within the recycling endosomal system as opposed to the non-ablatable GLUT4 pool, distinct from this compartment (Laurie *et al.*, 1993).

3.4.3 Co-Localisation of γ-adaptin, the CD-M6PR and Syntaxin 4 with GLUT4-Containing Vesicles

To further define the non-ablatable GLUT4 compartment I examined the co-localisation of GLUT4 with γ-adaptin, CD-M6PR and syntaxin 4 by immunoadsorption of GLUT4-containing vesicles. Vesicles were isolated from the LDM fraction of adipocytes before and after ablation using a monoclonal antibody (IF8) or a polyclonal antibody for GLUT4. As a control, I performed immunoadsorption with non-specific IgG. Figure 3.6 shows the detection of the CD-M6PR and syntaxin 4 in the vesicles enriched in either GLUT4 or non-specific

IgG and in the depleted LDM fraction in each case. Figure 3.7 shows the detection of γ-adaptin in GLUT4-containing vesicles. Syntaxin 4, γ-adaptin and the CD-M6PR were all found to co-localise to some extent with GLUT4 both before and after ablation. The extent of syntaxin 4 and γ-adaptin localisation to GLUT4 vesicles was not significantly altered upon ablation, suggesting that the majority of these proteins detected in GLUT4 vesicles reside in the non-ablatable GLUT4 compartment. The loss of syntaxin 4 immunoreactivity in the depleted LDM fractions, further suggests that the vast majority of the intracellular pool of syntaxin 4 is associated with the GLUT4 non-ablatable compartment. In the case of the CD-M6PR, although also localised to GLUT4 vesicles following ablation, a fairly large proportion of this protein remains in the LDM fraction following the complete depletetion of GLUT4.

3.4.4 Intracellular Distribution of GLUT4, γ-adaptin and the CD-M6PR in 3T3-L1 Adipocytes

The co-localisation of GLUT4 with TGN markers including the γ-adaptin subunit of the TGN-specific adaptor complex AP-1 and the CD-M6PR which recycles between the TGN and endosomal compartments, suggests that GLUT4 may traffic through this compartment. In order to analyse the co-localisation and intracellular distribution of these three proteins in greater detail, immunofluorescence microscopy and immuno-electron microscopy were used.

Double-labelled immunofluorescence showed partial overlap of GLUT4 with the CD-M6PR (Figure 3.8A) and γ-adaptin in the perinuclear area (Figure 3.8B). In the case of γ-adaptin this is consistent with a recent immunocytochemical study in which GLUT4 is observed to partially overlap with γ-adaptin positive structures in rat adipocytes (Malide *et al.*, 1997a).

In collaboration with S. Martin (University of Queensland, Australia), the extent of co-localisation between GLUT4 and the CD-M6PR or γ-adaptin was analysed using immuno-EM studies on intracellular vesicles of basal 3T3-L1 adipocytes. Vesicles were isolated from 3T3-L1 adipocytes and double-labelled using colloidal gold-tagged antibodies of different particle sizes and the extent of overlap between the proteins was determined. In agreement with a previous study in rat adipocytes (Martin *et al.*, 1997), a significant degree of overlap between GLUT4 and the CD-M6PR (~70%) was observed (Table 3.1). A high percentage (~90%) of the γ-adaptin labelled vesicles also co-labelled for GLUT4 in these cells (Figure 3.9, Table 3.1). Although the γ-adaptin labelling detected by immuno-EM in the isolated vesicles was very low, the high percentage of co-labelling with GLUT4 in these vesicles confirms the immunoadsorption data, where GLUT4 vesicles were found to immunoprecipitate γ-adaptin present in the intracellular (LDM) membranes (Figure 3.7).

The intracellular distribution of GLUT4, the CD-M6PR and γ-adaptin was analysed in detail using immuno-EM studies on cryosections of basal 3T3-L1 adipocytes by T. Meerloo (University of Queensland, Australia). All three proteins were found to be concentrated in tubulovesicular-elements in the perinuclear region of the cells, associated with the TGN. However, there was also some additional labelling in the periphery of the cells. Double-labelled sections showed GLUT4 to co-localise with both the CD-M6PR and γ-adaptin in the TGN region of the basal 3T3-L1 adipocytes (data not shown).

Table 3.1

Analysis of Vesicle Labelling and Co-Localisation of GLUT4 with γ-adaptin and the CD-M6PR

A. γ-adaptin	Total vesicles labelled (%)		% co-localisation	
	GLUT4	γ-adaptin	GLUT4 vesicles containing γ-adaptin	γ-adaptin vesicles containing GLUT4
3T3-L1 adipocytes	15.2 ± 2.8	4.9 ± 1.7	18.0 ± 3.5	90.6 ± 7.0

B.CD-M6PR	Total vesicles labelled (%)		% co-localisation	
	GLUT4	CD-M6PR	GLUT4 vesicles containing CD-M6PR	CD-M6PR vesicles containing GLUT4
3T3-L1 adipocytes	17.8 ± 4.9	21.5 ± 6.8	73.3 ± 3.8	70.0 ± 2.3

In collaboration with S. Martin (University of Queensland, Australia) intracellular vesicles were isolated from 3T3-L1 adipocytes and double-labelled with antibodies specific for GLUT4 and γ-adaptin or the CD-M6PR tagged with different sized particles of colloidal gold. The degree of co-localisation between GLUT4 and γ-adaptin or the CD-M6PR was determined as a function of the total population of either GLUT4 vesicles or γ-adaptin/CD-M6PR vesicles, that contained the other marker (mean ± s.e.m).

Figure 3.1

Subcellular Distribution of GLUT4, γ-adaptin, SCAMPs, the CD-M6PR, Syntaxin 4, CSP and Rab4 in 3T3-L1 adipocytes and the Effect of Insulin

Shown is the distribution of GLUT4 (~45kDa), γ-adaptin (~90kDa), SCAMPs (~37&39kDa), CD-M6PR (~46kDa), Syntaxin 4 (~32kDa), CSP (dimer of ~70kDa) and Rab4 (~24kDa) in subcellular fractions isolated from basal (non-stimulated) and insulin-stimulated 3T3-L1 adipocytes (insulin exposure for 15 min at 1 μM). Subcellular membrane fractions (PM, LDM and HDM) were prepared and subjected to SDS-PAGE, electrophoretically transferred to nitrocellulose membranes, and immunoblotted with the antibodies indicated. The immunoblots were developed using ECL. It should be noted that equal volumes of protein were added to each lane except in the case of the syntaxin 4 immunoblot where twice as much protein sample was loaded to the lanes representing the LDM fractions in order to examine the intracellular pool of this protein. Each immunoblot is representative of at least two other experiments.

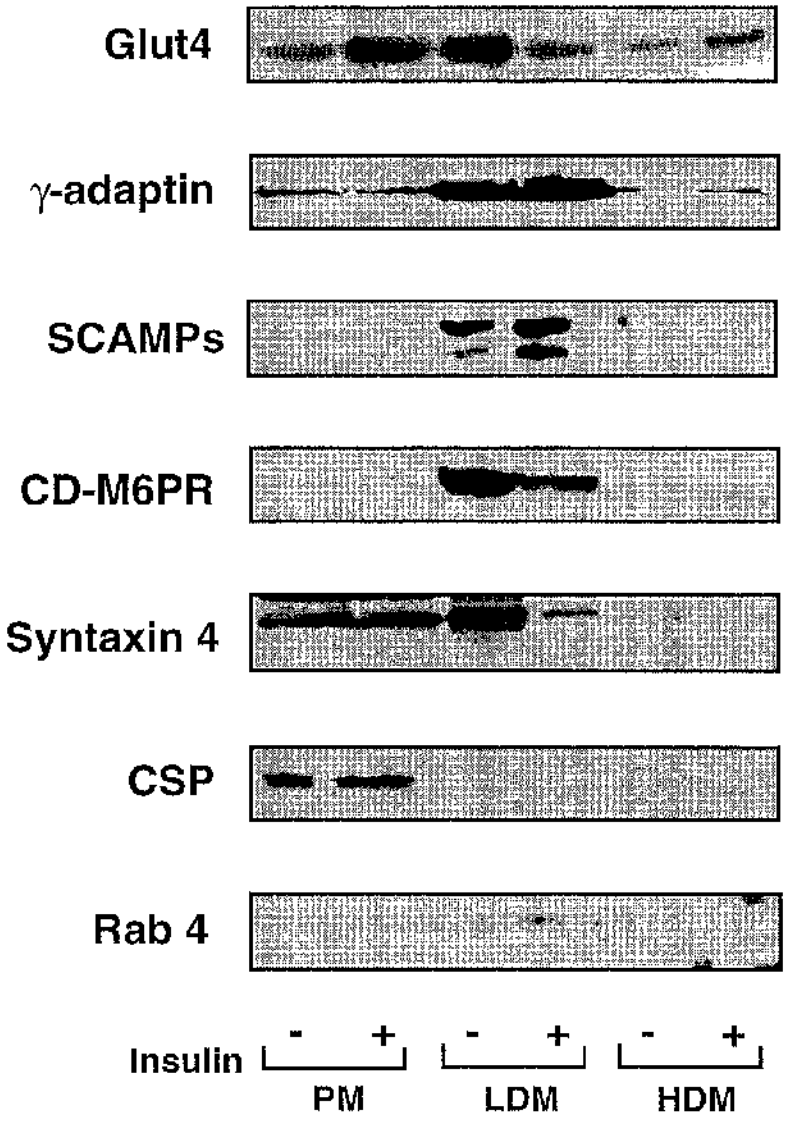
Glut4
γ-adaptin
SCAMPs
CD-M6PR
Syntaxin 4
CSP
Rab 4
Insulin
- + - + - +
PM
LDM
HDM

Figure 3.2

The Effect of Endosomal Ablation on the Intracellular Levels of GLUT4, TfR, γ-adaptin and CD-M6PR in 3T3-L1 Adipocytes

Duplicate plates of 3T3-L1 adipocytes were loaded with Tf-HRP at either 4°C or 37°C (as indicated) and incubated with DAB ± H_2O_2 as described in *Materials and Methods*. Intracellular (LDM) membrane fractions were isolated from these cells, and immunoblotted with the antibodies indicated. The effect of ablation at 37°C was determined by comparison of the signals in the - and + lanes. The 4°C experiment is included as a control to show that at this temperature there is no internalisation of the conjugate and hence no ablation. In each experiment, 25% of the LDM fraction from a single 10cm plate were loaded in each lane. Immunoblots were developed by ECL and quantified using densitometry. Quantitation of three individual immunoblots indicated that ~79% of the TfR signal was lost in the presence of peroxide whereas only ~38% and ~35% of the GLUT4 and the CD-M6PR signal were lost in the presence of peroxide, respectively.

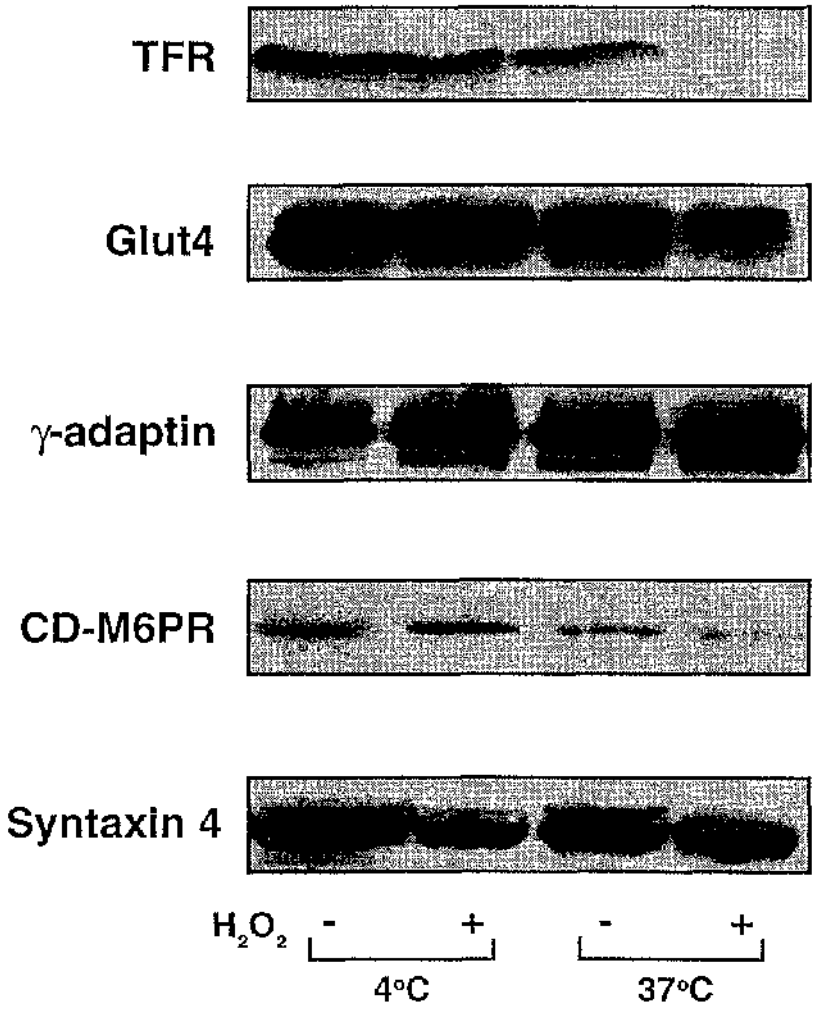
TFR
Glut4
γ-adaptin
CD-M6PR
Syntaxin 4
H2O2 - + - +
4°C
37°C

Figure 3.3

Sucrose Density Gradient Analysis of γ-adaptin Distribution in the Intracellular (LDM) Membranes of 3T3-L1 Adipocytes Before and After Ablation

3T3-L1 adipocytes were loaded with Tf-HRP at 37°C and incubated with DAB ± H_2O_2 as described in *Materials and Methods*. Intracellular (LDM) membranes were prepared and subfractionated on discontinuous sucrose gradients as described. Samples were collected and subjected to SDS-PAGE and immunoblot analysis using antibodies to γ-adaptin. The density of sucrose solutions increases from right to left (as indicated). There was no significant change in the density of membranes containing γ-adaptin following ablation. The experiment was repeated with similar results.

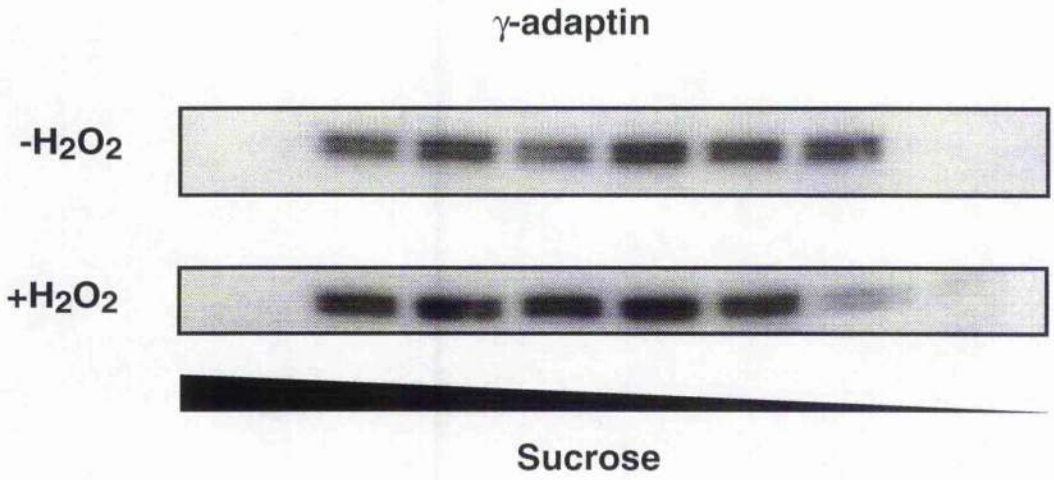
γ-adaptin
-H2O2
+H2O2
Sucrose

Figure 3.4

Sucrose Density Gradient Analysis of Rab4 Distribution in the Intracellular (LDM) Membranes of Basal and Insulin-Stimulated 3T3-L1 Adipocytes Before and After Ablation

3T3-L1 adipocytes were loaded with Tf-HRP and treated with (+) or without (-) insulin (1μM) for the last 15 min of the incubation at 37°C. The cells were then incubated with DAB ± H_2O_2 as descibed in *Materials and Methods*. Intracellular (LDM) membranes were prepared and subfractionated on discontinuous sucrose gradients as described. Samples were collected and subject to SDS-PAGE and immunoblot analysis using antibodies to Rab4. The density of sucrose solutions increases from right to left (as indicated). In the presence of peroxide (+ H_2O_2) the Rab4 signal is lost in a manner similar to that observed in insulin-stimulated cells both before and after ablation. Each immunoblot is representative of at least two other experiments.

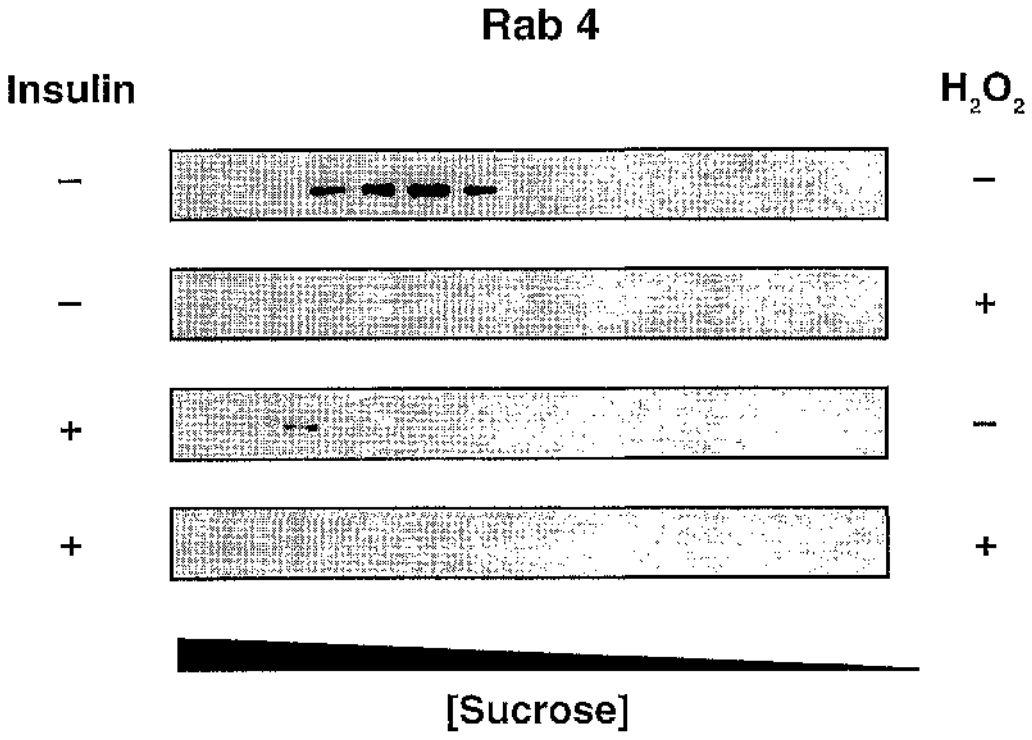
Rab 4
Insulin
H_2O_2
–
–
+
+
–
+
–
+
[Sucrose]

Figure 3.5

Sucrose Density Gradient Analysis of GLUT4 and SCAMPs Distribution in the Intracellular (LDM) Membranes of 3T3-L1 Adipocytes Before and After Ablation

3T3-L1 adipocytes were loaded with Tf-HRP at 37°C and incubated with DAB ± H_2O_2 as descibed in *Materials and Methods*. Intracellular (LDM) membranes were prepared and subfractionated on discontinuous sucrose gradients as described. Samples were collected and subject to SDS-PAGE and immunoblot analysis using antibodies to GLUT4 and SCAMPs as indicated. In the experiment shown, fraction 1 is the material which pelleted at the bottom of the gradient (far left); samples 2-12 were isolated from the gradient such that sample 2 contains the highest density of sucrose and sample 12 the lowest (far right). In the presence of peroxide, a partial loss of GLUT4 signal was observed whereas essentially all of the SCAMPs signal was recovered in sample 1.

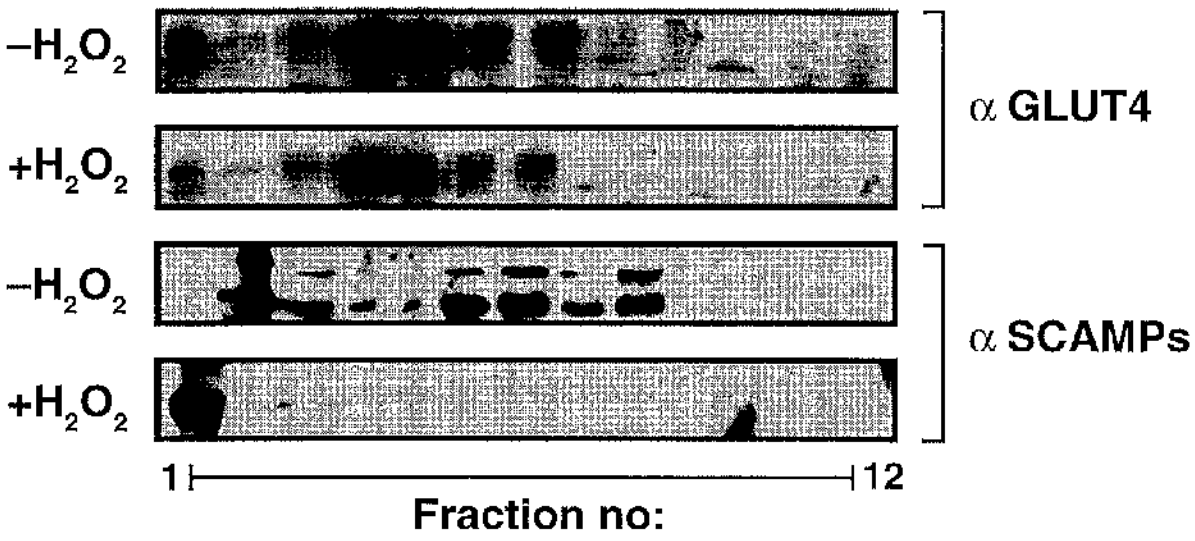
–H2O2
+H2O2
–H2O2
+H2O2
α GLUT4
α SCAMPs
1
12
Fraction no:

Figure 3.6

Co-Localisation of the CD-M6PR and Syntaxin 4 with GLUT4-Containing Vesicles

3T3-L1 adipocytes were loaded with Tf-HRP at 37°C and incubated with DAB ± H_2O_2 as descibed. Intracellular (LDM) membranes were isolated and incubated with anti-GLUT4 antibody or non-specific IgG (control) pre-coupled to *Staph. a.* cells as described in Section 2.11. Immunoadsorbed vesicles (GLUT4 and IgG) and depleted LDM fractions (GLUT4 and IgG) were subjected to SDS-PAGE and immunoblot analysis with antibodies, as indicated.

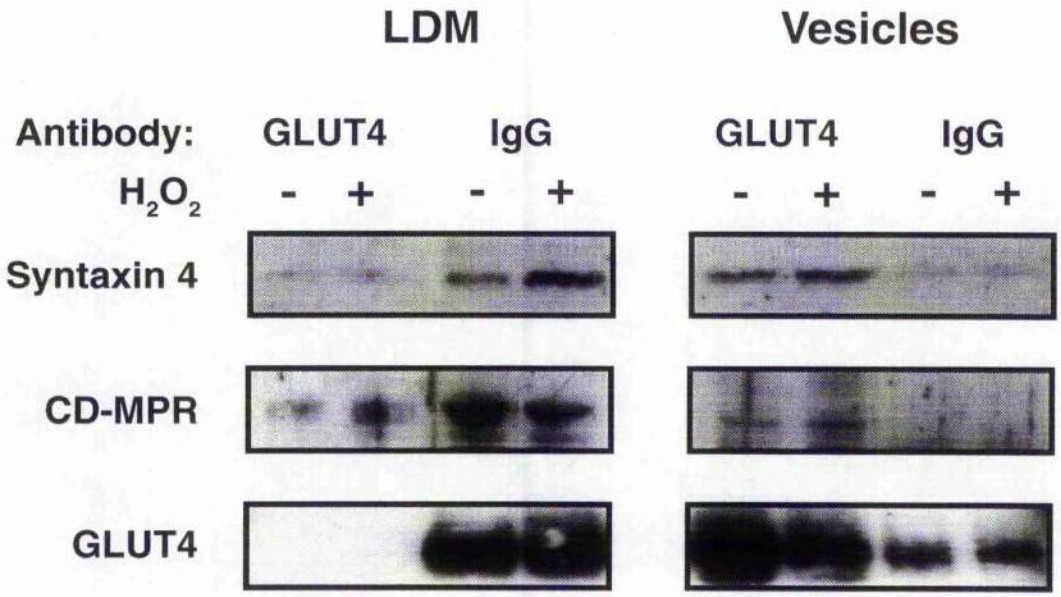
LDM
Vesicles
Antibody:
GLUT4
IgG
GLUT4
IgG
H_2O_2
- + - +
- + - +
Syntaxin 4
CD-MPR
GLUT4

Figure 3.7

Co-Localisation of γ-adaptin with GLUT4-Containing Vesicles

3T3-L1 adipocytes were loaded with Tf-HRP at 37°C and incubated with DAB ± H_2O_2 as descibed. Intracellular (LDM) membranes were isolated and incubated with anti-GLUT4 antibody pre-coupled to *Staph. a.* cells as described. Immunoadsorbed GLUT4 vesicles were subjected to SDS-PAGE and immunoblot analysis with γ-adaptin and GLUT4 antibodies.

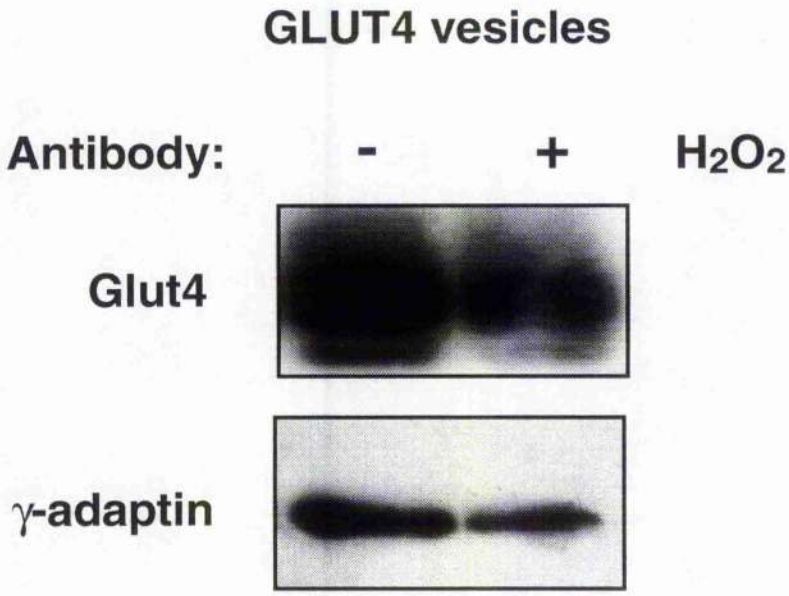
GLUT4 vesicles
Antibody:
-
+
H2O2
Glut4
γ-adaptin

Figure 3.8

Double-Labelled Immunofluorescence Analysis of Basal 3T3-L1 Adipocytes

Triton-permeabilised 3T3-L1 adipocytes were incubated with a mouse monoclonal anti-GLUT4 antibody and the corresponding secondary antibody (TRITC-conjugated goat anti-mouse IgG, stained red in A and B) in conjunction with either a rabbit anti-γ-adaptin antibody or a rabbit anti-CD-M6PR antibody and the corresponding secondary antibody (FITC-conjugated goat anti-rabbit IgG, stained green in A and B, respectively). All three proteins were predominantly present in the perinuclear region of the cells, although there was also some peripheral punctate labelling observed. The yellow colour indicates co-staining between proteins.

A

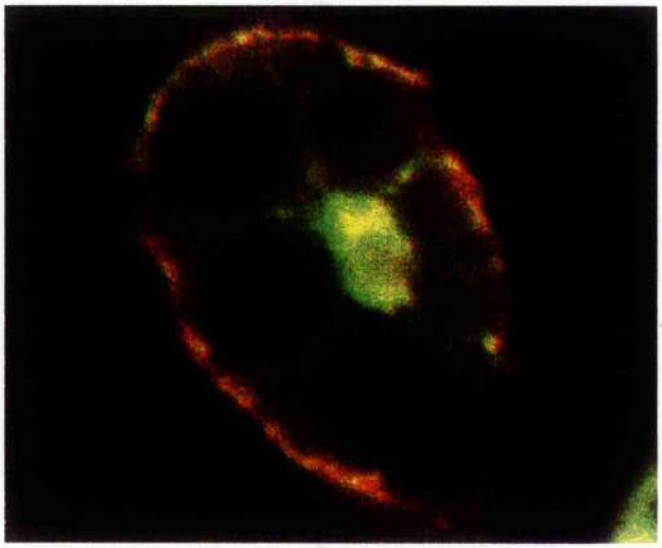

B

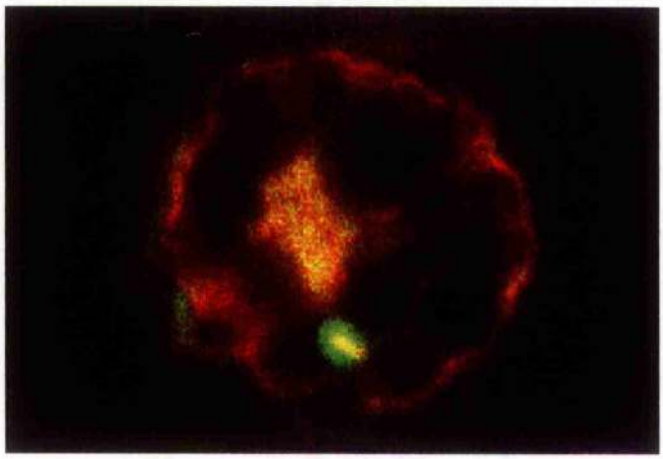

Figure 3.9

Immuno-EM of γ-adaptin and GLUT4 in Isolated Vesicles

In collaboration with S. Martin (University of Queensland, Australia), intracellular vesicles were prepared from basal (non-stimulated) 3T3-L1 adipocytes. Vesicles were absorbed to formvar carbon-copper coated grids and double-labelled using antibodies specific for γ-adaptin detected using 10nm protein A-gold, followed by antibodies for GLUT4 detected using 5nm protein A-gold. Similar results were obtained when the antibodies were applied in reverse order. Labelling of individual vesicles was quantified, the results of which are shown in Table 3.1.

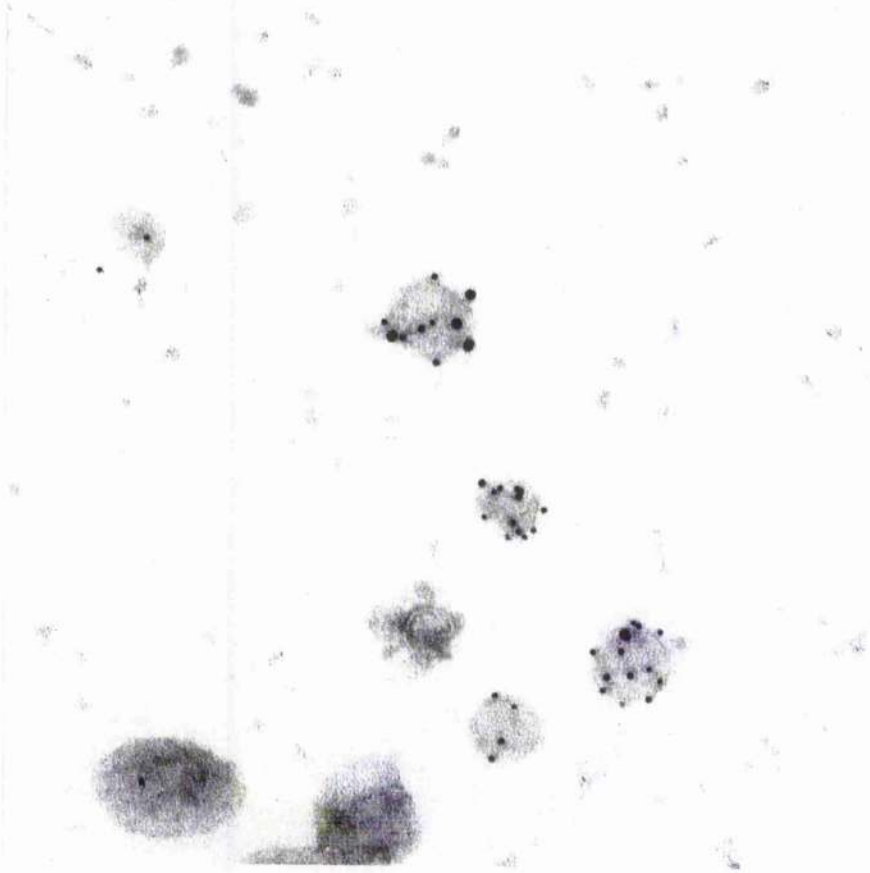

3.5 Discussion

Endosomal ablation and immuno-electron microscopy analysis have recently suggested that there is a GLUT4-containing compartment distinct from the recycling endosomal system (Livingstone *et al.*, 1996; Martin *et al.*, 1996). In 3T3-L1 adipocytes, under conditions in which all the recycling TfR-containing endosomes are destroyed (ablated), a large proportion of GLUT4 (~60%) is recovered in a post-endocytic compartment (referred to as the non-ablatable compartment) (Livingstone *et al.*, 1996). Moreover, GLUT4 was found to co-localise with VAMP2 in this post-endocytic compartment in both 3T3-L1 adipocytes (Martin *et al.*, 1996) and rat adipocytes (Malide *et al.*, 1997a), consistent with the notion that this may be a specialised secretory compartment from which the translocation of GLUT4 to the plasma membrane is regulated by insulin. Here, I have used endosomal ablation to determine the protein composition of the non-ablatable GLUT4 compartment with the aim of further defining the relationship of this compartment to other, well chararcterised, intracellular membrane structures.

In the present study, I wished to investigate the co-localisation of GLUT4 relative to marker proteins that define distinct intracellular compartments (γ-adaptin, the CD-M6PR and Rab4) and proteins known to be involved in exocytosis (SCAMPs, syntaxin 4 and CSPs) in 3T3-L1 adipocytes. To do this, I initially determined the subcellular distribution of these proteins in the absence and presence of insulin. On determining which proteins were localised to the intracellular membranes enriched in GLUT4, I examined the effect of endosomal ablation on the intracellular levels of these proteins and finally, determined their co-localisation with GLUT4 using vesicle immunoadsorption and / or immuno-electron microscopy analysis.

3.5.1 SCAMPs, Syntaxin 4 and CSPs: Markers for Exocytosis

The sequestration of GLUT4 from the recycling endosomal system into a specialised storage compartment in the absence of insulin is similar in many ways to the re-formation of synaptic vesicles in neuronal cells. Furthermore, the co-localisation of GLUT4 with synaptobrevin homologues (VAMP2 and cellubrevin / v-SNAREs) (Martin *et al.*, 1996; Volchuk *et al.*, 1995) and SCAMPs (Laurie *et al.*, 1993), suggests that GLUT4-containing vesicles are indeed analagous to small synaptic vesicles found in neuroendocrine cells. However, recent ablation studies have shown that the two v-SNAREs, although both found to co-localise with GLUT4 vesicles, are actually localised to distinct compartments (refer to Section 1.13) (Martin *et al.*, 1996), suggesting that they define separate classes of secretory vesicles. Indeed, the co-localisation of VAMP2 in the non-ablatable GLUT4 compartment suggests a possible role for this protein in the regulation of insulin-dependent GLUT4 trafficking, whereas the quantitative ablation of cellubrevin suggests that this v-SNARE may mediate the trafficking of the transporter through the endosomal system (Martin *et al.*, 1996).

In this study I have examined whether SCAMPs and syntaxin 4, secretory proteins previously identified in adipocytes, co-localise with GLUT4 in the non-ablatable compartment. The recent observation that CSPs are associated with secretory granules in endocrine cells as well as synaptic vesicles (Chamberlain *et al.*, 1996b), suggesting a role for these proteins in regulated exocytosis, also prompted me to to determine whether these proteins were present in adipocytes, and if they co-localised with GLUT4 vesicles.

SCAMPs are ubiquitously expressed proteins localised to membranes of both secretory and endocytic vesicles involved in transport both to and from the cell surface (Laurie *et al.*, 1993). They have previously been identified in adipocytes and have been shown to co-localise with GLUT4. In agreement with a previous study on

rat adipocytes (Laurie *et al.*, 1993), I observed the majority of SCAMPs to be localised to the intracellular (LDM) fraction enriched in GLUT4. However, in contrast to GLUT4, there was no significant decrease in the intracellular levels of SCAMPs in response to insulin (Figure 3.1). Prolonged exposure of the immunoblots did, however, reveal a small increase in SCAMP levels in the plasma membrane fraction in response to insulin. This increase is not apparent in the immunoblot shown in Figure 3.1, but is observed at higher protein loads, consistent with a previous study in adipocytes (Laurie *et al.*, 1993).

Syntaxin 4, a t-SNARE predominantly targeted to the plasma membrane of 3T3-L1 adipocytes, is thought to interact with VAMP2, facilitating the docking and fusion of GLUT4 vesicles in response to insulin (Olson *et al.*, 1997; Tellam *et al.*, 1997). However, a smaller but significant intracellular pool of syntaxin 4 was also observed in the intracellular (LDM) membrane fraction (Tellam *et al.*, 1997), suggesting a possible role for the t-SNARE in intracellular trafficking as well as in docking and fusion at the cell surface. As syntaxin 4 has been found to bind both VAMP2 and cellubrevin *in vitro* (Tellam *et al.*, 1997), I wished to determine whether this protein co-localised with GLUT4 in the GLUT4/VAMP2-positive post-endocytic compartment. In agreement with the aforementioned study in 3T3-L1 adipocytes, syntaxin 4 was predominantly localised to the plasma membrane, but a small fraction was also detected in the intracellular (LDM) membrane fraction. Similarily to GLUT4, in response to insulin there was a decrease in syntaxin 4 in this fraction. However, the low level of expression preluded quantitative analysis of the extent of this effect (Figure 3.1).

CSPs were found to be membrane-associated in 3T3-L1 adipocytes. However, in contrast to previous studies in endocrine cells where CSPs were found to be associated with secretory granules (Chamberlain *et al.*, 1996b), in 3T3-L1 adipocytes these proteins were localised to the plasma membrane, and were not detectable in the intracellular LDM fraction (Figure 3.1). There was no change in the distribution of

these proteins in response to insulin. These data suggest that CSPs are not associated with GLUT4 vesicles sequestrated within the cell in the absence of insulin.

As both SCAMPs and syntaxin 4 were observed in the intracellular (LDM) membrane fraction enriched in GLUT4, I examined the effect of endosome ablation on the intracellular levels of these proteins. As shown in Figure 3.2, I did not observe any ablation of syntaxin 4 in these cells, indicating that the intracellular complement of this protein does not reside in the recycling endosomal system. To determine whether this intracellular pool of syntaxin 4 co-localised with GLUT4 in the non-ablatable compartment, I examined the extent of co-localisation of syntaxin 4 and GLUT4 by vesicle immunoadsorption (Figure 3.6). Syntaxin 4 was found to co-localise to the same extent with GLUT4 vesicles both before and after ablation, suggesting that the majority, if not all, of the syntaxin 4 detected in GLUT4 vesicles resides in the non-ablatable compartment. Furthermore, the absence of syntaxin 4 in the depleted LDM membranes, suggests that almost the entire intracellular complement of this protein is associated with the GLUT4 non-ablatable compartment. Thus, it seems plausible that syntaxin 4 may also play a role in the intracellular trafficking of GLUT4, as well as regulating the docking of GLUT4 vesicles with the cell surface, as has been recently proposed (Olson *et al.*, 1997; Tellam *et al.*, 1997).

In marked contrast, the ablation procedure effectively removed the vast majority of the immunodetectable SCAMPs from the intracellular membrane pool, indicated by a shift of SCAMP immunoreactivity to the most dense fraction of the sucrose gradient (Figure 3.5). The quantitative ablation of these proteins indicates that the SCAMPs are localised within the recycling endosomal system in these cells, and that the co-localisation previously observed between GLUT4 and SCAMPs in rat adipocytes (Laurie *et al.*, 1993) was most likely within this endosomal compartment. The identification of a distinct compartment highly enriched in GLUT4 but not SCAMPs

may also explain the segregation of the two proteins in response to insulin as only GLUT4 was found to redistribute appreciably to the plasma membrane in a previous study on rat adipocytes (Laurie *et al.*, 1993). In response to insulin, GLUT4 may translocate to the plasma membrane from the non-ablatable compartment devoid of SCAMPs and also from the recycling endosomal system as constitutive recycling is upregulated in response to insulin (Tanner *et al.*, 1987; Tanner *et al.*, 1989). However, as SCAMPs are localised to the recycling endosomal system the upregulation of constitutive recycling alone will account for the smaller increase of these proteins at the plasma membrane in response to insulin. Taken together, these data further support the existence of an intracellular GLUT4 compartment which is distinct from the recycling endosomal system.

3.5.2 Rab4

The small GTP-binding protein Rab4, has previously been characterised as a compartmental marker for the endosomal system, where it mediates the recycling of early endosomes (Van Der Sluijs *et al.*, 1992; Bottger *et al.*, 1996). Recent studies have implicated Rab4 as a component of the GLUT4 trafficking machinery, involved in both insulin-stimulated GLUT4 translocation and the biogenesis of the storage compartment (Cormont *et al.*, 1996; Shibata *et al.*, 1996; Mora *et al.*, 1997). The association of Rab4 with GLUT4 vesicles is consistent with both these proteins being present in the recycling endosomal system. However, as Rab4 is thought to be involved in insulin-stimulated GLUT4 translocation I wished to determine whether a sub-population of Rab4 may associate with GLUT4 in the non-ablatable compartment in 3T3-L1 adipocytes. Analysis of the subcellular distribution of these proteins showed Rab4 to be localised to the intracellular (LDM) membranes enriched in GLUT4 (Figure 3.1), consistent with previous observations (Cormont *et al.*, 1993). However, in the aforementioned study, insulin induced a redistribution of both GLUT4 and Rab4 from this fraction to the plasma membrane and cytosolic fractions, respectively (Cormont *et al.*, 1993). I was unable to detect the

redistribution of Rab4 from the LDM fraction in this study. The fact that Rab4 was not detected in the cytosolic fraction (data not shown) may be explained by the degradation of this protein (despite the presence of proteinase inhibitors) following the complete subcellular fractionation of 3T3-L1 adipocytes. Indeed, a rapid and simple preparation of only total membranes and cytosol was required in rat adipocytes in order to observe the redistribution of Rab4 to the cytosolic compartment in response to insulin (Cormont *et al.*, 1993).

As Rab4 is not a transmembrane protein and therefore does not exhibit a lumenal domain within the vesicles to which they are associated, endosome ablation was analysed by sucrose density gradient analysis (Figure 3.4). Under these conditions, GLUT4 exhibited a partial loss of signal, consistent with the partial ablation of this protein (Figure 3.5). In contrast, the ablation procedure effectively removed all of the immunodetectable Rab4 from the intracellular membrane pool, suggesting that the entire cellular complement of this protein resides with the TfR within the recycling endosomal system. However, the complete lack of immunoreactivity in the immunoblot implies that Rab4 may no longer be associated with the LDM fraction possibly as a result of the ablation procedure, as observed for the dissociation of Rab4 from this fraction in response to insulin, as shown in Figure 3.4. However, as the ablation procedure did not appear to effect the association of Rab5 with intracellular membranes (Livingstone *et al.*, 1996), it is surprising that the same procedure would have an adverse effect on the association Rab4 with membranes. Unfortunately, as I was unable to detect Rab4 in the cytosolic fraction both after ablation or insulin treatment, we cannot confirm whether this is indeed the case (see above). On interpretation of these data at face value, the implication that the co-localisation of Rab4 and GLUT4 within 3T3-L1 adipocytes occurs within the recycling endosomal system is consistent with the notion that Rab4 participates in the trafficking of GLUT4 from the recycling endosomal system to the specialised storage compartment (Cormont *et al.*, 1996). However, a role for this small GTP-binding protein in insulin-stimulated GLUT4 translocation whilst localised to the

recycling system is not as clear. Although, if an alternative model of insulin-stimulated GLUT4 translocation to the cell surface is considered, where in response to insulin GLUT4 from the storage compartment fuses with the endosomal system instead of directly with the plasma membrane (Robinson *et al.*, 1992a), it is possible to envisage a possible role for Rab4 in this process. However, from these studies it is apparent that an alternative approach is required in order to further our understanding of the exact role of Rab4 in terms of GLUT4 intracellular trafficking.

3.5.3 γ-adaptin and the CD-M6PR: Markers for the TGN

As the TGN mediates the sorting of proteins destined for a wide variety of intracellular destinations including the endosomal system and the regulated secretory pathway, I wished to determine whether GLUT4 traffics through this compartment. Sorting of membrane proteins at the TGN involves the recruitment of cytosolic adaptors including AP-1 and AP-3 onto the membrane (refer to Section 1.4.3). The localisation of GLUT4 with clathrin-coated pits at the plasma membrane (Slot *et al.*, 1991b), suggests that the internalisation and / or intracellular targeting of the transporter may be mediated via interaction of the adaptor complex AP-2, associated with these pits. Similarily, sorting of GLUT4 at the TGN may be mediated by the clathrin-associated AP-1 complex. As γ-adaptin is a component of the AP-1 complex, we examined the extent of co-localisation between this protein and GLUT4 in 3T3-L1 adipocytes. Analysis of the subcellular distribution of γ-adaptin showed the majority of this protein to be localised to the intracellular (LDM) membranes (Figure 3.1), consistent with this fraction being enriched in the TGN. In contrast to GLUT4, γ-adaptin did not exhibit any significant redistribution in response to insulin. However, insulin-stimulated clathrin-coated budding from the TGN cannot be ruled out as many nascent secretory granules in the TGN are clathrin-coated, but shed their coat prior to exocytosis (Austin *et al.*, 1996).

Endosome ablation did not result in a significant loss of γ-adaptin immunoreactivity under conditions where quantitative ablation of the TfR from intracellular (LDM) membranes was observed (Figure 3.2). Similarily, no significant increase in the density of the intracellular membranes with which γ-adaptin is associated was observed following ablation (Figure 3.3). These data provide further evidence for the relatively low levels of γ-adaptin present in the recycling endosomal system. Analysis of GLUT4 vesicles immunoadsorbed both before and after ablation showed a significant level of co-localisation between these two proteins (Figures 3.7), suggesting that the majority of the γ-adaptin detected in the GLUT4 vesicles resides in the non-ablatable GLUT4 compartment. Furthermore, the co-localisation of GLUT4 with a component of AP-1 coated vesicles, suggests that GLUT4 is present within the TGN region of 3T3-L1 adipocytes.

Newly synthesised lysosomal enzymes are transported from the TGN to the prelysosome by a mannose 6-phosphate dependent pathway (Klumperman *et al.*, 1993). Most mammalian cells contain two distinct M6PRs: the cation-independent M6PR (CI-M6PR, also known as the insulin-like growth factor II receptor) of ~ 300kD and the cation-dependent M6PR (CD-M6PR), a homodimer of 46kD, both of which traffic from the TGN in AP-1 coated vesicles *en route* to the endosomes (Klumperman *et al.*, 1993). Although both the CI-M6PR and the CD-M6PR co-localise, a difference in distribution has been observed, probably due to functional differences between the two receptors (Klumperman *et al.*, 1993). The CI-M6PR is predominantly localised to early endosomes and to prelysosomal compartments (Klumperman *et al.*, 1993), consistent with the delivery of exogenous lysosomal enzymes to lysosomes via the endocytic pathway. In contrast, the requirement for the CD-M6PR to deliver ligands to both the lysosomes and the extracellular environment has localised this receptor predominantly to the TGN and tubulovesicular elements associated with the early endosomes (Klumperman *et al.*, 1993).

Previous studies have observed complete ablation of the CI-M6PR under conditions which resulted in only a ~ 40% ablation of GLUT4 (Livingstone *et al.*, 1996), suggesting that the pre-lysosomal compartments are unlikely to be the site of GLUT4 sequestration. In this study, we have examined the extent of co-localisation of the CD-M6PR with GLUT4 in 3T3-L1 adipocytes. The subcellular distribution of the CD-M6PR was found to be similar to that of GLUT4, as both proteins were localised to the intracellular (LDM) membranes and redistributed to the plasma membrane in response to insulin (Figure 3.1). However, the extent of this translocation to the plasma membrane was notably smaller in the case of the CD-M6PR. Under conditions in which ~ 38% of GLUT4 was ablated, a small proportion (~ 35%) of the CD-M6PR was also lost from the intracellular (LDM) membranes (Figure 3.2), suggesting that smaller pools of both of these proteins reside with the TfR in the recycling endosomal system. Vesicle immunoadsorption analysis showed that there was some degree of overlap between the two proteins after ablation, indicating that the CD-M6PR does co-localise to some extent with GLUT4 in the non-ablatable GLUT4 compartment (Figure 3.6). However, a significant proportion of the CD-M6PR remained in the depleted LDM fraction under conditions where the GLUT4 immunoreactivity was completely removed. Collectively, these data suggest that the CD-M6PR is localised in part to both the recycling endosomal system and the non-ablatable GLUT4 pool, but that these two fractions do not constitute the total cellular complement of this protein. Futhermore, the localisation of the CD-M6PR in the GLUT4 non-ablatable pool provides further evidence for the localisation of GLUT4 in the TGN region of 3T3-L1 adipocytes.

To determine whether the co-localisation observed between GLUT4 and γ-adaptin or the CD-M6PR was indeed within the TGN, I further examined the co-localisation and intracellular distribution of the three proteins by immunofluorescence microscopy and immuno-electron microscopy in collaboration with S. Martin and T. Meerloo (University of Queensland, Australia). Immuno-electron microscopy analysis of double-labelled intracellular vesicles of basal 3T3-L1 adipocytes revealed

a significant overlap between GLUT4 and the CD-M6PR (~70%), consistent with the co-localisation of these two proteins both within the recycling endosomal system and the GLUT4 non-ablatable compartment (Table 3.1). A high percentage (~90%) of the γ-adaptin labelled vesicles were also found to co-label for GLUT4, confirming the co-localisation of these two proteins in 3T3-L1 adipocytes (Table 3.1, Figure 3.9). Upon analysis of 3T3-L1 adipocyte cryosections by immuno-electron microscopy, all three of the proteins were found to be localised in tubulovesicular elements associated with the TGN. Furthermore, double-labelling of these sections revealed that both the CD-M6PR and γ-adaptin co-localised with GLUT4 within this region, consistent with the partial overlap of GLUT4 with the CD-M6PR (Figure 3.8A) and γ-adaptin (Figure 3.8B) in the perinuclear region of 3T3-L1 adipocytes observed by double-labelled immunofluorescence.

Together these data confirm that the co-localisation of GLUT4 with the CD-M6PR and γ-adaptin within the GLUT4 non-ablatable compartment is within the region of the TGN in 3T3-L1 adipocytes. The localisation of GLUT4 to AP-1 positive vesicles is consistent with the partial overlap of GLUT4 with γ-adaptin in perinuclear structures in rat adipocytes (Malide *et al.*, 1997a). However, as these vesicles are also enriched in CD-M6PR which does not appear to translocate to the cell surface in response to insulin to the same extent as GLUT4, it is unlikely that these vesicles bud directly from the TGN forming the insulin-responsive storage compartment. Indeed, co-localisation with the CD-M6PR suggests that the vesicles fuse with the endosomal system. Thus, we propose that GLUT4 traffics through the TGN in AP-1 positive vesicles, and suggest that along with the CD-M6PR, GLUT4 recycles back to the endosomal system where GLUT4 may be sorted into the specialised storage compartment.

3.6 Summary

By comparing the distribution and susceptibility to endosome ablation of GLUT4 and several other marker proteins, I have shown that a small pool of GLUT4 resides within the recycling endosomal system, consistent with the partial ablation of this transporter compared to the quantitative ablation of the TfR and SCAMPs, known markers for cell surface to endosome recycling. Within the larger non-ablatable pool, GLUT4 was found to co-localise with syntaxin 4, the CD-M6PR and γ-adaptin. These data confirm that the well-characterised recycling endosomal system plays a fundamental role in the constituive recycling of GLUT4. The co-localisation of GLUT4 with the CD-M6PR and γ-adaptin is consistent with the non-ablatable GLUT4 compartment deriving, at least in part, from the TGN. Moreover, this adds further support to the notion that GLUT4 traffics through the TGN as part of its recycling itinerary. The observation that a small proportion of syntaxin 4 co-localises with GLUT4 in an intracellular compartment suggests that this t-SNARE may be involved in intracellular protein sorting, but this point will require further characterisation. In short, these data add further support to the notion that a significant proportion of the intracellular GLUT4 resides in a specialised post-endocytic storage compartment. Regardless of the identity of the pools identified by endosome ablation, this appproach offers a powerful tool with which to resolve the intracellular segregation of GLUT4. In the following chapter I will consider how GLUT4 traffics from the GLUT4/VAMP2-positive non-ablatable compartment to the cell surface in response to insulin.

Chapter 4

Compartment Ablation Analysis of Insulin-and GTPγS-Stimulated GLUT4 Translocation from Multiple Intracellular Compartments

4.1 Aims

1. To examine the effect of endosomal ablation on protein trafficking through the recycling endosomal system.

2. To examine the effect of endosomal ablation on insulin- and GTPγS-stimulated GLUT4 and GLUT1 translocation.

3. To examine the effect of wortmannin on insulin-stimulated GLUT4 translocation following ablation of the endosomal system.

4. To examine the effect of endosomal ablation on constitutive secretion in 3T3-L1 adipocytes.

4.2 Introduction

Insulin stimulates the uptake of glucose in adipose cells by inducing the redistribution of GLUT4 from an intracellular site to the plasma membrane. Recent studies have shown that GLUT4 resides within at least two intracellular compartments, one of which is endosomal, marked by the presence of endosomal recycling proteins such as the TfR and SCAMPs (refer to Section 3.5.1), and the other a post-endocytic storage compartment (Livingstone *et al.*, 1996; Martin *et al.*, 1996; Malide *et al.*, 1997a). However, the exact mechanism of insulin-stimulated translocation from these intracellular compartments to the cell surface remains poorly understood.

Two models have been used to describe possible mechanisms for the insulin-stimulated translocation of GLUT4 to the cell surface (reviewed in Rea *et al.*, 1997). In the first model, the insulin-responsive storage compartment is thought to be sequestered within a topologically continuous subdomain of the endosomal system. Upon trafficking through the recycling system, interaction with various retention factors withdraws GLUT4 into this endosomal subdomain. Insulin stimulation is predicted to disrupt the interaction between GLUT4 and the retention factors, allowing the transporter to re-enter the constitutive recycling pathway and gain access to the cell surface. In this model, no specialised trafficking machinery is required for GLUT4 translocation as this function would presumably be fulfilled by the constitutive machinery utilised by the endosomal system.

The second model suggests that GLUT4 is sorted and removed from the endosomal system into a specialised secretory compartment, from which GLUT4 may translocate to the cell surface in response to insulin, independently of the recycling system. An important feature of this model is that a possible site of insulin action is the machinery that mediates the targeting and the docking/fusion of the GLUT4-containing vesicles with the plasma membrane.

The mechanism of insulin-stimulated GLUT4 translocation described by the second model is similar in many ways to the regulated exocytosis of synaptic secretory vesicles (SSVs) in neurons (refer to Section 1.13). In this regard, two independent studies have recently shown that VAMP2, a v-SNARE that targets SSVs to the pre-synaptic plasma membrane (refer to Section 1.5), co-localises with GLUT4 in the post-endocytic storage compartment (Martin *et al.*, 1996; Malide *et al.*, 1997a). In addition, syntaxin 4 and SNAP-23, homologues of neuronal VAMP2-binding proteins (t-SNAREs), have recently been identified in adipocyte plasma membranes (refer to Section 1.13) (Tellam *et al.*, 1997; Araki *et al.*, 1997). Furthermore, inhibition of the insulin-stimulated translocation of GLUT4 by VAMP2 peptides (Macaulay *et al.*, 1997) as well as syntaxin 4 fusion proteins (Olson *et al.*, 1997) in permeabilised or microinjected adipocytes, suggests that both of these proteins play an essential role in insulin-stimulated GLUT4 trafficking. Together these findings strongly support the regulated exocytosis model of GLUT4 trafficking, and further suggest that GLUT4 may be stored in intracellular vesicles that resemble SSVs.

Insulin-sensitive cells also express two other v-SNAREs, VAMP1 and cellubrevin, the latter of which is abundantly expressed in adipocytes (Volchuk *et al.*, 1995) (refer to Section 1.13). Similarily to VAMP2, cellubrevin translocates to the cell surface in response to insulin (Volchuk *et al.*, 1995) and binds to syntaxin 4 with reasonable affinity (Tellam *et al.*, 1997). However, in contrast to VAMP2, cellubrevin resides predominantly within the endosomal system (Martin *et al.*, 1996) (refer to Section 1.13). The differential distribution of these two v-SNAREs and their ability to interact with the t-SNARE syntaxin 4, further suggests that endosomes and GLUT4 vesicles derived from the post-endocytic compartment can independently dock and fuse with the cell surface.

In addition to insulin, various other stimuli can induce GLUT4 translocation to the cell surface. For example, the introduction of non-hydrolysable GTP analogs such as GTPγS markedly stimulates GLUT4 translocation in permeabilised 3T3-L1

adipocytes (Baldini *et al.*, 1991; Robinson *et al.*, 1992c; Clarke *et al.*, 1994). However, as the trafficking machinery involved in GTPγS-stimulated trafficking is still to be elucidated it is unclear whether GTPγS stimulates GLUT4 translocation through common and/or distinct trafficking pathways to that of insulin.

In the present study, I have used endosomal ablation to examine the translocation of GLUT4 from the endosomal and non-ablatable post-endocytic compartments to the cell surface in response to insulin and GTPγS. I have shown that ablation of the recycling endosomal system using Tf-HRP significantly inhibits GTPγS-stimulated GLUT4 and GLUT1 translocation. In contrast, insulin still elicits the translocation of GLUT4 to the cell surface after the ablation of the recycling pathway. However, insulin-stimulated GLUT1 translocation was blocked under the same conditions. I further show that insulin-stimulated GLUT4 translocation from the post-endocytic compartment is inhibited by wortmannin, suggesting a role for PI 3-kinase in trafficking from this post-endocytic compartment. On the basis of these and other data, I propose that GTPγS and insulin stimulate the exocytosis of GLUT4 from two distinct compartments, one being endosomal containing GLUT1 and the other being a separate post-endocytic GLUT4 compartment.

4.3 Materials and Methods

4.3.1 Transferrin Receptor Externalisation Assay

The rate of externalisation of the TfR was measured as described by Tanner and Lienhard (Tanner *et al.*, 1987).

Duplicate wells of 3T3-L1 adipocytes cultured on a 6-well plate were incubated in serum-free DMEM containing 1mg/ml BSA for 2 h at 37°C. During the last hour of the incubation, 3nM [^{125}I] transferrin was added directly to the media, together with Tf-HRP at a final concentration of 20μg/ml. After the cells were transferred onto ice,

cell surface attached [^{125}I] transferrin and Tf-HRP was removed by acid washing with ice-cold isotonic citrate buffer (150mM NaCl, 20mM Tri-sodium citrate, pH 5.0) over a period of 10 min with three changes of buffer and then the monolayer was washed once with ice-cold PBS (see Section 2.2.1). 1.9ml of PBS and 100µl of 3,3'-diaminobenzidine (DAB) (2mg/ml stock prepared freshly in PBS, vortexed thoroughly and filtered through a 0.22 µm-pore-size-filter) were added to each well, and H_2O_2 (0.02%) was added to one of each pair of wells. After a 60 min incubation at 4°C in the dark, the reaction was stopped by washing in PBS containing 1mg/ml BSA. The cells were washed once with KRP buffer (see Section 2.2.2) at 37°C containing 1mg/ml BSA, and then incubated in 1ml of KRP buffer containing unlabelled transferrin (1µM) ± insulin (1µM) at 37°C for the times shown. After this incubation, cells were rapidly washed three times with ice-cold PBS, and 1ml of 1M NaOH was added to each well. Cells were triturated, and the radioactivity associated with the cells was determined by γ counting. As a measure of non-specific binding, duplicate sets of plates were incubated with [^{125}I] transferrin in the presence of 10µM unlabelled transferrin and treated exactly as described above. The radioactivity associated with cells under these conditions was regarded as non-specific association, and this value was subtracted from measurements of cell-associated counts from all other conditions.

4.3.2 Cell-Surface Transferrin Receptor Internalisation Assay

An adaptation of the above method was employed to determine whether internalisation of the TfR is observed following the ablation of the endosomal system. As before, duplicate wells of 3T3-L1 adipocytes cultured on a 6-well plate were incubated in serum-free DMEM containing 1mg/ml BSA for 2 h at 37°C. For the last hour of this incubation the cells were loaded with Tf-HRP only and ablation was carried out as described above. The cells were washed once with KRP buffer at 37°C, and then incubated in 1ml of 3nM [^{125}I] transferrin in KRP containing 1mg/ml BSA at 37°C for the times shown. At the desired time, the cells were transferred

onto ice and subsequently washed three times with ice-cold isotonic citrate buffer (see above) and then the monolayer was washed once with ice-cold PBS. Following the addition of 1ml of 1M NaOH cell-associated radioactivity was measured as described above. Again, non-specific binding was measured by setting up duplicate sets of plates to which excess (10μM) unlabelled transferrin was added in addition to the radio-labelled transferrin.

4.3.3 Cell-Surface Transferrin Receptor Externalisation Assay

A further adaptation of the assay was employed to determine whether constitutive recycling of the TfR is observed following endosome ablation. Duplicate wells of 3T3-L1 adipocytes cultured on a 6-well plate were incubated in serum-free DMEM containing 1mg/ml BSA for 2 h at 37°C. For the last hour of this incubation the cells were loaded with Tf-HRP only and ablation was carried out as described above. The cells were then washed once with KRP buffer at 37°C, and incubated in 1ml of 3nM [^{125}I] transferrin in KRP buffer containing 1mg/ml BSA at 37°C for 20 min. This time was previously shown to allow internalisation of [^{125}I] transferrin (see Figure 4.8). Following washes with ice-cold citrate buffer and PBS as described above, the cells were washed once with KRP buffer containing 1mg/ml BSA and then the cells were incubated in 1ml of KRP containing unlabelled transferrin (1μM) at 37°C for the times shown. After this incubation, cells were rapidly washed three times with ice-cold PBS, 1ml of 1M NaOH was added to each plate and cell-associated radioactivity was measured as described above. Non-specific binding was measured as before.

4.3.4 Plasma Membrane Lawn Assay

During a 2 h incubation in serum-free DMEM, 3T3-L1 adipocytes cultured on collagen-coated coverslips were incubated with Tf-HRP conjugate (20μg/ml final concentration) for 60 min at 37°C. Endosomal ablation was carried out as described

in Section 2.9.2. Following the 1 h incubation at 4°C in the dark, the reaction was stopped by washing the monolayer with ice-cold PBS (see Section 2.2.1). The cells were washed with KRP buffer (see Section 2.2.2) at 37°C and then incubated in 1ml of KRP buffer containing 1mg/ml BSA ± insulin (1μM) for the times shown. At the desired time, the cells were rapidly washed with ice-cold buffer A (see Section 2.12.1) and plasma membrane lawns were prepared as described in Section 2.12.1.

Coverslips were viewed using a 40X objective lens on a Zeiss Axiovert microscope operated in a Laser Scanning Confocal mode. Samples were illuminated at 488nm and the signal at 510nm collected. For each condition, five to ten representative fields were collected using a constant set of parameters (contrast, brightness, laser intensity and pin-hole size) from triplicate coverslips at each experimental condition, and the data analysed for fluorescent intensity using MetaMorph software (Universal Imaging). Data was quantified and presented as mean ± s.e.m.

4.3.5 Permeabilisation of 3T3-L1 Adipocytes

α-toxin permeabilisation of 3T3-L1 adipocytes was carried out as described by Herbst *et al* (Herbst *et al.*, 1995). α-toxin is a 34kDa protein that inserts into the plasma membrane and then oligomerizes to form a 3nm diameter aqueous pore that allows the passage of molecules of ~ 5kDa or less (Fussle *et al.*, 1981). 3T3-L1 adipocytes were cultured on collagen-coated coverslips and incubated in serum-free DMEM for 2h prior to use. During the last hour of the incubation, Tf-HRP was added to the media at a final concentration of 20μg/ml. Following endosomal ablation as described in Section 2.9.2, the cells were washed three times in IC buffer (10mM NaCl, 20mM HEPES, 50mM KCl, 2mM K_2HPO_4, 90mM potassium glutamate, 1mM $MgCl_2$, 4mM EGTA, 2mM $CaCl_2$, pH7.2) at 37°C and then incubated in 0.5ml ICR buffer (IC buffer plus 4mM MgATP, 3mM sodium pyruvate, 100μg/ml bovine serum albumin, pH 7.4) containing α-toxin at 250 haemolytic units/ml (Calbiochem material, approximately 8μg/ml) for 5 min to permeabilise the plasma

membrane. The medium containing α-toxin was removed and the cells were incubated in 0.5ml of ICR buffer containing GTPγS (200μM), insulin (1μM) or buffer alone for 15 min at 37°C. The reaction was terminated by washing the cells rapidly in ice-cold buffer A (see Section 2.12.1) and plasma membrane lawns were prepared as described in Section 2.12.1. Coverslips were viewed and the data analysed and quantified as described above.

4.3.6 Adipsin Release:

Endosome Ablation

3T3-L1 adipocytes were cultured on 10cm plates and incubated in serum-free DMEM for 2 h at 37°C prior to use. For the last 60 min of the incubation Tf-HRP (20μg/ml final concentration) was added, and experimental plates were ablated by the addition of H_2O_2 as described in Section 2.9.2. Following incubation at 4°C for 60 min in the dark, the cells were washed extensively with PBS (see Section 2.2.1), washed a further two times with KRP buffer (see Section 2.2.2) at 37°C and adipsin release was measured as described in Section 2.14.

Wortmannin Treatment

3T3-L1 adipocytes were cultured on 10cm plates and incubated in serum-free DMEM for 2 h prior to use. For the last 30 min of the incubation, wortmannin (100nM) was added to experimental plates only. After the incubation, cells were washed twice with KRP buffer at 37°C and adipsin release was measured as described in Section 2.14.

4.3.7 Antibodies

The anti-GLUT4 antibody used for plasma membrane lawn assays was a rabbit polyclonal against a peptide comprising the C-terminal 14 amino acid residues of the human isoform of GLUT4 (see Section 2.4).

4.3.8 Statistical Analysis

Statistical analysis was performed using Statview 4.0 on a Mac Power PC.

4.4 Results

4.4.1 Effect of Endosomal Ablation on Transferrin Receptor Trafficking in 3T3-L1 Adipocytes

In the previous study,Ie used endosomal ablation analysis to resolve at least two intracellular pools of GLUT4 in 3T3-L1 adipocytes (refer to Section 3.2). Briefly, this technique relies on the ability of Tf-HRP to bind to TfRs on the cell surface and to traffic throughout the reycling endosomal pathway. The HRP enzyme activity can then be used to cross-link the proteins resident within the recycling system in the presence of 3,3'-diaminobenzidine and H_2O_2. By initiating the enzymatic activity of HRP within the living cell, it is possible to achieve compartment-specific ablation of proteins that co-localise with the conjugate within the recycling endosomal system.

As a first step to determine the effect of endosomal ablation on protein trafficking, I examined the recycling of TfRs as a marker of the constitutive recycling pathway. Cells were loaded with radiolabelled transferrin and Tf-HRP for 60 min at 37°C to fill the endosomal recycling pathway, after which endosomes were ablated as described in Section 4.3.1. Following ablation (DAB ± H_2O_2), cells were rapidly washed at 37°C, and the amount of cell-associated radiolabelled transferrin was followed over

time as a measure of transferrin recycling both in the absence and presence of insulin. As shown in Figure 4.1, there was a rapid loss of radiolabelled transferrin from cells that had been incubated with Tf-HRP and DAB in the absence of H_2O_2, indicating that the recycling pathway was still intact under these conditions. However, following the ablation of the endosomal system by the addition of H_2O_2, there was no reduction in cell-associated radiolabelled transferrin, indicating that the endosomal recycling pathway had been effectively disrupted (Figure 4.1).

4.4.2 Effect of Endosomal Ablation on Insulin-Stimulated GLUT4 and GLUT1 Translocation

I next wished to determine whether insulin was still capable of stimulating GLUT4 translocation to the cell surface in adipocytes following ablation of the endosomal system. In these experiments, duplicate sets of cells cultured on coverslips were exposed to Tf-HRP and DAB, but H_2O_2 was added to only one of each pair. Following ablation (DAB ± H_2O_2), cells were rapidly washed and incubated with or without insulin (1μM) at 37°C for the times indicated. Cell surface levels of GLUT4 were determined by immunofluorescence of plasma membrane lawns as described in Section 4.3.4. The results of a typical experiment are presented in Figure 4.2A. In the absence of insulin, cell surface levels of GLUT4 were very low both in ablated and non-ablated cells. Insulin-stimulated the time-dependent movement of GLUT4 to the plasma membrane even after ablation of the recycling system. However, the extent of translocation to the plasma membrane was reduced by ~20% in ablated cells, possibly due to the loss of endosomal GLUT4 (Figure 4.2B). It should also be noted that the time course of this translocation was slower than that observed in non-ablated cells.

Insulin also stimulates the translocation of other recycling proteins to the cell surface in adipocytes including GLUT1. However, in contrast to GLUT4, endosomal ablation analysis has previously shown GLUT1 to reside predominantly in the

recycling endosomal system (Livingstone *et al.*, 1996). Therefore, to provide further evidence that insulin stimulates the exocytosis of two distinct intracellular compartments I examined the effect of endosomal ablation on the insulin-stimulated recruitment of GLUT1 to the plasma membrane. If endosomal ablation disrupts trafficking through the recycling endosomal system, then in contrast to what we have observed for GLUT4 (Figure 4.2), insulin-stimulated recruitment of GLUT1 to the plasma membrane should be effectively inhibited. As shown in Figure 4.3, even after 20 min of incubation with insulin, there was no change in the cell surface levels of GLUT1, whereas there was a marked increase in cell surface levels of GLUT4 under the same conditions.

4.4.3 Effect of Endosomal Ablation on GTPγS-Stimulated GLUT4 and GLUT1 Translocation

It has previously been shown that non-hydrolysable GTP analogs such as GTPγS markedly stimulate the translocation of GLUT4 to the cell surface in 3T3-L1 adipocytes (Baldini *et al.*, 1991; Robinson *et al.*, 1992c). However, it has been suggested that the mode of action of GTPγS may differ from that observed with insulin (Shibata *et al.*, 1996). With this in mind, I therefore set out to determine whether GTPγS could also stimulate GLUT4 translocation after ablation of the endosomal system. I examined, by immunofluorescence of PM lawns, the effect of GTPγS on GLUT4 translocation in α-toxin permeabilised 3T3-L1 adipocytes following endosomal ablation, and compared these effects to those induced by insulin. Parallel experiments were performed in which cells had been ablated prior to permeabilisation and then treated with GTPγS or insulin as described in Section 4.3.5. As shown in Figure 4.4, the fold increase in GLUT4 cell surface levels induced by GTPγS was ~50% of that induced by insulin. Upon ablation of the endosomal system, insulin was still capable of inducing GLUT4 translocation. In contrast, GTPγS stimulated GLUT4 translocation was completely inhibited, suggesting that

GTPγS stimulates the translocation of GLUT4 primarily from the endosomal compartment.

I also examined the ability of GTPγS to stimulate the translocation of an endosomal protein, GLUT1. The observation that GTPγS-stimulated GLUT1 translocation was also blocked following endosomal ablation indicates that GTPγS-stimulates trafficking through the recycling endosomal system (Figure 4.5), consistent with the above data.

4.4.4 Effect of Wortmannin on Insulin- and GTPγS-Stimulated GLUT4 Translocation

It is well documented that PI 3-kinase activity is necessary to stimulate glucose transport activity and GLUT4 translocation to the cell surface (refer to Section 1.14). However, it has not been clearly established whether the effects of wortmannin, a potent inhibitor of PI 3-kinase activity, are specific for GLUT4 trafficking or apply to protein trafficking through the recycling system in general (refer to Section 1.6). In an effort to address this issue, I examined the role of PI 3-kinase in insulin-stimulated GLUT4 translocation after ablation of the endosomal system. 3T3-L1 adipocytes (± ablation) were treated with the selective PI 3-kinase inhibitor wortmannin (100nM) for 15 min prior to insulin stimulation. Insulin stimulated a large increase in the translocation of GLUT4 to the cell surface, which was completely inhibited by wortmannin in both non-ablated and ablated cells (Figure 4.6). These data indicate that the translocation of GLUT4 from the non-ablatable compartment to the cell surface is PI 3-kinase dependent.

As PI 3-kinase activity is thought to be involved in trafficking through the endosomal system I also examined the effect of wortmannin on GTPγS stimulated GLUT4 translocation. Under the same conditions where insulin-stimulated GLUT4 translocation was completely inhibited (Figure 4.7), pretreatment with wortmannin

was without effect on GTPγS-stimulated GLUT4 translocation, suggesting that the site of action of GTPγS lies downstream of PI 3-kinase.

4.4.5 Effect of Endosomal Ablation on Cell-Surface Transferrin Receptors

Although insulin is still capable of eliciting a significant increase in cell surface levels of GLUT4, there is however, a notable delay in the insulin-stimulated arrival of GLUT4 under these conditions (Figure 4.2). If we hypothesize that GLUT4 translocates from the non-ablatable compartment directly to the cell surface independently of the recycling system, the delay observed may be explained if insulin stimulates GLUT4 movement from the endosomal system to the plasma membrane more rapidly than the exocytosis of GLUT4 vesicles from the post-endocytic compartment (refer to Section 4.2). Therefore, in ablated cells the significant reduction of insulin-stimulated GLUT4 translocation at early times may be accounted for by loss of endosomal GLUT4. However, it is also possible that GLUT4 derived from the non-ablatable compartment may join the endosomal pathway prior to its arrival to the cell surface and this pathway is blocked immediately after ablation but not at later times when endosomes have had the chance to reform.

In order to address this issue, I set out to determine whether we could observe the *de novo* formation of endosomes following endosomal ablation. I therefore performed an experiment to determine whether TfRs present at the cell surface, which are not destroyed by the ablation procedure, are internalised following ablation of the endosomal system. After ablation (± H_2O_2), cells were warmed to 37°C and the internalisation of radiolabelled transferrin was followed as a function of time. As shown in Figure 4.8, radiolabelled transferrin was internalised in ablated cells with indistinguishable kinetics from that observed in non-ablated cells.

To ensure that the TfR was internalised into a functional endosomal system, I carried out a further experiment to determine whether the radiolabelled transferrin could be re-externalised, thus indicating the re-formation of a recycling system. In this experiment, following the internalisation of radiolabelled transferrin, cell-surface bound transferrin was removed by acid washing. On re-warming the cells to 37°C, the externalisation of radiolabelled transferrin was measured as a function of time (Figure 4.9). There was no significant difference between the rate of externalisation of radiolabelled transferrin from non-ablated cells compared to ablated cells. Taken together these data show that following ablation of the endosomal system, cell surface TfRs are capable of recycling, indicating that a functional endosomal system has reformed.

4.4.6 Effect of Endosomal Ablation and Wortmannin on Constitutive Secretion in 3T3-L1 Adipocytes

As well as inducing the translocation GLUT4, insulin also stimulates the secretion of adipsin, a serine protease, from adipocytes in culture (Kitagawa *et al.*, 1989). To determine whether these two processes share a common pathway, I examined the effect of endosomal ablation on the constitutive (basal) and insulin-stimulated release of adipsin. Following ablation as described in Section 2.9.2, cells were warmed to 37°C and adipsin release was assayed as a function of time. Figure 4.10 represents the results obtained at 5 and 10 min after exposure to insulin. In agreement with previous studies, insulin caused a modest stimulation of adipsin secretion (Kitagawa *et al.*, 1989). In both basal and insulin-stimulated cells, adipsin secretion was significantly attenuated by ablation of the endosomal system, suggesting that the vast majority of this soluble protein traffics through the endosomal system *en route* to the cell surface.

Consistent with the notion that PI 3-kinase plays a role in trafficking through the endosomal system, prior treatment of 3T3-L1 adipocytes with wortmannin

inhibited the secretion of adipsin in both basal and insulin-stimulated 3T3-L1 adipocytes (Figure 4.11), providing further evidence for the trafficking of this soluble protein through the endosomal system.

Figure 4.1

Effect of Endosomal Ablation on Transferrin Receptor Exocytosis

3T3-L1 adipocytes were incubated with 3nM [^{125}I] transferrin together with Tf-HRP at 20μg/ml. Subsequently, cell surface attached Tf/Tf-HRP was removed, and DAB with (ablated) or without (control) H_2O_2 was added. Cells were incubated at 4°C in the dark for 60 min to complete the ablation reaction. Thereafter, the cells were rapidly washed and incubated at 37°C and cell-associated radioactivity was measured at the times shown allowing the rate of radioactive transferrin release to be determined. Data from a representative experiment are shown. Each point is the mean of three determinations at each time point (± s.e.m).

Figure 4.1

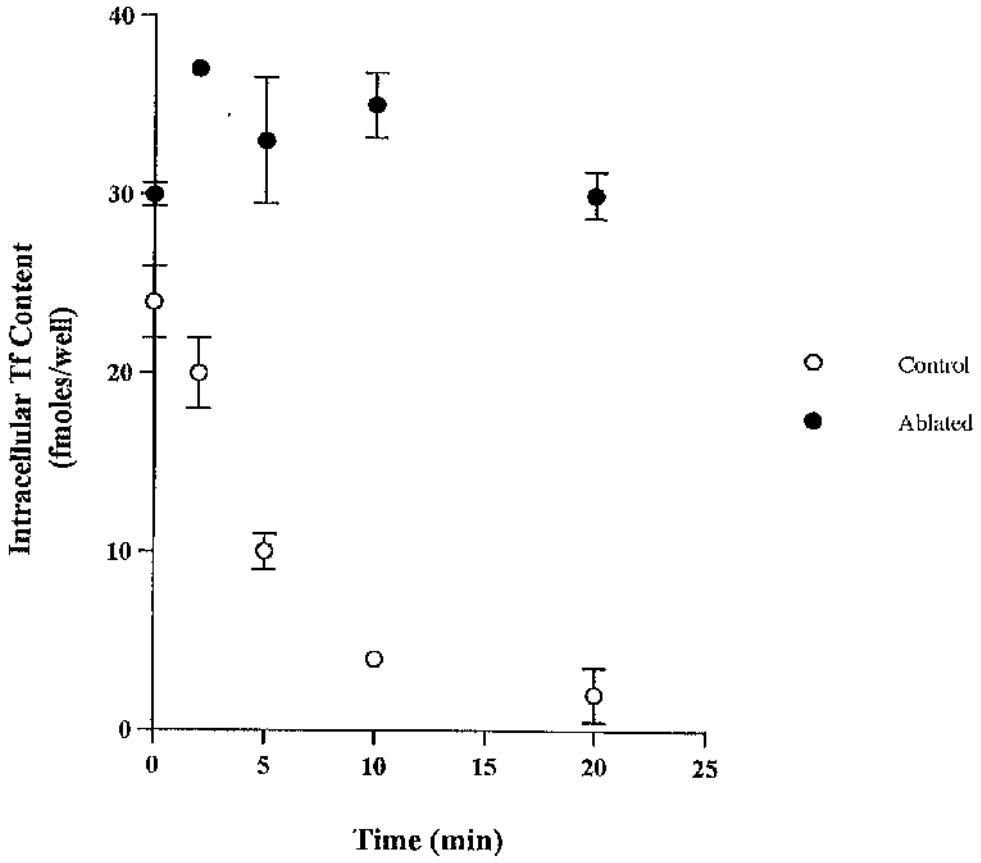
Intracellular Tf Content
(fmoles/well)
40
30
20
10
0
0
5
10
15
20
25
Time (min)
Control
Ablated

Figure 4.2

Effect of Endosomal Ablation on Insulin-Stimulated GLUT4 Translocation

Duplicate coverslips of 3T3-L1 adipocytes were loaded with Tf-HRP and incubated with DAB with (ablated) or without (control) H_2O_2 as described in *Materials and Methods*. After completion of the DAB cytochemistry, the cells were rapidly washed and incubated with or without insulin (1μM) for the times shown. At the end of this incubation, plasma membrane lawns were prepared and labelled with an antibody specific for GLUT4. **A**, a representative experiment. **B**, quantitation of three similar experiments (mean ± s.e.m).

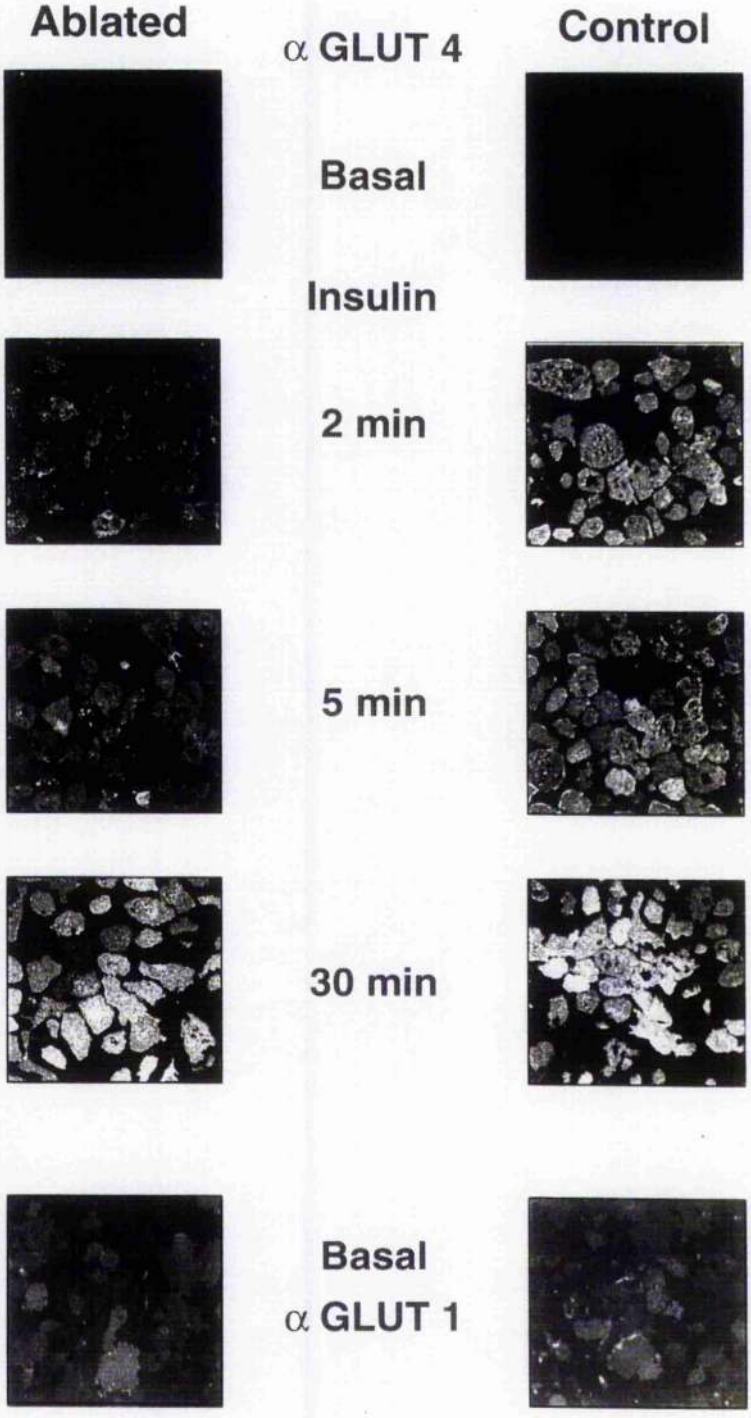
Ablated
α GLUT 4
Control
Basal
Insulin
2 min
5 min
30 min
Basal
α GLUT 1

Figure 4.2B

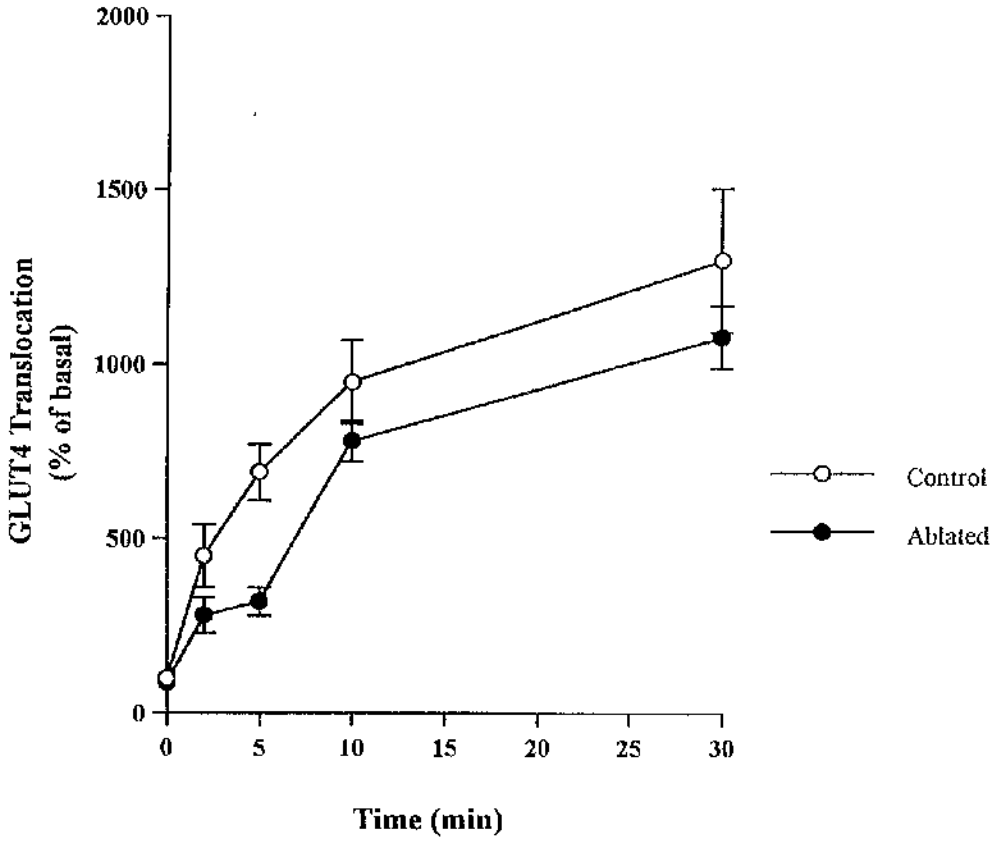
2000
1500
1000
500
0
GLUT4 Translocation
(% of basal)
0
5
10
15
20
25
30
Time (min)
Control
Ablated

Figure 4.3

Effect of Endosomal Ablation on Insulin-Stimulated GLUT1 Translocation

Duplicate coverslips of 3T3-L1 adipocytes were loaded with Tf-HRP and incubated with DAB with (ablated) or without (control) H_2O_2 as described in *Materials and Methods*. After completion of the DAB cytochemistry, the cells were rapidly washed and incubated with or without insulin (1μM) for the times shown. At the end of this incubation, plasma membrane lawns were prepared and labelled with antibodies specific for either GLUT1 or GLUT4. Shown is a representative experiment, repeated three times with similar results.

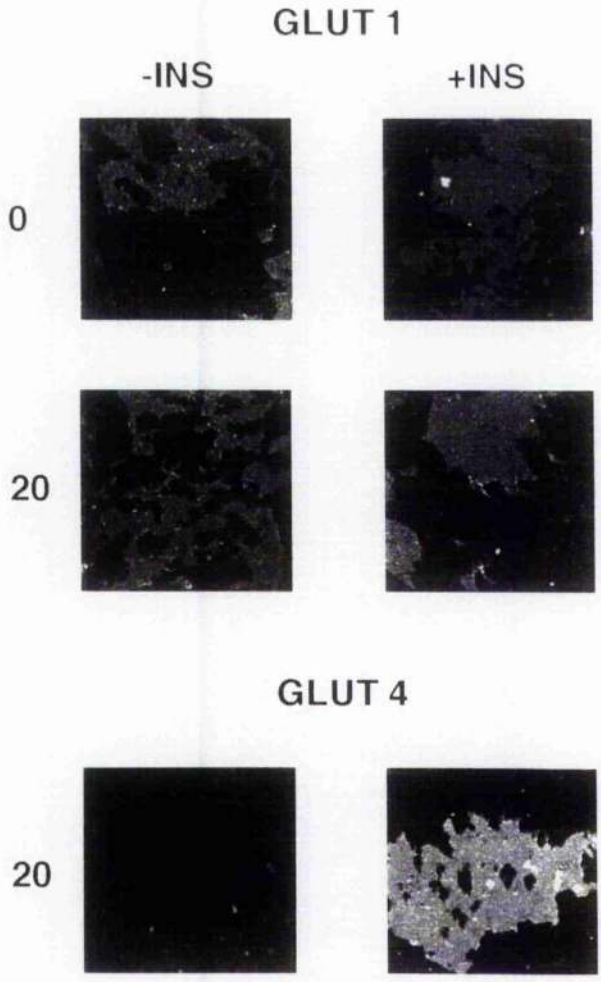
GLUT 1
-INS
+INS
0
20
GLUT 4
20

Figure 4.4

Effect of Endosomal Ablation on GTPγS-Stimulated GLUT4 Translocation

Triplicate coverslips of 3T3-L1 adipocytes were loaded with Tf-HRP and incubated with DAB ± H_2O_2 as described in *Materials and Methods*. After completion of the DAB cytochemistry, the cells were rapidly washed and permeabilised with α-toxin at 37°C. The cells were then treated for 15 min with buffer alone or buffer containing insulin (1μM) or GTPγS (200μM). Plasma membrane lawns were prepared and the extent of GLUT4 translocation relative to the basal value was determined using scanning laser confocal immunofluorescence microscopy. Shown are data of a representative experiment (n = 2). Data are presented as the mean fold increase relative to basal (unstimulated cells) ± s.e.m. (*$p<0.05$, compared to cells without H_2O_2, ** $p<0.05$ compared to cells treated with insulin).

Figure 4.4

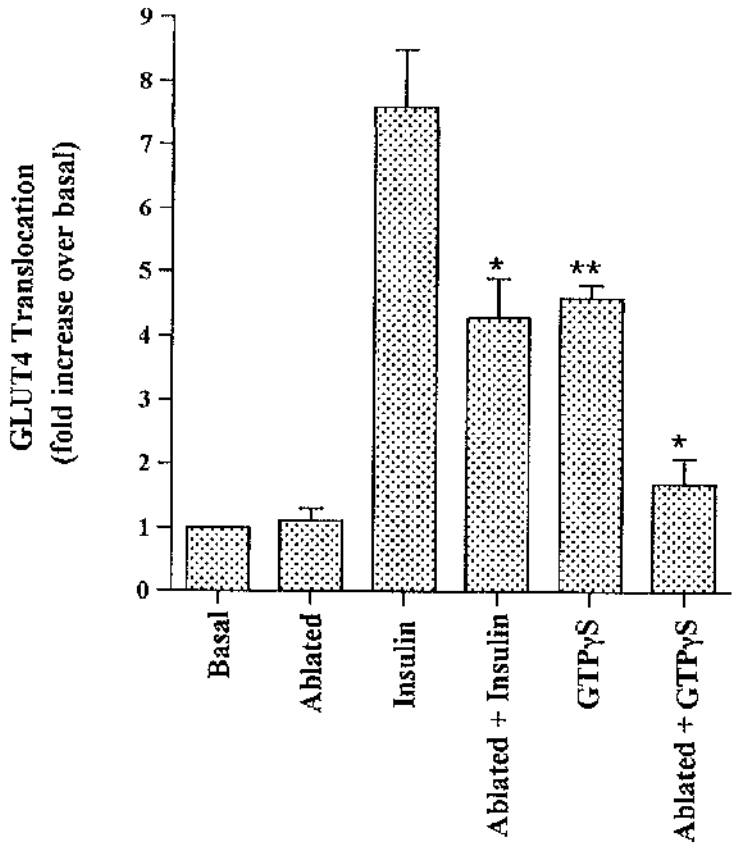
GLUT4 Translocation
(fold increase over basal)
0
1
2
3
4
5
6
7
8
9
*
**
*
Basal
Ablated
Insulin
Ablated + Insulin
GTPγS
Ablated + GTPγS

Figure 4.5

Effect of Endosomal Ablation on GTPγS-Stimulated GLUT1 Translocation

Triplicate coverslips of 3T3-L1 adipocytes were loaded with Tf-HRP and incubated with DAB ± H_2O_2 as described in *Materials and Methods*. After completion of the DAB cytochemistry, the cells were rapidly washed and permeabilised with α-toxin at 37°C. The cells were then treated for 15 min with buffer alone or buffer containing insulin (1μM) or GTPγS (200μM). Plasma membrane lawns were prepared and the extent of GLUT1 translocation relative to the basal value was determined using scanning laser confocal immunofluorescence microscopy. Shown are data of a representative experiment (n = 2). Data are presented as the mean fold increase relative to basal (non-stimulated) cells ± s.e.m.

Figure 4.5

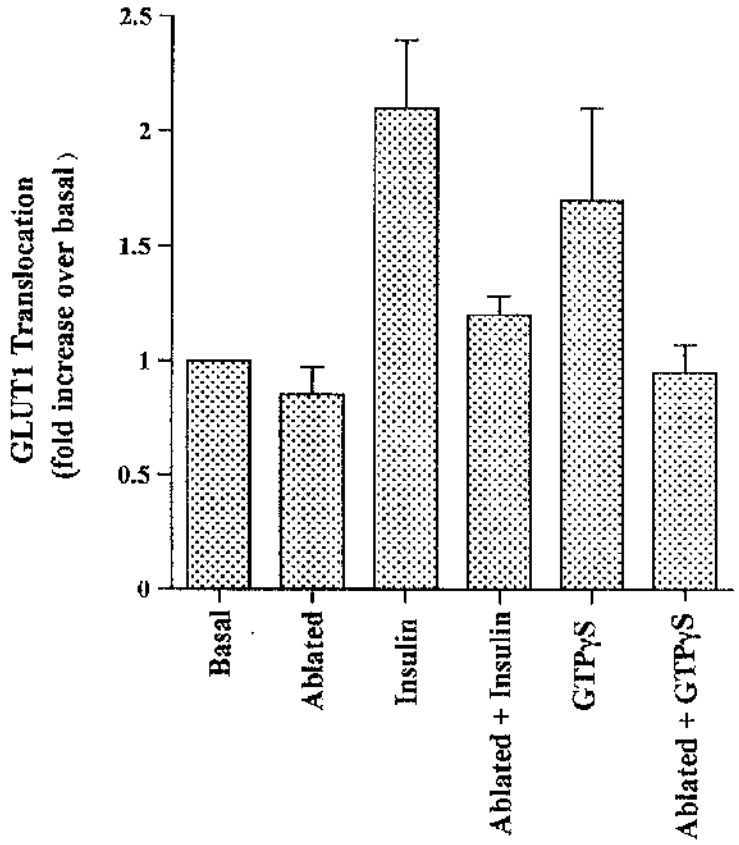
GLUT1 Translocation
(fold increase over basal)
2.5
2
1.5
1
0.5
0
Basal
Ablated
Insulin
Ablated + Insulin
GTPγS
Ablated + GTPγS

Figure 4.6

Effect of Wortmannin on Insulin-Stimulated GLUT4 Translocation

Triplicate coverslips of 3T3-L1 adipocytes were loaded with Tf-HRP and incubated with DAB ± H_2O_2 as described in *Materials and Methods*. After completion of the DAB cytochemistry, the cells were rapidly washed and treated with or without wortmannin (100nM) at 37°C. After 15 min, the cells were incubated with or without insulin (1μM) for a further 15 min. Thereafter, GLUT4 levels at the plasma membrane were determined using the plasma membrane lawn assay. Shown is the quantitation of three experiments of this type. Data are presented as the mean fold increase relative to basal (non-stimulated) cells ± s.e.m.

Figure 4.6

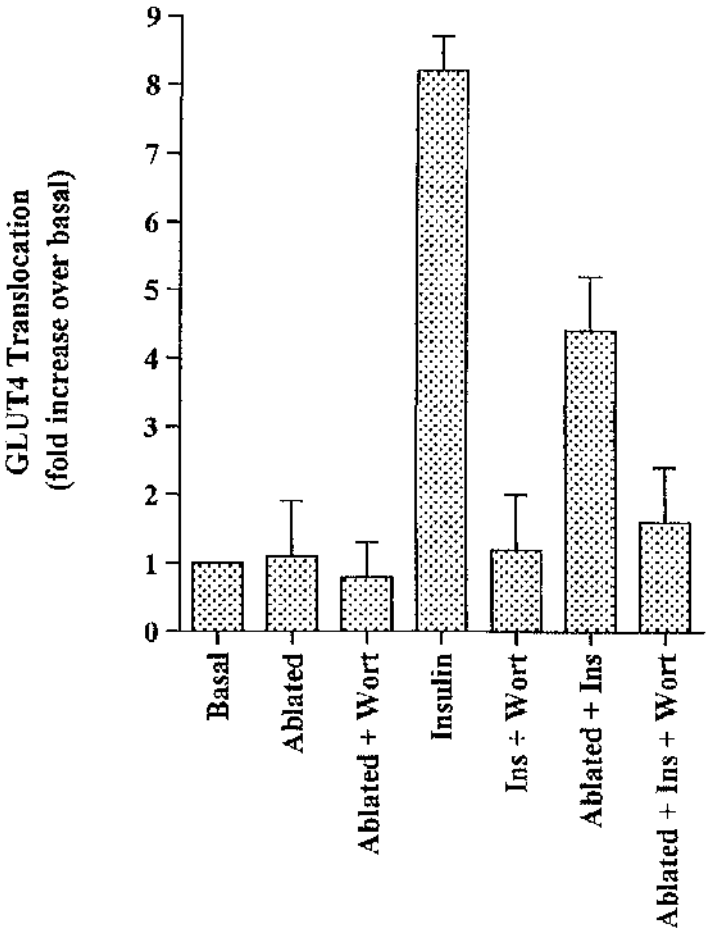
GLUT4 Translocation
(fold increase over basal)
0
1
2
3
4
5
6
7
8
9
Basal
Ablated
Ablated + Wort
Insulin
Ins + Wort
Ablated + Ins
Ablated + Ins + Wort

Figure 4.7

Effect of Wortmannin on GTPγS-Stimulated GLUT4 Translocation

Triplicate coverslips of 3T3-L1 adipocytes were loaded with Tf-HRP and incubated with DAB ± H_2O_2 as described in *Materials and Methods*. After completion of the DAB cytochemistry, the cells were rapidly washed and permeabilised with α-toxin at 37°C. The cells were then treated for 15 min with buffer alone or buffer containing wortmannin (100nM) before treatment with insulin (1μM) or GTPγS (200μM) for a further 15 min. Thereafter, GLUT4 levels at the plasma membrane were determined using the plasma membrane lawn assay. Shown are data of a representative experiment (n = 2). Data are presented as the mean fold increase relative to basal (non-stimulated) cells ± s.e.m.

Figure 4.7

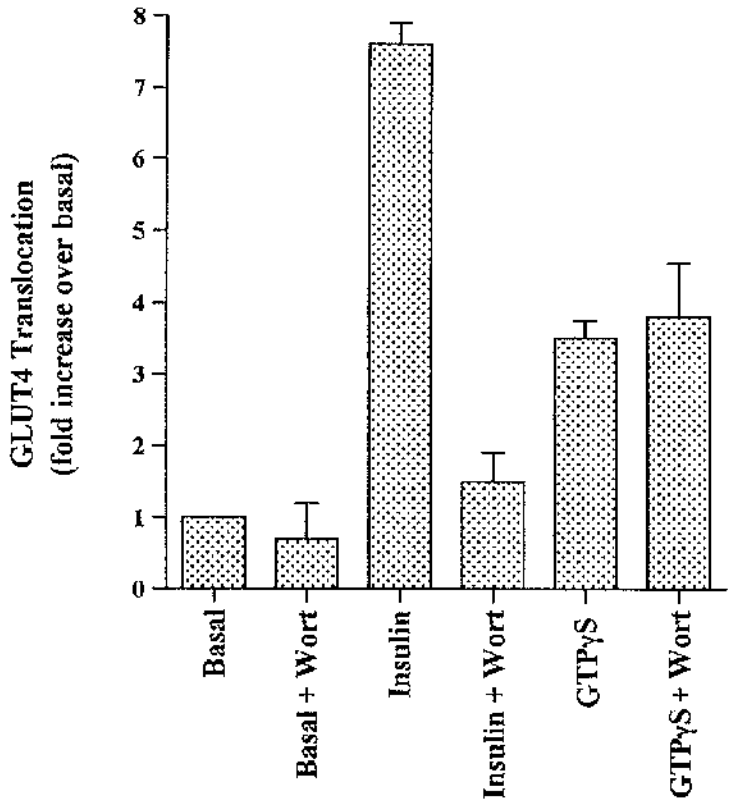
GLUT4 Translocation
(fold increase over basal)
0
1
2
3
4
5
6
7
8
Basal
Basal + Wort
Insulin
Insulin + Wort
GTPγS
GTPγS + Wort

Figure 4.8

Effect of Endosomal Ablation on the Internalisation of Cell-Surface Transferrin Receptors

3T3-L1 adipocytes were loaded with Tf-HRP and incubated with DAB ± H_2O_2 as described in *Materials and Methods*. After completion of the DAB cytochemistry, the cells were rapidly washed and incubated with 3nM [^{125}I] transferrin at 37°C for the times shown. After the desired time, cell surface attached transferrin was removed and cell-associated radioactivity was measured in cells that were incubated with (ablated) or without (control) H_2O_2. Data from a representative experiment are shown (n = 2). Each point is the mean of three determinations at each time point (± s.e.m.).

Figure 4.8

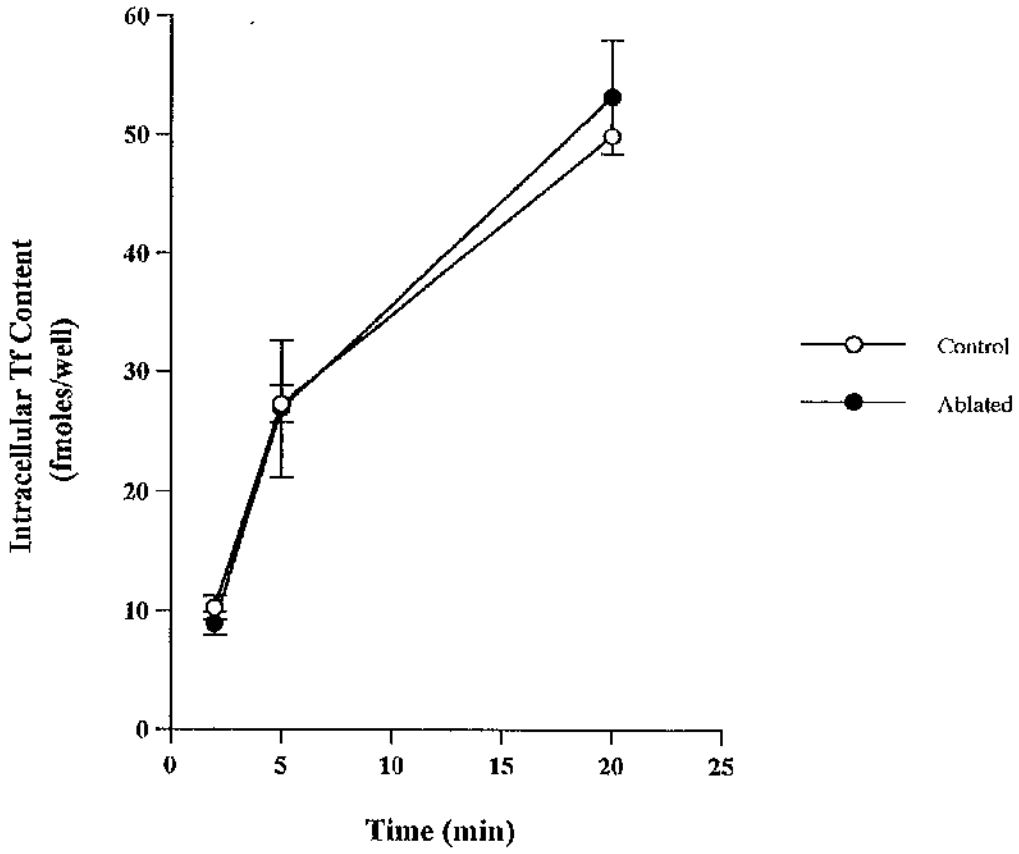
Intracellular Tf Content
(fmoles/well)
60
50
40
30
20
10
0
0
5
10
15
20
25
Time (min)
Control
Ablated

Figure 4.9

Effect of Endosomal Ablation on the Recycling of Cell-Surface Transferrin Receptors

3T3-L1 adipocytes were loaded with Tf-HRP and incubated with DAB ± H_2O_2 as described in *Materials and Methods*. After completion of the DAB cytochemistry, the cells were rapidly washed and incubated with 3nM [^{125}I] transferrin at 37°C for 20 min. After the removal of cell surface attached transferrin, the cells were incubated at 37°C and cell-associated radioactivity was measured at the times shown allowing the rate of radioactive transferrin release to be determined in cells that were incubated with (ablated) or without (control) H_2O_2. Data from a representative experiment are shown (n = 2) . Each point is the mean of three determinations at each time point (± s.e.m.).

Figure 4.9

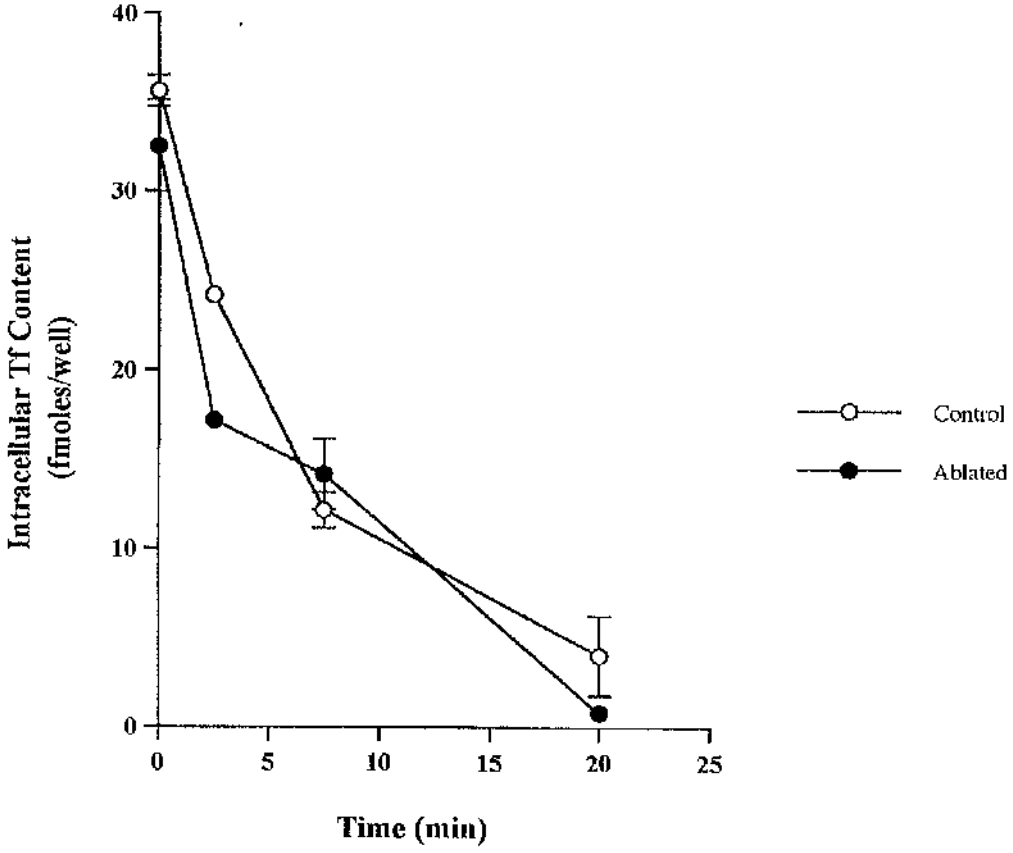
Intracellular Tf Content
(fmoles/well)
40
30
20
10
0
0
5
10
15
20
25
Time (min)
Control
Ablated

Figure 4.10

Effect of Endosomal Ablation on Adipsin Secretion from 3T3-L1 Adipocytes

3T3-L1 adipocytes were loaded with Tf-HRP and incubated with DAB ± H_2O_2 as described. Cells were then rapidly washed and incubated in buffer with or without insulin at 37°C. Adipsin secretion was assayed as described in *Materials and Methods*. **A**, a representative immunoblot of adipsin secretion at 5 and 10 min after exposure to insulin. **B**, quantitation of adipsin secretion. Adipsin secretion is expressed in arbitrary units as described in Section 2.14.

Adipsin release

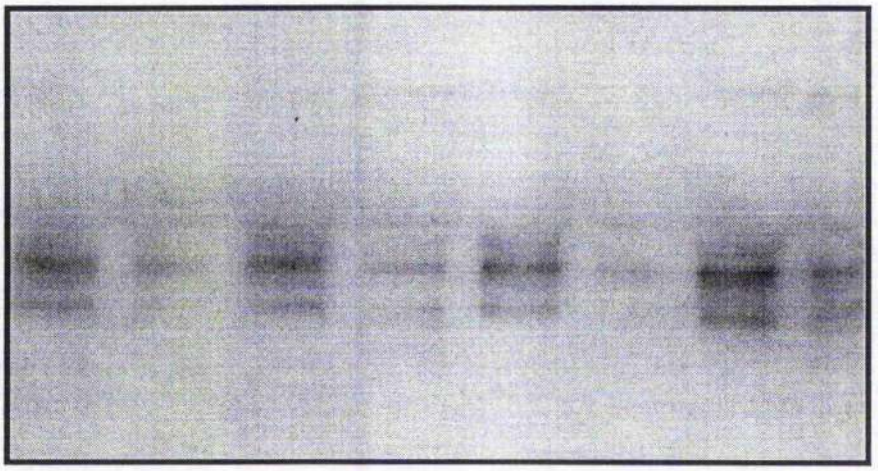

INS	-	-	+	+	-	-	+	+
H_2O_2	-	+	-	+	-	+	-	+
	5min				10min			

Figure 4.10B

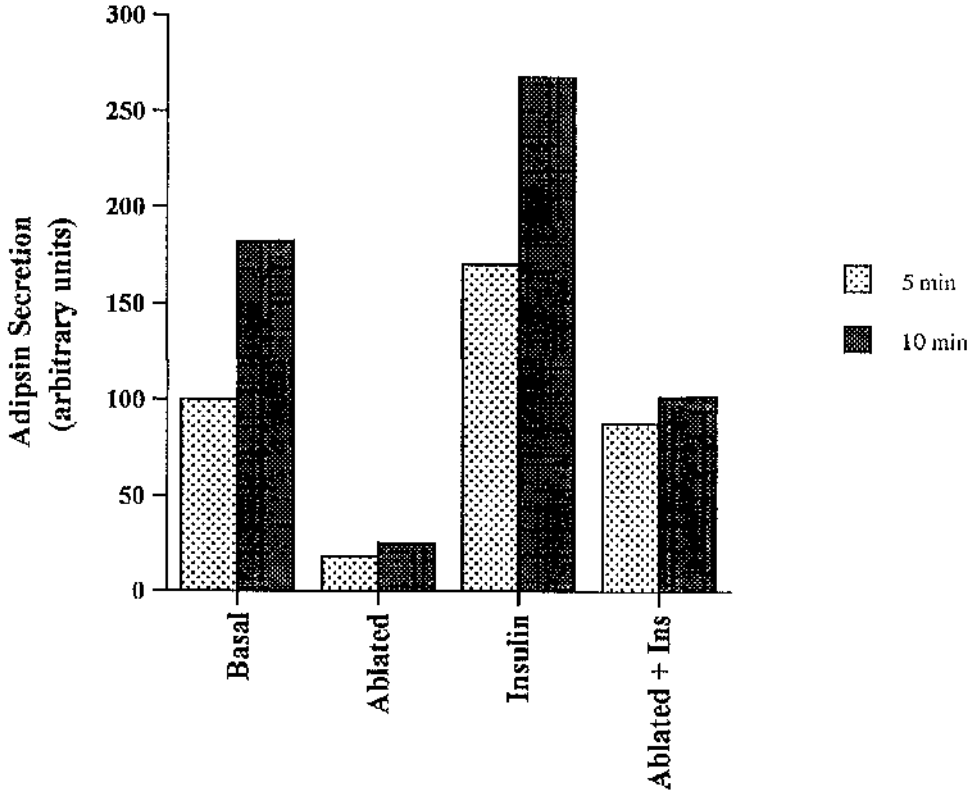
Adipsin Secretion
(arbitrary units)
300
250
200
150
100
50
0
Basal
Ablated
Insulin
Ablated + Ins
5 min
10 min

Figure 4.11

Effect of Wortmannin on Adipsin Secretion from 3T3-L1 Adipocytes

3T3-L1 adipocytes cultured on 10cm plates were pre-treated with wortmannin at the indicated concentrations for 15 min at 37°C. Thereafter, the cells were treated with insulin (1μM) for a further 15 min. Adipsin secretion was assayed and quantified as described. Shown is a representative experiment of at least three similar experiments, with wortmannin inhibition being expressed as a % of adipsin secretion measured in the absence of wortmannin. Note that both basal and insulin-stimulated adipsin secretion were wortmannin sensitive, with indistinguishable IC_{50}s. Hence for clarity, only the data for insulin-stimulated adipsin secretion is presented.

Figure 4.11

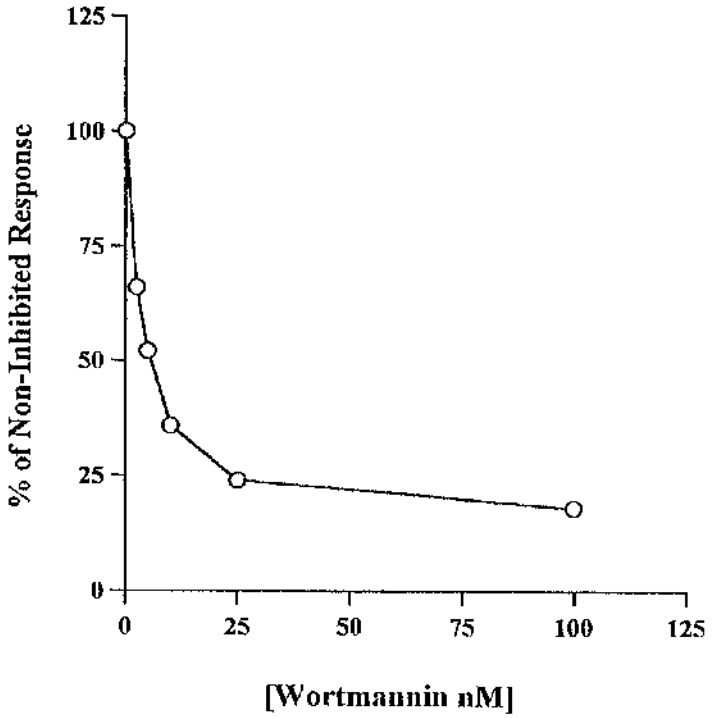
125
100
75
50
25
0
% of Non-Inhibited Response
0
25
50
75
100
125
[Wortmannin nM]

4.5 Discussion

The segregation of GLUT4 within two intracellular compartments, one enriched in cellubrevin and the other VAMP2, is consistent with a model in which insulin stimulates the exocytosis of GLUT4 from a storage compartment to the plasma membrane in a manner analagous to the exocytosis of SSVs (Rea *et al.*, 1997). To examine such a model in 3T3-L1 adipocytes, I used endosomal ablation to determine whether insulin-stimulated GLUT4 translocation remains intact following the disruption of the recycling endosomal system. In collaboration with D.E. James and colleagues (University of Queensland, Australia) this model was further tested by examining the effect of recombinant glutathione S-Transferase (GST) fusion proteins encompassing the entire cytoplasmic tails of VAMP1, VAMP2 and cellubrevin and N-terminal VAMP2 peptides on insulin-stimulated GLUT4 translocation in streptolysin O (SLO) permeabilised 3T3-L1 adipocytes. The results for this study are not shown and shall be referred to in this discussion for comparative purposes only.

On determining that the ablation procedure effectively disrupted recycling of the TfR through the endosomal system (Figure 4.1), I set out to examine whether insulin was still capable of stimulating GLUT4 translocation to the cell surface under the same conditions. As shown in Figure 4.2, insulin still elicits a significant increase in GLUT4 cell-surface levels following disruption of the endosomal system, suggesting that the post-endocytic VAMP2-positive pool of GLUT4 translocates directly to the plasma membrane, independently of the recycling pathway. In addition, endosomal ablation effectively inhibited the translocation of the endosomal protein, GLUT1 to the cell surface (Figure 4.3). In agreement with these findings, D.E. James' group have shown that the introduction of N-terminal VAMP2 peptides into SLO-permeabilised 3T3-L1 adipocytes inhibited the insulin-dependent movement of GLUT4 by ~35% but had no significant effect on insulin-stimulated GLUT1 translocation (Martin *et al.*, 1998). In addition, this collaborative study also showed

that the introduction of a GST-cellubrevin fusion protein under the same conditions inhibited GLUT1 but not GLUT4 insulin-stimulated translocation (L. Martin and D.E. James, personnel communication). Collectively, these data not only provide further evidence for the segregation of GLUT1 and GLUT4 within distinct compartments, but also support the notion that the individual compartments independently translocate to the cell surface in response to insulin. On the basis of these and previous data, we suggest that one of these compartments is a post-endocytic storage compartment for GLUT4 and the other is the constitutive recycling endosomal system. The localisation of cellubrevin to the endosomal system (Martin *et al.*, 1996) suggests that this v-SNARE regulates the docking and fusion of the recycling endosomes with the cell surface, while VAMP2 may be involved predominantly in the regulation of GLUT4 exocytosis from the post-endocytic compartment. It is important to note that a significant proportion of GLUT4 (~35%) resides within the endosomal system (refer to Section 1.10), which may explain the lower levels of GLUT4 observed at the cell surface following endosomal ablation (Figures 4.2 and 4.4) and the inability of the N-terminal VAMP2 peptide to completely block GLUT4 translocation (see above).

Although the above data provide strong evidence for the direct translocation of GLUT4 from the post-endocytic compartment to the cell surface independently of the recycling pathway, I noted that there was a significant delay in the insulin-stimulated arrival of GLUT4 at the cell surface following ablation of the endosomal system (Figure 4.2). This delay may simply be explained by insulin stimulating protein trafficking through the endosomal system more rapidly than the exocytosis of GLUT4 from the post-endocytic compartment. Therefore, in ablated cells the significant reduction of GLUT4 at early times may be accounted for by the loss of endosomal GLUT4. However, on considering an alternative model of insulin-stimulated GLUT4 translocation to the cell surface, where in response to insulin GLUT4 derived from the storage compartment merges with the endosomal system instead of directly with the plasma membrane (refer to Section 4.2), it is possible that

the delay observed may be a result of the time taken for the re-formation of endosomes, following disruption of the recycling system. To try to distinguish between these two possibilities, I examined the effect of endosomal ablation on the recycling of TfRs localised to the plasma membrane which are not destroyed by the ablation procedure. As shown in Figures 4.8 and 4.9, the internalisation and subsequent externalisation of radiolabelled transferrin, clearly shows that cell-surface TfRs are capable of recycling following the ablation of the endosomal system. Therefore, on the basis of endosomal ablation analysis alone I cannot discount the possibility that GLUT4 from the post-endocytic compartment may traffic through the endosomal system *en route* to the cell surface. Consistent with this possibility is the observation that a small proportion of syntaxin 4 co-localises with GLUT4 in the non-ablatable storage compartment in adipocytes (refer to Section 3.5.1), suggesting a role for this VAMP2-binding protein at an intracellular location. However, as the majority of syntaxin 4 is localised to the plasma membrane in adipocytes, it is most likely that the syntaxin 4 peptides and antibodies previously shown to inhibit insulin-stimulated GLUT4 translocation (refer to Section 1.13) do so by inhibition of vesicle docking and fusion with the plasma membrane.

It is well documented that the non-hydrolysable GTP analogue, GTPγS markedly stimulates the translocation of GLUT4 to the cell surface (Clarke *et al.*, 1994; Herbst *et al.*, 1995; Robinson *et al.*, 1992c). However, it has been suggested that the mode of action of this stimulus may differ from that observed with insulin (Shibata *et al.*, 1996). I therefore reasoned that examining the GTPγS stimulation of GLUT4 translocation following endosomal ablation might provide further insight by identifying common and / or distinct pathways for GLUT4 trafficking. Consistent with previous studies (Herbst *et al.*, 1995), I showed both insulin and GTPγS to stimulate GLUT4 translocation in α-toxin permeablised 3T3-L1 adipocytes (Figure 4.4). In contrast to insulin, GTPγS-stimulated GLUT4 and GLUT1 translocation were effectively blocked following ablation of the endosomal system, suggesting that GTPγS selectively targets the recycling endosomal pool as opposed to the post-

endocytic storage compartment. Further support for this idea was provided by the observation that the N-terminal VAMP2 peptide previously shown to inhibit insulin-stimulated GLUT4 translocation (see above), had no significant effect on GTPγS-stimulated GLUT4 translocation (Martin *et al.*, 1998).

Previous studies have reported contradictory findings regarding the extent of GTPγS-stimulated GLUT4 translocation in 3T3-L1 adipocytes. A study by Clarke *et al* found the extent of GTPγS-stimulated GLUT4 translocation to be significantly less than that observed for insulin (Clarke *et al.*, 1994), whereas several other groups reported both GTPγS and insulin to stimulate GLUT4 translocation to the same extent (Herbst *et al.*, 1995; Robinson *et al.*, 1992c). Although the basis of this difference is not apparent, our endosomal ablation and VAMP2 peptide studies show GTPγS-stimulated GLUT4 translocation to be ~50% of that induced by insulin. A plausible explanation for this data is that GTPγS stimulates the exocytosis of only one of the GLUT4 pools in 3T3-L1 adipocytes, in this case the endosomal compartment.

Several biochemical studies have shown that wortmannin, a potent inhibitor of PI 3-kinase, blocks the translocation of GLUT4 to the plasma membrane in 3T3-L1 adipocytes by inhibiting the exocytic movement of GLUT4-containing vesicles (Clarke *et al.*, 1994; Yang *et al.*, 1996) (refer to Section 1.14). However, it has also been reported that wortmannin blocks the insulin-stimulated exocytosis of the CI-M6PR and the TfR in 3T3-L1 adipocytes (Shepherd *et al.*, 1995a; Shepherd *et al.*, 1995b), suggesting a more general role of PI 3-kinase activity for insulin stimulation of the steps along the recycling pathway. My data clearly demonstrate that insulin-stimulated GLUT4 translocation is completely blocked upon prior treatment of 3T3-L1 adipocytes with wortmannin both in ablated and non-ablated cells (Figure 4.6), suggesting that the translocation of GLUT4 from the post-endocytic compartment is PI 3-kinase dependent. In support of this interpretation, a recent confocal microscopy study has shown that upon pre-treatment of intact rat adipose cells with

wortmannin, the pattern of GLUT4 intracellular staining following insulin treatment is indistinguishable to that observed in basal cells not treated with wortmannin (Malide *et al.*, 1997b). The inability of GLUT4 to redistribute within the cell as well as to translocate to the cell surface under these conditions further suggests that GLUT4 translocation is blocked or markedly delayed at a very early step in the forward movement of the vesicles out of the post-endocytic compartment to the plasma membrane. In addition, these data argue against the possibility that the inhibitory effect of wortmannin observed after endosomal ablation may indeed be a general effect on the recycling pathway following the re-formation of the endosomal system (see above). It is also important to note that in contrast to the some-what modest inhibiton of insulin-stimulated GLUT4 translocation by the VAMP2 peptide (~35%), wortmannin completely blocks insulin-stimulated GLUT4 translocation, suggesting that PI 3-kinase plays a role in at least two distinct steps in GLUT4 translocation and recycling. In this regard, my observation that GTPγS-stimulated GLUT4 translocation is wortmannin-insensitive (Figure 4.7) suggests that GTPγS acts at a step(s) distal to PI 3-kinase, possibly by a direct interaction with vesicle trafficking machinery.

It is well documented that insulin induces a 2 to 4 -fold increase in cell surface levels of several endosomal proteins including the TfR, the CI-M6PR and GLUT1 (Tanner *et al.*, 1987; Tanner *et al.*, 1989), indicating that insulin stimulates general recycling through the endosomal system. However, the constitutive secretion of the serine protease adipsin, has also been reported to be stimulated by insulin in 3T3-L1 adipocytes (Kitagawa *et al.*, 1989). Hence, I wished to determine whether this protein may exhibit a similar mode of translocation to that of GLUT4 in response to insulin. In contrast to GLUT4, both basal (constitutive) and insulin-induced adipsin release were effectively inhibited following endosomal ablation (Figure 4.10), suggesting that the increase in secretion observed in response to insulin was most likely a result of the general stimulation of the recycling endosomal system. Furthermore, these data also argue against direct trafficking from intracellular

membranes to the plasma membrane, suggesting that protein transport utilises the endosomal system *en route* to the cell surface in 3T3-L1 adipocytes.

In summary, the use of endosomal ablation analysis has enabled me to uncouple insulin- and GTPγS-stimulated GLUT4 translocation in 3T3-L1 adipocytes. I have shown that insulin is still capable of stimulating GLUT4 translocation following endosomal ablation under conditions where GTPγS-stimulated GLUT4 translocation was effectively inhibited. In addition, both insulin- and GTPγS-stimulated GLUT1 translocation were blocked following ablation of the recycling endosomal system. In accordance with these results, a collaborative study by D.E. James and co-workers showed a requirement for VAMP2 in insulin-stimulated but not GTPγS-stimulated translocation (Martin *et al.*, 1998). The most plausible explanation for these data is that insulin stimulates the exocytosis of two distinct intracellular compartments. We suggest that one of these is the VAMP2-positive post-endocytic storage compartment containing GLUT4 and the other is the constitutive recycling endosomal system containing GLUT1 which may also be stimulated by GTPγS.

Chapter 5

Analysis of the Role of ARF Proteins and Phospholipase D in Insulin-Stimulated GLUT4 Translocation

5.1 Aims

1. To examine the effect of insulin on the subcellular distribution of ARF proteins in 3T3-L1 adipocytes.

2. To investigate the role of ARF proteins in insulin-stimulated GLUT4 translocation and 2-deoxy-D-glucose transport.

3. To examine the expression of PLD isoforms in 3T3-L1 adipocytes.

4. To investigate the role of PLD in insulin-stimulated GLUT4 translocation and 2-deoxy-D-glucose transport.

5.2 Introduction

ADP-ribosylation factors (ARFs) are ubiqitous small GTPases that play an important role in membrane trafficking and secretory processes in eukaryotic cells (Boman *et al.*, 1995). The ARF family consists of 15 structurally related gene products that include 6 ARF proteins and 11 ARF-like (ARL) proteins. The ARF proteins are divided into 3 classes on the basis of size and amino acid identity. ARFs 1 to 3 form class I, ARF 4 and 5 form class II and ARF6 forms class III. All the ARFs contain a glycine at position 2 that is a site for N-terminal myristoylation (reviewed in Donaldson *et al.*, 1994;Moss *et al.*, 1995).

Although ARFs are implicated in several intracellular trafficking events including endosome fusion (Lenhard *et al.*, 1992) and endocytosis (D' Souza-Schorey *et al.*, 1995), the most extensively studied process is the secretory pathway, mediated at least in part, by ARF1 (for examples see Chen *et al.*, 1996; Ktistakis *et al.*, 1996). Like other members of the Ras superfamily, ARF1 interconverts between an inactive GDP-bound form and an active GTP-bound form as it cycles between the cytosol and the Golgi membranes. Upon binding to the Golgi it promotes binding of the adaptor protein-1 (AP-1), a component of the clathrin coat (Traub *et al.*, 1993; Seaman *et al.*, 1996b) and coatomer, the protomer of the COP1 coat (Donaldson *et al.*, 1992) to the membrane allowing the budding of secretory vesicles (Chen *et al.*, 1996; Ktistakis *et al.*, 1996).

ARF1 is also a possible site of action for phosphoinositides in membrane trafficking. Both the guanine nucleotide exchange factor (GEF) (Chardin *et al.*, 1996) and the GTPase activating protein (ARF-GAP) (Randazzo *et al.*, 1994) which are thought to regulate the guanine nucleotide exchange status of ARF1, are dependent upon phosphatidylinositol 4,5-bisphosphate (PIP_2). Furthermore, ARF1 is also an effective activator of phospholipase D (PLD) (Cockcroft *et al.*, 1994; Brown *et al.*, 1993). PLD hydrolyses phosphatidylcholine to choline and phosphatidic acid (PA),

which along with PIP_2 has been proposed to be involved in regulated secretion (Stutchfield *et al.*, 1993; Fensome *et al.*, 1996).

As insulin-stimulated GLUT4 translocation may be mechanistically similar to regulated secretion (discussed in Chapter 1), I wished to investigate the role of both ARFs and PLD in this event in 3T3-L1 adipocytes. In the present study, I examined the role of ARF proteins 1/3, 5 and 6 and PLD in insulin-stimulated GLUT4 translocation and glucose transport. Previous studies have shown that myristoylated N-terminal ARF peptides inhibit ARF function (Kahn *et al.*, 1992; Galas *et al.*, 1997). Introduction of myristoylated peptides corresponding to the N-terminus of ARF6 into α-toxin permeabilised 3T3-L1 adipocytes, markedly inhibited insulin-stimulated GLUT4 translocation and 2-deoxy-D-glucose transport, whereas ARF5 and ARF1 peptides were without effect. In addition, I demonstrate that 3T3-L1 adipocytes express two isoforms of phospholipase D, PLD1 and PLD2. However, prior treatment of 3T3-L1 adipocytes with butan-1-ol, had no affect on insulin-stimulated glucose transport and GLUT4 translocation, suggesting that PLD does not function as a downstream effector of ARF in this event. Taken together with the above data, I propose that ARF6 plays a crucial role in insulin-stimulated GLUT4 translocation, consistent with a general role for this small GTP-binding protein in regulated exocytosis in endocrine cells (Galas *et al.*, 1997).

5.3 Materials and Methods

5.3.1 Permeabilisation of 3T3-L1 Adipocytes

α-toxin permeabilisation of 3T3-L1 adipocytes was carried out as previously described (see Section 4.3.5). 3T3-L1 adipocytes were cultured on collagen-coated coverslips and incubated in serum-free DMEM for 2h prior to use. The cells were then washed three times in IC buffer (10mM NaCl, 20mM HEPES, 50mM KCl, 2mM K_2HPO_4, 90mM potassium glutamate, 1mM $MgCl_2$, 4mM EGTA, 2mM

$CaCl_2$, pH7.2) at 37°C and then incubated in 0.5ml ICR buffer (IC buffer plus 4mM MgATP, 3mM sodium pyruvate, 100μg/ml bovine serum albumin, pH 7.4) containing α-toxin at 250 haemolytic units/ml (Calbiochem material, approximately 8μg/ml) for 5 min to permeabilise the plasma membrane. The medium containing α-toxin was removed and the cells were incubated in 0.5ml of ICR buffer containing peptides at the required concentration for 10 min, followed by the addition of insulin (1μM) or vehicle for a further 15 min at 37°C. Insulin stimulation was terminated by washing the cells rapidly in ice-cold buffer A (see Section 2.12.1) and plasma membrane lawns were prepared as described in Section 2.12.1. Coverslips were viewed and the data analysed as described in Section 4.3.5.

5.3.2 2-Deoxy-D-Glucose Transport Assays:

Effect of Myristoylated Peptides

In order to measure the uptake of glucose following the treatment of 3T3-L1 adipocytes with myristoylated peptides, cells cultured on 6-well plates were permeabilised with α-toxin and treated with peptides and insulin as described above. At the end of the 15 min insulin stimulation, glucose transport was measured by the uptake of 2-deoxyglucose, according to a method previously described for 3T3-L1 adipocytes permeabilised with α-toxin (Herbst *et al.*, 1995). A small volume of (25μl) of radiolabeled 2-deoxy-D-glucose and sucrose was added to the 0.5ml of buffer in each well, such that the final concentration was 50μM 2-deoxy-D-glucose (0.5μCi of [^{3}H] 2-deoxy-D-glucose) and 50μM sucrose (0.06μCi of [^{14}C] sucrose), and incubated for 5 min at 37°C. Transport was terminated by 'flipping' the plates rapidly to remove the incubation buffer and then 'dipping' them sequentially into 3 volumes of ice-cold PBS (see Section 2.2.1). The plates were left to air dry and 1ml of 1% Triton X-100 in H_2O was added to each well. Following incubation for 60 min at room temperature, [^{3}H] 2-deoxy-D-glucose and [^{14}C] sucrose uptake was determined by liquid scintillation dual-labelled counting. The amount of sucrose

remaining with the cells provided a measure of non-specific trapping and uptake from the medium, and the raw values for 2-deoxy-D-glucose uptake were corrected by subtraction of the corresponding amount of this compound. Each experiment consisted of transport assays on triplicate wells of cells in the basal state and cells treated with insulin alone or peptide and insulin.

Effect of Butan-1-ol

3T3-L1 adipocytes cultured on 6-well plates were incubated in serum-free DMEM for 2 h prior to use. For the last 30 min of the incubation, butan-1-ol (30mM) or butan-2-ol (30mM) were added to experimental plates only. After the incubation, cells were washed twice with KRP buffer (see Section 2.2.2) at 37°C and 2-deoxy-D-glucose transport was measured as described in Section 2.13.

5.3.3 Double-Labelled Immunofluorescence Microscopy

Double-labelled immunoflurescence microscopy was carried out as described in Section 2.12.2. In this case, triton-permeabilised 3T3-L1 adipocytes were incubated with a mouse monoclonal anti-GLUT4 antibody and the corresponding secondary antibody (TRITC-conjugated goat anti-mouse IgG) in conjunction with a rabbit anti-ARF5 antibody (see Section 5.3.5) and the corresponding secondary antibody (FITC-conjugated goat anti-rabbit IgG).

5.3.4 Adipsin Release:

Effect of Butan-1-ol

3T3-L1 adipocytes were cultured on 10cm plates and incubated in serum-free DMEM for 2 h prior to use. For the last 30 min of the incubation, butan-1-ol (30mM) or butan-2-ol (30mM) were added to experimental plates only. After the

incubation, cells were washed twice with KRP buffer (see above) at 37°C and adipsin release was measured as described in Section 2.14.

5.3.5 Peptide Synthesis

Peptides corresponding to the residues 2 through 16 of murine ARF5 were synthesised by Thistle Research (Glasgow, UK) and were > 99% pure as determined using HPLC. A myristoyl group was included at the position corresponding to Gly-2. Myristoylated ARF6 and ARF1 peptides were supplied by Dr M-F. Bader (INSERM, Strasborg, France).

5.3.6 Antibodies

The anti-GLUT4 antibody used for immunoblotting and vesicle immunoadsorption was a rabbit polyclonal against a peptide comprising the C-terminal 14 amino acid residues of the human isoform of GLUT4 (see Section 2.4). For double-labelled immunofluorescence a monoclonal GLUT4 antibody (1F8) was used (see Section 2.4). Anti-ARF5 antibodies were from Professor J. Moss (NIH, Bethesda, Maryland, USA) and Professor R.A. Kahn (NIH, Bethesda, Maryland, USA). Anti-ARF 1/3 antibody was a generous gift from M.J.O Wakelam (University of Birmingham, UK) and anti-ARF6 antibodies were supplied by Dr M-F. Bader (INSERM, Strasborg, France) and Dr J. Donaldson (NIH, Bethesda, Maryland, USA). Anti-adipsin antibody was generously provided by Professor B. Spiegelman (Dana Farber Cancer Institute, Boston, USA). Anti-PLD1 and PLD2 were from Quality Controlled Biochemicals Inc (Hopkinton, MA, USA).

5.3.7 Statistical Analysis

Statistical analysis was performed using Statview 4.0 on a Mac Power PC.

5.4 Results

5.4.1 Distribution of ARF Proteins and the Effect of Insulin and Wortmannin in 3T3-L1 Adipocytes

Initially, I wished to examine the effect of insulin on the subcellular distribution of ARF isoforms in 3T3-L1 adipocytes. Adipocytes treated with or without insulin for 15 min were fractionated into plasma membrane (PM), low density microsomal (LDM), high density microsomal (HDM) and soluble protein (SP, corresponding to cytosolic proteins) fractions as previously described in Section 2.10. Equal amounts of protein (40μg) from each fraction were resolved by SDS-PAGE, transferred to nitrocellulose membranes and immunoblotted with antibodies to ARF1/3 (an antibody known to cross react with both ARF1 and 3 was used), ARF5, ARF6 and GLUT4. 3T3-L1 adipocytes were found to express ARFs 1/3, 5 and 6. In basal (non-stimulated) adipocytes ARF1/3 was localised mainly in the SP fraction with smaller amounts in the LDM and HDM fractions, while ARF6 was present to some extent in most fractions although clearly enriched in the PM, consistent with previous studies for this cell type (Yang *et al.*, 1998) (Figure 5.1).

ARF5, found to be localised to the LDM and SP protein fractions in basal cells, was the only isoform observed to exhibit altered subcellular distribution in response to insulin (Figure 5.2). When adipocytes were stimulated with insulin (1μM), an increase in both ARF5 and GLUT4 levels was observed at the PM. In the case of GLUT4 there was a concommitant decrease in the LDM fraction, as has been well documented. In contrast, the redistribution of ARF5 to the PM was from both the the SP fraction and the LDM fraction.

It is well documented that PI 3-kinase is involved in insulin-induced glucose uptake (reviewed in Shepherd *et al.*, 1996a). Indeed, GLUT4 translocation is blocked by PI 3-kinase inhibitors such as wortmannin and LY294002 (Cheatham *et al.*, 1994;

Clarke *et al.*, 1994; Yang *et al.*, 1996). To investigate a possible involvement of PI 3-kinase in insulin-induced ARF5 translocation, adipocytes were treated with insulin (1μM) for 15 min in the presence or absence of wortmannin (100nM). As expected, wortmannin blocked the insulin-induced departure of GLUT4 from the LDM fraction (Figure 5.2). In contrast, the inhibitor enhanced ARF5 levels present within the plasma membrane, almost completely depleting the SP and LDM fractions. These results suggest that the cycling of ARF5 between the cytosol and the plasma membrane is PI 3-kinase dependent.

The observation that ARF6 was predominantly localised to the plasma membrane in 3T3-L1 adipocytes, together with the recent data that this small GTP-binding protein has been involved in regulated exocytosis (Galas *et al.*, 1997), tempted me to examine the effect of wortmannin on the subcellular distribution of this protein in adipocytes. Consistent with the initial fractionation study, ARF6 was clearly enriched in the plasma membranes (Figure 5.2). No change in distribution was observed on exposure to insulin with or without prior treatment with wortmannin.

5.4.2 Co-Localisation of ARF5 and GLUT4 within 3T3-L1 Adipocytes

The translocation of ARF5 to the PM in response to insulin and the localisation of this isoform in the LDM fraction in which GLUT4 is enriched, prompted me to determine whether ARF5 co-localised with GLUT4 in 3T3-L1 adipocytes. Further analysis of their subcellular distribution was examined by immunoadsorption of GLUT4 vesicles and immunofluorescence microscopy.

Vesicles were immunadsorbed from the LDM fraction of basal 3T3-L1 adipocytes using either the affinity-purified GLUT4 antibody or a non-specific IgG as described in Section 2.11. Both the vesicles and the depleted LDM were analysed for the presence of ARF5 and GLUT4. Under my experimental conditions, most of the GLUT4 protein was immunoadsorbed, as indicated by the depletion of GLUT4 from

the LDM fraction, where anti-GLUT4 was used but not non-specific IgG (Figure 5.3). The lack of detection of GLUT4 in the GLUT4 vesicles suggests that upon removal of the vesicles from the *Staph. a.* cells, the GLUT4 remained firmly attached to the cells, thus preventing any detection of the protein in this fraction. ARF5 was not detected in either the GLUT4 vesicles or the vesicles obtained using the non-specific IgG. The lack of immunoprecipitation of ARF5 with GLUT4 was confirmed by the analysis of the GLUT4-depleted LDM, which did not show any significant reduction in the amount of ARF5 compared to that in the non-depleted LDM (Figure 5.3).

The co-localisation of ARF5 and GLUT4 in insulin-stimulated adipocytes was analysed using double-labelled immunofluorescence. Figure 5.4 shows paraformaldehyde fixed, Triton-permeabilised basal and insulin treated cells labelled with a GLUT4 monoclonal antibody (IF8) and an anti-ARF5 antibody. Under basal conditions, GLUT4 immunofluorescence is almost entirely intracellular and is found in the perinuclear region with some evidence of fine punctate spots distributed at the cell surface. In contrast, ARF5 immunofluorescence is both cytoplasmic and perinuclear in disribution in basal cells. Only partial co-localisaton between GLUT4 and ARF5 is observed in the perinuclear region. After a 15 min treatment with insulin (1μM), redistribution of both GLUT4 and ARF5 to the plasma membrane is observed, consistent with the subcellular fraction data. Translocation of GLUT4 and ARF5 to the plasma membrane results in an increase in co-localisation, although the extent of overlap is still limited. This is probably a result of the constant cycling of ARF5 between the plasma membrane and the cytosol, thus at any one time ARF5 will still be observed in the cytoplasm in insulin-stimulated cells. Together, these results confirm the subcellular fractionation data as GLUT4 and ARF5 are localised to distinct compartments in the basal state from which they translocate to the plasma membrane in response to insulin.

5.4.3 Role of ARFs in Insulin-Stimulated GLUT4 Translocation

To investigate whether ARF5 or ARF6 play an essential role in insulin-stimulated GLUT4 translocation we introduced peptides designed to inhibit ARF function into α–toxin permeabilsed 3T3-L1 adipocytes and examined the effect on insulin action. As previous studies have shown that only peptides with a myristoyl group at Gly-2 inhibit ARF function (see Table 5.1) (Kahn *et al.*, 1992; Galas *et al.*, 1997), I examined, by immunofluorescence of PM lawns, the effects of both myristoylated $ARF5_{(2-17)}$ and $ARF6_{(2-13)}$ peptides on cell surface levels of GLUT4 in response to insulin. In the absence of peptides, insulin (1μM) increased cell surface levels of GLUT4 by 6.3-fold in permeabilised cells (Figure 5.5a). In cells incubated with myristoylated $ARF5_{(2-17)}$ (100μM), insulin increased surface levels of GLUT4 by 6.8-fold, similar to that observed in the absence of peptides. However, in the presence of myrisoylated $ARF6_{(2-13)}$ (100μM) insulin-stimulated GLUT4 translocation was reduced by over 60%, indicating that insulin action was specifically inhibited by the myristoylated $ARF6_{(2-13)}$ peptide (Figure 5.5). I also examined the effect of a myristoylated ARF1 $peptide_{(2-17)}$ (Figure 5.5). However, this peptide had no significant effect on insulin-stimulated cell surface levels of GLUT4, indicating that the strong inhibition of insulin-stimulated GLUT4 translocation observed in the presence of myristoylated $ARF6_{(2-13)}$ was not due to some non-specific effect.

Under similar conditions, I also examined the effect of the myristoylated ARF peptides on insulin-stimulated glucose transport. The effects of insulin and myristoylated ARF1, 5 and 6 peptides on the uptake of 2-deoxy-D-glucose by α-toxin permeabilised adipocytes are shown in Figure 5.6. In the absence of peptides, insulin (1μM) stimulated glucose transport by 8.3-fold. Similarily, in cells incubated with myristolated $ARF5_{(2-17)}$ (100μM) and myristolated $ARF1_{(2-17)}$ peptides (100μM), insulin stimulated glucose transport by 7.3 to 8.8-fold. However, in accordance with the plasma membrane lawn data, incubation with myristoylated

$ARF6_{(2-13)}$ (100μM) reduced insulin-stimulated glucose transport by ~ 60%. Taken together, these results provide evidence that ARF6 plays an essential role in insulin-induced GLUT4 translocation.

5.4.4 Subcellular Distribution of PLDs and the Effect of Insulin in 3T3-L1 Adipocytes

As previous reports have shown that ARF is an effective activator of PLD (Cockcroft *et al.*, 1994; Brown *et al.*, 1993), it is possible that ARF6 may act catalytically via this enzyme at the docking and / or fusion stage of GLUT4 vesicles with the plasma membrane. It is also possible that ARF isoforms yet to be identified in 3T3-L1 adipocytes, may be involved in the budding of GLUT4 vesicles from the intracellular storage compartment, similar to the role of ARF1 in the formation of secretory vesicles at the Golgi (Chen *et al.*, 1996; Chen *et al.*, 1997b). Again, PLD may act as a downstream effector of ARF in this process.

As a first step in determining whether PLD may be involved in the insulin-regulated exocytosis of GLUT4, I examined the expression and localisation of PLD isoforms in 3T3-L1 adipocytes using antibodies specific for PLD1, PLD2 and GLUT4. As shown in Figure 5.7, both PLD1 and 2 were expressed and localised to the LDM fraction in adipocytes, with no change in their redistribution in response to insulin. This is in marked contrast to GLUT4, which, in the same cells, exhibited a large movement from the LDM fraction to the PM fraction.

5.4.5 Role of Phospholipase D in Insulin-Stimulated Trafficking in 3T3-L1 Adipocytes

Next, I wished to examine the role of PLD in insulin-stimulated GLUT4 translocation. To inhibit PLD activity I utilised the primary alcohol butan-1-ol, and compared the effect of this alcohol to that of butan-2-ol which does not inhibit PLD

activity (Cook *et al.*, 1991). Treatment with butan-1-ol (30 or 60mM) for 30 min before adipocytes were stimulated with insulin (1μM) for 15 min, had no effect on GLUT4 translocation to the cell surface as assessed using the plasma membrane lawn assay (Figure 5.8). Under similar conditions, I also investigated the effect of butan-1-ol (30 or 60mM) on insulin-stimulated glucose transport. In accordance with the immunofluorescence data, butan-1-ol was without effect on 2-deoxy-D-glucose uptake in basal and insulin stimulated cells (Figure 5.9).

To ensure that the treatment of adipocytes with butan-1-ol was indeed targeting PLD activity in these cells, I decided to examine the effect of the inhibitor on the insulin-stimulated secretion of the serine proteinase adipsin. In agreement with previous studies, insulin increased adipsin secretion from 3T3-L1 adipocytes by ~ 2-fold (Figure 5.10) (Kitagawa *et al.*, 1989). Treatment of adipocytes with butan-1-ol (30 mM) for 30 min prior to insulin stimulation inhibited both basal (constitutive) and insulin-stimulated adipsin secretion (Figure 5.11). Butan-2-ol was without effect, consistent with the inability of this secondary alcohol to inhibit PLD activity (Cook *et al.*, 1991).

Table 5.1

Sequence Alignment of ARF Proteins at the Amino Terminus

```
ARF1aa      MGNIFANLFKGLFGKK...
ARF2aa      MGNVFEKLFKSLFGKK...
ARF3aa      MGNIFGNLLKSLIGKK...
ARF4aa      MGLTISSLFSRLFGKK...
ARF5aa      MGLTVSALFSRIFGKK...
ARF6aa      MGKVLSK----IFGNK...
```

Shown is a sequence alignment of the murine isoforms of the ARF family (Hosaka *et al*, 1991). The myristoylated ARF6 peptide used in Figures 5.5 and 5.6 is underlined. The same peptide was also found to inhibit secretion from chromaffin cells (Galas *et al.*, 1997).

Figure 5.1

Subcellular Distribution of GLUT4, ARF1/3 and ARF6 in 3T3-L1 Adipocytes and the Effect of Insulin

Shown is the distribution of GLUT4, ARF1/3 and ARF6 in subcellular fractions isolated from basal (unstimulated) and insulin-stimulated 3T3-L1 adipocytes (insulin exposure for 15 min at 1 μM). Subcellular membrane fractions (PM, LDM HDM and SOL) were prepared, subjected to SDS-PAGE, electrophoretically transferred to nitrocellulose membranes, and immunoblotted for GLUT4, ARFs 1/3 and 6. In each immunoblot, 40μg of protein was loaded per lane. Note that GLUT4 exhibits translocation from the intracellular (LDM) membrane fraction to the plasma membrane, but neither ARF1/3 nor ARF6 exhibited altered distribution in response to insulin treatment. This set of immunoblots was from the same preparation of cellular fractions, and is representative of at least two other experiments.

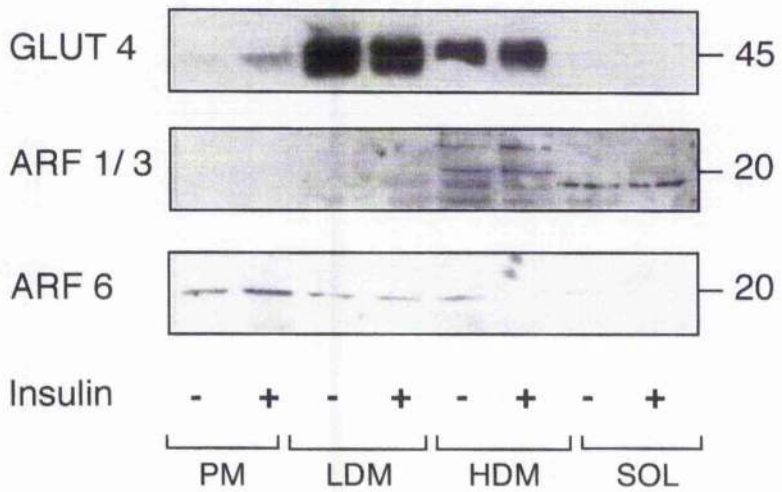
GLUT 4
45
ARF 1/ 3
20
ARF 6
20
Insulin
- + - + - + - +
PM
LDM
HDM
SOL

Figure 5.2

Subcellular Distribution of GLUT4, ARF5 and ARF6 in 3T3-L1 Adipocytes and the Effect of Insulin and Wortmannin

Shown is a representative immunoblot of subcellular fractions (PM, LDM, SP) of 3T3-L1 adipocytes from basal (non-stimulated), insulin-stimulated (1μM) for 15 min, or cells pre-treated with 100nM wortmannin before insulin treatment. Note the insulin-stimulated re-distribution of GLUT4 from the LDM fraction to the PM, which is inhibited by prior exposure of the cells to 100nM wortmannin. In contrast, insulin-stimulated ARF5 movement to the PM arises from both the SP and LDM fractions, and is markedly potentiated by prior exposure of the cells to wortmannin. Similar data were obtained using two different anti-ARF5 antisera. No change in ARF6 distribution was observed in response to insulin or wortmannin treatment.

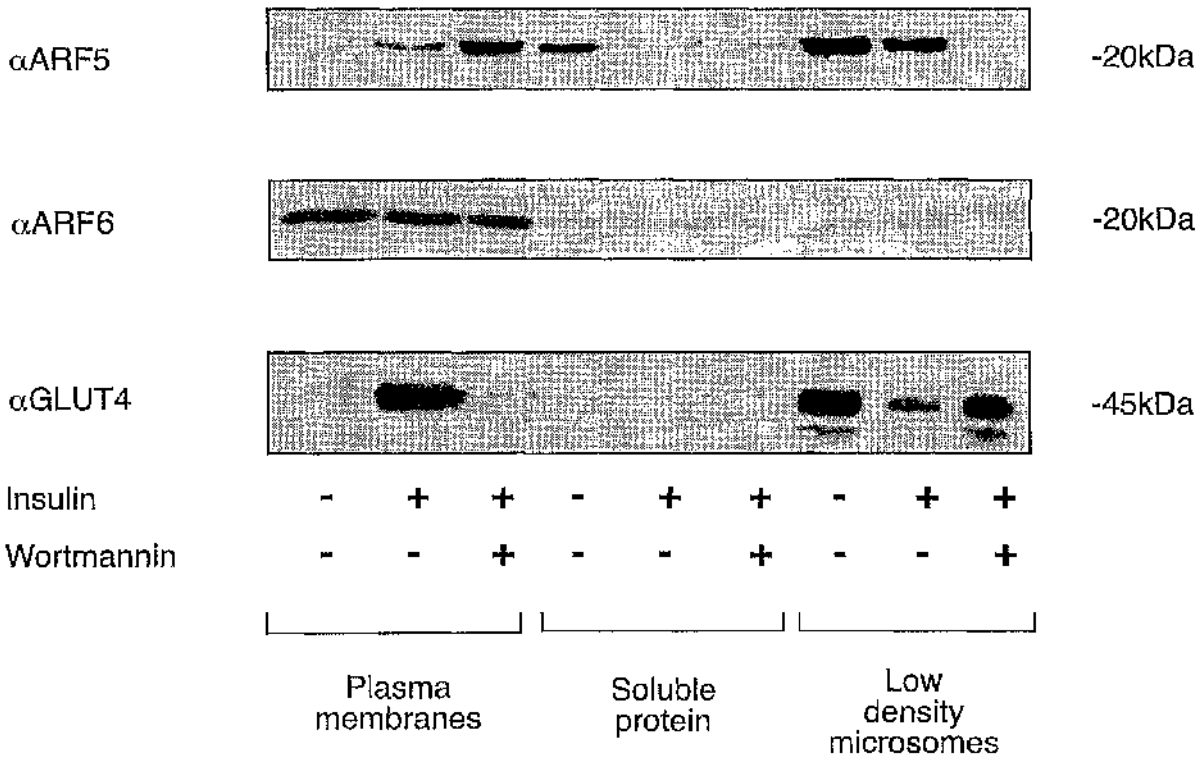
αARF5
-20kDa
αARF6
-20kDa
αGLUT4
-45kDa
Insulin
- + + - + + - + +
Wortmannin
- - + - - + - - +
Plasma membranes
Soluble protein
Low density microsomes

Figure 5.3

Immunoadsorption of GLUT4-Containing Vesicles

Intracellular (LDM) membranes were isolated from basal 3T3-L1 adipocytes and incubated with anti-GLUT4 antibody or non-specific IgG (control) pre-coupled to *Staph. a.* cells as described in Section 2.11. Immunoadsorbed vesicles (GLUT4 and IgG) and depleted LDM fractions (GLUT4 and IgG) were subjected to SDS-PAGE and immunoblot analysis with anti-GLUT4 and anti-ARF5 antibodies as indicated.

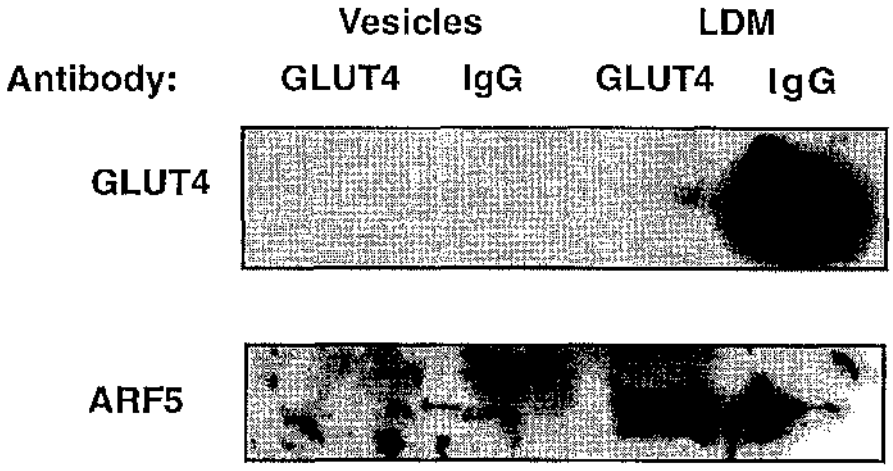
Vesicles
LDM
Antibody:
GLUT4
IgG
GLUT4
IgG
GLUT4
ARF5

Figure 5.4

Double-labelled Immunofluorescence Analysis of GLUT4 and ARF5 in Basal and Insulin-Stimulated 3T3-L1 Adipocytes

Triton-permeabilised (BASAL) basal (non-insulin-stimulated) and (INSULIN) insulin-stimulated 3T3-L1 adipocytes were incubated with a mouse monoclonal anti-GLUT4 antibody and the corresponding secondary antibody (TRITC-conjugated goat anti-mouse IgG, stained red) in conjunction with a rabbit anti-ARF5 antibody and the corresponding secondary antibody (FITC-conjugated goat anti-rabbit IgG, stained green). The yellow colour indicates co-staining of the proteins at the plasma membrane in the insulin-stimulated cells.

Basal

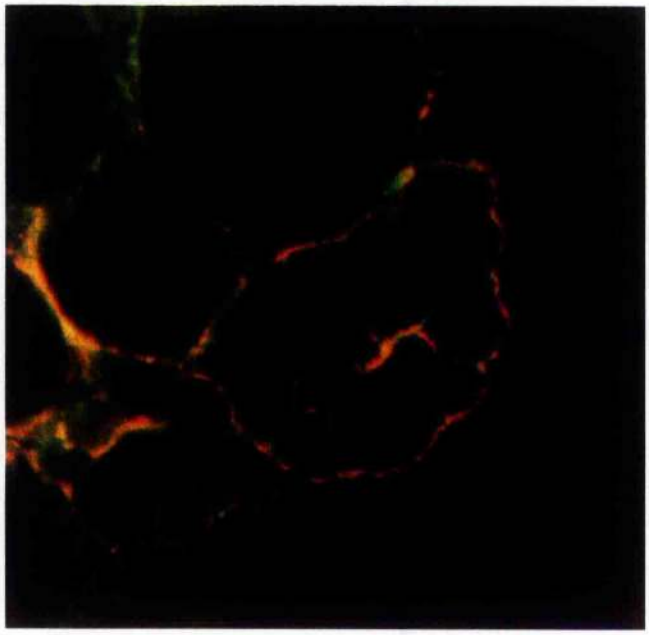

Insulin

Figure 5.5

Effect of Myristoylated ARF Peptides on Insulin-Stimulated GLUT4 Translocation in Permeabilised 3T3-L1 Adipocytes

Triplicate coverslips of α-toxin permeabilised 3T3-L1 adipocytes were incubated at 37°C in buffer alone or in buffer containing myristoylated ARF peptides (100μM) as indicated. After 10 min, the cells were treated with or without insulin (1μM) for a further 15 min. Plasma membrane lawns were prepared and the extent of GLUT4 translocation relative to the basal value was determined using scanning laser confocal immunofluorescence microscopy. Shown are data of a representative experiment (n = 3). Data are presented as the mean fold increase relative to basal (non-stimulated) cells ± s.e.m.

Figure 5.5

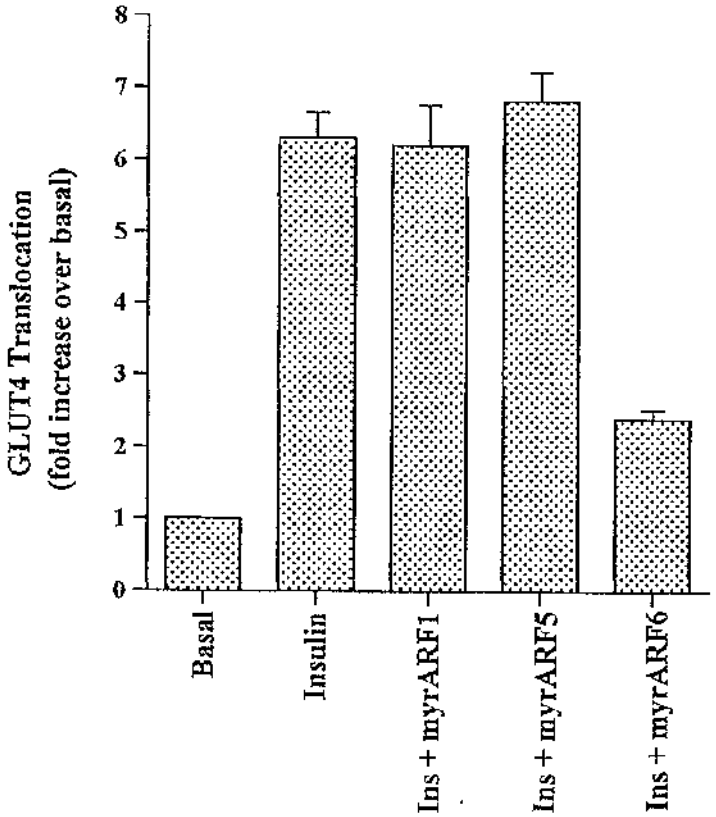
GLUT4 Translocation
(fold increase over basal)
0
1
2
3
4
5
6
7
8
Basal
Insulin
Ins + myrARF1
Ins + myrARF5
Ins + myrARF6

Figure 5.6

Effect of Myrisoylated ARF Peptides on Insulin-Stimulated 2-Deoxy-D-Glucose Transport in Permeabilised 3T3-L1 Adipocytes

Triplicate wells of α-toxin permeabilised 3T3-L1 adipocytes were incubated at 37°C in buffer alone or in buffer containing myristoylated ARF1 (100μM), ARF5 (100μM) and ARF6 (100 and 10μM) peptides as indicated. After 10 min, the cells were treated with or without insulin (1μM) for a further 15 min. Glucose transport was measured by the assay of 2-deoxy-D-glucose uptake for 5 min as described in *Materials and Methods*. Shown are data from a representative experiment (n = 3). Data are represented as the mean fold increase relative to basal (non-stimulated) cells ± s.e.m

Figure 5.6

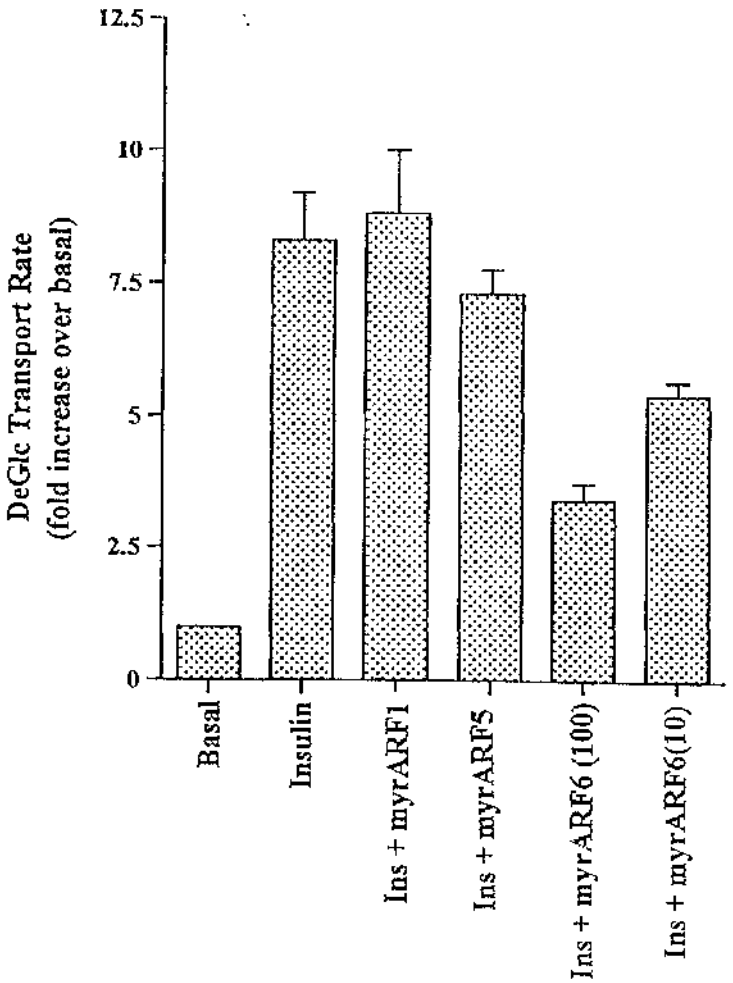
DeGlc Transport Rate
(fold increase over basal)
12.5
10
7.5
5
2.5
0
Basal
Insulin
Ins + myrARF1
Ins + myrARF5
Ins + myrARF6 (100)
Ins + myrARF6(10)

Figure 5.7

Subcellular Distribution of GLUT4, PLD1 and PLD2 in 3T3-L1 Adipocytes and the Effect of Insulin

Shown is the distribution of GLUT4, PLD1 and PLD2 in subcellular fractions isolated from basal (non-stimulated) and insulin-stimulated 3T3-L1 adipocytes (insulin exposure for 15 min at 1μM). Subcellular membrane fractions (PM, LDM HDM and SOL) were prepared, subjected to SDS-PAGE, electrophoretically transferred to nitrocellulose membranes, and immunoblotted for GLUT4, PLD1 and PLD2. In each immunoblot, 40μg of protein was loaded per lane. Note that GLUT4 exhibits translocation from the intracellular (LDM) membrane fraction to the plasma membrane, but neither PLD1 or PLD2 exhibited altered distribution in response to insulin treatment. This set of immunoblots was from the same preparation of cellular fractions used for the immunodetection of ARF proteins in 3T3-L1 adipocytes (Figure 5.1).

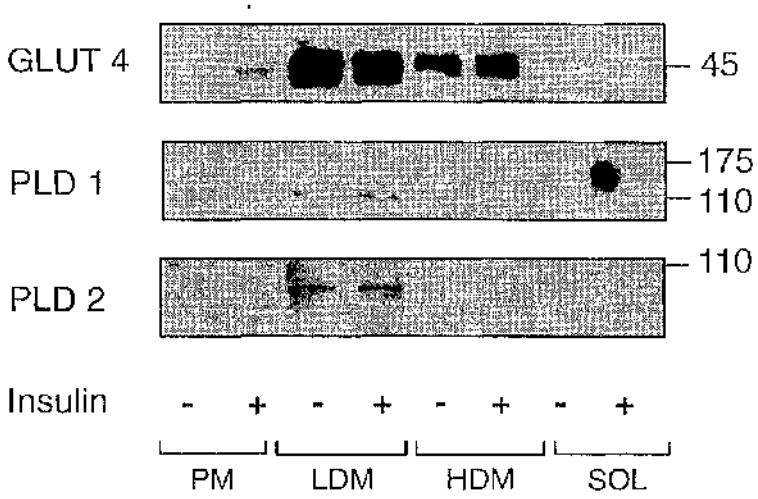
GLUT 4
45
PLD 1
175
110
PLD 2
110
Insulin
- + - + - + - +
PM
LDM
HDM
SOL

Figure 5.8

Effect of Butan-1-ol on Insulin-Stimulated GLUT4 Translocation in 3T3-L1 Adipocytes

Triplicate coverslips of 3T3-L1 adipocytes were incubated in buffer containing butan-1-ol (30mM) or butan-2-ol (30mM, as a control) for 30 min at 37°C, before being treated with or without insulin (1μM) for a further 15 min. GLUT4 translocation was assessed using the plasma membrane lawn assay. Butan-1-ol and butan-2-ol were without effect on GLUT4 translocation, even at concentrations of up to 60mM. Quantification of three experiments of this type revealed no significant differences in fluorescence intensity in the butan-1-ol, butan-2-ol and non-treated coverslips in either basal (non-stimulated) or insulin-stimulated state. Data are presented as the mean fold increase relative to basal cells ± s.e.m.

Figure 5.8

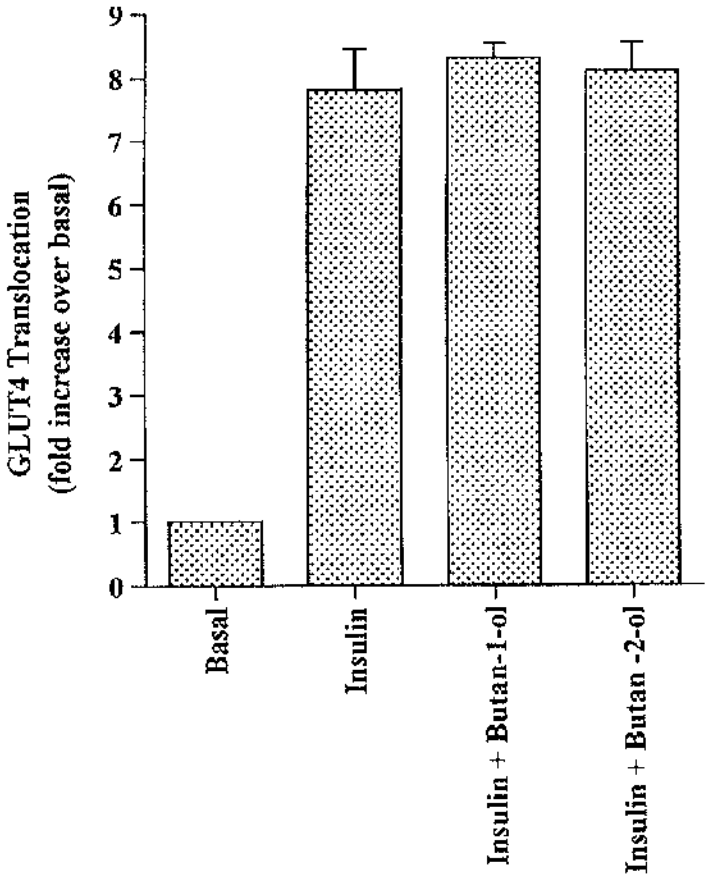
GLUT4 Translocation
(fold increase over basal)
0
1
2
3
4
5
6
7
8
9
Basal
Insulin
Insulin + Butan-1-ol
Insulin + Butan -2-ol

Figure 5.9

Effect of Butan-1-ol on Insulin-Stimulated 2-Deoxy-D-Glucose Transport in 3T3-L1 Adipocytes

3T3-L1 adipocytes were incubated in buffer containing butan-1-ol (30mM) or butan-2-ol (30mM, as a control) for 30 min at 37°C, before being treated with or without insulin (1μM) for a further 15 min. Glucose transport was measured by the assay of 2-deoxy-D-glucose uptake as described in Section 2.13. At concentrations up to 60mM, butan-1-ol had no effect on either basal or insulin-stimulated glucose transport. Shown is a representatative experiment of three similar experiments. Data are presented as the mean 2-deoxy-D-glucose transport rate ± s.e.m.

Figure 5.9

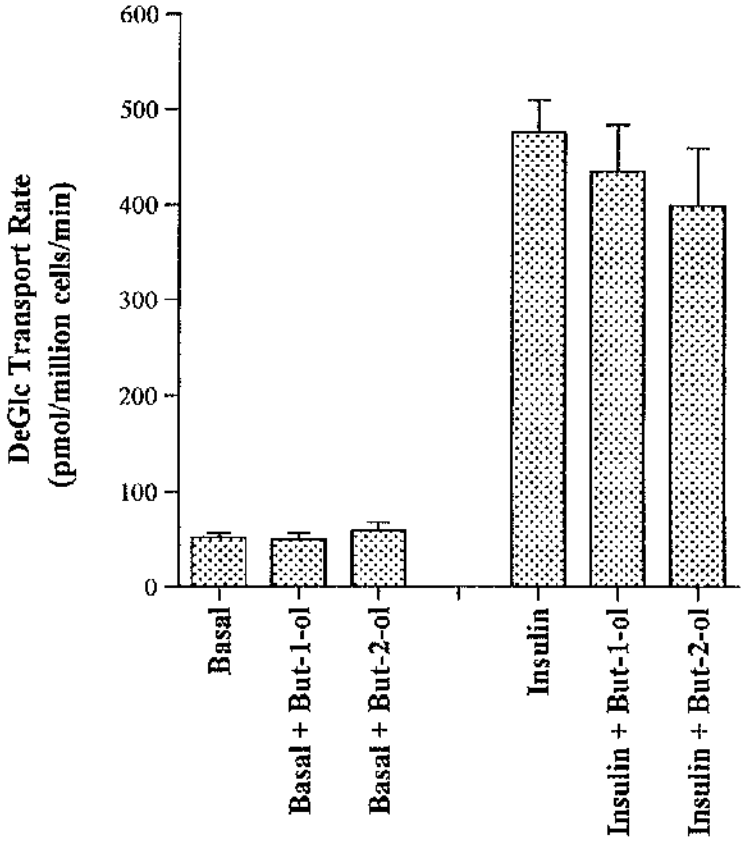
DeGlc Transport Rate
(pmol/million cells/min)
600
500
400
300
200
100
0
Basal
Basal + But-1-ol
Basal + But-2-ol
Insulin
Insulin + But-1-ol
Insulin + But-2-ol

Figure 5.10

Effect of Butan-1-ol on Adipsin Secretion in 3T3-L1 Adipocytes

A. Time course of adipsin secretion from 3T3-L1 adipocytes. Cells were treated with or without insulin (1μM) for the indicated times. The relative amount of adipsin in the medium was determined by immunoblotting. Adipsin secretion is expressed in arbitrary units as described in Section 2.14. This experiment was repeated with similar results.

B. Time course of adipsin secretion from cells pre-treated with butan-1-ol (an inhibitor of PLD activity) and butan-2-ol (as a control) as described. Cells were treated with or without insulin for the indicated times. Shown is a representative experiment of at least two similar experiments.

Figure 5.10A

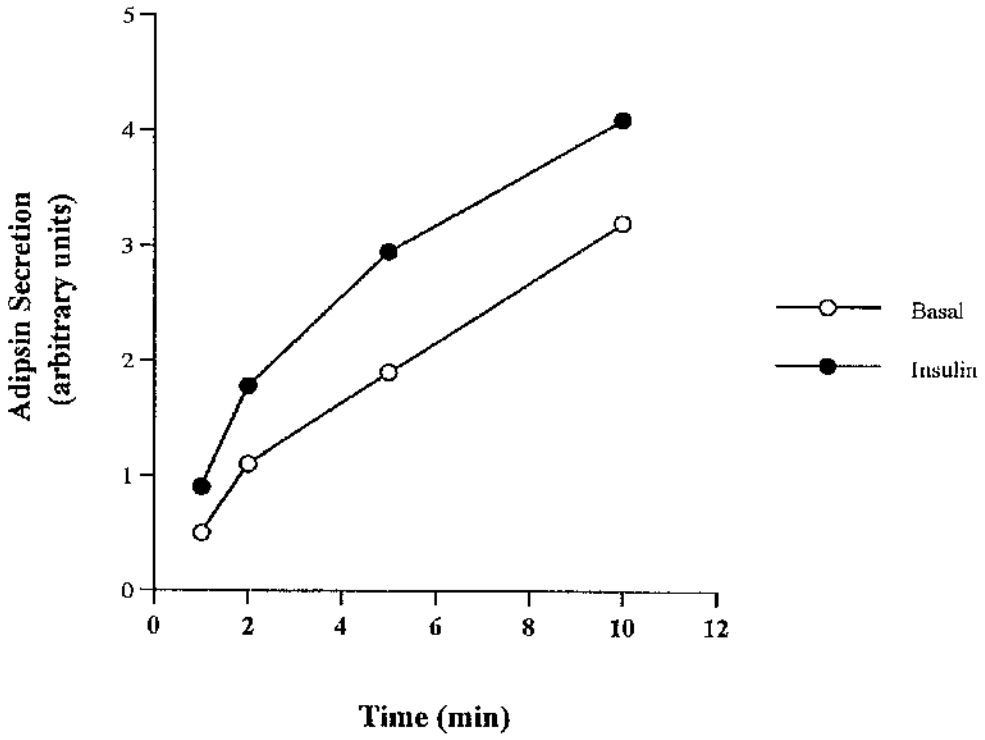
Adipsin Secretion
(arbitrary units)
5
4
3
2
1
0
0
2
4
6
8
10
12
Time (min)
Basal
Insulin

Figure 5.10B

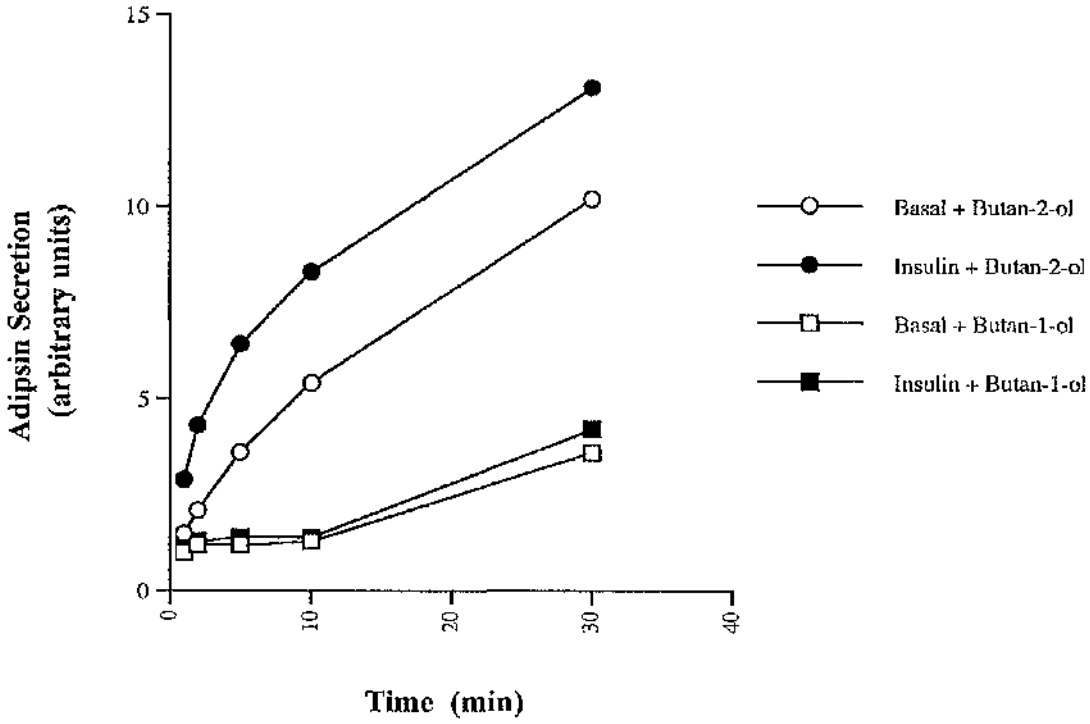
Adipsin Secretion (arbitrary units)
15
10
5
0
0
10
20
30
40
Time (min)
Basal + Butan-2-ol
Insulin + Butan-2-ol
Basal + Butan-1-ol
Insulin + Butan-1-ol

5.5 Discussion

ARF proteins have been implicated in the regulation of vesicular transport through the secretory pathway (reviewed in Moss *et al.*, 1995). Recent studies have shown that ARFs may play a role in both the formation of secretory vesicles (Chen *et al.*, 1996) and the initiation or facilitation of vesicle fusion at the plasma membrane (Galas *et al.*, 1997) in endocrine cells. As insulin-stimulated GLUT4 translocation to the cell surface in adipocytes exhibits many similarities to regulated secretion in neuroendocrine and endocrine cells, I wished to investigate whether ARF proteins may also be an important component of the GLUT4 trafficking machinery.

As a first step towards identifying ARF proteins involved in insulin-stimulated GLUT4 translocation we examined the effect of insulin on the subcellular distribution of ARFs 1/3, 5 and 6 in 3T3-L1 adipocytes. An antibody reported to cross-react mainly with ARF1 and 3 identified a protein present within the intracellular (LDM) membrane fraction and the cytosolic fraction (Figure 5.1), consistent with previously published data (Hosaka *et al.*, 1991). In agreement with a previous study on 3T3-L1 adipocytes (Yang *et al.*, 1998), ARF6 was predominantly localised within the plasma membrane, with some immunoreactivity present in the cytosolic and intracellular membrane fractions. However, under our experimental conditions, neither of these isoforms exibited an altered distribution in response to insulin. In contrast, both GLUT4 and ARF5 levels increased within the plasma membrane in response to insulin. In the case of GLUT4, this was concomitant with a decrease in the intracellular (LDM) fraction, as has been well documented. However, ARF5, localised to the intracellular (LDM) fraction and the soluble protein (cytosolic) fraction in the basal state, redistributed to the plasma membrane from both of these fractions in response to insulin (Figure 5.2). Consistent with these findings, double-labelled immunofluorescence showed little overlap between GLUT4 and ARF5 in basal cells, with an increase in co-localisation at the plasma membrane in response to insulin (Figure 5.4). The extent of co-localisation at the plasma membrane is

possibly limited due to the cycling of ARF5 between the cytosol and plasma membrane.

As PI 3-kinase is known to play an important role in insulin-stimulated GLUT4 translocation (reviewed in Shepherd *et al.*, 1996a), I also examined the effect of wortmannin on ARF5 translocation. As expected, wortmannin effectively inhibited insulin-stimulated GLUT4 translocation to the plasma membrane. In marked contrast, in the same cells, ARF5 translocation to the plasma membrane was markedly enhanced, suggesting that the cycling of ARF5 between the cytosol and the plasma membrane is dependent upon PI 3-kinase.

Conversion of ARF_{GDP} to ARF_{GTP} is promoted *in vivo* by a guanine nucleotide exchange factor (GEF). Several of these proteins have recently been identified, all of which contain a central sec7 domain responsible for nucleotide exchange and a pleckstrin homology (PH) domain which interacts with inositol phospholipids (Chardin *et al.*, 1996; Klarlund *et al.*, 1997). Recent evidence suggests that the interaction between the PH domain and the inositol phospholipid mediates GEF association at the membrane, thus increasing GEF and ARF localisation resulting in enhanced catalytic activity (Paris *et al.*, 1997). Interestingly, a protein previously identified in 3T3-L1 adipocytes, GRP1, has recently been reported to catalyse guanine nucleotide exchange for ARFs 1 and 5 *in vitro* (Klarlund *et al.*, 1998). Furthermore, binding of the PI 3-kinase product, phophatidylinositol 3,4,5-trisphosphate (PIP_3), markedly enhances the exchange activity (Klarlund *et al.*, 1998), suggesting a model in which the selective recruitment of GRP1 to PIP_3 in membranes activates ARFs 1 and 5.

Based on these recent studies and the observation that inhibition of PI 3-kinase activity in insulin-stimulated 3T3-L1 adipocytes leads to an increase in ARF5 levels at the plasma membrane, I hypothesise that ARF5 cycles between the cytosol and the plasma membrane, mediated in part via guanine nucleotide exchange. In response

to insulin, PI 3-kinase activation results in the synthesis of PIP_3, which in turn recruits a guanine nucleotide exchange factor such as GRP1 or its homologs to the plasma membrane where it localises with $ARF5_{GDP}$ resulting in its activation and the subsequent hydrolysis of GTP. Inhibition of PI 3-kinase by wortmannin would block PIP_3 production thus preventing the recruitment of the GEF to the plasma membrane, resulting in the accumulation of the weakly bound $ARF5_{GDP}$ at the plasma membrane as guanine nucleotide exchange and hydrolysis of ARF5 is impaired. However, although this hypothesis provides an attractive working model for insulin-stimulated PI 3-kinase-dependent trafficking in 3T3-L1 adipocytes, further studies are required to determine whether GRP1 catalyses nucleotide exchange of ARF5 at the plasma membrane *in vivo*. Interestingly, a most recent study has reported that upon expression of ARNO (ARF nucleotide-binding-site opener) in 3T3-L1 adipocytes, insulin stimulates the translocation of the GEF to the plasma membrane in a PI 3-kinase dependent manner (Kanamarlapudi *et al.*, 1998), suggesting that our model may indeed be a reasonable hypothesis.

Previous studies have shown that myristoylated N-terminal ARF peptides inhibit ARF function (Kahn *et al.*, 1992; Galas *et al.*, 1997). To investigate whether ARF5 plays a specific role in GLUT4 insulin-stimulated trafficking in 3T3-L1 adipocytes, I used myristoylated peptides corresponding in sequence to the N-terminal residues of ARF5. In addition, the predominant localisation of ARF6 to the plasma membrane in adipocytes, together with the recent data that this small GTP-binding protein has been implicated in the regulated exocytosis of chrommaffin granules in endocrine cells (Galas *et al.*, 1997), prompted us to examine the effect of myristoylated ARF6 peptides on insulin-stimulated GLUT4 translocation. As illustrated in Figures 5.5 and 5.6, the myristoylated $ARF6_{(2-13)}$ peptide strongly inhibited both insulin-stimulated GLUT4 translocation and glucose transport in 3T3-L1 adipocytes, consistent with a role for this small GTPase in regulated exocytosis. In contrast, the myristoylated $ARF5_{(2-17)}$ peptide had no effect on insulin-stimulated GLUT4 translocation or glucose transport. Although the role of ARF5 is unclear, it is

possible that this small GTP-binding protein may be involved in general trafficking processes within these cells.

It is important to note, however, that the myristoylated $ARF6_{(2-13)}$ peptide did not completely block insulin-stimulated GLUT4 translocation. On considering the localisation of GLUT4 to two distinct intracellular compartments within adipocytes (refer to Section 3.2), a plausible explanation for these data is that ARF6 is involved in the exocytosis of GLUT4 from the insulin-responsive storage compartment in response to insulin but does not regulate the docking and fusion of recycling endosomes with the cell surface. Thus, stimulation of the recycling endosomal system in response to insulin (Tanner *et al.*, 1987; Tanner *et al.*, 1989) would result in an increase in GLUT4 levels at the plasma membrane even when GLUT4 translocation from the storage compartment is blocked. To determine whether ARF6 is involved predominantly in the regulation of the insulin-responsive storage compartment, further studies may be carried out to investigate whether this ARF protein regulates the insulin-dependent trafficking of proteins previously shown to be localised to the recycling endosomal system such as the transferrin receptor (TfR) and GLUT1 (Livingstone *et al.*, 1996).

I cannot rule out the possibility, however, that complete inhibition is not observed due to experimental limitations. In this regard, myristoylated peptides are difficult to solubilise thus reducing the efficiency of the internalisation of the peptide, resulting in a possible reduction of the inhibitory effect. Again, further studies are required to determine the efficiency of internalisation of the peptide in order to resolve this issue. However, due to the time constraints of this work I was unable to pursue either of the aforementioned studies.

Taken together, these data implicate ARF6 as a key component of the insulin-responsive GLUT4 trafficking machinery. Although this present study does not enable me to define a precise role for ARF6 in GLUT4 trafficking, the predominant

localisation of ARF6 at the plasma membrane suggests that the small GTP-binding protein may function in the latter stages of trafficking, possibly at the stage of docking / fusion of GLUT4 vesicles at the cell surface. Similar to the cycling of ARF1 between the cytosol and Golgi membranes (see above), ARF6 may function by cycling between the cytosol or indeed another membrane compartment and the plasma membrane as it interconverts between an inactive GDP-bound form and an active GTP-bound form in response to insulin. In this regard, a recent study has shown that ARF6 cycles between the plasma membrane and a novel internal membrane compartment in HeLa cells (Radhakrishna *et al.*, 1997). It should be noted however, that the subcellular fractionation immunoblots (Figures 5.2 and 5.3) did not reveal any significant change in ARF6 subcellular distribution in response to insulin. One plausible explanation for this finding is that the membrane compartments between which ARF6 cycles in response to insulin, may be isolated in the same fraction by the fractionation procedure employed in this study. Interestingly, the ARF6-associated membrane compartment in HeLa cells is distinct from the early endosomal compartment containing TfRs (Radhakrishna *et al.*, 1997). Accordingly, it would not be detected as an 'early endosome' in the intracellular membrane fraction, but may be isolated with the plasma membrane under the experimental conditions used in this study. However, further studies are required in order to determine whether such an ARF6-associated internal membrane compartment exists in 3T3-L1 adipocytes.

There is an accumulating body of evidence which proposes a role for PLD as a downstream effector of ARF in regulated secretion (see for example Stutchfield *et al.*, 1993; Ktistakis *et al.*, 1996; Chen *et al.*, 1997b). With this in mind, I wished to identify which PLD isoforms are expressed in 3T3-L1 adipocytes, and determine whether PLD activity plays a role in insulin-stimulated GLUT4 translocation. Using antibodies for PLD1 and PLD2, I showed that both these isoforms are expressed in 3T3-L1 adipocytes, and are both localised to the intracellular (LDM) membrane fraction (Figure 5.7). In the case of PLD1, this observation is consistent with the

localisation of PLD1 activity to intracellular membranes thought to be involved in ARF-regulated vesicular budding and secretion (Chen *et al.*, 1997b; Ktistakis *et al.*, 1996; Fensome *et al.*, 1996). However, although PLD2 has been localised to the plasma membrane in overexpression studies (Colley *et al.*, 1997), there is little data on the location of endogenous PLD2 as relatively few cell types or tissues have been examined in this regard. Indeed, to my knowledge this is the first terminally differentiated, growth arrested cellular context in which PLD1 and PLD2 distribution has been examined. As neither of the isoforms exhibited an insulin-dependent redistribution to the plasma membrane it seems improbable that ARF6 may regulate PLD activity at the cell surface in response to insulin. In collaboration with M.J.O Wakelam (University of Birmingham), we have been unable to effectively assay PLD activity in 3T3-L1 adipocytes, probably due to the high level of lipid in these cells interfering with the lipid micellar structures required for PLD assays in broken cells. However, it is tempting to speculate that these PLD isoforms may act as downstream effectors of ARF isoforms localised to the intracellular membranes in these cells.

To determine whether PLD may be involved in insulin-stimulated GLUT4 translocation we used the primary alcohol, butan-1-ol, to divert the production of phosphatidic acid to phosphatidylbutan-1-ol, previously shown to inhibit PLD activity (Cook *et al.*, 1991). Here I have shown that even at concentrations known to inhibit PLD activity (Cook *et al.*, 1991), butan-1-ol has no affect on insulin-stimulated GLUT4 translocation and 2-deoxy-D-glucose transport (Figures 5.8 and 5.9). However, under the same conditions, both the constitutive and insulin-stimulated secretion of adipsin from adipocytes is inhibited by butan-1-ol but not butan-2-ol, a secondary alcohol unable to inhibit the PLD catalysed reaction (Figure 5.11). These data indicate that butan-1-ol is effectively targeting PLD activity within the adipocytes. However, this activity appears to play a role in adipsin secretion but does not appear to be involved in the ability of insulin to recruit GLUT4 to the cell surface.

The data presented in the previous study (refer to Section 4.4.6) suggests that adipsin secretion utilises the recycling endosomal system. The most likely mechanism of secretion would involve the fusion of TGN-derived secretory vesicles with the endosomal network *en route* to the plasma membrane, consistent with a PLD-mediated step. However, although I have also shown GLUT4 to traffic through the TGN in AP-1 positive vesicles (refer to section 5.3.3), the data imply that the insulin-responsive GLUT4 storage compartment does not bud directly from the TGN and therefore inhibition of PLD activity at the TGN will have no effect on insulin-stimulated GLUT4 translocation. Furthermore, recent evidence suggests that the recruitment of AP-1 adaptors onto the TGN does not involve PLD activity even though AP-1 recruitment is ARF-mediated (West *et al.*, 1997). Thus, inhibition of PLD activity localised to the TGN would effectively block adipsin secretion but not insulin-stimulated GLUT4 translocation.

In summary therefore, I have shown that the introduction of myristoylated ARF6 peptides inhibits both insulin-stimulated GLUT4 translocation and glucose transport in 3T3-L1 adipocytes. On the basis of these and other data, I propose that ARF6 plays a crucial role in the regulated exocytosis of GLUT4 in response to insulin. In the view of the current proposed functions for ARF proteins in vesicular traffic, it is tempting to speculate that ARF6 facilitates fusogenic events at the plasma membrane in response to insulin.

Chapter 6

Construction of an ssHRP Chimera for Compartment Ablation Analysis in 3T3-L1 Adipocytes

6.1 Aims

1. To construct a chimeric cDNA comprising the human growth hormone signal sequence (sshGH) fused in frame at the N-terminus of horseradish peroxidase (HRP).

2. To subclone the ssHRP chimera into a suitable vector for high-level expression in mammalian cells.

3. To establish stable 3T3-L1 adipocyte cell lines expressing the ssHRP protein.

4. To use the expression of this protein in conjunction with DAB-cytochemistry to carry out compartment ablation analysis in 3T3-L1 adipocytes.

6.2 Introduction

In a previous study (refer to Chapter 4) I used a transferrin-horseradish peroxidase (Tf-HRP) conjugate in combination with DAB-cytochemistry to selectively target trafficking through the recycling endosomal system. In addition to defining the constitutive recycling pathway, HRP probes may also be used to target other trafficking pathways. By coupling targeting signals from other proteins to HRP, intracellular pathways which cannot be readily accessed from the cell surface can be examined. In this regard, a secretory form of peroxidase comprising the signal sequence of the human growth hormone and HRP (ssHRP) has previously been used as a probe for the exocytic pathway (Connolly *et al.*, 1994). Upon expression of the chimeric protein in mammalian cells, HRP was shown to be active from the earliest part of the secretory pathway and was efficiently secreted from the cells via the *trans* cisternae of the Golgi complex, thus acting as an excellent tracer for the exocytic pathway (Connolly *et al.*, 1994).

I have previously shown GLUT4 to extensively co-localise with γ-adaptin and the CD-M6PR within the TGN region of 3T3-L1 adipocytes (refer to Chapter 3), suggesting that this membrane sorting compartment plays an important role in GLUT4 trafficking. To further investigate the role of the TGN in this regard, I set out to construct an ssHRP chimeric protein with the intention of targeting this protein to the exocytic pathway in 3T3-L1 adipocytes. Blocking the secretion of ssHRP from the TGN by incubating the cells at 20°C (Connolly *et al.*, 1994) would enable me to disrupt trafficking through this compartment using HRP-mediated ablation analysis (refer to Section 3.2), thus allowingmes to investigate the role of the TGN in GLUT4 trafficking.

In the present study, I show that ssHRP may be targeted to the exocytic pathway and efficiently secreted from 3T3-L1 adipocytes. Furthermore, I demonstrate that the secretion of the HRP from the cells may be stimulated by insulin. However,

preliminary ablation studies of the TGN did not show a change in the level of TGN38 in the intracellular (LDM) membranes, suggesting that the technique adopted needs to be optimised before it may be employed to study the role of the TGN in GLUT4 trafficking.

6.3 Materials and Methods

6.3.1 Construction of pOP13.ssHRP.aP2

DNA manipulations were carried out by standard procedures as described in Materials and Methods (refer to Chapter 2).

I obtained the HRP cDNA as an engineered gene from *Armoracia rusticana* cloned between the *Hind* III and *Eco* R1 sites in the polylinker of pUC19. To enable entry into the secretory pathway, the signal sequence from human growth hormone (Hall *et al.*, 1990) was added. The signal sequence was removed from the polylinker site of pMTL22p (Chambers *et al.*, 1988) where it had been inserted as a *Bam* HI-*Hind* III fragment to produce pEKSP. To construct the ssHRP chimera, the sshGH fragment was excised from pEKSP with *Bam* HI-*Hind* III and inserted into the multiple cloning site of pGEM-7Zf(+)® (Promega) linearised with *Bam* HI-*Hind* III. The DNA encoding HRP was excised by *Hind*III-*Eco*RI from pUC19, and ligated downstream of the sshGH into the *Hind* III-*Eco* RI sites of pGEM-7Zf(+)®. As shown in Figure 6.2, the ssHRP construct was subsequently excised by *Bam* HI from pGEM-7Zf(+) and subcloned into the polylinker site of the shuttle vector pNotNot (a pGEM11z and pBluescript polylinker fusion kindly provided by Professor K. Siddle, University of Cambridge) (Figure 6.2) cut with *Bam* HI from which the chimera could be subcloned into a suitable mammalian expression vector.

pOP13CAT.aP2 was chosen as a suitable expression vector for transfection into 3T3-L1 adipocytes as the aP2 element has been shown to function as an adipocyte

specific promoter (Graves *et al.*, 1992). ssHRP cDNA was excised from pNotNot by *Not* I and inserted into pOP13CAT.aP2 following the removal of the CAT reporter gene using *Not* I (Figure 6.2). The plasmid DNA was digested to ensure that the cDNA was inserted in the correct orientation (Figure 6.3).

6.3.2 Calcium Phosphate Transfection of 3T3-L1 Fibroblasts and Selection of Stable Transfectants

The method of transfection used was calcium phosphate precipitation, a procedure which is especially suitable for fibroblastic cell lines. The transfection mixture outlined below was sufficient to transfect one 10cm plate of cells which were seeded to be approximately (but no more than) 50% confluent at the time of transfection.

3-4 h prior to transfection the media was changed and the cells were incubated at 37°C in a humidified atmosphere of 10 % CO_2. 3 h after the media change, the transfection mixture was prepared by adding 36µl of 2M $CaCl_2$ and 10 or 20µg of DNA made up to 300µl with sterile water, to a 10ml polypropylene tube. 300µl of HEPEs Buffered Saline (HBS) was added to a separate tube and the $CaCl_2$-DNA mixture was added dropwise (over 2 min) using a pasteur pipette to the HBS, while bubbling air through the HBS with another pipette. This resulted in the formation of a fine precipitate which was incubated at room temperature for 30 min before being added dropwise to the cells. The cells were then incubated at 37°C in a humidified atmosphere of 10% CO_2 for a further 48 h.

Subsequent selection was then carried out by replacing the media with fresh DMEM/10% (v/v) newborn calf serum, 1% (v/v) penicillin and streptomycin containing G418 (500µg/ml) as the selection antibiotic. Selection was maintained for 2-3 weeks with frequent media changes changes to eliminate dead cells and was continued until discrete colonies could be visualised. Individual colonies were then

trypsinised using cloning rings and transferred to 6cm plates for subsequent propagation.

6.3.3 HRP Assay

To measure the release of HRP activity into the media, transfected or wild type 3T3-L1 adipocytes cultured on 6-well plates were incubated for 2 h at 20°C in external solution ([ES] 140mM NaCl, 5mM KCl, 2mM $CaCl_2$, 1mM $MgCl_2$, 10mM glucose, 10mM HEPES, pH7.4) to block secretion. After the incubation, the buffer was removed and ES at 37°C was added. Cells were incubated at 37°C and 100µl fractions of ES were collected every 30 min for 2 h. To measure cell-associated HRP activity, cells cultured on 10cm plates were incubated in serum-free DMEM for 2h at 20°C and then rinsed three times in PBS (refer to Section 2.2.1) containing 0.5% BSA. Cells were suspended in 500µl of 50mM Tris/Cl (pH 2.5) and lysed by three cycles of freezing and thawing in liquid nitrogen before being centrifuged in a microfuge for 5 min at 10,000 x g to produce a high speed supernatant.

The assay to measure HRP activity was carried out as described by Connolly *et al* (Connolly *et al.*, 1994). Reactions were carried out in a 96-well microtitre plate. Equal volumes of reagent (250µl of a saturable solution of *o*-phenylene diamine in methanol, 10ml of 100mM sodium citrate / 1% Triton X-100 [pH 5.5)] and 7µl 30% H_2O_2) and sample (ES fractions or supernatant from the above procedures) were added to the microtitre plate and incubated at 37°C in the dark. After 60 min, the reaction was stopped by the addition of 0.5 volumes of 2M HCl. HRP activity released into the media was quantitated by measuring the absorbance at 450nm and is expressed in arbitrary units. Buffer alone (as a negative control) and Tf-HRP loaded cells (as a positive control) were assayed in parallel.

6.3.4 Ablation of the Intracellular (LDM) Membranes using ssHRP

Cells cultured on 10cm plates were incubated in serum-free DMEM for 2 h at 20°C to block protein trafficking through the TGN (Matlin *et al.*, 1983). The cells were transferred onto ice and treated with DAB ± H_2O_2 (Section 3.3.1), incubated at 4°C in the dark for 60 min, washed and the intracellular membranes were prepared as described in Section 3.3.1.

6.3.5 Antibodies

The anti-GLUT4 antibody used for immunoblotting the intracellular (LDM) membranes was a rabbit polyclonal against a peptide comprising the C-terminal 14 amino acid residues of the human isoform of GLUT4 (see Section 2.4). Anti-TGN38 was a generous gift from Dr G. Banting (University of Bristol, UK).

6.4 Results

6.4.1 Restriction Digestion Analysis of pOP13.ssHRP.aP2

The chimeric cDNA of ssHRP was excised from the pNotNot vector as a *Not* I fragment of ~1kb in length. The fragment was subsequently purified and ligated into pOP13.aP2 following the digestion of pOP13CAT.aP2 with *Not* I to remove the CAT reporter gene (Figure 6.2). Following the transformation of competent *E. coli* cells, individual clones were screened by digestion with *Not* I for the presence of the ~ 1kb insert. On selection of positive clones, restriction with *Sma* I and *Kpn* I would yield a fragment ~ 1.5kb in length if in the correct orientation as shown in Figure 6.3, or a smaller fragment ~ 0.5kb in length if in the incorrect orientation.

6.4.2 Secretion of HRP from 3T3-L1 Adipocytes and the Effect of Insulin

To target HRP to the exocytic pathway in 3T3-L1 adipocytes, I constructed a chimeric cDNA comprising the signal sequence of the human growth hormone attached to the amino terminus of HRP (Figure 6.1). This chimeric cDNA ssHRP, was then cloned into a suitable mammalian expression vector to create pOP13.ssHRP.aP2 (Figure 6.2) and transfected into 3T3-L1 fibroblasts.

I then attempted to establish stable lines of 3T3-L1 adipocyte cells expressing ssHRP. This was successful, although the extent of differentiation varied between the cell lines. Initially, cells were screened for ssHRP expression by measuring the activity of cell-associated HRP activity (refer to Section 6.3.3). In preliminary studies I found that HRP activity was barely detectable when cells were incubated at 37°C. I therefore reduced the incubation temperature to 20°C to block trafficking through the TGN and induce an increase in the level of intracellular HRP. Figure 6.4 illustrates the level of cell-associated HRP activity of two pOP13.ssHRP.aP2 clones referred to as SS-2 and SS-3, compared to wild type 3T3-L1 adipocytes. The difference in the levels of cell-associated HRP activity exhibited by SS-2 and SS-3 is most likely a function of the level of expression exhibited by the individual clones. However, it should be noted that such a difference in cell-associated activity may also be a reflection of the extent of differentiation. In each passage, the SS-3 cell line consistently produced a uniform lawn of cells, whereas the SS-2 cell line was noticably more patchy upon differentiation.

To test if the ssHRP was entering the exocytic pathway, I investigated whether the HRP activity was efficiently secreted from the 3T3-L1 adipocytes by assaying for enzyme activity in the medium. As before, to increase the level of detectable HRP activity secreted into the medium, the cells were incubated at 20°C to allow HRP activity to accumulate within the cell before being released at 37°C. As shown in Figure 6.5A and B, HRP activity is secreted from both basal (non-stimulated) SS-2 and SS-3 cell lines, indicating that the ssHRP chimera has been targeted to the

constitutive secretory pathway in 3T3-L1 adipocytes. Consistent with the cell-association data, the SS-3 clone exhibited a much higher level of secretion than the SS-2 clone. Upon exposure to insulin, both cell lines exhibited an increase in the secretion of HRP activity, consistent with the insulin-stimulated secretion of adipsin in 3T3-L1 adipocytes (refer to Section 5.4.5).

6.4.3 Ablation of Intracellular (LDM) Membranes using ssHRP

Having established stable cell lines of 3T3-L1 adipocytes in which HRP activity is present within the secretory pathway, I wished to use the peroxidase probe to ablate the TGN compartment within these cells. To do this I incubated SS-2 and SS-3 adipocytes at 20°C for 2 h in order to allow HRP activity to accumulate within the TGN. I then exposed the cells to DAB ± H_2O_2 as described in Section 3.3.1. To determine whether the TGN was effectively ablated under these conditions, I immunoblotted the intracellular (LDM) membranes of the cells for the presence of a putative TGN marker, TGN38. As shown in Figure 6.6, there was no significant change in the immunoreactivity of the TGN marker following ablation of either of the cell lines, indicating that the experimental conditions employed did not result in ablation of the TGN. In addition, I also immunoblotted the samples for GLUT4. No significant change was observed in the immunoreactivity of this protein in the presence of H_2O_2.

Figure 6.1
Structure of ssHRP

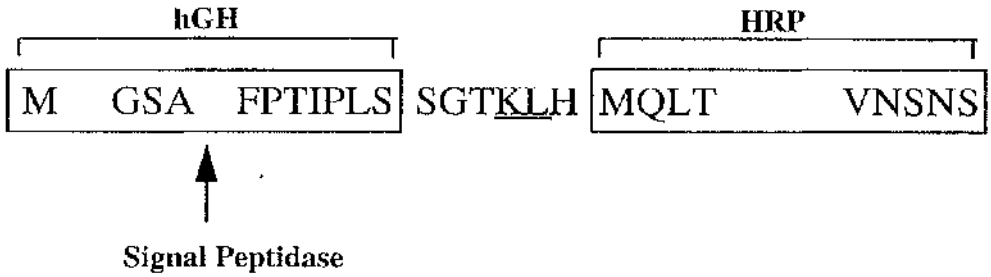

This figure shows the elements of the ssHRP construct used in this study. Boxed sequences are the main components (hGH, human growth hormone); KL indicates the site of fusion of hGH to the N-terminus of HRP. The predicted site of signal peptidase cleavage is shown.

Figure 6.2

Construction of pOP13.ssHRP.aP2

pOP13CAT.aP2 was chosen as a suitable expression vector for transfection into 3T3-L1 adipocytes as the aP2 element has been shown to function as an adipocyte specific promoter (Graves *et al.*, 1992). The ssHRP construct was excised by *Bam* HI from pGEM-7Zf(+)® and subcloned into the polylinker site of the shuttle vector pNotNot (a pGEM11z and pBluescript polylinker fusion) cut with *Bam* HI. ssHRP cDNA was excised from pNotNot by *Not* I and inserted into pOP13CAT.aP2 following the removal of the CAT reporter gene using *Not* I.

Figure 6.2

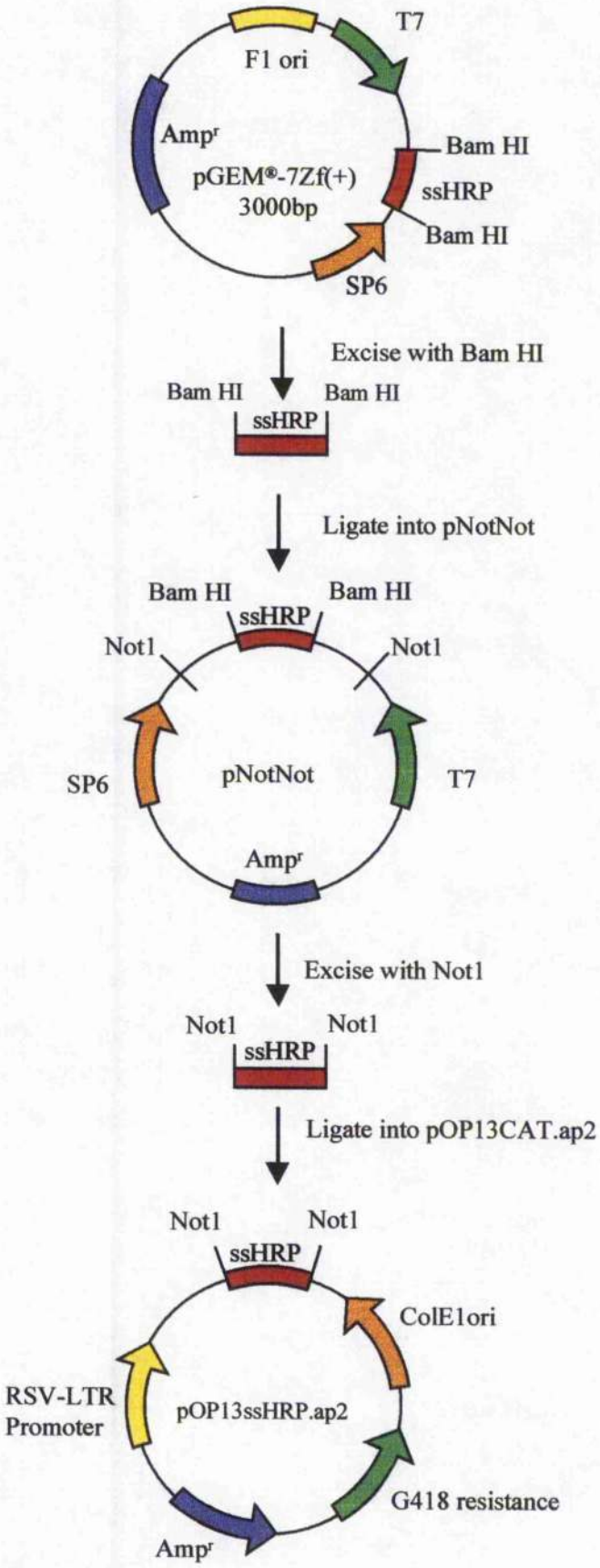
T7
F1 ori
Amp^r
Bam HI
pGEM®-7Zf(+)
3000bp
ssHRP
Bam HI
SP6
Excise with Bam HI
Bam HI
Bam HI
ssHRP
Ligate into pNotNot
Bam HI
Bam HI
ssHRP
Not1
Not1
SP6
pNotNot
T7
Amp^r
Excise with Not1
Not1
Not1
ssHRP
Ligate into pOP13CAT.ap2
Not1
Not1
ssHRP
ColE1ori
RSV-LTR
Promoter
pOP13ssHRP.ap2
G418 resistance
Amp^r

Figure 6.3

Restriction Digestion Analysis of the pOP13.ssHRP.aP2 Construct

Following the transformation of competent *E. coli* cells, individual clones were screened by digestion with *Not* I for the presence of the ~ 1kb insert. In order to determine whether the chimeric cDNA was inserted into the vector in the correct orientation, the positive clones were subjected to restriction digestion analysis. Restriction with *Sma* I and *Kpn* I would yield a fragment ~ 1.5kb in length if in the correct orientation or a smaller fragment ~ 0.5kb in length if in the incorrect orientation.

Figure 6.3

Correct Orientation

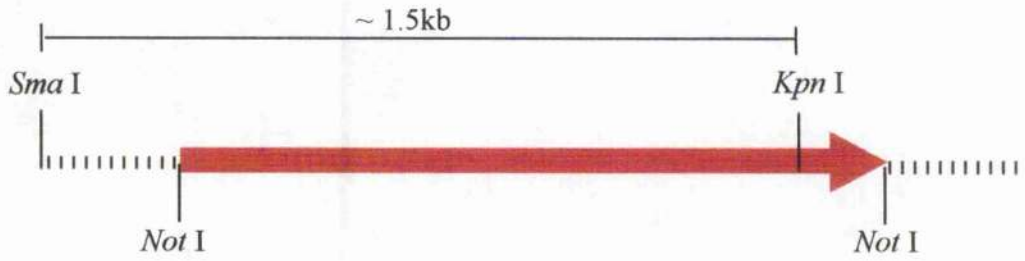

Incorrect Orientation

Figure 6.4

Cell-Associated HRP Activity of SS-2 and SS-3 Adipocytes

Transfected (SS-2 and SS-3) or wild type 3T3-L1 adipocytes cultured on 10cm plates were incubated in serum-free DMEM for 2h at 20°C and then rinsed three times in PBS containing 0.5% BSA. Cells were suspended in Tris/Cl, lysed and centrifuged to produce a high speed supernatant as described in *Materials and Methods*. HRP activity in the supernatant was assayed as described. As the cell-associated HRP activity was only measured for the purpose of screening the individual clones, this experiment was only carried out once for each cell line.

Figure 6.4

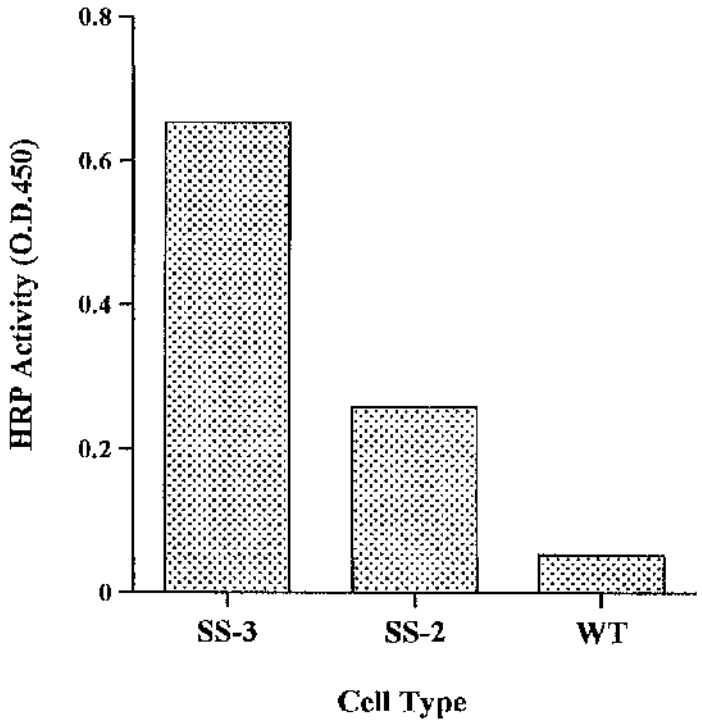

Figure 6.5

Secretion of HRP Activity from SS-2 and SS-3 Adipocytes

Duplicate wells of SS-2 (**A**) and SS-3 or wild type (WT) (**B**) 3T3-L1 adipocytes were incubated in ES buffer for 2 h at 20°C. Cells were then incubated in fresh ES buffer with or without insulin at 37°C. Secreted HRP activity was assayed as described in *Materials and Methods*. In each case, the data shown are of a representative experiment (n = 2).

Figure 6.5A

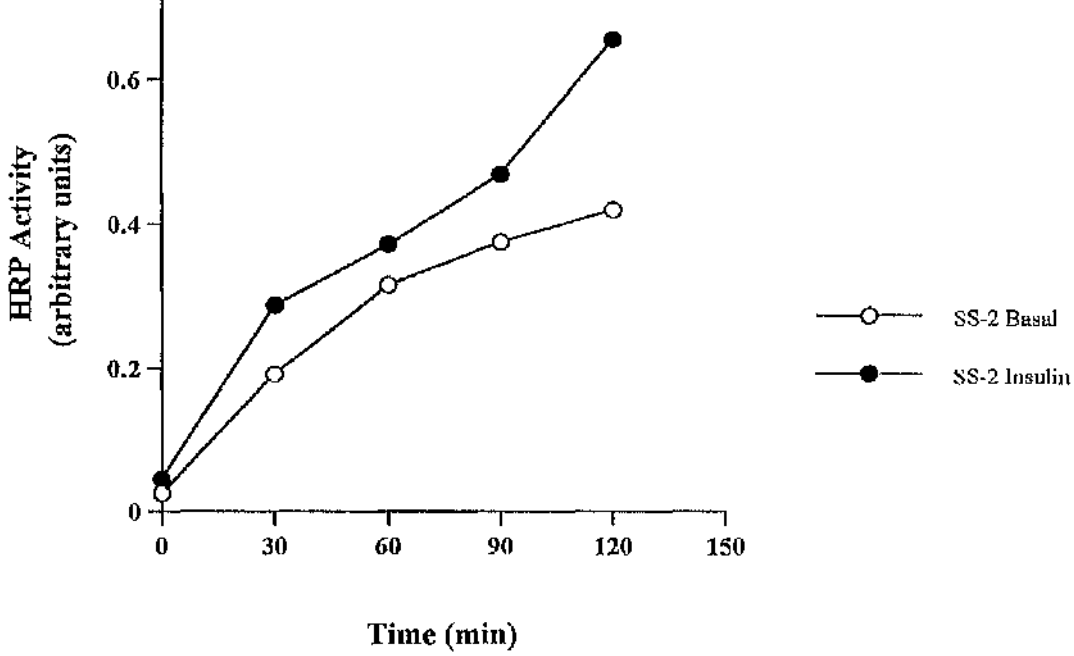
0.8
0.6
0.4
0.2
0
HRP Activity
(arbitrary units)
0
30
60
90
120
150
Time (min)
SS-2 Basal
SS-2 Insulin

Figure 6.5B

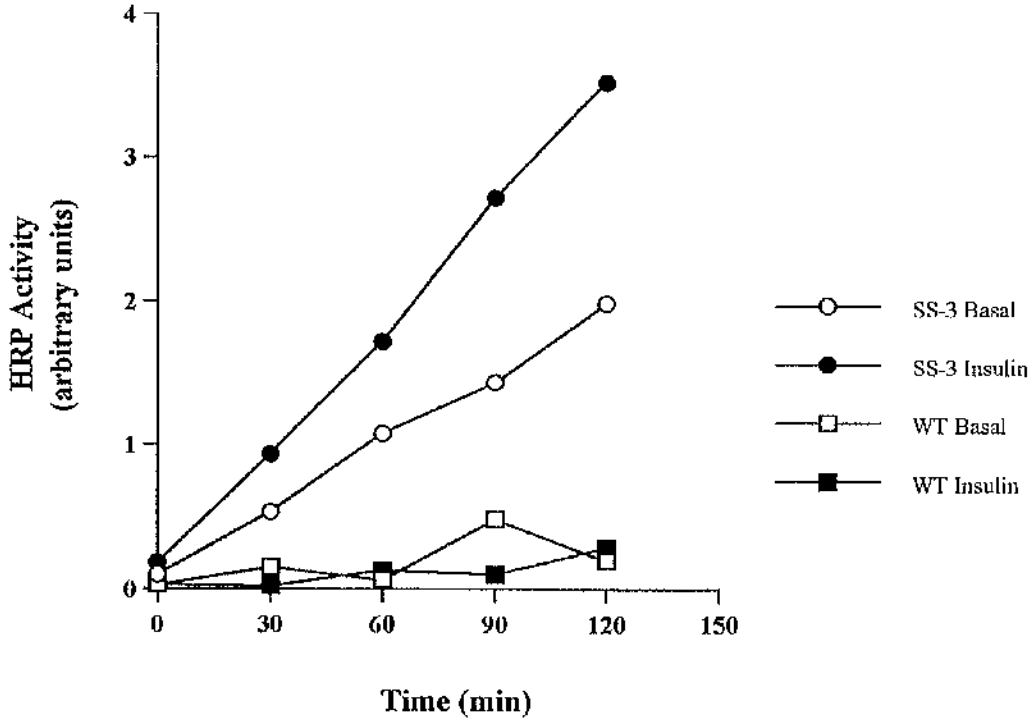
HRP Activity
(arbitrary units)
4
3
2
1
0
0
30
60
90
120
150
Time (min)
SS-3 Basal
SS-3 Insulin
WT Basal
WT Insulin

Figure 6.6

Ablation of Intracellular (LDM) Membranes using ssHRP

Duplicate plates of SS-2 and SS-3 adipocytes were incubated with DAB ± H_2O_2 as described. Intracellular (LDM) membrane fractions were prepared and subjected to SDS-PAGE (20μg/lane), electrophoretically transferred to nitrocellulose membranes, and immunoblotted with the antibodies indicated. The immunoblots were developed using ECL. The effect of ablation was determined by comparison of the signals in the - and + lanes. It should be noted that due to time constriants n = 1.

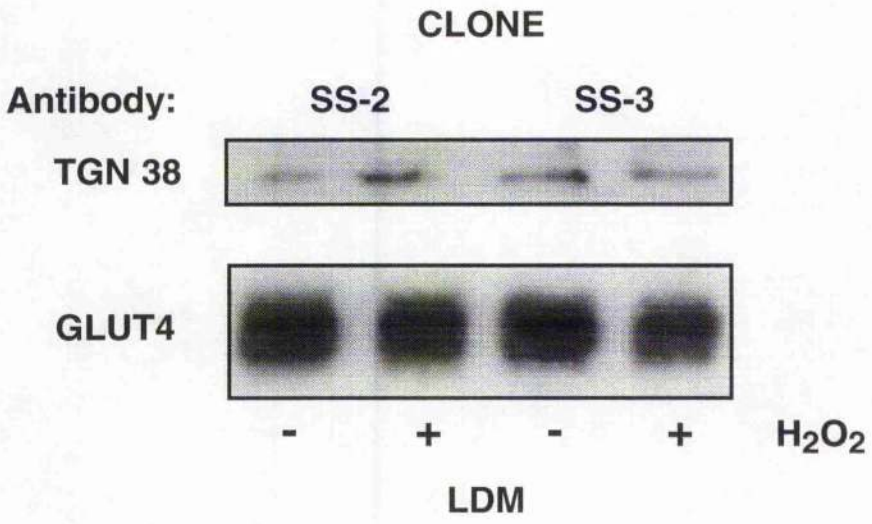
CLONE
Antibody:
SS-2
SS-3
TGN 38
GLUT4
-
+
-
+
H_2O_2
LDM

6.5 Discussion

In previous studies (refer to Chapters 3 and 4) we exploited the ability of HRP in the presence of DAB and H_2O_2, to render co-localised proteins insoluble in the endocytic pathway. This ablation technique proved to be extremely useful for quantitative studies of protein distribution between intracellular compartments within 3T3-L1 adipocytes. In this regard, we observed GLUT4 to co-localise with TGN specific markers, γ-adaptin and the CD-M6PR, suggesting that GLUT4 traffics through this membrane sorting compartment.

As an attempt to investigate the role of the TGN in GLUT4 trafficking, we wished to further exploit this ablation technique by targeting an HRP probe to the exocytic pathway in 3T3-L1 adipocytes. To do this, we set about constructing a cDNA chimera comprising the human growth hormone signal sequence fused in frame to the N-terminus of HRP (Figure 6.1). By doing so, we wished to establish stable 3T3-L1 adipocyte cell lines in which a chimeric protein, ssHRP, would be targeted to the exocytic system.

As a first step to determine whether the antibiotic selected cell lines expressed HRP activity, we initially screened the cell lines by measuring the cell-associated HRP activity. Due to low levels of detectable HRP activity in preliminary studies, we carried out a temperature block at 20°C to allow the HRP to accumulate within the intracellular membranes. This resulted in the identification of two cell lines, referred to as SS-2 and SS-3, both of which expressed HRP activity compared to wild type 3T3-L1 adipocytes (Figure 6.4). The level of HRP activity observed in the SS-3 cell line was much higher than that of SS-2, suggesting a higher level of expression in the SS-3 cells. However, it should be noted that the extent of differentiation was much poorer in the case of the SS-2 cell line, which may also result in a lower level of HRP activity.

Next, to determine whether the ssHRP was entering the exocytic pathway in 3T3-L1 adipocytes, we measured the HRP activity secreted from the cells into the medium. Preliminary studies showed both basal (non-stimulated) SS-2 and SS-3 adipocytes to secrete HRP into the medium, consistent with the targeting of the protein to the constitutive secretory pathway within these cells (Figure 6.5A and B). Furthermore, both cell lines exhibited an increase in HRP secretion in response to insulin. This data is consistent with the insulin-stimulated release of adipsin, a soluble protein which is also constitutively secreted from 3T3-L1 adipocytes (Kitagawa *et al.*, 1989). However, further studies are required to compare the time course of insulin-stimulated adipsin release with that for insulin-stimulated HRP release.

The expression of such a protein in several other mammalian cell lines has shown that the HRP is active from the beginning of the secretory pathway (Connolly *et al.*, 1994). Furthermore, morphological studies on these cells have shown that it is possible to load the *trans* side of the Golgi stack with this activity by incubating the cells at 20°C. The accumulation of HRP activity is thought to result as at 20°C trafficking is blocked from the TGN, but the processes which concentrate secretory product still operate within compartments proximal to this block (Connolly *et al.*, 1994). With this in mind, we set out to attempt to ablate the TGN of 3T3-L1 adipocytes. Initially, we incubated SS-2 and SS-3 adipocytes at 20°C for 2 h in order to allow the accumulation of HRP activity within the TGN before exposing the cells to DAB and H_2O_2. Under these conditions, proteins localised to the TGN should be rendered 'insoluble' and therefore quantitatively ablated upon immunoblot analysis of the intracellular (LDM) membranes. However, as shown in Figure 6.6, there was no significant difference in either cell line in the immunoreactivity of the TGN38 in the presence of H_2O_2, suggesting that the experimental conditions employed in this preliminary study did not result in the ablation of the TGN.

In these initial experiments, the procedure for HRP-mediated ablation was performed as described for the ablation of the endosomal system (refer to Section 3.3.1).

However, from this data it is apparent that the conditions under which ssHRP-mediated ablation of the TGN is carried out need to be optimised. In this regard, we need to determine the conditions required for the accumulation of ssHRP in the TGN in terms of the incubation period at 20°C. This may be achieved by determining the amount of ssHRP localised to TGN38 vesicles immunoadsorbed from the intracellular membranes of cells incubated at 20°C for varying periods of time. In addition, as the TGN is likely to be a much more restricted compartment than the endosomes loaded with Tf-HRP, it is possible that in order to target this compartment with DAB and H_2O_2, higher concentrations of these reagents may be required for the disruption of the TGN function in a manner analagous to that performed using Tf-HRP. However, due to the time constraints of this work I was unable to pursue such studies.

In summary, we have established stable cell lines of 3T3-L1 adipocytes expressing an ssHRP chimeric protein which is targeted to the exocytic pathway within these cells. However, the experimental conditions required to exploit this protein for ssHRP-mediated ablation of the TGN have yet to be optimised.

6.6 Future Work

Unfortunately, due to the time constraints of this work we were unable to exploit the compartment ablation technique to further investigate the role of the TGN in GLUT4 trafficking. In this regard, it would be of interest to examine insulin-stimulated GLUT4 translocation following the disruption of the TGN. In addition, by studying the re-internalisation and / or intracellular distribution of GLUT4 upon insulin withdrawl, following the disruption of the TGN, it may be possible to determine whether the TGN is required for the sorting of GLUT4 into the post-endocytic storage compartment. However, the ability to carry out such experiments will depend on the optimisation of the conditions required for ssHRP-mediated ablation of the TGN.

Chapter 7

Overview

In the post-prandial state, high levels of circulating blood glucose induce the release of insulin from the pancreas. In turn, insulin stimulates the disposal of glucose from the circulation into the peripheral tissues, fat and muscle. It is well established that the rapid increase in glucose uptake into these cells in response to insulin is due to the translocation of a pool of intracellular glucose transporters (GLUT4) to the cell surface. Defects in glucose uptake into these peripheral tissues have a profound effect on whole body glucose homeostasis, leading to insulin resistance, such as is observed in individuals with diabetes. A potential defect in this system is the impairment of GLUT4 translocation in response to insulin. Such a defect may arise due to defective insulin signalling to the intracellular GLUT4 pool, abnormalities in the GLUT4 trafficking machinery or mistargeting of GLUT4 within the cells intracellular compartments. Thus, it is important that we gain further insight into the nature of the GLUT4 intracellular compartment(s) and the mechanism of GLUT4 translocation to the cell surface in response to insulin.

Recently, several independent studies have indicated that GLUT4 resides within at least two distinct intracellular compartments in adipocytes, one of which is endosomal, the other a non-ablatable post-endocytic compartment (Livingstone *et al.*, 1996; Martin *et al.*, 1996; Malide *et al.*, 1997a). It is thought that this non-ablatable post-endocytic compartment represents the insulin-responsive GLUT4 pool. However, to date the nature of this compartment remains poorly defined. With this in mind, I wished to elucidate the protein composition of the non-ablatable GLUT4 storage compartment in the expectation that this may further our understanding of the relationship of this compartment with other, well established, intracellular compartments. Using endosomal ablation analysis in combination with several other techniques, I have provided further evidence for the segregation of GLUT4 between the recycling endosomal system, enriched in cell surface to endosome recycling markers such as the TfR and SCAMPs, and a non-ablatable post-endocytic compartment. The observation that syntaxin 4 co-localised with GLUT4 in the latter compartment suggests that this t-SNARE may be involved in

GLUT4 trafficking at an intracellular level. In addition, I found GLUT4 to co-localise with two distinct TGN markers; the γ-adaptin subunit of the TGN-specific adaptor complex AP-1 and the CD-M6PR which recycles between the TGN and endosomal compartments. These data suggest that the GLUT4 trafficking pathway in basal 3T3-L1 adipocytes includes trafficking through the TGN in AP-1 coated vesicles. However, as these vesicles also contain a significant proportion of the CD-M6PR it is unlikely that they fuse directly with the cell surface, but rather recycle back as far as the TGN before GLUT4 is withdrawn from the endosomal system into the post-endocytic storage compartment.

The observation that several of the components of the insulin-regulatable trafficking machinery are indeed homologous if not indentical to the molecules used for SSV exocytosis in neurons, suggests that vesicles from the GLUT4 storage compartment have the potential to dock and fuse directly with the cell surface in response to insulin. In an effort to address this issue, I used endosomal ablation to examine the translocation of GLUT4 from the endosomal and non-ablatable post-endocytic compartments to the cell surface in response to insulin. Initial studies showed insulin to stimulate GLUT4 translocation following the disruption of trafficking through the endosomal system, suggesting that GLUT4 vesicles derived from the post-endocytic storage compartment may indeed fuse directly with the plasma membrane. However, further studies indicated that under the experimental conditions used in this study recycling through a re-formed endosomal system was possible. Thus, endosomal ablation analysis did not provide definitive evidence for the translocation of GLUT4 from the post-endocytic compartment to the plasma membrane independently of the endosomal system. Under the same conditions, however, I found GTPγS-stimulated GLUT4 translocation to be inhibited. In addition I observed both insulin and GTPγS-stimulated GLUT1 translocation to be inhibited following ablation of the recycling endosmal system. Together these data suggest that insulin stimulates the exocytosis of GLUT4 from two distinct

compartments, one being the post-endocytic storage compartment and the other being the endosomal system,which may also be stimulated by GTPγS.

Recent studies have implicated ARF proteins as key components of the regulated exocytotic machinery in endocrine cells (Chen *et al.*, 1996; Galas *et al.*, 1997). As insulin-stimulated GLUT4 translocation exhibits many similarities to regulated secretion in neuroendocrine and endocrine cells, I set out to investigate whether ARF proteins may also be an important component of the GLUT4 trafficking machinery. By introducing myristoylated N-terminus ARF1, 5 or 6 peptides into α-toxin permeabilised 3T3-L1 adipocytes, I found that the ARF6 peptide markedly inhibited insulin-stimulated GLUT4 translocation and glucose transport, whereas the ARF5 and ARF1 peptides were without effect. These results suggest that ARF6 plays a crucial role in insulin-stimulated GLUT4 translocation, consistent with a general role for this small GTP-binding protein in regulated exocytosis. In addition, I investigated the role of PLD in insulin-stimulated GLUT4 translocation, as this enzyme has recently been shown to act as a downstream effector of ARF in regulated secretory events (Stutchfield *et al.*, 1993; Ktistakis *et al.*, 1996; Chen *et al.*, 1997b). However butan-1-ol, an effective inhibitor of PLD activity, had no effect on insulin-stimulated GLUT4 translocation or glucose transport, suggesting that PLD does not function as a downstream effector of ARF in this event.

Finally, the observation that GLUT4 traffics through the TGN (see above), prompted me to construct a chimeric cDNA comprising the signal sequence of the human growth hormone and HRP (ssHRP) with the intention of targeting the resultant protein to the exocytic pathway in 3T3-L1 adipocytes. By doing so,Ie wished to further examine the role of the TGN in GLUT4 trafficking by disrupting trafficking through this sorting compartment by HRP-mediated ablation. However, although I established several stable cell lines expressing ssHRP activity which was constitutively secreted from the cells, I was unable to demonstrate that such a technique may be employed to ablate the TGN.

References

Allard, W.J., Lienhard, G.E. and Lodish, H.F. (1985) Science 229, 941-945

Alvarez, J., Lee, D.C., Baldwin, S.A. and Chapman, D. (1987) J. Biol. Chem. **262**, 3502-3509

Araki, E., Lipes, M.A., Patti, M.E., Bruning, J.C., Haag, B., Johnson, R.S. and Kahn, C.R. (1994) Nature **372**, 186-190

Araki, S., Tamori, Y., Kawanishi, M., Shinoda, H., Masuga, J., Mori, H., Niki, T., Okazawa, H., Kubota, T. and Kasuga, M. (1997) Biochem. Biophys. Research Comm. **234**, 257-262

Austin, C.D. and Shields, D. (1996) J. Cell Biol. **135**, 1471-1483

Baldini, G., Hohman, R., Charron, M.J. and Lodish, H.F. (1991) J. Biol. Chem. **266**, 4037-4040

Baldwin, S.A. (1987) Biochem. Biophys. Acta. **905**, 295-310

Baldwin, S.A. (1993) Biochem. Biophys. Acta 1154, 17-49

Bell, G.I., Burant, C.F., Takeda, J. and Gould, G.W. (1993) J. Biol. Chem. **268**, 19161-19164

Bennett, M.K. (1995) Curr. Opin. Cell Biol. **7**, 581-586

Biber, J.W. and Lienhard, G.E. (1986) J. Biol. Chem. **261**, 16180-16184

Birnbaum, M.J. (1989) Cell **57**, 305-315

Boll., W., Gallusser., and Kirchausen, T., (1995) Curr. Biol. **5**, 1168-1178

Boman, A.L. and Kahn, R.A. (1995) TIBS **20**, 147-150

Bottger, G., Nagelkerken, B. and Van Der Sluijs, P. (1996) J. Biol. Chem. **271**, 29191-29197

Brant, A.M., Jess, T.J., Milligan, G., Brown, C.M. and Gould, G.W. (1993) Biochem. Biophys. Res. Comm. **192**, 1297-1302

Brown, H.A., Gutowski, S., Moomaw, C.R., Slaughter, C. and Sternweiss, P.C. (1993) Cell **75**, 1137-1144

Bruning, J.C., Winnay, J., Bonner-weir, S., Taylor, S.I., Accili, D. and Kahn, C.R. (1997) Cell **21**, 561-572

Burant, C.F., Takeda, J., Brot-Laroche, E., Bell, G.I. and Davidson, N.O. J. Biol. Chem. **267**, 14523-14526

Burgering, M. and Coffer, P. (1995) Nature **376**, 599-602

Cain, C.C., Trimble, W.S. and Lienhard, G.E. (1992) J. Biol. Chem. **267**, 11681-11684

Cairns, M.T., Alvarez, J., Panico, M., Gibbs, A.F., Morris, H.R., Chapman, D. and Chin, J. J., Jung, E.K.Y. and Jung, C.Y. (1986) J. Biol. Chem. **261**, 7101-7104

Calderhead, D.M., Kitagawa, K., Tanner, L.I., Holman, G.D. and Lienhard, G.E. (1990) J. Biol. Chem. **265**, 13800-13808

Calera, M.R., Martinez, C., Lui, H., Jack, A.K., Birnbaum, M.J. and Pilch, P.F. (1998) J. Biol. Chem. **273**, 7201-7204

Chamberlain, L.H. and Burgoyne, R.D. (1996a) J. Biol. Chem. **271**, 7320-7323

Chamberlain, L.H., Henry, J. and Burgoyne, R.D. (1996b) J. Biol. Chem. **271**, 19514-19517

Chambers, S.P., Prior, S.E., Barstow, D.A. and Minton, N.P. (1988) Gene **68**, 139-149

Chardin, P., Paris, S., Antonny, B., Robineau, S., Beraud-Dufour, S., Jackson, C.L. and Chabre, M. (1996) Nature **384**, 481-484

Charron, M.J., Brosius III, F.C., Alper, S.L. and Lodish, H.F. (1989) Proc. Natl. Acad. Sci. USA **86**, 2535-2539

Cheatham, B., Vlahos, C.J., Cheatham, L., Wang, L., Blenis, J. and Kahn, C.R. (1994) Mol. Cell. Biol. **14**, 4902-4911

Chen, F., Foran, P., Shone, C.C., Foster, K.A., Melling, J. and Dolly, J.O. (1997a) Biochemistry **36**, 5719-5728

Chen, Y. and Shields, D. (1996) J. Biol. Chem. **271**, 5297-5300

Chen, Y.-G., Siddhanta, A., Austin, C.D., Hammond, S.M., Sung, T.-C., Frohman, M.A., Morris, A.J. and Shields, D. (1997b) J. Cell Biol. **138**, 495-504

Clarke, J.F., Young, P.W., Yonezawa, K., Kasuga, M. and Holman, G.D. (1994) Biochem. J. **300**, 631-635

Cockcroft, S., Thomas, G.M.H., Fensome, A., Geny, B., Cunningham, E., Gout, I., Hiles, I., Totty, N.F., Truong, O. and Heuan, J.J. (1994) Science **263**, 523-526

Colley, W.C., Sung, T.-C., Roll, R., Jenco, J., Hammond, S.M., Altshuller, Y., Barsagi, D., Morris, A.J. and Frohman, M.A. (1997) Curr. Biol. **7**, 191-201

Cong, L.N., Chen, H., Li, Y., Zhou, L., McGibbon, M.A., Taylor, S.I. and Quon, M.J. (1997) Mol. Endocrinol. **11**, 1881-1890

Connolly, C.N., Futter, C.E., Gibson, A., Hopkins, C.R. and Cutler, D.F. (1994) J. Cell Biol. **127**, 641-652

Cook, S.J., Briscoe, C.P. and Wakelam, M.J.O. (1991) Biochem. J. **280**, 431-438

Cormont, M., Bortoluzzi. M-N., Gautier, N., Mari, M., Van Obberghen, E. and Le Marchand-Brustel, Y. (1996) Mol. Cell. Biol. **16**, 6879-6886

Cormont, M., Tanti, J.-F., Gremeaux, T., Van Obberghen, E. and Le-Marchand-Brustel, Y. (1991) Endocrinology **129**, 3343-3350

Cormont, M., Tanti, J.F., Zahraoui, A., Van Obberghen, A., Tavatian, A. and Le Marchand-Brustel, Y. (1993) J. Biol. Chem. **268**, 19491-19497

Cosson, P. and Letourner, F. (1997) Current Opinion in Cell Biology **9**, 484-487

Cushman, S.W. and Wardzala, L.J. (1980) J. Biol. Chem. **255**, 4758-4762

D' Souza-Schorey, C., Guangpu, L., Colombo, M.I. and Stahl, P.D. (1995) Science **267**, 1175-1177

Damke, H., Baba, T., Van Der Bliek, A.M. and Schmid, S.L. (1995) J. Cell Biol. **131**, 69-80

Davidson, N.O., Hausman, A.M.L., Ifkovits, C.A., Buse, J.B., Gould, G.W., Burant, C.F. and Bell, G.I. AM. J. Physiol. **262**, C795-C800

Davies, A., Meeran, K., Cairns, M.T. and Baldwin, S.A. J. Biol. Chem. **262**, 9347-9352

Del Vecchio, R.L. and Pilch, P.F. (1991) J. Biol. Chem. **266**, 13278-13283

Dell'Angelica, E., Ohno, H., Eng Ooi, C., Rabinovich, E., Roche, K.W. and Bonifacino, J.S. (1997) EMBO J. **16**, 917-928

Denton, R.M. and Tavare, J.M. (1995) Eur. J. Biochem. **227**, 597-611

Ditte, A.S., Thomas, L., Thomas, G. and Tooze, S.A. (1997) EMBO J. **16**, 4859-4870

Donaldson, J.G., Cassel, D., Kahn, R.A. and Klausner, R.D. (1992) Proc. Natl. Acad. Sci. USA **89**, 6408-6412

Donaldson, J.G. and Klausner, R.D. (1994) Curr. Opin. Cell Biol. **6**, 527-532

Elliot, K.R.F. and Craik, J.D. (1983) Biochem. Soc. Trans.**10**, 12-13

Faundez, V., Horng, J-T. and Kelly, R.B. (1998) Cell **93**, 423-432

Fensome, A., Cunningham, E., Prosser, S., Khoon Tan, S., Swigart, P., Thomas, G., Hsuan, J. and Cockcroft, S. (1996) Curr. Biol. **6**, 730-738

Fischer, Y., Thomas, J., Sevilla, L., Monuz, P., Becker, C., Holman, G., Kozka, I.J., Palacin, M., Testar, X., Kammermeier, H. and Zorzano, A. (1997) J. Biol. Chem. **272**, 7085-7092

Froehner, S.C., Davies, A., Baldwin, S. A. and Lienhard, G.E. (1988) J. Neurocytol. 17, 173-178

Frost, C.S. and Lane, M.D. (1985) J. Biol. Chem. **260**, 2646-2652

Fukumoto, H., Seino, S., Imura, H., Seino, Y., Eddy, R.L., Fukushima, Y., Byers, M.G., Shows, T.B. and Bell, G.I. (1988) Proc. Natl. Acad. Sci. USA **85**, 5434-5438

Fukumoto, H., Kayano, T., Buse, J.B., Edwards, Y., Pilch, P.F., Bell, G.I. and Seino, S. (1989) J. Biol. Chem. **264**, 7776-7779

Fussle, R., Bhakdi, S., Sziegoleit, S., Tranumjensen, J., Kranz, J. and Wellensiek, H. (1981) J. Cell Biol. **91**, 83-94

Galas, M.-C., Helms, J.B., Vitale, N., Thierse, D., Aunis, D. and Bader, M.-F. (1997) J. Biol. Chem. **272**, 2788-2793

Garippa, R.J., Judge, T.W., James, D.E. and McGraw, T.E. (1994) J.Cell Biol. **124**, 705-715

Garvey, W.T., Maianu, L., Zhu, J.-H., Brechtal-Hook, G., Wallace, P. and Baron, A.D. (1998) J. Clin. Invest. **101**, 2377-2386

Gibbs, E.M., Lienhard, G.E. and Gould, G.W. (1988) Biochemistry **27**, 6681-6685

Gould, G.W and Bell, G.I. (1990) Trends Biochem. Sci. **15**, 18-23

Gould. G.W., Thomas, H.M., Jess, T.J. and Bell, G.I. (1991) Biochemistry **30**, 5139-5145

Gould, G.W. and Holman, G.D. (1993) Biochem. J. **295**, 329-341

Gould, G.W. (1997) Facilitative Glucose Transporters R.G. Landes Company

Graves, R.A., Tontonzo, P., Platt, K.A., Ross, S.R. and Spiegelman, B.M. (1992) J. Cell. Biochem. **49**, 219-224

Gruenberg, J. and Maxfield, F.R. (1995) Curr. Opin. Cell Biol. 7, 552-563

Guarnieri, F.G., Arterburn, L.M., Penno, M.B., Cha, Y. and August, J.T. (1993) J. Biol. Chem. **268**, 1941-1946

Hajduch, E., Aledo, J.C., Watts, C. and Hundal, H.S. (1997) Biochem. J. **321**, 233-238

Hajduch, E., Alessi, D.R., Hemmings, B.A. and Hundal, H.S. (1998) Diabetes **47**, 1006-1013

Hall, J., Hazlewood, G.P., Surani, M.A., Hirst, B.H. and Gibert, H.J. (1990) J. Biol. Chem. **265**, 19996-19999

Harrison, J.J.W., Zeidal, M.L., Jo, I. and Hammond, T.G. (1994) J. Biol. Chem. **269**, 11993-12000

Harter, C., Mellman, I. (1992) J. Cell Biol. **117**, 311-325

Haruta, T., Morris, A.J., Rose, D.W., Nelson, J.G., Mueckler, M. and Olefsky, J.M. (1995) J. Biol. Chem. **270**, 27991-27994

Hata, Y., Slaughter, C.A. and Sudhof, T.C. (1993) Nature **366**, 347-351

Hausdorff, S.F., Fingar, D.C. and Birnbaum, M.J. (1997) R.G. Landes Company

Hay, J.C. and Scheller, R.H. (1997) Curr. Opin. Cell Biol. **9**, 505-512

He, W., O'Neill, T.J. and Gustafson, T.A. (1995) J. Biol. Chem. **270**, 23258-23262

Hediger, M.A., Coady, M.J., Ikeda, T.S. and Wright, E.M. (1987) Nature **330**, 379-381

Heilker, R., Manning-Kreig, U., Zuber, J-F. and Spiess, M. (1996) EMBO J. **15**, 2893-2899

Herbst, J.J., Andrews, G.C., Contillo, L.G., Singleton, D.H., Genereux, P.E., Gibbs, E.M. and Lienhard, G.E. (1995) J. Biol. Chem. **270**, 26000-26005

Herman, G.A., Bonzelius, F., Cieutat, A.M. and Kelly, R.B. (1994) Proc. Natl. Acad. Sci. USA **91**, 12750-12754

Hinshaw, J.E. and Schmid, S.L. (1995) Nature **374**, 190-192

Holman, G.D. and Cushman, S.W. (1994a) BioEssays **16**, 753-759

Holman, G.D., Kozka, I.J., Clark, A.E., Flower, A.F., Saltis, J., Habberfield, A.D., Simpson, I.A. and Cushman, S.W. (1990) J. Biol. Chem. **265**, 18172-18179

Holman, G.D., Leggio, L.L. and Cushman, S.W. (1994b) J.Biol.Chem. **269**, 17516-17524

Holman, G.D. and Kasuga, M. (1997) Diabetologia **40**, 991-1003

Honing, S., Griffiths, J., Geüze, H.J. and Hunziker, W. (1996) EMBO J. **15**, 5230-5239

Honing, S., Sosa, M., Hille-Rehfeld, A. and von Figura, K. (1997) J. Biol. Chem. **272**, 19884-19890

Honing, S., Sandoval, I.V. and von Figura, K. (1998) EMBO J. **17**, 1304-1314

Hosaka, M., Toda, K., Takatsu, H., Torii, S., Murakami, K. and Nakayama, K. (1991) J. Biochem. **120**, 813-819

Hresko, S.D., Johnson, J.H., Quadde, C. and Newgard, C.B (1992) Proc. Natl. Acad. Sci. USA **89**, 677-692

Hudson, A.W., Fingar, D.C., Seidner, G.A., Griffiths, G., Burke, B. (1993) J. Cell Biol. **122**, 579-588

Iacopetta, B.J. and Morgan, H.E. (1983) J. Biol. Chem. **258**, 9108-9115

James, D.E., Brown, R., Navarro, J. and Pilch, P.F. (1988) Nature **333**, 183-185

James, D.E., Strube, M. and Mueckler, M. (1989) Nature **338**, 83-87

James, D.E. and Piper, R.C. (1993) J. Cell Sci. **104**, 607-612

James, D.E., Piper, R.C. and Slot, J.W. (1994) Trends Cell Biol. **4**, 120-126

Jhun, B.H., Rampal, A.L., Liu, H., Lachaal, M. and Jung, C.Y. (1992) J. Biol. Chem. **267**, 17710-17715

Johnson, K.F. and Kornfield, S. (1992) J. Cell. Biol. **119**, 249-257

Johnston, P.A. and Sudhof, T.C. (1990) J. Biol. Chem. **265**, 8869-8873

Kaback, H.R. (1996) The Lactose permease of *Escherichia coli*: an update. New York, Plenum Press

Kaburagi, Y., Satoh, S., Tamemoto, H., Yamamoto-Honda, R., Tobe, K., Veki, S.W., Yamauchi, T., Kono-sugita, E., Sekihara, H., Aizawa, S., Cushman., S.W., Akanuma, Y., Yazaki, Y. and Kadowaki, T. (1997) J. Biol. Chem. **272**, 25839-25844

Kaestner, K.H., Christy, R.J., McLenithan, J.C., Braiterman, L.T., Cornelius, P., Pekla, P.H. and Lane, M.D. (1989) Proc. Natl. Acad. Sci. USA **86**, 3150-3154

Kahn, B. (1992) J. Clin. Invest. **89**, 1367-1374

Kahn, C.R. (1995) Nature **373**, 384-385.

Kahn, R.A., Randazzo, P., Sefarini, T., Weiss, O., Rulka, C., Clark, J., Amherdt, M., Roller, P., Orci, L. and Rothman, J.E. (1992) J. Biol. Chem. **267**, 13039-13046

Kanamarlapudi, V., Oatey, P.B., Tavare, J.M. and Cullen, P.J. (1998) Curr. Biol. **8**, 463-466

Kandror, K.V. and Pilch, P.F. (1994) Proc. Natl. Acad. Sci. USA **91**, 8017-8021

Kandror, K.V. and Pilch, P.F. (1996) J. Biol. Chem. **271**, 21703-21708

Kasahara, M. and Hinkle, P.C. (1977) J. Biol. Chem. **252**, 7384-7390

Kayano, T., Burant, C.F., Fukumoto., H., Gould, G.W., Fan, Y-S., Eddy, R.L., Byers, M.G., Shows, T.B., Seino, S. and Bell, G.I. (1990) J. Biol. Chem. **265**, 13276-13282

Kayano, T., Fukumoto, H., Eddy, R.L., Fan, Y-S., Byers, M.G., Shows, T.B. and Bell, G.I. (1992) J. Biol. Chem. **263**, 15245-15248

Keller, S.R., Scott, H.M., Mastick, C.C., Aebersold, R. and Lienhard, G.E. (1995) J. Biol. Chem. **270**, 23612-23618

Kelly, R.B. (1995) Nature **374**, 116-117

Kirchhausen, T., Bonifacino, J.S. and Riezman, H. (1997) Curr. Opin. Cell Biol. **9**, 488-495

Kishida, Y., Olsen, B.R., Berg, R.A. and Prockop, D.J. (1975) J. Cell Biol. **64**, 331-339

Kitagawa, K., Rosen, B.S., Spiegelman, B.M., Lienhard, G.E. and Tanner, L.I. (1989) Biochem. Biophys. Acta **1014**, 83-89

Kitamaru, T., Ogawa, W., Sakaue, H., Hino, Y., Kuroda, S., Takata, M., Matsumoto, M., Maeda, T., Konishi, H., Kikkawa, U. and Kasuga, M. (1998) Mol. Cell. Biol. **18**, 3708-3717

Klarlund, J.K., Guilherme, A., Holik, J.J., Virbasius, J.V., Chawla, A. and Czech, M.P. (1997) Science **275**, 1927-1930

Klarlund, J.K., Rameh, L.E., Cantley, L.C., Buxton, J.M., Holik, J.J., Sakelis, C., Patki, V., Corvera, S. and Czech, M.P. (1998) J. Biol. Chem. **273**, 1859-1862

Klumperman, J., Hille, A., Veenendaal, T., Oorschot, V., Stoorvogel, W., von Figura, K. and Gueze, H.J. (1993) J. Cell Biol. **121**, 997-1000

Knutson, V.P., Donnelly, P.V., Lopez-Reyes, M.M. and Balba, Y.L.O. (1996) in Molecular Biology of Membrane Transport Disorders (S. G. Schultz, ed.), 303-319, Plenum Press, New York

Kobasyashi, M., Nikami, H., Morimatsu, M. and Saito, M. (1996) Neurosci. Lets. **213**, 103-106

Kohn, A.D., Kovacina, K. and Roth, R.A. (1995) EMBO J. **14**, 4288-4295

Kohn, A.D., Summers, S.A., Birnbaum, M.J. and Roth, R.A. (1996) J. Biol. Chem. **271**, 31372-31378

Kotani, K., Carozzi, A.J., Sakaue, H., Hara, K., Robinson, L.J., Clark, S.F., Yonezawa, K., James, D.E. and Kasuga, M. (1995) Biochem. Biophys. Res. Comm. **209**, 343-348

Ktistakis, N.T., Brown, H.A., Waters, M.G., Sternweiss, P.C. and Roth, M.G. (1996) J. Cell Biol. **134**, 295-306

Kuehn, M.J. and Schekman, R. (1997) Curr. Opin. Cell Biol. **9**, 477-483

Lamaze, C. and Schmid, S.L. (1995) Curr. Opin. Cell Biol. 7, 573-580

Laurie, S.M., Cain, C.C., Lienhard, G.E. and Castle, J.D. (1993) J. Biol. Chem. **268**, 19110-19117

Lavan, B.E., Lane, W.S. and Lienhard, G.E. (1997a) J. Biol. Chem. **272**, 11439-11443

Lavan, B.E., Fantin, V.R., Chang, E.T., Lane, W.S. Keller, S.R. and Lienhard, G.E. (1997b) J. Biol. Chem. **272**, 21403-21407

Le Borgne, R., Griffiths, G. and Hoflak, B. (1996) J. Biol. Chem. **271**, 2162-2170

Le Borgne, R. and Hoflack, B. (1997) J. Cell Biol. **137**, 335-345

Le Borgne, R.L., Alconada, A., Bauer, U. and Hoflack, B. (1998) J. Biol. Chem. **273**, 29451-29461

Lee, W. and Jung, C.Y. (1997) J. Biol. Chem. **272**, 21427-21431

Lenhard, J.M., Kahn, R.A. and Stahl, P.D. (1992) J. Biol. Chem. **267**, 13047-13052

Lewin, D.A. and Mellman, I. (1998) Biochem. Biophys. Acta **1401**, 129-145

Lippincott-Schwartz, J. (1996) in Molecular Biology of Membrane Transport Disorders (S. G. Schultz, ed.), 1-9, Plenum Press, New York

Livingstone, C., Dominiczak, A.F., Campbell, I.C. and Gould, G.W. (1995) Clin. Sci. **89**, 109-116

Livingstone, C., James, D.E., Rice, J.E., Hanpeter, D. and Gould, G.W. (1996) Biochem. J. **313**

Lobel, P., Fujimoto, K., Ye, R.D., Griffiths, G. and Kornfield, S. (1989) Cell **57**, 787-796

Macaulay, S.L., Hewish, D.R., Gough, K.H., Stoichevska, V., Macpherson, S.F., Jagadish, M. and Ward, C.W. (1997) Biochem. J. **324**, 217-224

Malide, D. and Cushman, S.W. (1997b) J. Cell Sci. **110**, 2795-2806

Malide, D., Dwyer. N.K., Blanchette-Mackie, E.J. and Cushman, S.W. (1997a) The J. Histochem. and Cytochem. **45**, 1083-1096

Marks, M.S., Ohno, H., Kirchhausen, T. and Bonifacino, J.S. (1997) Trends Cell Biol. **7**, 124-128

Marks, M.S., Woodruff, L., Ohno, H. and Bonifacino, J.S. (1996) J. Cell Biol. **135**, 341-354

Marsh, B.J., Alm, A.R., McIntosh, S.R. and James, D.E. (1995) J. Cell Biol. **130**, 1081-1091

Martin, L.B., Shewan, A., Millar, C.A., Gould, G.W. and James, D.E. (1998) J. Biol. Chem. **273**, 1444-1452

Martin, S., Reaves, B., Banting, G. and Gould, G.W. (1994) Biochem. J **300**, 743-749

Martin, S., Rice, J.E., Gould, G.W., Keller, S.R., Slot, J.W. and James, D.E. (1997) J. Cell Sci. **110**, 2281-2291

Martin, S., Tellam, J., Livingstone, C., Slot, J.W., Gould, G.W. and James, D.E. (1996) J. Cell Biol. **134**, 625-635

Martys, J.L., Wjasow, C., Gangi, D.M., Kielian, M.C., McGraw, T.E. and Backer, J.M. (1996) J. Biol. Chem. **271**, 10953-10962

Matlin, K. and Simons, K. (1983) Cell **34**, 233-243

Matter, K. and Mellman, I. (1994) Curr. Opin. Cell Biol. **6**, 545-554

Mauxion, F., Le Borgne, R., Munier-Lehmann, H., and Hoflack, B. (1996) J. Biol. Chem. **271**, 2171-2178

Mayer, A., Wickner, W. and Haas, A. (1996) Cell **85**, 83-94

Mellman, I. (1996) Annu. Rev. Cell Dev. Biol. **12**, 575-625

McCall, A.L., Van Bueren, A.M., Huang, L., Stenbit, A., Celnik, E. and Charron, M.J. (1997) Brain Res. 744, 318-326

Miller, S.G., Carnell, L. and Moore, H.H. (1992) J. Cell Biol. **118**, 267-283

Molloy, S.S., Thomas, L., VanSlyke, J.K., Stenberg, P.E. and Thomas, G. (1994) EMBO J. **13**, 18-33

Mora, S., Monden, I., Zorzano, A. and Keller, K. (1997) Biochem. J. **324**, 455-459

Morris, N.J., Ross, S.A., Lane, W.S., Moestrup, S.K., Petersen, C.M., Keller, S.R. and Lienhard, G.E. (1998) J. Biol. Chem. **273**, 3582-3587

Moss, J. and Vaughan, M. (1995) J. Biol. Chem. **270**, 12327-12330

Mueckler, M., Caruso, C., Baldwin, S. A., Panico, M., Blench, I., Morris, H.R., Thorens, B., Sarkar, H.K., Kaback, H.R. and Lodish, H.F. (1988) Cell **55**, 281-290

Nagamatsu, S., Kornhauser, J.M. Seino, S., Mayo, K.E. Steiner, D.F. and Bell, G.I. (1992) J. Biol. Chem. **267**, 467-472

Navé, B.T., Haigh, R.J., Hayward, A.C., Siddle, K. and Shepherd, P.R. (1996) Biochem. J. **318**, 55-60

Nesterov, A., Wiley, H.S. and Gill, G.N. (1995) Proc. Natl. Acad. Sci. USA **92**, 8719-8723

Novick, P. and Brennwald, P. (1993) Cell **75**, 597-601

Novick, P. and Zerial, M. (1997) Curr. Opin. Cell Biol. **9**, 496-505

Odorizzi, G., Cowles, C.R. and Emr, S.D. (1998)Trends Cell Biol. **8**, 282-288

Ogata, S. and Fukuda, M. (1994) J. Biol. Chem. **269**, 5210-7217

Ohno, H., Stewart, J., Fournier, M.C., Bosshart, H., Rhee, I., Miyatake, S., Saito, T., Gallusser, A., Kirchhausen, T. and Bonifacino, J.S. (1995) Science **269**, 1872-1875

Ohno, H., Fournier, M-C., Poy, G. and Bonifacino, J.S. (1996) J. Biol. Chem. **271**, 29009-29015

Oka, Y., Rozek, L.M. and Czech, M.P. (1985) J. Biol. Chem. **260**, 4435-4442

Olson, A.L., Knight, J.B. and Pessin, J.E. (1997) Mol. Cell. Biol. **17**, 2425-2435

Orci,. L., Thorens, B., Ravazzola, M., and Lodish, H.F. (1989) Science **245**, 295-297

Paris, S., Beraud-Dufour, S., Robineau, S., Bigay, J., Antonny, B., Chabre, M. and Chardin, P. (1997) J. Biol. Chem. **272**, 22221-22226

Pearse, B.M.F. (1988) EMBO J. **7**, 3331-3336

Pearse, B.M.F. and Robinson, M.S. (1990) Ann. Rev. Cell Biol. **6**, 151-171

Peterson, P.A. (1995) J. Biol. Chem. **270**, 19989-19997

Peyroche, A., Paris, S. and Jackson, C.L. (1996) Nature **384**, 479-481

Piper, R.C., Hess, L.C. and James, D.E. (1991) Am. J. Physiol. **260**, 570-580

Piper, R.C., Tai, C., Kulesza, P., Pang, S., Warnock, D., Baenziger, J., Slow, J.W., Geuze, H.J., Puri, C. and James, D.E. (1993) J.Cell Biol. **121**, 1221-1232

Ploug, T., Galbo, H., Vinten, J., Jorgensen, M. and Richter, E.A. (1987) Am. J. Physiol. **253**, E12-E20

Pond, L., Kuhn, L.A., Teyton, L., Schutze, M-P., Tainer, J.A., Jackson, M.R. and Rapoport, I., Chen, Y-C., Cupers, P., Shoelson, S.E and Kirchhausen (1998) EMBO J. **17**, 2148-2155

Radhakrishna, H. and Donaldson, J.G. (1997) J. Cell Biol. **139**, 49-61

Rameh, L.E., Arvidsson, A., Carraway, K.L., Couvillon, A.D., Rathbun, G., Crompton, A., VanRenterghem, B., Czech, M.P., Ravichandran, K.S., Burakoff, S.J., et al. (1997) J. Biol. Chem. **272**, 22059-22066

Randazzo, P.A. and Kahn, R.A. (1994) J. Biol. Chem. **269**, 10758-10763

Rea, S. and James, D.E. (1997) Diabetes **46**, 1667-1677

Ricort, J.-M., Tanti, J.-F., Cormont, M., Van Obberghen, E. and Le Marchand-Brustel, Y. (1994) FEBs Letts **347**, 42-44

Ricort, J.-M., Tanti, J.-F., Van obberghen, E. and Le Marchand-Brustel, Y. (1996) Eur. J. Biochem. **239**, 17-22

Robinson, L.J. and James, D.E. (1992a) Am. J. Physiol. **263**, 383-393

Robinson, L.J., Pang, S., Harris, D.S., Heuser, J. and James, D.E. (1992c) J. Cell Biol. **117**, 1181-1196

Robinson, M. (1990) J. Cell Biol. **111**, 2319-2326

Robinson, M., Watts, C. and Zerial, M. (1996) Cell **84**, 13-21

Robinson, M.S. (1992) Trends Cell Biol. **1992**, 293-297

Robinson, M.S. (1994) Curr. Opin. Cell Biol. **6**, 538-544

Rohrer, J., Schweizer, A., Russell, D. and Kornfield, S. (1996) J. Cell Biol. **132**, 565-576

Ross, S.A., Herbst, J.J., Keller, S.R. and Lienhard, G.E. (1997) Biochem. Biophys. Res. Comm. **239**, 247-251

Ross, S.A., Scott, H.M., Morris, N.J., Leung, W.Y., Lienhard, G.E. and Keller, S.R. (1996) J. Biol. Chem **271**, 3328-3332

Roth, M.G. and Sternweis, P.C. (1997) Curr. Opin. Cell Biol. **9**, 519-526

Rothman, J.E. (1994) Nature **372**, 55-63

Rybin, V., Ullrich, O., Rubino, M., Alexandrov, K., Simon, I., Seabra, M.C., Goody, R. and Zerial, M. (1996) Nature **383**, 266-269

Sabolic, I., Wuarin, F., Shi, L.B., Verkman, A.S., Ausiello, D.A., Gluck, S. and Brown, D. (1992) J. Cell Biol. **119**, 111-122

Sandoval, I.V. and Bakke, O. (1994) Trends Cell Biol. **4**, 292-297

Satoh, S., Nishimura, H., Clark, A.E., Kozka, I.J., Quon, M.J.,, Cushman, S.W. and Holman, G.D. (1993) J. Biol. Chem. **268**, 17820-17829

Schafer, W., Stroh, A., Berghofer, S., Seiler, J., Vey, M., Kruse, M.L., Kern, H.F., Klenk, H.D. and Garten, W. (1995) EMBO J. **14**, 2424-2435

Schmidt, A., Hannah, M.J. and Huttner, W.B. (1997) J. Cell Biol. **137**, 445-458

Schweizer, A., Kornfield, S. and Rohrer. (1996) J. Cell Biol. **132**, 577-584

Seaman, M.N.J., Burd, C.G. and Emr, S.D. (1996a) Curr. Opin. Cell Biol. **8**, 549-556

Scaman, M.N.J., Sowerby, P.J. and Robinson, M.S. (1996b) J. Biol. Chem. **271**, 25446-25451

Sharma, P.M., Egawa, K., Gustafson, T.A., Martin, J.L. and Olefsky, J.M. (1997) Mol. Cell Biol. **17**, 7386-7397

Shepherd, P.R., Gould, G.W., Colville, C.A., McCoid, S.C., Gibbs, E.M. and Kahn, B.B. (1992) Biochem. Biophys. Research Commun. **188**, 149-154

Shepherd, P.R., Nave, B.T. and Siddle, K. (1995a) Biochem. Soc. Trans. **23**, 201S

Shepherd, P.R., Soos, M.A. and Siddle, K. (1995b) Biochem. Biophys. Res. Comm. **211**, 535-539

Shepherd, P.R., Reaves, B.J. and Davidson, H.W. (1996b) Trends Cell Biol. **6**, 92-97

Shepherd, P.R., Nave, B.T. and O'Rahilly, S. (1996a) J. Mol. Endocrin. **17**, 175-184

Shepherd, P.R., Withers, D.J. and Siddle, K. (1998) Biochem. J. **333**, 471-490

Shibata, H., Omata, W. and Kojima, I. (1997) J. Biol. Chem. **272**, 14542-14546

Shibata, H., Omata, W., Suzuki, Y., Tanaka, S. and Kojima, I. (1996) J. Biol. Chem. **271**, 9704-9709

Shoelson, S.E., Chatterjee, S., Chaudhuri, M. and White, M.F. (1992) Proc. Natl. Acad. Sci USA **89**, 2027-2-31

Shpetner, H., Joly, M., Hartley, D. and Corvera, S. (1996) J. Cell Biol. **132**, 595-605

Simpson, F., Bright, N.A., West, M.A., Newman, L.S., Darnell, R.B. and Robinson, M.S. (1996) J. Cell Biol. **133**, 749-760

Simpson, F., Peden, A.A., Christopoulou, L. and Robinson, M.S. (1997) J. Cell Biol. **137**, 835-845

Skolnik, E.Y., Lee, C.H., Batzer, A., Vicenti, L.M. Zhou, M., Daly, R., Myers, M.G., Backer, J.M., Ullrich, A., White, M.F. and Schlessinger, J. (1993) EMBO Journal **12**, 1929-1936

Slot, J.W., Garruti, G., Martin, S., Oorschot, V., Posthuma, G., Kraegen, E.W., Latbutt, R., Thibault, G. and James, D.E. (1997) J. Cell Biol. **137**, 1-12

Slot, J.W., Geuze, H.J., Gigengack, S., James, D.E. and Lienhard, G.E. (1991a) Proc. Natl. Acad. Sci. USA **88**, 7815-7819

Slot, J.W., Geuze, H.J., Gigengack, S., Lienhard, G.E. and James, D.E. (1991b) J. Cell Biol. **113**, 123-135

Songyang, Z., Carraway, K.L., Eck, M.J., Harrison, S.C., Feldman, R.A., Mohammadi, M., Schlessinger, J., Hubbard, S.R., Smith, D.P., Eng, C. *et al* (1995) Nature **373**, 536-539

Spiro, D.J., Boll, W., Kirchausen, T. and Wesslinggresnick, M. (1996) Mol. Biol. Cell **7**, 355-367

Stack, J.H., De Wald D.B., Takegawa, K. and Emr, S.D. (1995) J. Cell Biol. **129**, 321-334

Stamnes, M.A. and Rothman, J.E. (1993) Cell **73**, 999-1005

Stenmark, H., Parton, R.G., Steele-Mortimer, O., Lutcke, A., Greunberg, J. and Zerial, M. (1994) EMBO J. **13**, 1287-1296

Stenmark, H., Vitale, G., Ullrich, O. and Zerial, M. (1995) Cell **83**, 423-432

Stephens, J.M. and Pilch, P.F. (1995) Endo. Rev. **16**, 529-546

Stoorvogel, W., Oorschot, V. and Geuze, H.J. (1996) J. Cell Biol. **132**, 21-33

Stutchfield, J. and Cockcroft, S. (1993) Biochem. J. **293**, 649-655

Sudhof, T.C. (1995) Nature **375**, 645-653

Sun , X.J., Rothenberg, P., Kahn, C.R., Backer, J.M., Araki, E., Wilden, P.A., Cahill, D.A., Goldstein, B.J. and White, M.F. (1991) Nature **352**, 73-77

Sun, X.J., Weng, L., Zhang, Y., Yenush, L., Myers, M.G., Glasheen, E., Lane, W.S., Pierce, J.H. and White, M.F. (1995) Nature **377**, 173-177

Suzuki, K. and Kono, T. (1980) Proc. Natl. Acad. Sci. USA **77**, 2542-2545

Takei, K., McPherson, P.S., Schmid, S.L. and De Camilli, P. (1995) Nature **374**, 186-189

Tamemoto, H., Kadowaki, T., Tobe, K., Sakuri, H., Hayakawa, T., Terauchi, Y., Ueki, K., Kaburagi, Y., Satoh, S., Sekihara, H., Yoshioka, S., Horikoshi, H., Furuta, Y., Ikawa, Y., Kasuga, M., Yazaki, Y. and Aizawa, S. (1994) Nature **372**, 182-186

Tanner, L.I. and Lienhard, G.E. (1987) J. Biol. Chem. **262**, 8975-8980

Tanner, L.I. and Lienhard, G.E. (1989) J. Cell Biol. **108**, 1537-1545

Tanti, J.-F., Gremeaux, T., Grillo, S., Calleja, V., Klippel, A., Williams, L.T., Van Obberghen, E. and Le Marchand-Brustel, Y. (1996) J. Biol. Chem. **271**, 25227-25232

Tellam, J.T., Macaulay, S.L., McIntosh, S., Hewish, D.R., Ward, C.W. and James, D.J. (1997) J. Biol. Chem. **272**, 6179-6186

Traub, L.M. and Kornfield, S. (1997) Curr. Opin. Cell Biol. **9**, 527-533

Traub, L.M., Ostrom, J.A. and Kornfield, S. (1993) J. Cell Biol. **123**, 561-573

Van Den Berghe, N., Ouwens, D.M., Maasen, J.A., Van Mackenlenbergh, M.G.H., Sips, H.C.M. and Krans, H.M.J. (1994) Mol. Cell Biol. **14**, 2372-2377

Van Der Sluijs, P., Hull, M., Webster, P., Male, P., Goud, B. and Mellman, I. (1992) Cell **70**, 729-740

Verhey, K.J., Yeh, J.I. and Birnbaum, M.J. (1995) J. Cell Biol. **130**, 1071-1079

Viyayasadhi, S., Xu, Y., Bouchard, B. and Houghton, A.N. (1995) J. Cell Biol. **130**, 807-820

Volchuk, A., Sargeant, R., Sumitani, S., Liu, Z.,, He, L. and Klip, A. (1995) J. Biol. Chem. **270**, 8233-8240

Volinia, S., Dhand, R., Vanhaesebroeck, B., MacDougall, L.K., Stein, R., Zvelebil. M.J., Domin, J., Panaretou, C. and Waterfield, M.D. (1995) EMBO J. **14**, 3339-3348

Walmsley, A.R., Barrett, M.P., Bringaud, F. and Gould G.W. (1998) Trends in Biochem. Sci. **23**, 476-481

Wan, L., Molloy, S.S., Thomas, L., Liu, G., Xiang, Y., Rybak, S.L. and Thomas, G. (1998) Cell **94**, 205-216

Waters, S.B., D'Auria, M., Martin, S.A., Nguyen, C., Kozma, L.M. and Luskey, K.L. (1997) J. Biol. Chem. **272**, 23323-23327

West, M.A., Bright, N.A. and Robinson, M.S. (1997) J. Cell Biol. **138**, 1239-1254

West, M.A., Lucocoq, J.M. and Watts, C. (1994) Nature **369**, 147-151

White, M.F. (1998) Mol. Cell. Biochem. **182**, 3-11

Withers, D.J., Gutierrez, J.S., Towery, H., Burks, D.J., Ren, J.M., Previs, S., Zhang, Y., Bernal, D., Pons, S., Shulman, G.I., Bonner-weir, S. and White, M.F. (1998) Nature **391**, 900-904

Wolf, G., Trub, T., Ottinger, E., Gronnga, L., Lynch, A., White, M.F., Miyazaki, M., Lee, J. and Schoelson, S.E. (1995) J. Biol. Chem. **270**, 27407-27410

Yamashiro, D.J. and Maxfield, F.R. (1984) J. Cell. Biochem. **26**, 231-246

Yang, C.Z., Heimberg, H., D'Souza-Schorey, C., Meukler, M.M. and Stahl, P.D. (1998) J. Biol. Chem. **273**, 4006-4011

Yang, J., Clarke, J.F., Ester, C.J., Young, P., W., Kasuga, M. and Holman, G.D. (1996) Biochem. J **313**, 125-131

Yang, J. and Holman, G.D. (1993) J. Biol. Chem. **268**, 4600-4603